LABORATORIO ULTRASUONI E CONTROLLI NON DISTRUTTIVI
DIPARTIMENTO DI INGEGNERIA ELETTRONICA
UNIVERSITÀ DEGLI STUDI DI FIRENZE

MINE IDENTIFICATION NOVELTIES EUROCONFERENCE

1 9 9 9

OCTOBER 1-3
VILLA AGAPE
FIRENZE - ITALY

Euroconference on:

SENSOR SYSTEMS AND SIGNAL PROCESSING TECHNIQUES APPLIED TO THE DETECTION OF MINES AND UNEXPLODED ORDNANCE

MINE'99 Proceedings

Euroconference on:

Sensor systems and signal processing techniques
applied to the detection of mines and unexploded ordnance

October 1-3, 1999

Villa Agape, Firenze, Italy

Laboratorio Ultrasuoni e Controlli Non Distruttivi
Università di Firenze, Italy

Edited by Leonardo Masotti and Lorenzo Capineri

Additional copies may be ordered from:

Mrs Annalisa Mettel

Dipartimento di Ingegneria Elettronica,

Universita' di Firenze,Via S.Marta 3, 50139, Firenze, Italy

Phone / Fax +39 055 4796517

e.mail : mine99@diefi.die.unifi.it

Internet: http//diefi.die.unifi.it/~mine99

Foreword

Welcome to the Euroconference on *Sensor systems and signal processing techniques applied to the detection of mines and unexploded ordnance – MINE'99* being held in Villa Agape, Firenze, Italy. This is the first scientific and technical Euroconference devoted to the demining problem planned to be organized again in the future.

The main goal of this workshop is to examine the present capabilities and features of different investigation techniques (magnetic, electromagnetic, thermographic, nuclear, chemical etc.) and to stimulate a strong exchange of knowledge and new ideas between different technological and scientific fields. To this end there will be appointed discussions after each session and poster presentations.

The scientific programme is organised in 10 plenary sessions and a poster session anticipated by a brief oral presentation of the works. The contributions have been submitted by authors from 13 countries in nearly 23 papers. Another important goal of this conference is to support the participation of young researchers from European Member States and scientists from Eastern European countries. At the end of the workshop participants will draft a consensus document to present the current status of each investigation method and to point out the most promising (and reliable?) image analysis methods in the specific areas. Proposals for a new meeting will be also discussed.

The Director and the Organizing Committee feel honoured by the European Commission confidence and mandate to organize this Euroconference. We wish to thank the Sponsors and the patronage of the University of Florence, Comune di Firenze a Centre of Optronic Excellence of Florence. Special thanks go also to the authors and session chairmen for their contributions to the conference and the staff of Laboratorio Ultrasuoni e Controlli Non Distruttivi at the Department of Electronic Engineering of the University of Florence.

Again welcome in the pleasant atmosphere of Villa Agape that we hope to stimulate new and fruitful projects and collaborations.

Director

Prof. Leonardo Masotti

Organizing Committee

Dr Lorenzo Capineri, Mr Gianfranco Mela , Prof Colin Windsor

Supported by:

EUROPEAN COMMISION

UNIVERSITÀ DEGLI STUDI DI FIRENZE

CNR - ITALIAN NATIONAL RESEARCH COUNCIL

CASSA DI RISPARMIO DI FIRENZE

THE BRITISH COUNCIL

Under the Patronage of:

COMUNE DI FIRENZE

CENTRO DI ECCELLENZA OPTRONICA FIRENZE

REGIONE TOSCANA

Organization

Director

Leonardo Masotti, Italy

Organizing Committee

Lorenzo Capineri, Italy
Gianfranco Mela, Italy
Colin Windsor, United Kingdom

Scientific Committee

Lorenzo Capineri, Italy
Jan Cornelis, Belgium
Arnaldo D'Amico, Italy
David Daniels, United Kingdom
Karl Langenberg, Germany
Leonardo Masotti, Italy
Jean Daniel Nicoud, Switzerland
Christian Pichot, France
Giorgio Sberveglieri, Italy
Colin Windsor, United Kingdom

Chairmen

Claudio Bruschini, Switzerland
Lorenzo Capineri, Italy
Jan Cornelis, Belgium
Arnaldo D'Amico, Italy
David Daniels, United Kingdom
Mikael Georgson, Sweden
Stefan Havlick, Slovakia
Karl Langenberg, Germany
Leonardo Masotti, Italy
Giancarlo Nebbia, Italy
Jean Daniel Nicoud, Switzerland
Christian Pichot, France
Giorgio Sberveglieri, Italy
Mario Sepe, Italy
Colin Windsor, United Kingdom

Secretary

Annalisa Mettel, Italy

Author Index

Subjects index

Table of Contents

THERMOGRAPHY AND THERMOVISION

NUCLEAR METHODS

CHEMICAL SENSORS

NOVEL METHODS (INGENIOUS AND INGENUOUS SOLUTIONS)

MULTIPLE SENSORS SYSTEMS AND DATA FUSION

INVERSION METHODS FOR GROUND PENETRATING RADAR

POSTERS PRESENTATIONS

Humanitarian demining
Is it worth to invest in technology?

J.D. Nicoud, LAMI-EPFL, CH 1015-Lausanne
jean-daniel.nicoud@epfl.ch http://diwww.epfl.ch/lami/detec/

ABSTRACT:
Anti-personnel mines are efficient weapons ; even with international treaties, mines will continue to be used in future conflicts, until technology will allow to remove them as easily as they are planted. Manual mine detection is slow, but efficient. Humanitarian demining teams just need more money to use more people, clear land, and contribute to the local economy. Validation of mine detection equipments is a long process to be conducted in interaction with demining teams. Our experience in Croatia and Cambodia, testing a GPR system for acquiring data, allows us to give several recommendations.

Keywords: Humanitarian demining, Standard operation procedures, Evaluation and qualification of equipment

Introduction

The cost for clearing manually all the important mined areas, over the next 5 or 10 years, is much lower than the expenses on govermental and military R&D on mine detection and neutralization, during the same period. Since we have no hope to find an applicable solution as soon, is it worth now to invest in technology?

About 50 millions mines are laid in the soils of 50 countries, maybe 10 times more are stockpiled and they are still easily available from many manufacturers in the world. For every mine painfully removed, about the same number is laid within the same time in the conflicts you see daily on CNN. Mines are indeed efficient weapons, low cost, easy to produce. International treaties have reduced their proliferation, but minorities and nations with land or ethnic claims have difficulties to accept the rules of high standing countries. Most existing mines have been laid by guerrilla armies as an offensive weapon to spread terror, destabilize the economy, destroy food sources and create refugee flows. The low cost of mines and the difficulty to neutralize them is their key advantage.

Organized armies use mines as a defensive weapon to protect their positions, and they keep track of their layout. They develop expensive equipment for breaching through the enemy's minefields and for testing the safety of the roads at a speed greater than 20 km/h. The military are now more concerned about humanitarian demining, but they are not used to release their experience and have a poor understanding of the cost-effectiveness constraints of humanitarian demining teams.

Many projects are underway to search for new technologies for mine detection and removal, and for developing products that could be used by deminers. Most of these projects are defined without a real understanding of the situation on a demining field, ignoring the deminers' requirements for accepting a new technology.

Lobbying is more active for the survival of the sensor and robotic researcher species than for Angolan kids. R&D activities will go on and have to go on; there is some hope that several projects will head toward a solution. It is good to dream about a demining robot that would

remove the mines as quickly as soldiers can place them, and for a cost per mine similar to the cost of a mine: that day, the military interest for planting mines may disappear.

The three demining dimensions

There are three phases of mine use, during and after a conflict, which will remain as long as anti-personnel mines are not definitively banned.

Phase one: During the war, the armies protect their strategic positions with antitank and antipersonnel mines. The opponent's activity is to breach through these minefields, regardless of the material and human losses. For this military demining|, neutralizing 90% of the mines is acceptable, at any cost.

Phase two: When the conflict is over, Kuwait being an exception, the country is economically ruined and the United Nation calls for the help of the armies of goodwill nations, in order to re-establish the communications, remove the anti-tank mines from the roads, delimit the minefields in which antipersonnel mines and unexploded ordnance (UXO) could be found. This very useful, but expensive activity, requires trained people and special equipment. In general, the objective is to get the local army trained to take this work over as soon as possible, with of course much more limited resources. This has happened in Cambodia 5 years ago, and is happening now in Bosnia. It is usually called humanitarian demining, but post-conflict demining| is better to avoid confusion with the third phase.

Phase 3: When the UN removes its support after several years, e.g. as in Cambodia (Afghanistan, Angola, Mozambique are or will be similar), the economy is still completely down, and the government has severe financial problems. Many people are killed or maimed everyday by antipersonnel mines without any compensation. Non profit demining organizations, supported by the UN and several NGOs (Non Governmental Organisations), start to train the cheap local deminers in probing the ground patiently in order to find all the mines. In Cambodia, at the present rate, this may take more than 20 to 50 years. This is sustainable humanitarian demining|.

Post-conflict demining

An important amount of research funding, worth about 100 Mio dollars per year, is spent for the development of technological solutions related to post-conflict demining, with the belief that the ultimate solutions will soon be available, if sufficient funding for R&D is available. Many projects for teleoperated or autonomous robots, cameras, sensors, data bases, airborne detection systems which can only recognize anti-tank mines, are developed by engineers who have not even seen a real mine-field. The objective appears to be to make a demonstration on some military test field, and get the project continued. From the point of view of humanitarian deminers, this is a complete waste of money.

Sustainable humanitarian demining

A major concern of the UN, ICRC and NGOs supporting humanitarian demining is the health, food, education and economic problems of the many defavored countries of the world. They are also concerned with the antipersonnel mine problem. They provide medical care and prosthesis, or pay for the demining activities. In Cambodia, the CMAC (Cambodian Mine Action Centre) has more than 2000 deminers. Together with 4 other mine clearance organizations (800 additional deminers), they clear about 15 km2 per year and removed in 5 years only 10% to 20% of the estimated number of mines in Cambodia. Additional areas claimed to be mined are verified and freed if not dangerous.

The idea to use a robot for replacing the men doing this not so dangerous work brings the same cost/effectiveness issues. In Angola or Cambodia, a deminer is paid about $150 a month and his family gets $5000 in case of an accident. Replacing these deminers by robots brings also a social and economic problem: will they find other equally well paid jobs? A teacher or

a policeman gets only 30 dollars a month. Tourism pays correctly, but there are rather few places like Angkor.

Demining technologies

Mechanical solutions are good for the military. They are usually inadequate for humanitarian deminers, since they neutralize only 90% of the mines, and make the removal of the mines left more difficult. The only advantage is to clear the vegetation; removing vegetation by hand is terribly slow and painful. But no research lab is ready to devote attention to such an apparently trivial problem. No industry will develop such a vehicle for a market of 10 to 20 pieces a year. Deminers have to do the development themselves, patching a standard vegetation cutter used on highway sides on a low cost Russian truck.

Fig 1. Vegetation cutter developed by HALO-Trust and used in Cambodia

The key problem is the sensor, which must be brought as close as possible from the mine location. Hence the need for removing vegetation, which is also a requirement for the rehabilitation of the land for agricultural needs.

Besides the widely used metal detectors, several technologies are being developed with the hope to accelerate the demining process. They will be covered by other papers. No one solution will be usable in all situations. It is hence easy to criticize any effort in a given direction, and claim the cost-effectiveness is not worth.

Genetically modified animals or plants, in which a special interest has been developed for TNT, could be a more efficient way for marking mines, or even eating them. Apparently, little work is being carried out in this direction. At the University of Groningen, a whasp is studied, that should get fluorescent color in presence of TNT. Sandia lab USA, tryes to check the explosive content of the dust brought back by bees when they return to the hive. In Belgium, rats are tested in place of dogs (APOPO project). We had hope with coakroaches, but the measurement of their odor sensors didn't show any particular sensitivity to TNT or RDX.

If odor sensors develop correctly over the next years, there is some hope that an autonomous small and reasonably cheap robot could explore every square meter of an area and come to the conclusion that there are no mines in it. It seems more easy to decide there is no mine in a given field, than to locate precisely existing mines. As an animal would do, the robot can stop as long as required to improve the measure. Such a robot must be able to navigate inside deep vegetation with a 10-20 mm tree every 50cm. This would save tremendous amount of time devoted now to prodding fields in which no mines are found after many weeks. When the field is known to be safe, the farmers can use their usual procedures for restoring to farmland.

Validation of demining equipment

We need urgently a good mine sensor, which will be likely a combination of sensors; but its development cannot follow the usual industry procedures. Any accident will be charged on the promoters of the changes, even if statistics prove a general reduction of accidents. Most products, specially PC software, are tested by the users, who patiently wait for the next release, trying to work around the bugs. With a new demining equipment, the first undetected mine will cause an accident and just make the product disappear from the market, and a similar technology may not be proposed again in a product for many years. Tests in laboratory

will never be convincing enough for a deminer. He will do the tests himself, and compare the results with the presently mastered technology, the metal detectors.

Validation of demining equipment is a long and difficult process developers should not ignore. Most projects have been and will continue to be interrupted before reaching this validation point, and frequently without a clear documentation allowing the subsequent projects to take benefit of the development and measurements done. Military and industrial confidentiality restricts the transfer of know-how and slows down the general progress. The technology is difficult, the market is very small, nobody is ready to pay what is really required, and no systematic approach is taken for the validation of equipment. This is a very bad set of parameters in a field where everybody agrees about the humanitarian need and urgence for getting a solution. It is good to see the increased effort from several governments and the European Community to support projects; open cooperation, adequation with requirements and validation methodology should be key criteria for acceptance of projects.

Standard Operation Procedure (SOP)

Researchers need a reference procedure to evaluate and qualify new demining equipment. The Standard Operation Procedure (SOP) documented and followed by each demining team is the only reference demining teams trust in. It specifies how to remove the vegetation, how to check, adjust and use the metal detector, how to prod, what to do when a dangerous object is found. For the seldom places which may feature non-metal mines, or when the soil does not allow the use of a metal detector, systematic prodding and excavationas deep as required is the reference procedure.

Any new demining equipment must be tested on the field against the reference procedure in use. Validation on a military proving ground will never be accepted by humanitarian deminers. The test procedure must be performed by the demining teams themselves. Due to the danger on the field, engineers will not be accepted close-by, and this complicates the test procedures.

Within the initial phases of the test, the developers need to check the operation and verify the quality of the data. They have of course done this abundantly in the lab and on different fields, but the situation on a real minefield brings a lot of new parameters. A solution has to be found in order to be able to give the deminers the equipment to be tested. Its operation has to be inserted inside the SOP, without removing any item, and not adding difficult or dangerous operations. Either the new sensor is used after removing vegetation (40cm at a time on the 1m wide lane), or the sensor is used on the potentially dangerous spots signalled by the metal detector. Then the usual prodding is performed and the cause of the alarm can be recorded. For the developers, the work is then to check the data given by the detector against the alarms, and see if a correct prediction could have been done. In the case a complete scan is performed, one could dream about a sensor able to find mines the metal detector would not see; in this case, it would be necessary to prod the entire ground to an important depth.

This seems to us the only procedure that will allow developers to check for the data, improve their algorithms, and get useful feedbacks from the deminers about the usability of their system. When the tests will be considered successful by the developers, they will have to be continued for a long period in cooperation with a demining team.

Tests of the system on the field

The system to be tested by the deminers on the field must include features to check the operation from the distance and collect as much data as possible. The first prototypes must be designed for testing the validation procedure, and get confidence in the proposed technology, and not with the idea of a product that could be sold. The evaluation system should be lightweight and easy to use. It should not give any indication to the deminer, except in case of misuse that will prevent the correct acquisition of data. Data should be radio transmitted 50m away toward a system allowing an immediate checking and saving of the data.

The first trial on the field should be done on a 100 m2 field prepared 6 months in advance next to a real minefield, having an average of 3 false alarms and 0.2 mine surrogates per square meter. Two parallel lanes (team of 4-6 deminers) can be open for an optimal use of the sensor system: during the prodding on one lane, data can be acquired on the other lane. A 5-day campaign will allow to clear the test field and record about 300 situations, adequate for a first evaluation. In Cambodia or Angola, the local costs charged by the local demining team may be in the $2000 range only.

The next step on a real field will need one equipment per lane, since the lanes will be 25 meter apart, and no direct crossing will be possible. Several equipment transmitting their data to the data collecting unit will be cost-effective, since one or two designers will be here to take care of the problems and check for acquired data.

The product to be used by the deminers will then at least be redesigned and built. Subsequent tests will be done by the deminers alone, according to procedures that will depend on the experiences done during the evaluation phase, and to the characteristics of the equipment.

Our experience with Detec-1 and Detec-2

The DeTeC project (1995-97) provided us with the experience of a medium project (5 persons) initially intended to validate a combined MD-GPR (Metal Detector - Ground Penetrating Radar Combination) mine detector, in order to reduce the number of false alarms. We restricted the objective to the development of a portable system for doing data acquisition on the field, in order to ease further industrial development of a product.

We realized talking to several deminers in Cambodia (November 96) that the reference was the metal detector, and deminers didn't want to change their SOP about it. We hence decided to do a succesive usage of the existing MD, followed by a scan with our GPR. In order to have the deminer operating a lighter system, we split the Detec-1 system in two parts: the antenna, raw processing and wireless transmission were in a box handled by the deminer, and the processing, visualization an storage of the data, in another box within a safe zone, 50m away. It was considered as an advantage that the platoon chief could look at the images taken by several deminers in parallel, and provide a better diagnostic about false alarms then the less educated deminers doing the work. We demonstrated the equipment to experienced deminers in June 97, and tested it in Karlovac, Croatia, early July 1997. Two drawbacks appeared: the manual scanning was too difficult to be done precisely, with a clear danger of handling a too heavy antenna just above the mine. The other point was that the deminer doing the work cannot be told from a distance if it is a false alarm or not; he has to take the decision himself. In case of accident, he would be the only responsible for a wrong decision.

We then rebuilt Detec-2, using a mechanical arm for directing the antenna movement. This proved to be convenient. We also put the processor, screen and disk storage in the same box, with this idea of a future product having to be under the complete control of the deminer. This was a major error that prevented us from doing acquisitions on a real field while we were in Cambodia, since the equipment was too complicated to operate. The interest of the engineers to look at the freshly acquired data was slowing down excessively the work of the deminers. We now consider it would have been wise to design specifically a system for our main objective of acquiring data in order to test algorithms for false alarm recognition, and not to try to build an equipment that could also have been used for trial use, after the implementation of the best algorithms.

Fig 2 Detec-2 system in test at Thmar-Puk (Cambodia)

Support for the researchers

We consider it urgent to create a center which can help the engineers carrying out sensor projects. As typical actions, this center should be able to distribute mine surrogates at a reasonable cost, document where to find test facilities (sand boxes, military fields) and redistribute without any restriction the results of all the tests done within these facilities, and serve as an intermediary agent between the developers and the deminers in action, in order to define and facilitate the validation steps.

Experts within international centers should in the future collect, integrate and update all the experiences, in order to recommend procedures, and define the validation steps that would minimize both the risk of accident when using a new equipment for tests or trial use, and maximize the chance of commercial success of the sensors and auxiliary equipment the demining community badly needs.

EUDEM CE project is a useful step in this direction. A list of organizations doing research and producing demining equipment has been established. An open data base is accessible (http://www.eudem.vub.ac.be/), and the project has summarized existing techniques and new technology development.

References

C. Bruschini et al, "Study on the State of the Art in the EU related to humanitarian demining technology, products and practice", EU-EUDEM project report draft, Aug 1999, 50pp

D. Barlow et al. (ed) "Sustainable Humanitarian Demining: Trends, Techniques and Technologies" JMU, 1998 (copies can be obtained from hdic@jmu.edu)

J. Brooks, J.D. Nicoud "Applications of GPR Technology to Humanitarian Demining Operations in Cambodia: Some Lessons Learned", Third Annual Symposium on Technology and the Mine Problem, Mine Warfare Association, Monterey, CA, USA, 6-9.4.1998. Proceedings available on CD ROM.

J.D. Nicoud, F. Guerne, J. Brooks "Report on the DeTec-2 Testing in Cambodia, November 18-21 1998", The Journal of Humanitarian Demining, Issue 2.2, June 1998. Available online at http://www.hdic.jmu.edu/hdic/journal/2.2/features/nicoud.htm.

F. Guerne, B. Gros, M. Schreiber, J.D. Nicoud, "DETEC-1 and DETEC-2: GPR Mine Sensors for Data Acquisition in the Field", Proceedings SusDem'97, Zagreb, 1997, pp. 5.34-5.39 (also http://diwww.epfl.ch/lami/detec/susdem_detec2.html).

International and Local Demining Experience. Update of the Italian Ministry for Foreign Affairs for Demining Initiatives

Sepe Mario – A.B.C. Consultant and Relator
Gianfranco Mela – A.B.C. General Manager

ABSTRACT:
A.B.C. is the only Italian clearing company that operates even on an international scale. Since 1994, they have set up and successfully developed some effective and innovative demining procedures.
They combine mechanical demining with the use of suitably trained dogs to detect mines and explosive devices, and they also have highly specialised staff equipped with adequate modern detectors. With these means, A.B.C. have carried out, quickly and safely, many demining operations for humanitarian purposes in countries whose land is spread with numerous mines, such as Croatia, Bosnia Herzegovina and Angola.

Key words: Mine and UXOs Clearance – Mechanical Demining – Mine Sensing Dogs – Manual Demining.

The history of A.B.C.'s experience in the field of demining in Italy, is a long one. Indeed, it dates back to the 1960s, and actually started with the clearance experiences acquired since 1947.
A.B.C. are still demining in Italy - mostly from underground uxos - for infrastructure building. However, they are still finding some World War II minefields, like in the Sila area (Calabria, southern Italy), where in 1998 one intact and still efficient German Teller A/T minefield was found.

The demining necessities caused by the Kuwait War involved A.B.C. in land and underwater demining projects, which demonstrated the Italian capability to manage operations abroad. At the same time, however, these operations showed that it was time to enhance the acquired experiences by new procedures and technologies to safely handle new types of mine and uxo pollution (infestation) and guarantee the minimum required final demining quality of 99.6%. The target included the use of minimum time/money consuming procedures in compliance with the limits imposed on international demining prices.

The co-operation between A.B.C. and Mine Action Services started around that time, and, together, we were able to present to the European Commission (at the beginning of 1996) a new demining method which combines three different systems: mechanical demining, trained dogs and deminers. This method is compliant with all stated requirements.

We have obtained good results thanks to our full commitment. We started our work with the identification and gathering of all available demining systems, procedures, technologies and equipment. We have compared them, trying to classify the aspects which better meet the

requirements of realistic demining scenarios, which are rarely represented by desert areas and most often involve forests and thick woods.
Considering the subjects that are being discussed in the present conference, we think it necessary to underline that we too looked for a technological "short-cut" in the first place. We were looking for technological aids (detectors, etc.) which would allows us to waste less time, but all systems available on the market were only able to detect explosive devices without taking into account all difficulties created by woods, which would prevent the use of such systems from an aircraft (except for special conditions, e.g. desert areas).
These new detectors had greater detecting performances as compared to traditional electronic mine detectors, but they did not bring about significant improvements as concerns their general use. In fact they were very complex, and had to be operated by specialists of new technologies, who were often not prepared to work on mine fields.
Besides, even the best detectors only gave an indication of the presence of explosive devices, which – due to vegetation - were identified only at a minimum distance from the detector. As a consequence, human action was needed to physically identify and locate explosive devices, and operators ran the risk of getting caught in snares that could not be sensed by any detecting system.

Therefore, the problem was – and still is – that of demining in thick-wood areas potentially covered with snares, which slow down sensibly all clearing activities. Indeed, in the presence of snares, demining is completely manual, regardless of the type of detector used.

MANUAL DEMINING

International Organisations have established a limit for the cost of demining, which varies between 1.5 and 3 Euros (Lit.3,000/6,000) with an expected monthly output of demined land equivalent to at least 100,000 square metres.

Detectors and their methods for use were - and still are – good for military demining operations, but they did not fit in the targets established by Financial Organisations for demining of infrastructures and for humanitarian purposes.

The method which we have studied and used on land, instead, is fully compliant with the above targets. What follows is an illustration of the reasons for the success of our method:

- through mechanical demining, all vegetation is removed from soil, and the latter is then ploughed to the required depth. Consequently, 100% of snares and explosive devices are destroyed. However, it may well be that some devices are simply broken up without exploding. Therefore, mechanical demining alone does not guarantee the needed level of quality, and a further step is needed;

MECHANICAL DEMINING

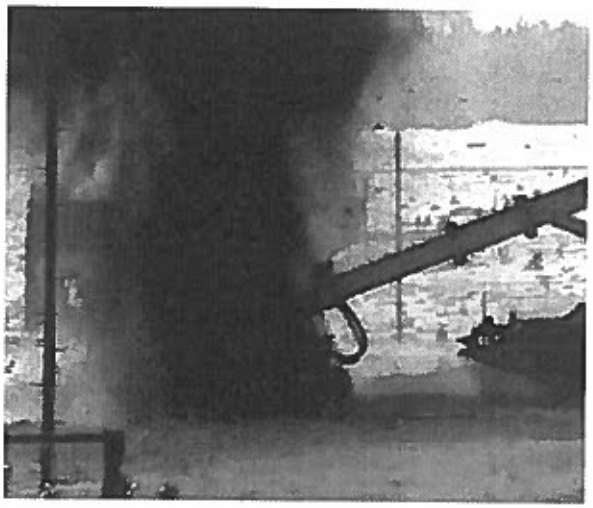

MECHANICAL DEMINING

- this step consists in checking the whole area which has been demined mechanically with teams of dogs trained to detect mines and explosives. These dogs, which are lead by "handlers", can sense even the smallest parts of devices containing explosive.

MINE SENSING DOGS

This technique was extensively used during World War II, and is particularly effective and safe, especially if it is carried out on areas which have been cleared from vegetation and snares. Under these ideal conditions, handlers can notice even the smallest deviation from the normal behaviour of their trained dogs, and therefore they can obtain the best results. It is important to point out that almost all accidents occurred while using dogs with no prior mechanical demining, were caused by snares with trip-up wires, which cannot be spotted by dogs because they are deftly hidden in the thickness of the vegetation.

The use of mechanical demining + dogs already provides the minimum legally required quality level: 99.6% . Actually, this is a very hard quality level to obtain *a priori* on land and – consequently – only with a 100% quality can a company state that the contract acceptability limits have been exceeded, and that their operators have taken every possible human action to eliminate all further hazards. Indeed, demining operators are then the first people to walk over a demined area.
Therefore, in order to reach our highest targets, the two methods mentioned earlier have been completed with the following technique:

- an electronic double-check is carried out by teams of demining operators equipped with the most sensitive mine detectors that are currently available on the market (Forster Minex). In some cases, they also use "georadars" and Forster Ferex to spot unusual underground findings at considerable depths, or in special areas which have been scattered deliberately with fragments of metal or explosive to impair the sensing capacity of both mine detectors and trained dogs.

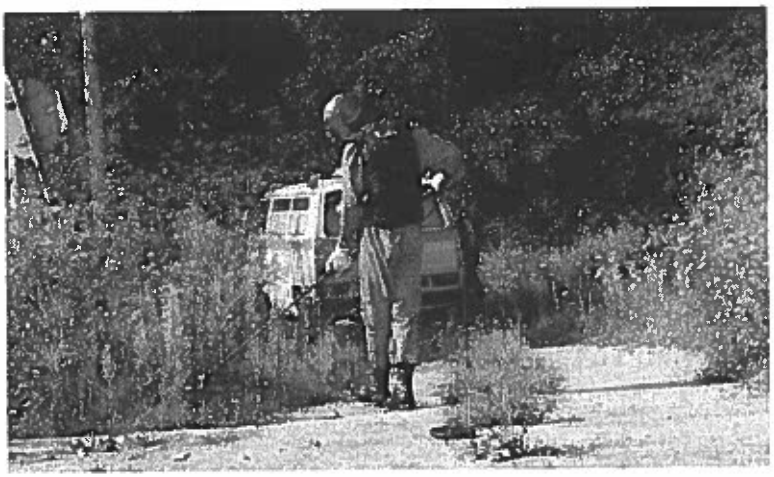

MANUAL DEMINING

A.B.C. have used this integrated operating procedure to carry out several demining operations, such as the following:

- demining of the Sisak-Sunja-Volinja railway in Croatia, funded by IFOR;
- demining of the banks and its environs on the Sava river at Odzak (northern Bosnia) , funded by World Bank;
- demining of the railway line from the harbour of Lobito to the border with Congo, funded by the Ministry of Transports of Angola (this project is suspended due to the renewal of hostilities in this area);
- demining of a tourist/recreational area in the town of Slavonski Brod in Croatia, funded by UNDP-UNMAAP and Croatian Mine Action Centre.

In all the above projects, we have obtained excellent results, and works have been completed in less than 60% of the assigned time. As confirmed by successive quality checks carried out independently by clients, we have achieved a 100% demining quality, and – most of all – no accidents whatsoever have occurred to people, animals or mechanical means.
Our experience in the present operational scenario lead us to hope that modern research will soon give out new systems and methods. And our hope is also that these systems will sensibly improve those which are currently being used, and that they will take into account the conditions and the limits under which they will be used.
Starting from the same experience, we also believe that there should be a greater commitment for the research of innovative solutions geared towards each industrial "niche", which would add more value to new technology. On this subject, we are fully available for those who wish to consider and develop this field of research, because we would be the ideal experienced final users of any potential new technology.
Finally, we believe that international efforts for research and development of innovative systems for non-military demining should be aiming to improve the present systems and solve their many little but dangerous problems. In fact, modern research is still too concentrated in finding a "global solution" which does not exist – as it is clear from demining and from any other industrial activity.
In February 1999, the Central Office of the Co-operation for Development Unit of the Ministry of Foreign Affairs promoted the creation of the National Committee for Humanitarian Actions against Anti-Personnel Mines. Its aim is to foster and co-ordinate national projects to solve this major problem.
A.B.C. were very pleased to take part in this project, since they are a member of Assobon - Associazione Italiana delle Società di Bonifica - (Italian Demining Companies' Association), and they are the only Italian company that is carrying out demining operations abroad for humanitarian purposes. Moreover, back in 1997, A.B.C. had already declared their total commitment for such projects.
The above Committee has set up special Work Teams operating in different fields and dealing with several problems, such as the constitution of a national data bank to be added to the existing international data banks, and the training of qualified demining staff in Italy. The Committee also organises press campaigns to make the public aware of principles, methods, public relations, scientific and technological research concerning demining for humanitarian purposes and any other aspect of the issue of anti-personnel mines.

References:

La Nazione – 28.06.1995: *Tecnologia Fiorentina Per La Bonifica Delle Mine*

Gazzettino – 14.07. 1995: *Tele-Sminamento: Sistema Italiano Presentato All'Onu*

Toscana Oggi – 23.07. 1995: *Pace E Tecnologia A Braccetto*

The Namibian - 20th March 1996: *Summit Acts On Landmines Legacy*

La Nazione 16.04.1996: *Sminamento, Firenze La Capitale*

Panorama Difesa – n. 132 May 1996 pp. 54-57: *Gli Uomini Del Grano*

Toscana Qui – May-June 1996 pp. 80-82: *Sfida Alla Morte*

Panorama Difesa – n. 137 November 1996 pp. 36-38: *.....E Il Treno Va*

Toscana Oggi 10.11.1996: *Ex-Jugoslavia, Sminata Dai Toscani La Ferrovia Tra La Bosnia E a Croazia*

Panorama Difesa n. 141 - Marzo 1997 p 57, : *A.B.C. - Progetto Bonifica*

Raids – n. 138 October 1998 pp. 32-34: *A.B.C. Specialisti In Sminamento*

L'unita' – 11.06. 1999: *L'incubo Mine Sul Ritorno Dei Profughi*

Il Sole 24 Ore – 11.06.1999: *Fassino: Una Legge Per Le Imprese Italiane*

Business Week July 5th 1999: *What Kosovo Doesn't Need: A Battle Over Aid*

Il Giornale - – 14.07.1999: *Kosovo. Le Società Fiorentine Investono Sulla Ricostruzione*

Metal Detectors for Humanitarian Demining: from Basic Principles to Modern Tools and Advanced Developments

Claudio Bruschini

EPFL-LAMI, INF-Ecublens, CH-1015 Lausanne, Switzerland

Tel. +41 (0)21 693 3911, Fax. 5263

E-mail: Claudio.Bruschini@epfl.ch, Web: http://diwww.epfl.ch/lami/detec/

ABSTRACT

We will focus on the low frequency electromagnetic detection of metallic objects, concentrating in particular on induction devices ("metal detectors") and their application to Humanitarian Demining. We will begin by reviewing the basic principles of such systems, having a look at some features of the primary and secondary magnetic field and of the induction mechanism.

The introductory part will be followed by a description of present-day commercial systems, which are the result of many years' efforts in increasing sensitivity and autonomy, and mastering background rejection and ergonomics. The last section will then focus on advanced developments and how they could be used with profit in Humanitarian Demining, possibly in selected scenarios.

Keywords: humanitarian demining, metal detectors, electromagnetic induction, imaging systems

Introduction

Detection and clearance are still being very often carried out in Humanitarian Demining using manual methods as the *primary procedure. When operating in this way* the detection phase still relies heavily on metal detectors (see Fig. 1), whereby each alarm needs to be carefully checked until it has been fully understood and/or its source removed [1]. This is normally done visually, and by prodding and/or excavating the ground.

Unfortunately, metal detectors cannot differentiate a mine (see Fig. 3) or UXO from metallic debris (an example is shown in Fig. 2). In most battlefields, but not only there, the soil is contaminated by large quantities of shrapnel, metal scraps, cartridge cases, etc., leading to between 100 and 1,000 false alarms for each real mine. Each alarm means a waste of time and induces a loss of concentration [1]. When manual methods follow other procedures, such as mechanical clearance, constraints on the need to check each alarm are often somewhat relaxed.

In the following we shall more closely focus on metal detectors and how their use in humanitarian demining could be improved, possibly using input from other fields in which similar devices are used with profit.

Theoretical Background

The detectors we will consider are electromagnetic sensors exploiting low frequency electromagnetic fields up to some hundred kHz roughly. These sensors are capable of detecting metallic objects buried in the ground at usually shallow depth, whilst indirectly providing "limited" information on their nature (depth, shape, size, etc.). Proximity to the surface is usually required.

Fig. 1: HALO Trust deminer in Cambodia, checking the ground with an Ebinger 420SI metal detector

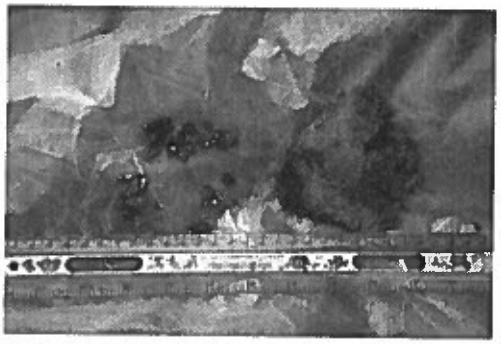

Fig. 2: Example of metallic debris (ruler: 25 cm long)

Fig. 3: Chinese Type 72 mine minimum-metal AP mine (78 mm large, 38 mm high)

Metal Detectors (Electromagnetic Induction Devices)

Metal detectors, actually electromagnetic induction devices, are usually composed of a search head containing one or more coils carrying a time-varying electric current. The latter generates a corresponding time-varying magnetic field which "propagates" towards the metallic target (and in other directions as well). This primary field reacts with the electric and/or magnetic properties of the target (the soil itself or any metallic object), which responds to it by modifying the primary field or, as a more accurate description, by generating a secondary magnetic field. This effect links back into the receiver coil(s) in the search head, where it induces an electrical voltage which is detected and converted, for example, into an audio signal [2].

The secondary field depends, both temporally and spatially, on a large number of parameters such as the distance, material type, orientation, shape and size of the buried object, but target characterisation is very difficult in the general case. The secondary field is due to eddy currents, which are induced by the primary field in conductive materials. Low conductivity metals, such as some alloys and stainless steel, are in general more difficult to detect, whereas the detector's response is magnified for ferromagnetic objects (induced magnetisation).

In the case of a circular coil of radius R for example, the primary field behaves at a distance z on the coil axis as $1/(R^2+z^2)^{3/2}$, i.e. decreases with the cube of the distance far away from the coil. Given that the secondary magnetic field has to "propagate" all the way back to the receiver coil(s) it is not surprising that the "art" of building metal detectors consists, in a certain sense, in discriminating small target signals from background signals. Smaller coils

provide better sensitivity (at closer ranges) and spatial resolution, but do not allow to go as deep, and scan as fast, as the larger ones.

Frequency and Time Domain Metal Detectors

Metal detectors can be subdivided in Frequency Domain, or Continuos Wave (CW), and Time Domain systems. Frequency Domain instruments make use of a discrete number of sinusoidal signals, very often just one. They can employ separate transmit/receive circuits, and the measurement of the amplitude and phase of the received signal in background conditions can be used to reject part of the background signal itself.

Time Domain, or "pulse", instruments work by passing pulses of current through a coil (typical repetition rate of the order of 1 kHz), taking care to minimise the current switch-off time (a few μsec). Eddy currents are thus induced in nearby conductive objects and their exponential decay with time observed. The eddy current decay time constant itself, some hundred μsec, depends (predominantly) on the target's conductivity, permeability and size. Pulse systems are the detector of choice when it comes to working in salt water or strongly mineralised soils.

Metal Detectors for Humanitarian Demining

Metal detectors for humanitarian demining are capable of detecting tiny amounts of metal, from a fraction of a gram onwards, at shallow depths. They mostly share the following characteristics:

- **Weight**: less than 2 kg. **Price**: in the 2000-4000 EURO range.
- **Size**: round, oval or rectangular head. In the former case the diameter is between 20 and 30 cm, to achieve sufficient depth and a reasonable scanning surface and speed.
- **Operating depth**: shallow, i.e. from flush (even with the surface) down to about 10-15 cm for minimum-metal mines, 20-30 cm for mines with an appreciable metallic content, and about 50-70 cm for large metallic objects such as UXO or metallic mines.
- **Electrical/Mechanical**: capable of working with standard cell batteries for a long time (tens of hours), and usually simple to use. Many demining teams pay more attention to the ergonomics rather than to the pure performances of the detector itself.
- **Output**: normally an audio signal, usually already the result of extensive internal data processing, from which an experienced operator can make some qualitative statement on the target and its position. When using manual methods as the *primary procedure*, **each** alarm is carefully checked until it has been fully understood and/or its source removed.

These detectors have indeed become more and more refined and sensitive over the years, and it has been often said that they have reached their limits. In fact there are a number of other technical fields in which metal detectors are used with profit to deliver additional information on the object under study, albeit often for specific cases only.

Imaging Metal Detectors: Input from Civil Engineering Applications

One of the fields mentioned above is civil engineering, in which we identified and tested a commercial "imaging metal detector" [2], trying to assess its potentialities and understand if such systems could be useful to "provide the deminer with a visual image of shape and size of the metal signature" [1] (being well aware that spatial resolution and depth penetration constitute conflicting requirements). Results could be a priori expected for "larger" metallic

objects of regular size, such as UXO (Unexploded Ordnance), and to be useful in regions where only a few type of mines exist and one has to differentiate them from metallic debris.

Civil Engineering Applications

Cylindrical reinforcing bars in concrete are widely employed in civil engineering and are mostly made of steel. They can be detected and characterised using metal detectors, whose head sizes are normally much smaller than the ones employed in humanitarian demining. They are therefore more accurate at shallow depths (increased spatial resolution) and able to resolve closely spaced objects, but lack in depth of penetration given that the detection range is strongly related to the coil dimensions.

The Ferroscan System

The Ferroscan system (Fig. 4) is targeted at the visualisation of steel rebars in concrete; it uses a multi-sensor and differential detector, basically measuring (an approximation of) the horizontal gradient, along the scanning direction, of the vertical component of the induced magnetic field. The differentiated signal curves can then be used to produce a composite bidimensional grey scale image [3]. The data processing is tuned to ferromagnetic objects.

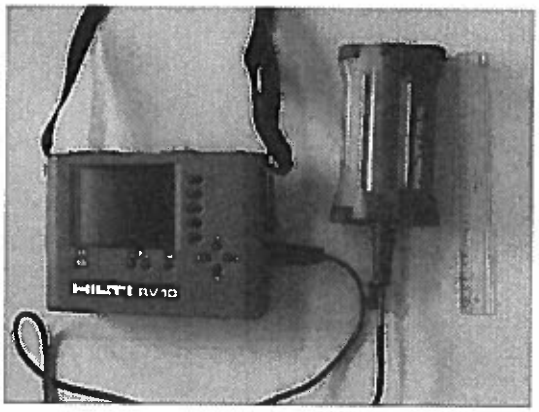

Fig. 4: Ferroscan RV 10 monitor (left) and RS 10 scanner (right) (ruler length: 30 cm)

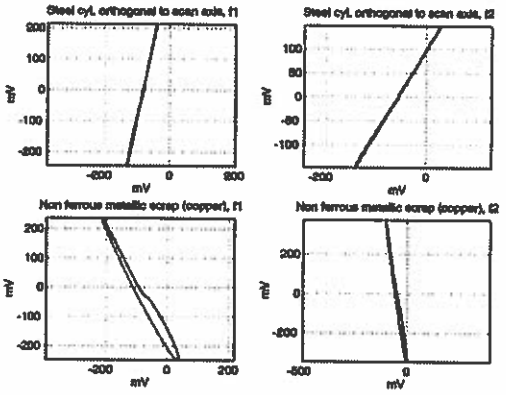

Fig. 5: Example of Metal Detector response at 5 increasing depths (general trend, differential sensor, line scan over the object)

Tests in the "Sandbox" and Discussion

A number of objects were tested in a "sandbox" at different depths, in particular (Fig. 6):

- *PMN* "like" AP mine: a "classical" AP mine, diameter 11 cm, height 5 cm, with cover retaining ring (ferromagnetic!) placed at about 1.5 cm from the top. The cover retaining ring is clearly visible (Fig. 6 left half), with the darker spot probably corresponding to the area around the pin used to secure the ring.
- *BLU 26 "bomblet"*, round (65 mm diameter), 430 grams. Large quantities of similar UXO are still found in Laos for example. Its mixed nature is probably at the origin of some of the complex image details displayed (Fig. 6 right half).

Images of the objects are shown up to a depth which gives roughly, *with the current hardware and data processing*, reasonable images, but which has not to be taken as a precise indication of the actual sensor performances. In general an object's image gets larger with increasing depth, as expected (see also Fig. 5).

Preliminary Conclusions

We can summarise our findings as follows:

- Ferroscan images are indeed a precious aid in localising and interpreting the underlying metallic structure, without pretending to deliver a true representation of it. This task has been solved by employing multi-sensor hardware and simple and elegant data processing software. Imaging in civil engineering is "eased" by the fact that the nature of the problem is rather well defined a priori.
- The multi-sensor arrangement is practical to rapidly scan a large area, and its resolution looks indeed sufficient for large or extended objects such as AP mines with relevant metal content and UXO. On the other hand using more than one sensor, and the differential arrangement itself, have some side effects on the visualisation of smaller isolated (ferromagnetic) objects, for which the system was indeed not intended, and in presence of edges. In these cases a single sensor might be scanned in more detail over the object, possibly providing a more accurate image. In any way, the increased spatial resolution comes as expected at the price of decreased depth penetration.

The images obtained confirm that this approach is potentially interesting, especially if one has to look for (larger) ferromagnetic objects. Detailed imaging of smaller objects is and remains a very challenging task.

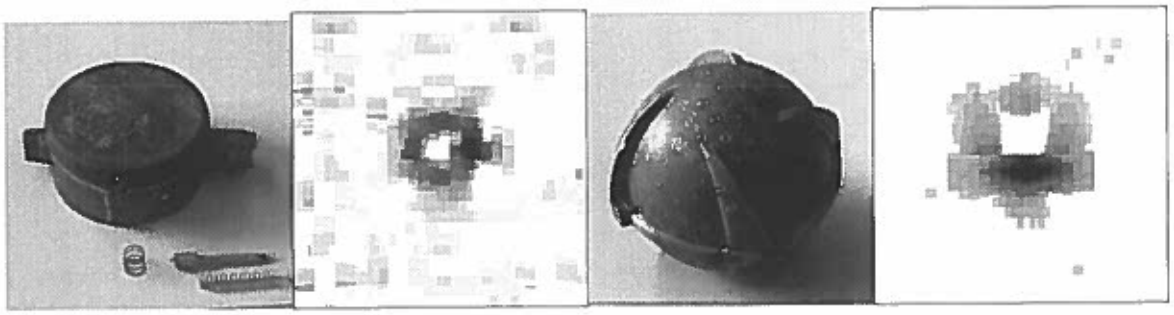

Fig. 6: PMN AP Mine, image at a depth of 1.6cm; BLU 26 "bomblet", image at a depth of 5cm (both: 60x60cm)

Imaging Metal Detectors: Deconvolution Approach

Another way of obtaining an "image" is to scan a single sensor over a surface to then try to deconvolve the detector's intrinsic response from the acquired data. A knowledge of the detector's response to a point-like object (Point Spread Function, or PSF) is mandatory in such a strategy, and can be obtained either theoretically by modelling the detector's response, or experimentally via direct measurements on small objects for example. We note in passing that the PSF will certainly be a function of the object's depth (see Fig. 5). Whether this approach will be practically applicable in the field, from the point of view of the resulting resolution, scanning speed and cost for example, remains to be demonstrated.

Other Advanced Developments:

Object Characterisation:

As we have seen in the introduction to metal detectors, their internal signals do depend on the nature of the object under study, its depth and size. It is therefore very tempting to try to harness at least part of this information. *Fig. 7* shows an example, for a two-frequency continuos wave instrument, of how information on the target's nature can be contained in the

amplitude and phase of the received signal. Multifrequency systems might lead to some kind of "induction spectroscopy", and similar arguments are valid for pulse instruments.

In an ideal case one might provide object classification (mine or debris) or identification (mine type), possibly starting from a database of templates. Even without going that far it might still be possible to extract valuable additional information for the deminer, for example small object *vs.* large object. Problems with this approach are again represented by weak target signals and irregular background signals, nearby objects distorting the response, and obviously by the presence of unforeseen or unaccounted objects. The response signal does also depend on a large number of parameters such as the object's orientation, the exact metal type, etc.

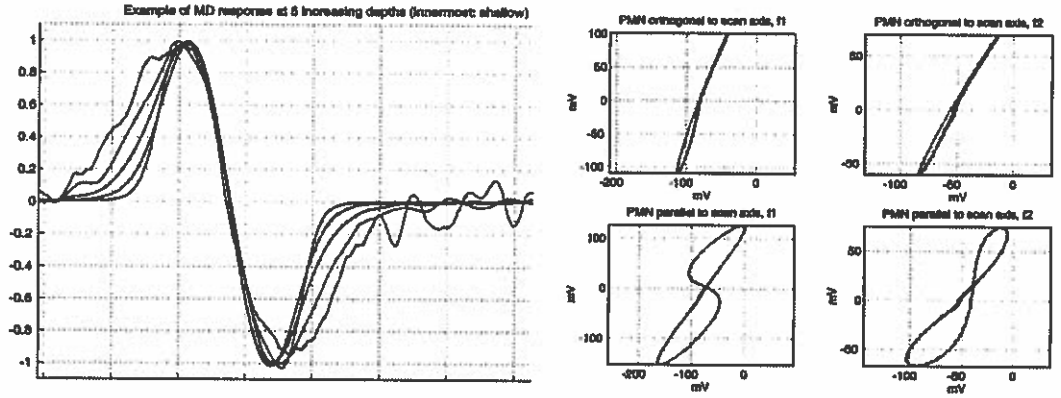

Fig. 7: Example of amplitude and phase dependencies when passing with a Continuos Wave detector, using two frequencies f1 and f2, over a PMN mine and two other objects.

Information on an object's depth should also be among the most easily recoverable object parameters. It could be delivered for example either by scanning the detector across the object and analysing the width of the response (or other parameters; see again Fig. 5), or by taking at least two measurements under different conditions, for example employing two overlapping coils. Some of these techniques are in use for Non Destructive Testing applications, but the need of having to be careful here can not be stressed sufficiently.

This last point is even more true when it comes to giving an estimate of the object's size, which would undoubtedly be an interesting piece of information. One way of doing it consists in measuring the magnetic field over an area in order to try to calculate an object's magnetic dipole moment (typically using a simple, dipolar model), which gives an indication of its "magnetic" volume. Again, applicability in the field and sources of errors have to be very carefully studied.

Sensors other than Standard Coils (Hardware Improvements):

It has been suggested to study sensors other than the ordinary coils currently used in metal detectors, for example giant magnetoresistive elements, or miniature fluxgate elements. They are expected to be broadband and provide better spatial accuracy; the construction of linear or bidimensional arrays should also be possible, delivering some kind of localised "image" of the soil metallic/magnetic contents. On the other hand their overall sensitivity is likely to be smaller, which might very well discourage their use for certain applications (their use might for example be envisaged for the detection of UXO or mines with a relevant metal content, but not for minimum metal mines).

Another direction of research could consist in the study of "improved" magnetic field shapes, for example more compact than what obtained with ordinary circular or rectangular coils, or featuring some other special structure (e.g. spatially periodic).

References:

[1] K. Eblagh, "Practical Problems in Demining and Their Solutions", *Proceedings of the EUREL Int. Conference on The Detection of Abandoned Landmines*, Edinburgh, UK, pp. 1-5, 7-9 Oct. 1996.

[2] C. Bruschini, "*Evaluation of a Commercial Visualizing Metal Detector for UXO/Mine Detection: the HILTI Ferroscan System*", in Sustainable Humanitarian Demining: Trends, Techniques and Technologies, Mid Valley Press, Verona, VA, USA, pp. 314-325, Dec. 1998 (hdic@jmu.edu).

[3] K. Kousek, et al., "Apparatus for Determining Location of an Element of Magnetizable Material in a Construction Structure", US Patent # 5,296,807, 22 Mar. 1994.

An overview of RF sensors for mine detection: Part 1 Radiometry

David J Daniels
ERA Technology Ltd, Cleeve Road, Leatherhead, Surrey, KT22 7SA, UK
Tel 00 44 1 372 367 081 Fax 00 44 1 372 367 081
e-mail david.daniels@era.co.uk

Key words: Mine detection, Radiometry

1. Introduction

This paper is part 1 in a series that provides an overview of radio frequency (RF) techniques for the detection of buried plastic and metal mines. The three basic techniques that are considered in the series of papers are radiometry, quadrupole resonance and active radar, Radiometry is suitable for the detection of surface laid mines or very shallowly buried mines in dry conditions.

2. The problem

Landmines are weapons, which are used, in the military role to frustrate and slow down the manoeuvrability of enemy forces. There are internationally agreed procedures for lying down and recording the position of minefields and individual mines. The problem of mines is associated with operations in regions where agreed military procedures are ignored. There is a clear distinction between the scope and quality of humanitarian demining or post conflict clearance operations and military mine clearance. For the mine problem, new technical solutions are sought and RF techniques are among the leading contenders from among a number of possible methods of detecting minimum metal / plastic mines. The fundamental problem is that mines can be found in such a wide variety of conditions that it is unlikely that one single technique can be used to provide an adequate performance.

3. Research and Development

Considerable efforts are being made on a world-wide basis to develop a solution to the problem of mine detection both for military and humanitarian applications. National Military Organisations, Universities, Industrial Research and Technology Organisations as well as private companies are conducting these programmes. Among the leading contacts for the dissemination of information in the United States is; the US Department of Defence [1], DARPA, Minawara, James Madison University [2], etc. Information can also be obtained from the United Nations particularly concerning field operations and statements of operational requirements. In Europe the European Commission Joint Research Centre (JRC) is implementing a network of excellence (ARIS) which acts as a focal point for interchange between active research members. This group also has links to the Nordic NRDF. Many European research and development programmes for humanitarian demining are co-ordinated and supported by both the European Commission and by various European Industrial partners via Esprit and other projects. Information on European Commission support for R and D on demining can be found on a CD produced by the JRC. The proceedings of the JRC De-mining Technologies Conference [3] held in Sept/Oct 1998 provides useful references to the R and D activities of the majority of the international participants. EUREL, via the IEE [4 5] in the UK, has organised several conferences each held in Edinburgh on the subject of research and development. Information on research publications can be found from organisations such as; SPIE, IEEE, IEE, and are included in their proceedings, transactions and conference publications.

4. Mines

Most of the mines encountered in infested countries are metallic mines, but some proportion of plastic or minimum metallic mines can be found in a variety of countries and terrains. Conventional mine detectors detect the metal content of a mine, hence the plastic mine or minimum metal mine remains largely undetectable by current technology particularly in areas where battlefield debris and shrapnel

causes a high false alarm for the metal detector.
Mines can be buried or surface laid and are emplaced by a variety of techniques including being scattered on the surface by vehicles or helicopters. Thus mines may be found in regular patterns, or in irregular distributions. Where environmental conditions result in soil erosion and movement caused by rain over several seasons the mines may be lifted and moved to new locations and can be covered or exposed. Mines are encountered in desert regions (i.e. Somalia, Kuwait), mountains (i.e. Afghanistan, El Salvador), jungles (i.e. Cambodia, Vietnam) as well as urban areas (i.e. Beirut, Former Yugoslavia). The variety of mines that can be encountered is considerable and details can be found on the US Department of Defense CD Minefacts © which contains details of over 675 landmines as well as the US Department of Defense, Naval Explosive Ordnance, CD Ordata © which is a guide to UXO identification.
In general most pressure sensitive mines are not designed to operate when buried deeply. The overburden ground material acts as a mechanical bridge and inhibits triggering of the detonator mechanism and also reduces the force of the explosion. This fact is often taken into account in the specification of performance for a mine detector. For example a hand held mine detector should be able to detect AT mines at depths up to 300mm and AP mines at depths up to 100mm with spacing between the detector head and ground surface of 100mm. Vehicle based mine close-in mine detectors generally require a greater ground clearance. However mines can be encountered at depth well beyond the range of most detection systems. Mine detection systems can be employed in several different roles: for close-in hand-held detection, for vehicle mounted stand-off detection or as a remote sensor mounted on low flying fixed or rotary wing aircraft. These are mostly synthetic aperture radars (SAR).

5. Environmental conditions

The variety of environmental conditions in which mines can be found is enormous. Minefields are not only neat ordered rows of mines in flat deserts but can also be found among the debris of burnt out buildings and post-conflict urban and rural environments. An example of a mine-infested situation is shown in Figure 1. Clearly, mine detection equipment has to be designed to work in a wide range of physical environments and the statement of

Figure 1 Photograph of mine infested area in Croatia

operational requirements issued by end-users will reflect this need. Detection equipment must be able to be operated in climatic conditions, which range from arid desert, hillside scree to overgrown jungle. Ambient operating temperatures can range from below $-20\ ^{0}$C to $60\ ^{0}$C. Rain, dust, humidity and solar insolation all must be considered in the design and operation of equipment. The transport conditions of equipment can be arduous and these as well as man-machine interface issues are vitally important to the design of detectors.

6. Introduction to electromagnetic techniques

There are many introductory and advanced texts, which describe the various factors that need to be considered regarding the propagation and reflection of electromagnetic waves in earth materials. The general principles of the propagation of ground probing radar signals are described by Daniels [6], while the principles of the detection of visually obscured targets is described by Baum[7]. A full description of electromagnetic probing in geophysics is given by Wait[8], who also discusses propagation in stratified media Wait[9]. It is not the objective of this paper to repeat material already well covered and the reader is also referred to Olhoeft[10] who provides a useful introduction to the physics of propagation in soils.

6.1 Geological conditions

The determination of the dielectric properties of earth materials remains largely experimental. Rocks, soils and concrete are complex materials composed of many different minerals in widely varying proportions and their dielectric parameters may differ greatly even within materials which are nominally similar. Most earth materials contain moisture, usually with some measure of salinity. Since the relative permittivity of water is in the order of 80 even small amounts of moisture cause a significant increase of the relative permittivity of the material. A large number of workers have investigated the relationships between the physical, chemical and mechanical properties of materials and their electrical and in particular microwave properties. In general they have sought to develop suitable models to link the properties of the material to its electromagnetic parameters. Such models provide a basis for understanding the behaviour of electromagnetic waves within these media. Information on the geological properties of earth soils can be found in the Digital Soil Map of the World and Derived Soil Properties CD © published by the Food and Agriculture Organisation of the United Nations. This enables the ten map sheets of the world to be classified in terms of parameters such as pH, organic carbon content, C/N ratio, clay mineralogy, soil depth, soil moisture capacity and soil drainage class. Such information is useful in assessing the potential of RF techniques for particular geographic regions and an example is shown in fig.2:

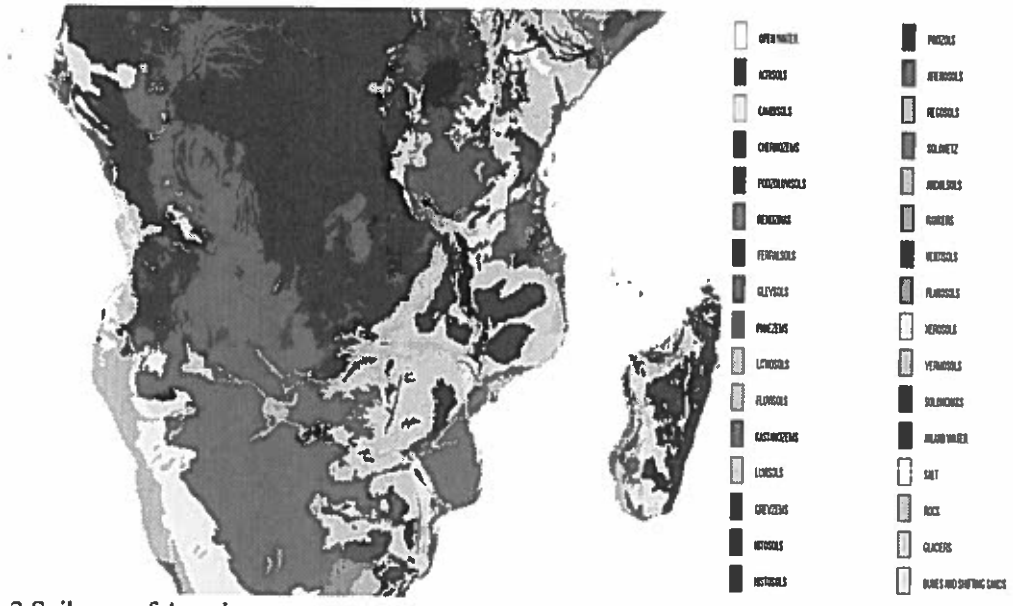

Fig.2 Soil map of Angola

7. Passive radio frequency techniques

7.1 Introduction

The remote detection of surface laid metallic and non-metallic mines by optical or infrared methods is feasible provided there is no obscuration by local vegetation and there is an adequate contrast ratio. In the situation where vegetation obscures the mine, one method of detecting the mine is by means of a passive microwave radiometer. The principle of passive microwave radiometry is based on a

receiving antenna that intercepts the microwave radiation emitted by the scene, providing an output that is proportional to the integrated power gathered by the antenna beam pattern. The output from terminals of the antenna is processed by means of a receiver and the radiometer effectively functions as a power meter. The following description is based largely on a paper by Daniels[11] first published by the IEE

7.2 Principles

A radiometer is an instrument that measures the power incident on an antenna. The antenna beam of a microwave radiometer is normally scanned over the scene of interest. In order to detect a target there must be a difference in microwave temperature between the target and its background that is within the resolving capability of the radiometer. In the case of a surface laid mine, the soil and vegetation acts as the background. The microwave temperature of the soil varies with the annual cycle and the diurnal cycle and, amongst other things, depends on the level of incoming solar radiation (insolation), soil composition, soil water content and microwave frequency. The soil temperature can be classified in terms of the Annual Equilibrium Temperature (AET) which is defined as that temperature where the sum of the incoming insolation and sky radiation and the outgoing emission from the surface are in balance. Typically in the 10-20 GHz region the predicted soil surface temperature for soil with a dielectric constant (real part = 4, imaginary part = -1.5) and with a water content of 17%, varies between 255 to 310 Kelvin. The surface laid mine is predominantly illuminated by the emission from the sky, through the atmosphere, and over the frequency range 1-10 GHz the microwave temperature of the sky is in the order of 6K. The mine is considered to act as a specular reflector and effectively mirrors the general sky background. Only at a particular combination of angles, in relation to the sun, will the radiometer see the sun as a hot reflector and over the majority of viewing angles the mine will reflect the cold sky. Evidently incoming insolation and emission from the soil will serve to raise the microwave temperature of the mine. The difference between the brightness of the sun at 10 GHz and infrared frequencies is nearly a factor of 10 to the power 8. Thus the mine could have a physical temperature well in excess of its microwave temperature which would be due to the reflection from a cold sky.

The brightness of the mine will be dependent on the properties of the material from which the mine is constructed, such as its reflectivity, absorptivity and emissivity, as well as the aspect angle from which the mine is viewed. In the microwave region the brightness (in Wm-1 Hz-1 sr-1) of a material is given by the thickness of the dielectric and its microwave emissivity will affect the measured temperature. If the mine can be regarded as a dielectric slab then its emissivity is a complex function, but for a lossless dielectric it can be shown that the emissivity tends to zero. Figure shows the ratio of reflectivity to emissivity as a function of angle and thickness for a low loss dielectric slab. Note that the nadir angle and a thin section provides the highest ratio and hence the optimum viewing position.

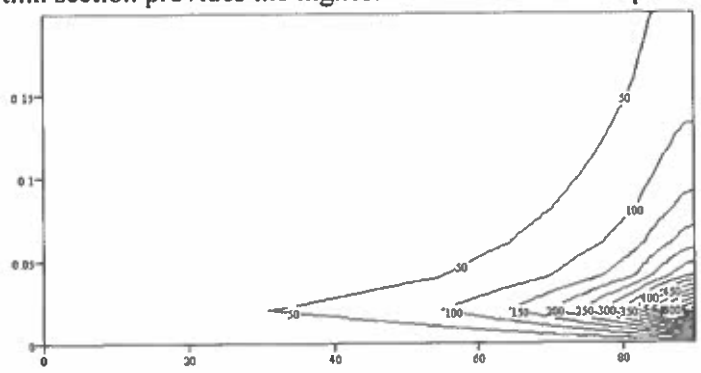

Figure 3 Graph of the ratio of reflectivity to emissivity for viewing angle in degrees (*horizontal axis*) versus thickness in metres (*vertical axis)* for a thin dielectric sheet (e_r=2)

For loamy soils with a 5% moisture content the soil emissivity is approximately equal to 0.9 at an angle of incidence of 30°. A metal mine could intuitively be regarded as equivalent to a specular reflector with very low emissivity. There is, therefore, a worst case microwave temperature difference

of approximately 250K between the mine and the soil in winter conditions, while in summer conditions the difference will increase. Although there is a large difference in temperature between the mine and the soil, several factors will tend to reduce the apparent difference measured by the radiometer. The effect of the vegetation cover will be to mask the temperature of the terrain and will be noticeable at higher microwave frequencies. Although frequencies in the order of 2-3 GHz or less are needed to minimise the effect experimental work was carried out in the range of 11-12 GHz where components were readily available. The received energy will be the convolution of the area of ground intercepted by the antenna beam pattern and the effective area of the mine that is radiating as a cold spot. Evidently a warm ground and a cold mine will combine to give a lower temperature than an equivalent area of warm ground. The impact of mine size in relation to antenna footprint can be seen in Figure 4This shows the predicted temperature difference, in 0.5K increments, between an area of ground containing the mine to an area of ground at ambient temperature. The contours are plotted as a function of mine diameter in metres (x-axis) and the temperature of the mine in Kelvin (y-axis). The ambient temperature of the ground is taken as 256K and the antenna footprint is assumed to be a circle of diameter 1-m.

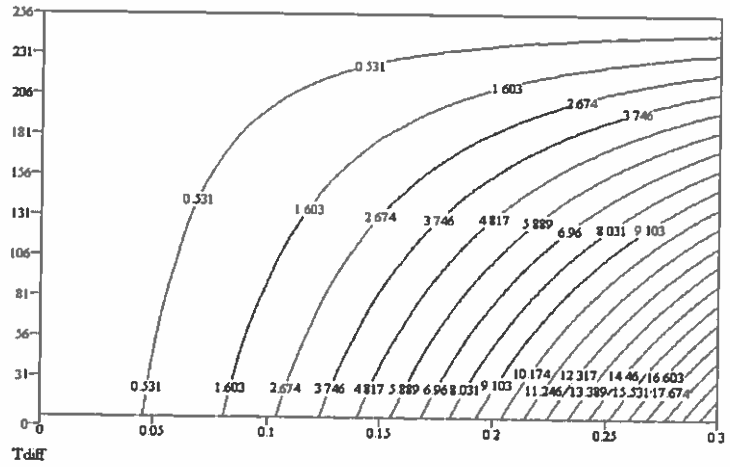

Figure 4 Graph of the temperature difference in 0.5K increments plotted as a function of mine diameter in metres (*x-axis*) and the temperature of the mine in Kelvin (*y-axis*)

As can be seen from the graph, when the mine is large, i.e. 0.3 m diameter with a surface temperature of 6K, the temperature difference measured by the radiometer would be 22K (see bottom right hand corner of graph), even though the surface microwave temperature difference between the ground and the mine is 250K. Conversely, when the mine has a small diameter and is warmer than the normal reflected sky background of 6K, then its predicted measured temperature difference can fall below 0.5K (contour line on the left-hand side). On the basis of this simplified model, if a radiometer with a temperature resolution of better than 0.5K can be used, then the surface laid mine should be detectable.

7.3 Radiometer system

A low cost radiometer was designed and built and consisted of two receiver channels formed by two single output LNB receivers operating over the 10.7 GHz to 11.8 GHz band as shown in Figure 5. .The typical noise figure of each is 0.8 dB; the output IF frequency lies within the 950 MHz to 2050 MHz band and the gain of each is in the order of 50 dB. Each can be switched between vertical and horizontal polarisation. The two receiver channels and antennas are arranged to view a different footprint on the ground. The design uses standard satellite receiver technology, which has the great advantage of both keeping the cost of materials low and reducing the amount of development effort.

Figure 5 Photograph of prototype handheld radiometer

Both LNBs were substantially similar in terms of temperature, noise figure and gain, as well as temperature gradients of noise figure and gain. Mounting the two units in a similar environment ensures that changes in outside ambient effects affect each equally. The output from each LNB is a signal in the 950 - 2050 MHz range and is fed to a difference amplifier to provide an output which is proportional to the difference power measured by the two LNB's. This enables common mode signals to be rejected while allowing difference mode signals to be measured. A detector circuit provides a DC output, which is fed to a centre zero meter. As the system is scanned over the ground, any microwave temperature differences between the different footprints will be measured. The footprint of each antenna on the ground will define the sensitivity. In wet conditions in the UK, vegetation caused two problems; obscuration of targets and false alarms from dense patches of vegetation. Further work is underway to resolve this issues. However in dry, desert-like conditions the concept design showed considerable promise for the detection of surface laid or very near surface mines.

8. Reference

[1] Humanitarian Demining Operations Equipment Planning Guide, US Dept of Defense, August 1997, also reference 1

[2] Sustainable Humanitarian Demining : Trends Techniques and Technologies Zagreb, Croatia, Sept 30th Oct 2nd 1997, pub. by Humanitarian Demining Information Center at James Madison University

[3] Proceedings of the European Commission JRC De-mining Technologies Conference Ispra, Italy, Sept/Oct 1998

[4] EUREL International Conference Detection of Abandoned Landmines Edinburgh, UK, 7th- 9th October 1996, IEE Conference Publication 431

[5] EUREL 2nd International Conference Detection of Abandoned Landmines Edinburgh, UK, 12th-14th October 1998, IEE Conference Publication 458

[6] D J Daniels Surface Penetrating Radar 1996 IEE Radar Sonar Navigation and Avionics Series Volume 6 ISBN 0 85296 862 0

[7] Carl Baum Ed. The detection and identification of visually obscured targets 1998 pub Taylor and Francis ISBN 1-56032-533-X

[8] James R Wait. Electromagnetic probing in Geophysics, 1971, pub Golem Press, ISBN 0911762-09-4

[9] James R Wait. Electromagnetic waves in stratified media, 1962, pub Pergammon Press

[10] Gary R Olhoeft, Electrical, Magnetic and Geometric properties that determine ground penetrating radar performance. Proceedings of the Seventh International Conference on Ground Penetrating Radar Kansas USA May 27-30 1998

[11] Daniels D. J., A low cost, hand-held, microwave radiometer for surface laid mines.EUREL/IEE International Conference – The Detection of Abandoned Landmines, Edinburgh, Scotland, UK, 12-14 October 1998

An overview of RF sensors for mine detection: Part 2 quadrupole resonance

David J Daniels
ERA Technology Ltd, Cleeve Road,
Leatherhead, Surrey, KT22 7SA, UK
Tel 00 44 1 372 367 081 Fax 00 44 1 372 367 081
e-mail david.daniels@era.co.uk

Key words: Mine detection, Nuclear quadrupole resonance

ABSTRACT

This paper is part 2 in a series that provides an overview of radio frequency (RF) techniques for the detection of buried plastic and metal mines. The technique that is considered in this paper is quadrupole resonance. The solid explosive contained within the mine can be detected by quadrupole resonance techniques.

1. Quadrupole resonance

Nuclear quadrupole resonance (NQR) is a radio frequency technique that is used for characterising the structural chemistry of nitrogen based compounds Rowe and Smith[1], Hibbs et al[2] and Engelbeen[3]. The NQR technique identifies the radio frequency (RF) spectral characteristics of a particular explosive when the nuclei of the explosive are caused to resonate following exposure to a transient RF magnetic field. The data output from an NQR system takes the form of a repetitive series of transient signals of a known centre frequency or range of frequencies whose short time amplitude time envelope decays exponentially as shown in Figure 1. This is known as free induction decay (FID) and is a type of short time, sample waveform. In general, this is a repetitive function, which is intrinsically formed by virtue of the physical process rather than being classified as a truncated function.

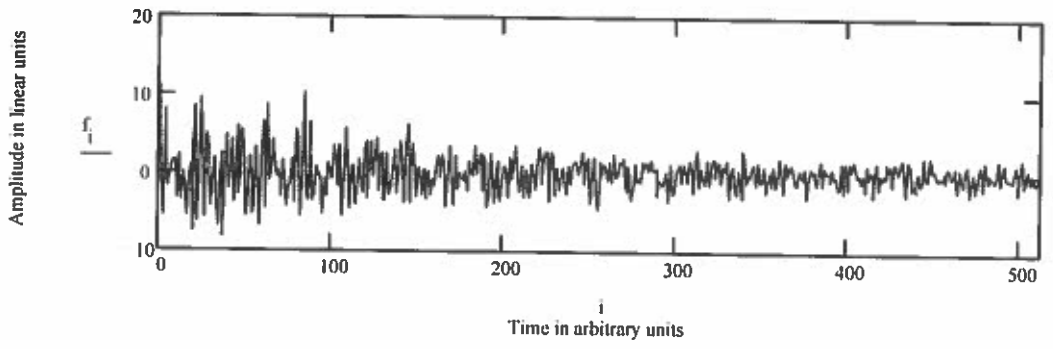

Figure 1 Simulation of the time domain response of an NQR signal, with a 10dB signal to noise ratio, from an hypothetical explosive

The application of a pulse of RF energy to a sample causes transitions between energy levels of the nuclei of the compound or alternatively it causes the nuclei to precess about the axis of the electric field gradient at the quadrupole precession frequency. The magnitude of the precession is dependant on the product of the nuclear electric quadrupole moment Q and the electric field gradient q. When the energy related to the pulse is no longer present, the nuclei precess to the original rest state and in doing so radiate a weak RF signal. The re-radiated field from the sample is in the order of femtoTeslas for sample of some tens of grammes of explosive. Thus the receiver of the detector must exhibit high sensitivity. The pulse radiated by the transmit coil are usually a sequence of phase coherent, high power RF pulses at centre frequencies dictated by the sample. In the case of TNT within the general range 500 to 1500kHZ, RDX, 0.4MHZ to 6MHz and PETN 400kHz to 1MHz. The pulse lengths, intervals and coherency all influence to magnitude and frequency of the re-radiated signal.

The time domain signature of the NQR response may be free induction decay or a series of echoes in which a time reversed image of the FID response precedes the normal one-sided FID response once the series is established. In essence the signal-processing requirement is that of a time series analysis with particular reference to the characteristics of the time series as shown in fig.2. The principal characteristics of the NQR signals which can be classified as a non-stationary time series are; an exponential decay, the presence of multiple frequencies, a short time response, an echo series, either causal or non-causal, and most importantly, a low signal to noise ratio.

Normally considerable averaging is applied to recover the weak signal from the noise and this is achieved by repetitively subjecting the sample to a series of phase coded, transmitted pulses. Generally it is considered that Fourier methods are most appropriate to the analysis of statistically stationary functions whereas non-stationary functions may be better analysed by alternative methods.

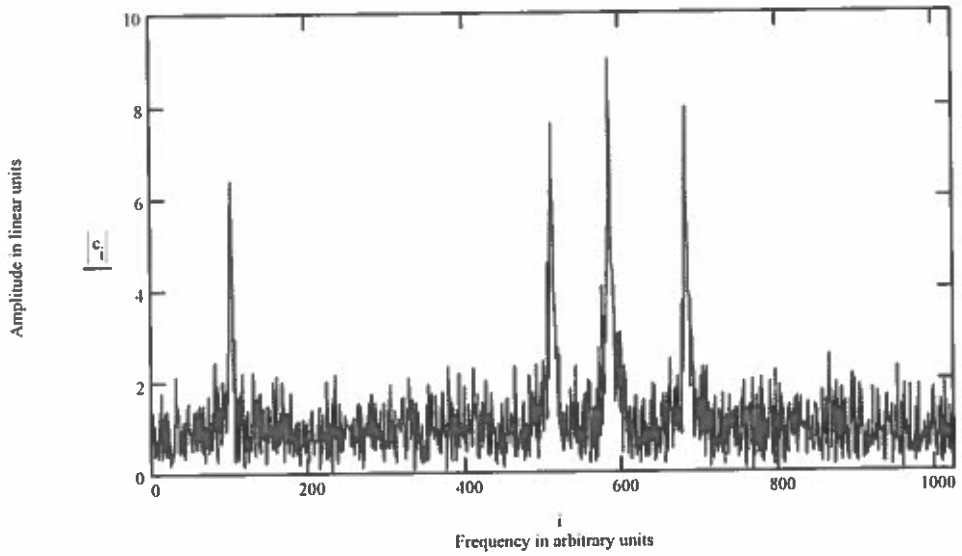

Figure 2 The frequency domain response, obtained by an FFT, of an NQR signal, with a 10dB signal to noise ratio, from an hypothetical explosive

The limitations of the Fourier method of spectral estimation are that it has a frequency resolution that is approximately equal to the reciprocal of the sample time window in seconds. The action of sampling the data for a defined time causes leakage of energy from the main lobe of a spectral response into the sidelobes. Alternative methods, such as the Prony algorithm, model functions as decaying exponentials, hence may at first consideration appear ideal. However it is well known that early Prony algorithms are very vulnerable to noise and have met with mixed fortunes, hence more modern adaptations such as the eigenvalue realisation of Prony may give better results. Wavelet transforms such as the Wigner or STFT may be better adapted to the transient nature of the NQR response but again noise may prove a limiting factor. In the case of the multiple spectral lines generated by TNT some form of template correlation may prove useful in improving the signal to noise and classification performance. In the case of the recovery of the principal from a series of echoes, methods such as homomorphic deconvolution are indicated. Techniques such as cepstrum analysis are well known and can be considered.

As can be appreciated the effect of interference from radio stations is potentially significant while the interaction of the transmit and receive coils requires careful and meticulous design. It could be postulated that interference from statistically stationary signals such as radio transmitters would appear in the sampled data and will "breakthrough" in terms of adjacent spectral lines as shown in Figure 3. It may be that the algorithms that provide the highest spectral resolution will be the best in the situations where multiple spectral lines caused by the particular explosive occur and are contaminated with interference.

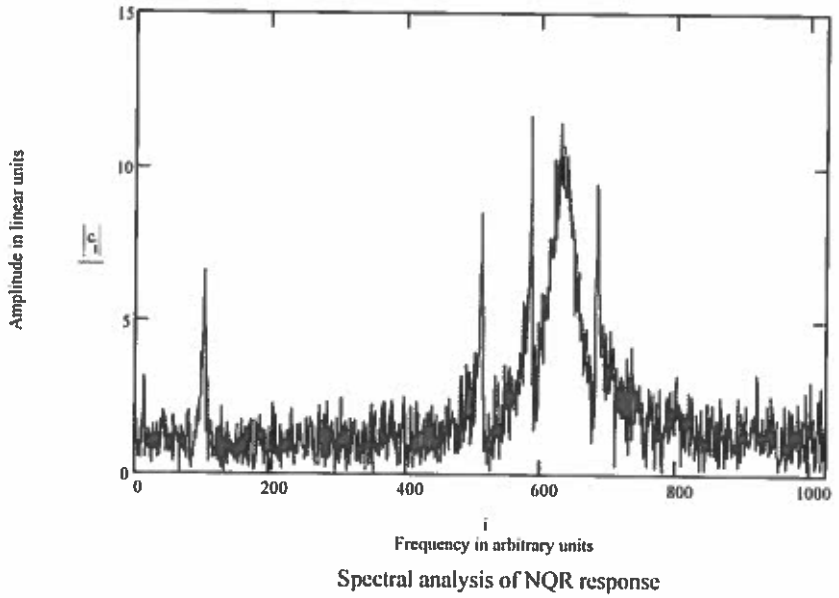

Figure 3 The frequency domain response of an NQR signal with a 10dB signal to noise ratio from an hypothetical explosive together with a source of RF interference

2. Summary

Advances in the performance and design of NQR RF sensors have been significant over the last few years. If the current rate of progress is maintained, NQR technology may help to make a significant contribution to meeting the challenge of mine detection. However there is a need to ensure that scarce scientific resources are applied in the most effective manner. However, such technology needs industrial development if it is to reach the minefield. Issues such as the size of the market, the means of procurement, continued development and logistic support will be just as important as the technology. Unless these aspects are addressed the technical solution will never leave the laboratory. Research programmes should involve industrial development and field assessment at an early stage if they are to stand any chance of real use and benefit to the deminer.

3. Acknowledgements

I would like to thank the Directors of ERA Technology for their support of this work.

4. References

1 Rowe M.D. and Smith J.A.S. Mine detection by nuclear quadrupole resonance, EUREL International Conference Detection of Abandoned Landmines Edinburgh, UK, 7th- 9th October 1996, IEE Conference Publication 431 p62

2 Hibbs A.D., et al Landmine detection by nuclear quadrupole resonance, In press 1998, pp 11

3 Engelbeen A., Nuclear quadrupole resonance mine detection, Revue H,F part 3 pp 35-43 1998

An overview of RF sensors for mine detection: Part 3 Radar

David J Daniels
ERA Technology Ltd, Cleeve Road, Leatherhead, Surrey, KT22 7SA, UK
Tel 00 44 1 372 367 081 Fax 00 44 1 372 367 081
e-mail david.daniels@era.co.uk

Key words: Mine detection, Ultra-Wideband Radar, Ground probing Radar

1. Introduction

This paper is the third in a series of papers that provides an overview of radio frequency (RF) techniques for the detection of buried plastic and metal mines. Radar is the most advanced and prototype mine detection systems are currently being evaluated. Current demonstrator radar systems may be able to detect buried AT mines, but the detection of AP mines will require further development of antennas, clutter rejection algorithms and target detection methods.

2. Radar

2.1 Introduction

There are many introductory and advanced texts, which describe the various factors that need to be considered regarding the propagation and reflection of electromagnetic waves in earth materials. The general principles of the propagation of ground probing radar signals are described by Daniels [1], while the principles of the detection of visually obscured targets is described by Baum[2]. A full description of electromagnetic probing in geophysics is given by Wait[3], who also discusses propagation in stratified media Wait[4]. It is not the objective of this paper to repeat material already well covered and the reader is also referred to Olhoeft[5] who provides a useful introduction to the physics of propagation in soils.

Ultra-wideband, ground penetrating radar radiates a short pulse or frequency modulated burst of electromagnetic energy into the ground and detects the backscattered energy from the buried target. The radiated pulse is typically a wavelet of several nanoseconds duration and in the frequency domain, covers a wide range of frequencies. Typically the spectral characteristics of the pulse consist of a series of individual frequencies whose spacing is related to the pulse repetition interval and whose envelope is related to the temporal characteristics of the wavelet. The power radiated per spectral line is in the order of a few nanowatts. For close-in systems the radar antenna beam is moved in a known pattern over the surface of the ground and an image of the ground can be generated, in real time, on a display either in gray scale or in colour. The image can be a cross-section or a plan view. The radar image is not identical to an optical image because the wavelengths of the illuminating radiation are similar in dimension to the target. This results in a much lower definition in the radar image and one that is highly dependent on the propagation characteristics of the ground. In addition the beam pattern of the antenna is widely spread and this degrades the spatial resolution of the image, unless corrected. For longer-range systems where the objective is to detect surface laid or very shallowly buried mines, synthetic aperture techniques are used. The topic of general radar system design is covered in many texts and useful information will be found in the following Cook[6], Skolnik[7], Nathanson[8], Wehner[9], Galati[10] and Astanin[11]. Mine detection is covered by Scheers[12], Earp[13], Steinway[14], Carin[15], Duvoisin[16], Bourgeois[17], Earp[18], Vitebskiy[19] as well as Daniels[20 21 22 23 24]

2.2 Waveform design

In general the power incident on the mine should be restricted because of the possibility that high levels could trigger detonation of future generation smart electronic mines. The key parameter for most radar systems is the mean power. For portable, close-in radars the capacity of the power sources limits the radiated power. Most radar systems for the close-in application will radiate a mean power in

the range 10mW to 100mW. The power incident on the mine will in general be lower than this due to spreading losses and propagation path losses. The UWB SAR radars will produce much high peak voltages levels but the power incident on the mine should be limited.

The factors relevant to radar system design and hence transmitted waveform are discussed by Daniels[25] and Noon[26]. The choice of system design, and hence modulation technique, is to a large extent governed by the need to work in field conditions where both the ground attenuation and clutter levels can be expected to be high. Under these conditions the depth range of the radar system is likely to be primarily defined by the soil attenuation and clutter, once a particular range of frequencies has been chosen. It can be shown that considerable variations (10-30 dB) in the sensitivity of competing system designs actually translate to comparatively small changes in depth performance. The selection of a suitable waveform for transmission, at least in terms of resolution, can be considered a function of the duration of the complex envelope of the measured signal. The output from most ultra-wideband radar systems can be compared in terms of a time domain representation of the waveform. Almost all types of radar can be assessed not just by their signal to noise and signal to clutter ratios but also by comparing their inherent range resolution. Such a procedure reveals the characteristics that define the radar performance. An assessment of such signals is described by Daniels[27] and can be summarised as follows.

Generic radar systems using a direct detection receiver and a matched filter receiver are compared. Normally the resolution of a radar system is defined by considering the case of identical targets and in the case of Gaussian pulses, resolution can be achieved at pulse separations between 1.25 and 1.5 of the pulse width. This is not likely to prove satisfactory in the case of a target of low radar cross section in close proximity to a target of high radar cross section i.e. an AP mines next to an AT mine. The envelopes of the time domain and frequency domain receivers were compared. It is shown that although the main lobe bandwidths of both signals are nearly identical, the time duration of the envelope of the detected frequency domain signal is twice that of the envelope of the Ricker wavelet. Hence a radar design using a time domain, direct receiver, has a considerably better resolution at the 10% resolution criteria level, than frequency domain radar. This is primarily because the receiver of the frequency domain radar, cross-correlates the received signal. In essence improved resolution has been achieved in the time domain system at the expense of signal to noise ratio, but this may not be so relevant to attenuation limited operation.

2.3 Time domain radar

Most commercially available ground probing radar systems use short pulses or impulses. The high-speed sequential sampling approach used to acquire RF waveforms produces a low S/N ratio because the spectrum of the sampling pulse is a poor match for that of the received pulse. In general, the dynamic range of the sampling receiver is typically 60 dB, without time varying gain, and with time varying gain is equivalent to 90 dB or more. Signal averaging can increase the effective sensitivity by the amount of averaging and this can be typically 10 to 30 dB. The overall dynamic range is largely set by the ratio of the mean power to the effective receiver sensitivity and can be up to 150 dB.

2.4 Frequency domain

The main advantages of the FMCW radar are the wider dynamic range, lower noise figure and higher mean powers that can be radiated. In addition a much wider class of antenna is available for use by the designer. The sensitivity of the receiver is much better than the time domain equivalent simply by virtue of its lower bandwidth and hence lower thermal noise. Typically a sensitivity of 120 dBm is achieved and a system dynamic range of 180 dB is feasible. FMCW radar transmits a continuously changing carrier frequency by means of a voltage-controlled oscillator (VCO) over a chosen, frequency range on a repetitive basis. The received signal is mixed with a sample of the transmitted waveform and results in a difference frequency which is related to the phase of the received signal, hence its time delay and hence range of the target. The difference frequency or intermediate frequency (IF) must be derived from an I/Q mixer pair if the information equivalent to a time domain representation is required, as a single ended mixer only provides the modulus of the time domain waveform. The FMCW radar system is particularly sensitive to certain parameters. In particular it

requires a high degree of linearity of frequency sweep with time to avoid spectral widening of the IF and hence degradation of system resolution. Dennis and Gibbs[28] made an assessment of the sensitivity of sidelobe level to linearity and showed the ratio of sidelobe to peak level was dependent on the sweep linearity. Practically the effect of a non-linearity of a few percent is to cause significant sidelobes.

The further advantage of a stepped frequency or FMCW ground probing radar is its ability to adjust the range of frequencies of operation to suit the material and targets under investigation if the antenna has an adequate pass-band of frequencies. It can adjust the radiated power on a spectral line basis and its ability to integrate the received signal level improves the system sensitivity. The calibration of the radar does, of course, depend on stable system characteristics and antenna parameters that are invariant with the spacing of the front surface and the antenna. Although on first consideration frequency domain radars should offer a superior sensitivity to time domain radars, because of their lower receiver bandwidth and, hence thermal noise, both the type of receiver and the range sidelobes of the radiated spectrum may result in an equivalent or worse sensitivity in terms of range resolution as discussed above.

2.5 Antennas

In the wideband case the radar antennas are considered in terms of their transfer function rather than their gains or effective apertures. In many cases a separate transmit and receive antenna is used hence their transfer functions may not be identical. The type of antenna that is used with ultra-wideband radar has important role in defining the performance of the radar.
The types of antenna that are useful to the designer of ultra-wideband radar fall into two groups, dispersive antennas and non-dispersive antennas. However, in principle, all antennas are dispersive to some extent. Examples of dispersive antennas that have been used in ultra-wideband radar are the exponential spiral, the Archimedean spiral, the logarithmic planar antenna, the Vivaldi antenna, slot antennas and the exponential horn. The impulse response of this class of antennas is extended and generally results in a 'chirp' waveform if the input is an impulse. Examples of non-dispersive antennas are the TEM Horn, the bicone, the bow tie, the resistive, lumped element loaded antenna and the continuously, resistively loaded, antenna. The input voltage driving function to the terminals of the antenna in impulse radar is typically a Gaussian pulse and this requires the impulse response of the antenna to be extremely short. The main reason for requiring the impulse response to be short is that it is important that the antenna does not distort the input function and generate time sidelobes. These time sidelobes would obscure targets that are close in range to the target of interest; in other words the resolution of the radar can become degraded if the impulse response of the antenna is significantly extended.

Element antennas are characterised by linear polarisation; low directivity and relatively limited bandwidth unless either end loading or distributed loading techniques are employed in which case bandwidth is increased at the expense of radiation efficiency. Details of resistive loading techniques are given by Montoys[29]. Horn antennas have found most use with FD ultra-wideband radars where the generally higher frequency of operation and relaxation of the requirement for linear phase response permit the consideration of this class of antenna. FD ultra-wideband radars have used an offset paraboloid fed by a ridged horn. This arrangement was designed to focus the radiation into the ground at a slant angle to reduce the level of the reflection from the ground. Care needs to be taken in such arrangements to minimise the effect of back and side lobes from the feed antenna, which can easily generate reflection from the ground surface.

One method of radiating circular polarisation is to use an equi-angular spiral antenna. Unfortunately, the dispersive nature of this type of antenna causes an increase in the duration of the transmitted waveforms and the radiated pulse take the form of a "chirp" in which high frequencies are radiated first, followed by the low frequencies. This effect, however, may be compensated by a "spiking" filter, which may take the form of a conventional matched filter or a more sophisticated filter such as Wiener filter.

A spiral antenna could be implemented as a multi-element planar structure; however, this realisation may often fail to provide the expected performance because of several deficiencies. Firstly, the limited physical dimensions of the spiral result in elliptical polarisation at low frequencies which can degrade to essentially linear polarisation; second, reflections from the ends of the arms cause both clutter and degradation of the circularity of the polarisation and, thirdly, the proximity of the ground affects the reactive field of the antenna, resulting in non-symmetrical loading and degradation of the far field pattern. However, at low frequencies the axial radio degrades quite rapidly reaching unacceptable values. Similarly with commercially available baluns the high frequency axial ratio degrades. This situation has a significant effect on the envelope of the polarisation vectors of the transmitted pulse.

2.6 Signal processing

There is no fundamental difference in the information content of the data output from any modulation scheme provided, of course, that the amplitude and phase information is retained in the receiver conversion process. In general it is the range to the target, which is of most interest, and as this is fundamentally equivalent to time, the time series data set is most relevant Many of the processing techniques that have been applied to surface penetrating radar data have been developed for other applications and in addition to radar, acoustic, ultrasonic and seismic processing methods have been freely employed.

. The general processing problem encountered in dealing with surface penetrating radar data is in the widest sense the extraction of a localised wavelet function from a time series which displays very similar time domain characteristics to the wavelet. Unlike conventional radar systems in which the target can sometimes be regarded as being in motion compared with the clutter; in the surface penetrating radar case, the target and the clutter are spatially fixed and the radar antenna is moved with respect to the environment. Most antennas used in surface penetrating applications have a limited low frequency response and tend to act as high pass filters effectively differentiating the applied impulse, hence creating a wavelet. In most cases near identical antenna are used and if these are spaced sufficiently far from the ground surface then their transfer response is unaffected by the proximity of the ground. In the case of antennas operated in close proximity to the ground then their transfer response will vary with changes in the ground surface electrical parameters. The image of the target is convolved with the footprint of the antenna and a simulation of a suitable pseudo-inverse filtering operation is shown in Fig1.

Any processing scheme, which relies on invariant antenna parameters, should take into account the mode of operation of the antennas and the degree of stability that is practically realisable. The antenna cross coupling response is composed of a fixed contribution due to antenna cross coupling or reflection and a variable contribution the effect of the ground or nearby objects. It has been found possible to reduce the amplitude of the cross coupled signal to very low levels; in the case of crossed dipole antennas to below -70 dB and in the case of parallel dipole antennas to below -60 dB. However, the random effect of main, side and back lobe perturbations can be significant and degrades the overall value of cross coupling to -40 dB. The value of the cross coupling is thus determined by any local inhomogeneities in the soil or by any covering material whether of mineral or vegetable origin. There is unfortunately little that can be done to predict variations in cross coupling and it is not amenable to treatment by many processing algorithms

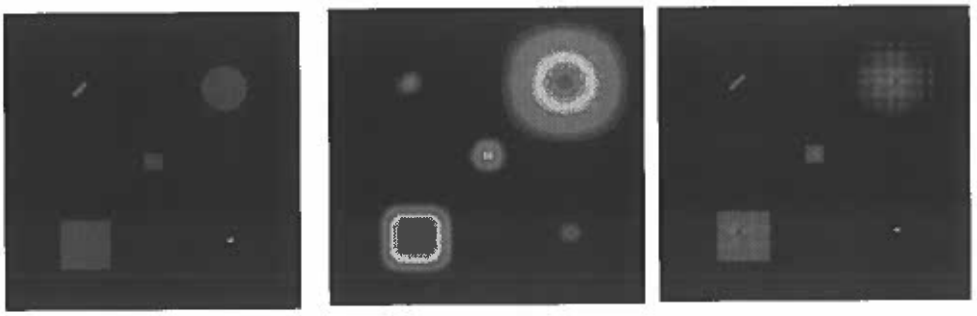

Figure 1 Modelling of the inverse filtering operation to compensate for antenna blurring. Left to right original, blurred image, deconvolved image.

. The variation in cross coupling is much greater with the crossed dipole antenna than the parallel dipole. The ground impulse response can be determined from its attenuation and dielectric constant across the frequency range of interest.
The target impulse response can be composed of the convolution of the wanted target response, together with many other reflectors which may not be wanted by the user but which are valid reflecting targets as far as electromagnetic waves are concerned.

The time separation of the targets is related to their physical spacing as well as the velocity of propagation, which can vary depending on the material properties. Where the targets are well separated in range it is relatively straightforward to separate the radar reflections but this becomes progressively more difficult as targets become closer together, as instead of individual delta functions a series of overlapping (in time) wavelet functions of different characteristics exists. Much work has been done on a variety of signal processing techniques and Astanin[30] and Daniels[31] describe various approaches

2.7 Ultra-wideband synthetic aperture radar (SAR)

UWB SAR systems for mine detection are under development for both vehicle and airborne application.
A real antenna coherently integrates an incident echo signal distributed across its aperture. The azimuth resolution is limited by the directivity of the antenna; improved resolution can be achieved using a ultrawideband synthetic aperture approach. Resolution in the down range from the radar can be obtained by transmitting wideband signals and cross-range resolution can be obtained by coherent processing of echo energy returned from the ground as the platform carrying the radar sensor travels above and or alongside the ground area to be mapped. The synthetic aperture size is the length along the track over which coherent integration occurs. This is limited by range and real antenna beamwidth. Synthetic aperture size shrinks for echoes arriving from distances closer to the platform and increases for echoes arriving at distances further from the platform. The effect, after azimuth focusing, is to produce constant cross-range resolution independent of range, which is approximately equal to one-half of the real aperture's cross-range dimension. Likewise, echo signals collected along a synthetic aperture length must be coherently summed in order to realise the narrow beamwidth associated with a long, synthetically generated aperture. This is achieved by first correcting all forms of platform-to-ground movements that deviate from straight-line motion. What remains is a response for each surface scatterer that varies quadratically in phase with distance along the survey path. The quadratic phase response is produced by quadratic range change associated with straight-line motion of the radar past the scatterer. Removal of the quadratic phase is called azimuth focusing. The synthetic aperture processing, as evident from above, consists principally in the phase compensation of the echoes received from each point to be imaged in the subsequent positions of the synthetic array. The main problem of vehicle or airborne mounted SAR is the exact knowledge of the phase terms to be used in the aperture synthesis. The errors in the knowledge of the track path are given from: errors in navigation instrumentation, resonance frequency of the platform structure, platform structural flexure, antenna pointing errors, platform roll, pitch and yaw motion. To perform phase correction, in the presence of motion errors, an estimation of the actual relative motion between radar and scene-centre is necessary. The techniques to estimate the quadratic phase term are named autofocus because they are used to control an automatic focusing of the SAR image, through the estimation of the coefficient of the quadratic phase term. Two basic autofocusing algorithms are the multilook registration autofocus and the contrast optimisation autofocus. Although the underlying physical principles are different, the performance obtained is comparable. To implement an accurate SAR motion compensation, usually a combination of both hardware estimation and autofocusing is used.

Recent technical developments in remote detection of minefields are in airborne ultra-wideband (UWB), synthetic aperture radar (SAR) systems and, at SRI and subsequently Environmental Mapping Services, R.Vickers has developed airborne systems that can detect buried and surface laid objects from 1000m. These airborne radars are very different from the conventional closely coupled GPR systems in commercial ground survey use. An example of radar SAR image (courtesy of Dr R Vickers

and SRI) is shown in Figure 2. This was taken from an altitude of 400metres above the Yuma desert. The radar operated at a depression angle of 45 degrees and achieved a nominal resolution of 80cm. It was capable of detecting metal AT mines of 30cm diameter buried at a depth of 15-30cm in a soil of conductivity 8-10mmhos/m. Further details can be obtained from SRI USA. In this case of vehicle-mounted SAR systems, the problems of motion compensation are less than in the airborne case and generally, lower powers are needed. Many countries are developing vehicle-based systems to detect both surface laid and buried mines

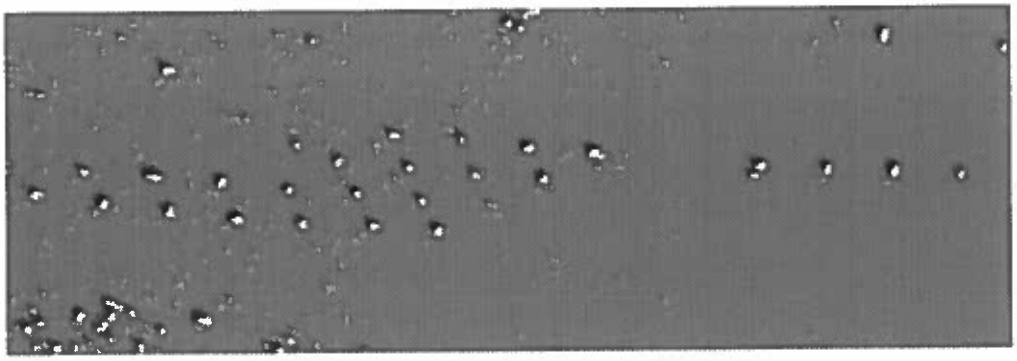

Figure 2 UWB SAR image of buried AT mines in the Yuma Desert, aircraft at 400m altitude (Courtesy SRI, Dr R Vickers)

2.8 Summary

Frequency domain systems are generally more expensive than time domain systems and often inherently slower, due to the need for additional processing operations, i.e. FFT operations to transform the data back to a time domain equivalent. Provided that the antennas have an excellent performance, the better dynamic range of the frequency domain radar can be exploited but realistically the cross coupling and side/back lobe characteristics of the antennas will always limit the sensitivity and performance of the system. As antenna cross-coupling and side/back lobe performance is rarely better than 60 dB to 70 dB this suggests that the dynamic range of the time domain radar is more than adequate and the >100 dB dynamic range of the frequency domain radar is out of reach. This suggests that the main effort in terms of improvements in probing range should be devoted to increasing the performance of the antenna. The range of designs that at under evaluation for close-in and stand-off sensing is considerable and impressive results are being obtained. However the main challenge for radar technology is the high loss ground condition and until systems with dynamic ranges well in excess of 100dB become available performance will always be limited by soil conditions

3. Acknowledgements

I would like to thank the Directors of ERA Technology for their support of this work and the Partners, Daimler-Benz Research, Ebinger, NPA, Thomson Human Factors, Thomson-TME, Thomson-Airsys and Thomson-TCO, in the Esprit Project 26331 (DREAM). The author is also grateful to Dr M. Philipakis of ERA Technology for his modeling and simulation of the antennas. I would also like to thank to Dr R Vickers and SRI for their permission to use the material acknowledged in this paper.

References

1 D J Daniels Surface Penetrating Radar 1996 IEE Radar Sonar Navigation and Avionics Series Volume 6 ISBN 0 85296 862 0

2 Carl Baum Ed. The detection and identification of visually obscured targets 1998 pub Taylor and Francis ISBN 1-56032-533-X

3 James R Wait. Electromagnetic probing in Geophysics, 1971, pub Golem Press, ISBN 0911762-09-4

4 James R Wait. Electromagnetic waves in stratified media, 1962, pub Pergammon Press

5 Gary R Olhoeft, Electrical, Magnetic and Geometric properties that determine ground

penetrating radar performance. Proceedings of the Seventh International Conference on Ground Penetrating Radar Kansas USA May 27-30 1998
6 Cook and Bernfeld, Radar Signals, An introduction to theory and application, ISBN 0-89006-733-3, Artech House, p9
7 M Skolnik, Radar Handbook 2nd Edition, ISBN 0-07057913-X, Ed, McGraw-Hill, Chap 10
8 Nathanson, Radar Design Principles, ISBN 07-046047-7 Chap 8
9 Wehner, High Resolution Radar, ISBN 0-089006-194-7 Chap 4
10 Galati, Advanced Radar Techniques and Systems IEE Radar Sonar Navigation and Avionics Series Volume 4 ISBN p104
11 Astanin and Kostylev, Ultra-wideband Radar Measurements Systems IEE Radar Sonar Navigation and Avionics Series Volume 7 ISBN 0 85296 894 9 Chap 1
12 Scheers B, Ground Penetrating Radar for Anti-personnel Mine Detection, Revue HF, Part 3 (25-33) 1998
13 Earp S.L., Hughes E.S., Ultra Wideband Ground Penetrating Radar For The Detection of Buried Metallic Mines, IEEE Aerospace and Electronics Systems Magazine, Vol.11, Part 9, pp 30-34, Sep 1996
14 Steinway W.J., Duvoisin H.A., Tomassi M. S. et al., Multi-Sensor System for Mine Detection Proceedings IGAAS '98, Seattle, USA, Vol.1, pp 228-233, 1998
15 Carin L., Felsen L., (Editors), Ultra-Wideband Short Pulse Electromagnetics, Proceedings 2nd Int. Conf. Brooklyn, USA, pp 125-131, April 1994
16 Duvoisin H.A., Steinway W.J. et al., Multi-Sensor System for Mine Detection Proceedings Conf. On Infrared Technology and Applications, San Diego, USA, pp 705-715, July 1998
17 Bourgeois Jacqueline M., Smith Glenn S., A Complete Electromagnetic Simulation of the Separated-Aperture Sensor for Detecting Buried Land Mines, IEEE Transactions on Antennas and Propagation, Vol.46, No.10, October 1998
18 Earp S.L., Hughes E.S. et al., Ultra-Wideband Ground Penetrating Radar for the Detection of Buried Metallic Mines, Proceedings, IEEE National Radar Conf. Ann Arbor, USA, pp 7-12, May 1996
19 Vitebskiy S., Carin L. et al., Ultra-Wideband, Short-Pulse Ground-Penetrating Radar: Simulation and Measurement, IEEE Transaction of Geoscience and Remote Sensing, Vol.35, Part 3, pp 762-72, May 1997
20 Daniels, D J High Resolution Radar Detection of Buried Anti-Personnel Mines for Humanitarian Clearing Operations ISMCR '96, Brussels, Belgium, 9-11 May 1996
21 Daniels D J Radar techniques for mine detection SUSDEM '97, Zagreb, 29 Sep – 1 Oct 1997
22 Daniels D J Multi-sensor radar techniques for mine detection, IEEE CESA '98, Tunisia, 1-4 April 1998
23 Daniels D J Ground Probing Radar Techniques for Mine Detection, GPR '98, Kansas, USA, 26-30 May 1998-05-14
24 Daniels D J Detection of ground probing radar target images in clutter, EUREL/IEE Meeting on Radar and Sonar Signal Processing, Peebles, Scotland, UK, 5-8 July 1998
25 Daniels D J, Ultra-wideband detection of buried objects, IEEE IGARSS Proceedings, Singapore pp1278-1281 August 3 -8 1997
26 Noon D, Stickley G F, Antenna ring-down, range sidelobes and quality factor of time and frequency domain GPR systems Proceedings of the Seventh International Conference on Ground Penetrating Radar Kansas USA May 27-30 1998
27 Daniels D J. Resolution of Ultrawideband Signals, IEE Procs Radar Sonar and Navigation, (to be published Aug 1999)
28 Denniss., Gibbs Solid state linear FMCW systems –their promise and their problems. Proc. IEEE Int. Mic. Conf. Atlanta, GA, USA pp 340-342, 1974
29 Montoys T.P., Smith G.S.,VEE Dipoles With Resistive Loading for Short Pulse Ground Penetrating Radar Microwave and Optical Technology Letters, Vol.13, Part 3, pp 132-137), Oct 1996
30 Astanin L.Y., Greppener V.V. et al.., Ultrawideband Ground Probing Radar Signal Processing Methods Proceedings Image and Multidimensional Digital Signal Processing '98, Alpbach, Austria, pp 259-261, July 1998
31 Daniels D. J., Surface penetrating radar image quality EUREL/IEE International Conference – The Detection of Abandoned Landmines, Edinburgh, Scotland, UK, 12-14 October 1998

Digital Signal/Image Processing For Mine Detection. Part 1 : Airborne Approach

L. van Kempen, A. Katartzis, V. Pizurica, J. Cornelis and H. Sahli
Department of Electronics - ETRO-IRIS
Vrije Universiteit Brussel
Pleinlaan 2, 1050 Brussel - Belgium

tel. +32/629 28 58 fax. +32/629 28 83
email : {lmkempen,akatarzi,vpizuric,jpcornel,hsahli}@etro.vub.ac.be

Keywords. Airborne minefield detection, remote sensing, image processing.

Abstract. Experiments on airborne minefield identification are reviewed in "Part 1". "Part 2", in these same proceedings, describes ground based experiments. The emphasis in this part is on the processing and pattern recognition algorithms. Preliminary results are shown, further refinement and redesign are needed before going to real life situations.

1 Introduction.

"Humanitarian demining, and UXO removal" is an *interdisciplinary problem*, involving several types of actors with specific motivations, personal views on action priorities, and sometimes strong susceptibilities. It is a worldwide problem which cannot be tackled without considering the complex interactions between politics, industrial interests, NGO/MAC demining actions and mine awareness training, military involvement and technology, humanitarian/medical and environmental consequences, economic cost/benefit analysis, fundamental and applied R&D results [1].

Like in many EU countries, also in Belgium the scientific research community was interpellated by the problem in 1995, driven by a clear political incentive against mine production, trade, storage and usage. Under the initiative of the Royal Military Academy and two universities, namely VUB and ULB, government funding for an interuniversity project, HUDEM, was obtained [2]. Although, right from the start the good will and collaboration of end users was obtained, this initiative raised the concern of demining campaign organizers, because it was seen as yet another way to extract finances, which would normally go to real demining actions on the field. In the meanwhile, it has been proven that on the contrary, *researchers have attracted supplementary funds to the domain* which otherwise would be allocated to other technical and scientific application domains. It is well recognized how military procedures and technology have influenced, through a process of adaptation, the field of humanitarian demining, but *also other domains are providing new insights*, like non destructive testing, signal/image processing, remote sensing, Geographical Information Systems, medical imaging, ([3], [4]) ... Some of them will be illustrated in the paper.

It is important to understand the extent to which the design of mine detection and minefield delineation technology is based on military operational doctrine, compared to humanitarian or post-conflict requirements. For the latter the needs of real time operation and testing following military practice, are not so relevant. Hence objectives as acceptance and ergonomy adapted to usage by indigenous deminers and NGO's, as well as increased performance in sensitivity at a reasonable False Alarm Rate should be emphasized. Achieving these goals opens perspectives for research and development at the university level in the fields of combined sensing principles, signal and image processing, data fusion, improved human interfaces, and new platforms.

Our department, ETRO, stepped into the field of humanitarian mine and minefield detection, some 4 years ago, with the goal of contributing to the optimization of detection algorithms and equipment. Starting from our background knowledge in *image/video processing and machine vision*, we have extended the application projects from medical imaging, satellite image analysis, industrial visual inspection, tele-publishing, teleradiology, remote sensing, towards antipersonnel mine and minefield detection. Although our initial objective was to apply expertise on data fusion into the latter domain, we soon found out that this is not feasible without familiarizing ourselves with the nature of the signals coming out of the individual sensors. Initially we have explored the signal properties and discrimination power of GPR, US signals and thermal IR image sequences without explicitly taking into account the physical models of the scene and the image formation systems. This approach, although useful, has severe limitations and we were convinced that we could only bring something new to the domain by working in association to instrumentation builders and end users. This explains why we gradually became more and more involved in mine detection itself. We have built our own test measurement

set-up, funded by an internal VUB project [5], starting from the DeTeC EPFL equipment [6]. Currently, we are conducting a survey on the State of the Art on humanitarian demining technology, products and practice in the EU (EUDEM - HPCN: 501853). In a TELSAT4 project (T4/03/55), we verify if temporal satellite image sequences are a useful source of information for enhanced detection of minefield indicators. The DEMINE (HPCN 29902) project allows us to develop signal processing algorithms in collaboration with GPR equipment designers and end users. In a pilot project on Airborne Minefield detection in Mozambique: (REG/661-97/2, DG VIII), we are investigating the role of image processing for the delineation of minefields in a test situation (Belgium), and in realistic surroundings (Mozambique).

The goal of the current papers (Part 1 & Part 2) is to summarize some results and technological research, which has been carried out in the framework of these projects.

2 Theoretical Background and Materials.

Minefield detection is usually carried out using short-range ground-based sensors. These are sometimes fairly effective, but without large-area coverage capability, which makes the whole process very slow. On the other hand, recent developments in airborne remote sensing open new perspectives for minefield detection. Compared with ground-based methods, airborne minefield detection (AMD) can provide low-cost, fast and wide area surveillance. Having a global overview of the suspected area, helps delineating the minefield. Several different sensors (e.g. Optical, Multispectral, Thermal, Radar) have been used in AMD in recent years. Each of them has different characteristics, with some advantages and limitations depending on several environmental circumstances, like weather, soil, vegetation and the type of mines.

Our department is participating in the pilot project *Airborne Minefield Detection in Mozambique (DGVIII)* in which two tests have been made.

The first airborne campaign took place over a military domain in Leopoldsburg, covering an area of approximately 500000 m^2. The one year old field contains 9 minefields, with AT and anti-personal (AP) mines and some UXO's. The terrain was mostly covered by low vegetation, with high dense bushes. Depending on the altitude of the aircraft, the scales of the images that have been recorded are in the range between 1:500 and 1:6000. The following sensors have been used; ZeissLMK2000 (optical), LeicaRC30 (optical), VOS80C (digital optical), Recon CA-860 (thermal), AES-1 (radar). At an altitude of 200m, the highest ground resolution for optical sensors is in the range of several millimeters. The films that have been used are black and white, colour and colour infra red. Digitized images are produced with a scanning resolution of 15μm. Typically, for the scale 1:500, a ground resolution of 7.5mm has been reached. The digital data provided by the VOS80C camera have a typical spatial resolution of 32 cm at a flying height of 200 m. The resolution achieved by the Recon CA-860 sensor is 8cm, at 300m. For the AES-1 sensor the ground resolution in P-band at the altitude of 600m is 2.5m x 0.5m.

During the second campaign, four sites in Mozambique have been chosen, each of them with different type of environmental conditions. The total surveyed area covers around 750km2. Two LeicaRC30 cameras were mounted on the aircraft equipped with different films (colour and colour infra red). Images were obtained in scales varying from 1:500 to 1:2000. Only one minefield was surveyed at scale 1:500, yielding a ground resolution in the digitized images of 7.5 mm.

The problem of AMD can be approached using either direct or indirect methods [7]. Direct methods can be generally divided in two steps: mine cues detection and minefield pattern recognition. The first step concerns the identification of the location and the assessment of all the mine candidates, based on a specific model (shape, size, contrast appearance), whereas the second step uses the a priori knowledge about the minefield shape, e.g. regularity like colinearity and equal spacing, in order to identify minefield patterns [8]. Indirect methods are focused on the delineation of the minefields by using several indicators. These can be either man-made objects close to the minefield (sticks, wires, concrete blocks, fences, paths) or the absence of recent human activities inside the suspected areas.

2.1 Mine cues and minefield pattern detection

The mine cues extraction concerns the detection and localization of mine candidates, and the production of their detection confidence values. Depending on the image modality used, several approaches are proposed in the literature [9], [10], [11], [12], [13]. All these methods are *model-based*. The expected contrast appearances, shape and size of the target objects, are used to guide the detection and labeling process. For each detected target, features, such as location, size, shape and contrast are measured. These features are used for the estimation of a target confidence value.

The application of a single-mine detection method on a particular image modality is usually insufficiently specific, and hence we combine it with techniques for the identification of minefield patterns that may be present in the surveyed region. For patterned minefields, which exhibit a particular regularity (e.g. equal spacing and colinearity) compared to the surrounding clutter, several minefield models can be found in the literature [14],[15],[16],[17],[18],[19].

2.2 Detection of minefield indicators

Under most real life circumstances, the detection of the individual mines from airborne images becomes a very difficult task. In the case of Mozambique, the

minefields are very old, containing mainly buried AP mines, mostly covered with dense vegetation. These reasons forced us to search for minefield indicators, for the detection and delineation of the minefields. Using this indirect method for AMD, we focused our research on the detection of the following features:

- indicators placed in a periodic pattern (poles, sticks, concrete blocks);
- roads, paths, fences and other linear features;
- homogeneous regions.

3 Experimental Results

3.1 Mine cues and minefield pattern detection

We have developed a method for mine cues detection that follows a general approach. The mine targets are considered as changes in the vegetation/soil textures. Texture parameter extraction, and clustering methods are used for classification of background (vegetation, soil, etc...) and mine-like objects. The decision mine/no-mine is made in a post-processing step, which considers mine shape and size characteristics. This is obtained by using several morphological operators. Our proposed method is based on a general *supervised image segmentation* scheme (see figure 1).

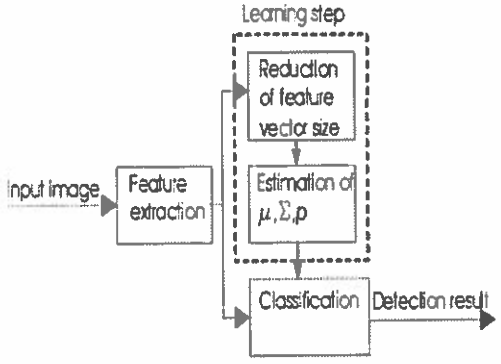

Figure 1: *Supervised image segmentation.*

For the problem of minefield pattern detection, a geometrical model-based approach is proposed. The method is applied to the configuration of points that are extracted after the classification and clutter reduction steps. First the Hough transform is used for line detection (linearity criteria), and then line patterns that tend to exhibit equal spacing regularity of the detected points are selected using the FFT transform.

We have applied these techniques on the images obtained during the Belgium test. The one year old test field contains 9 minefields, with AT and antipersonal (AP) mines and some UXO's. We have concentrated our work only on images taken by optical sensors, since the quality of the digital images obtained with the other sensors does not allow us to search for individual mines. Figure 2 shows the detection of two linearly arranged mine patterns. They are delineated by detecting AT mines laying on the ground. The minefield has a V shape containing 36 AT mines (see figure 2(a)), where 17 of them are extracted (see figure 2(c)). In a second case, the minefield contains 20 AT mines and 10 AP mines. Among them, 10 AT mines are found. One of them is laying on the ground and directly detected. The rest of the minefield is identified by detecting the difference in vegetation following a regular pattern.

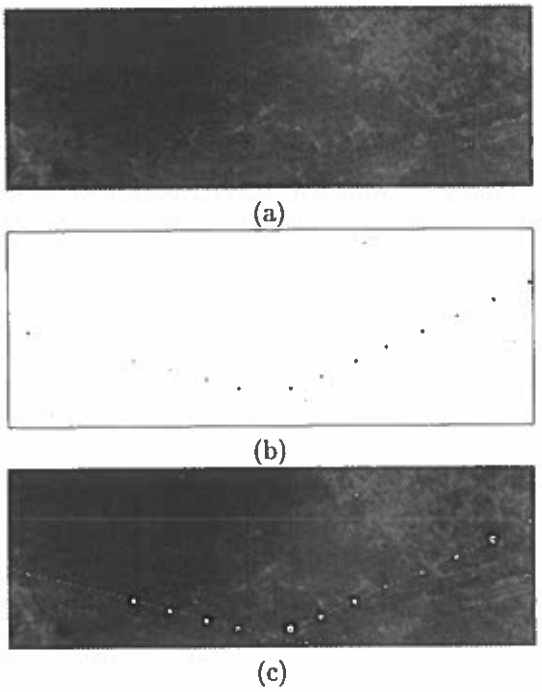

Figure 2: *(a) Minefield region, (b) Result of mine-cues detection, (c) Delineation of the minefield.*

3.2 Detection of minefield indicators

Detection of periodic indicators

One specific defensive minefield in the Buzi region in Mozambique is delineated by poles, which exhibit a periodic pattern at both sides. The total length is 4km and the width is 5m. The terrain is flat and outside the minefield agricultural land is in exploitation.

The poles appear on the images as elongated objects with their shadow oriented in a certain direction. For their detection we have applied two algorithms. The first one involves wavelet frame analysis (see figure 3) for the enhancement of image features in a certain direction (pole's shadow), while the second performs watershed segmentation [20] from which dark elongated objects are extracted (see figure 4).

Linear feature extraction

One type of basic minefield indicators consists of elongated structures that often can be found around the minefields. These elongated features correspond to wires and fences delineating the minefield, or roads and paths that designate safe passage areas. A char-

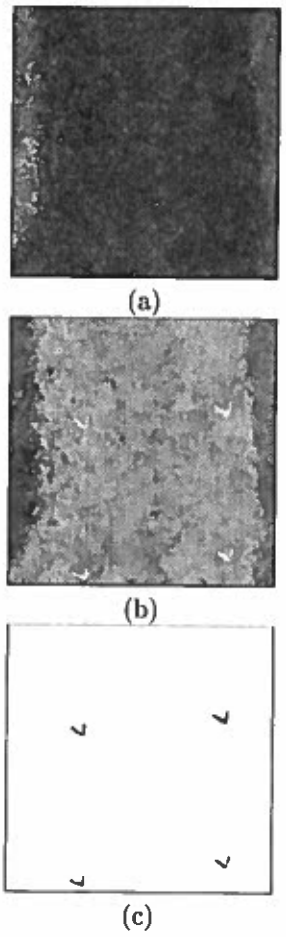

Figure 3: *Wavelet approach (a) Buzi minefield, (b) Enhanced reconstructed image, (c) Poles detection.*

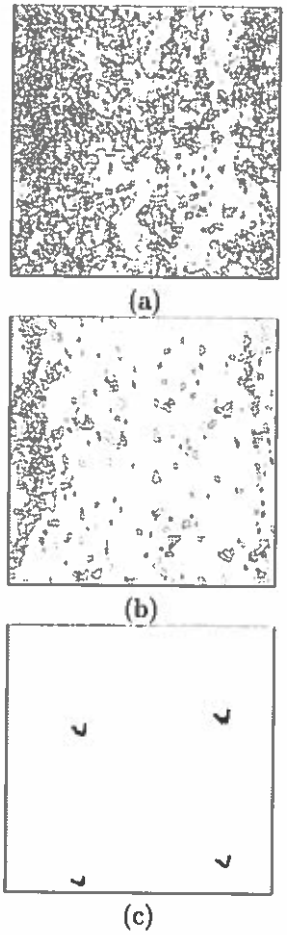

Figure 4: *Watershed approach (a) Oversegmented image, (b)Region merging step, (c) Poles extraction.*

acteristic example is the case of the Songo minefield, where linear features like roads give a good information about the position of the minefield (see figure 5 (a)).

Our approach identifies roads and paths in airborne imagery by combining two criteria: a local criterion evaluating the intensity in a small neighborhood surrounding a target pixel to discriminate lines from background, and a global criterion introducing some large-scale knowledge about the structures to be detected. Initially, we apply a line detector algorithm based on the work of J. Chanussot and P. Lambert [21]. This utilizes several morphological operators that identify elongated objects with a specific width that corresponds to the size of the roads to be extracted (figure 5(b)). As a next step, we apply a linking process that generates a set of line segments (figure 5(d)) by making use of the response of the morphological operators together with information about orientation (figure 5(c)) (for each pixel this corresponds to the direction where the response of the line detector has the highest value). The extraction of the road is carried out using contextual, a priori knowledge about its shape which can be introduced by associating an energy function to the segments with the use of Markov Random Field theory [22]. A graph is built that contains all possible connected segments (figure 5(e)) created by using some connectivity criteria: the distance between two segments must be less than a fixed threshold, and alignment of the two segments must be acceptable. The road identification process is modeled as the extraction of the best graph labeling (figure 5(f)).

Segmentation in homogeneous regions Most of the time, minefield areas are undisturbed homogeneous regions with no human activity inside. In some cases they are surrounded by agricultural fields. For this reason, segmentation of the image in homogeneous regions may lead to the delineation of meaningful areas in terms of land usage, some of them being minefields. The segmentation technique (Fig. 6), based on a variant of k-means clustering, was previously used in the context of cloud identification in satellite images [23].

4 Conclusions and Discussion

Several image processing and image analysis methods have been developed and tested. Detection of buried minefields, using airborne images presents a great challenge, and presently it is an unsolved problem, which cannot be tackled by direct methods only, especially in the presence of high and dense vegetation. This makes designing direct methods, which include the detection

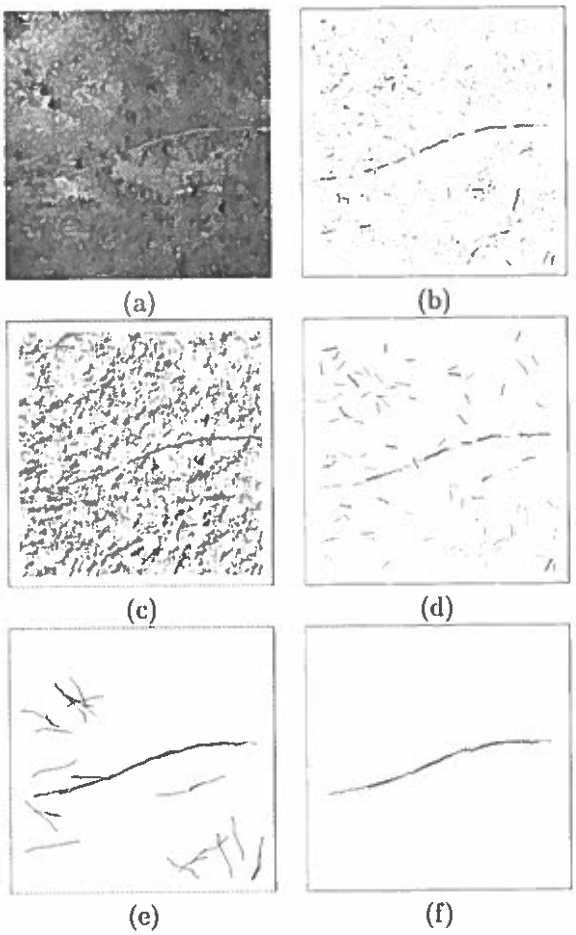

Figure 5: *Linear feature extraction (a) Original airborne image, (b) Response of the morphological operators, (c) Orientation image, (d) Set of detected line segments, (e) All possible connected segments (f) Final result.*

of individual mine candidates, a very difficult task. These methods highly depend on the environmental conditions, sensors used and types of mines. In cases where AT mines lay on the ground, as it was proved during the campaign in Belgium, direct methods are feasible by using image analysis. For this reason, we have developed a supervised image segmentation technique for individual mine detection followed by morphological processing. The minefields were delineated with the use of a regular pattern detection algorithm.

A promising approach for the delineation of the minefields, which does not consider detection of the individual mines and can be used in a wide-area surveillance, is the identification of several minefield indicators. We have done some research on this topic using the images obtained during the Mozambique campaign. Several features can be derived for indirect AMD, such as elongated structures, homogeneous regions, and periodic indicators. The results of our proposed algorithms carry different kinds of information (roads showing safety passages, fencing systems delineating suspected areas, homogeneous regions indicating different vegetation types). All this information

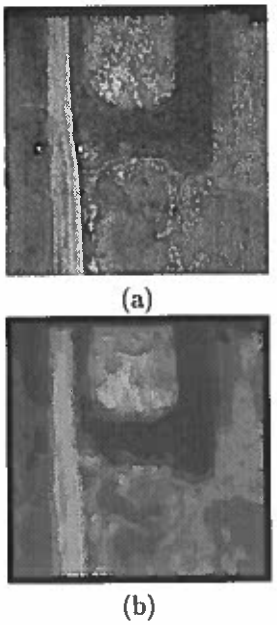

Figure 6: *Segmentation in homogeneous regions (a) Original image of Buzi minefield, (b) Segmented image.*

can be integrated in a multi-layer representation of the scene, where each layer adds additional knowledge about the image.

One of the limitations of our work is that we have modeled neither the physical characteristics of the sensors nor the scanning conditions during the digitization. By formulating the degradation process during the image acquisition (e.g. inherent noise), we could probably develop efficient enhancement techniques that improve the quality of the images. As far as the problem of detection of minefield indicators is concerned, we didn't use any texture model for different types of vegetation. By borrowing these models from existing land-usage studies, segmentation results could probably be improved, as we take into account a priori knowledge about the regions that we want to extract. These two limitations will be considered in our future work.

Most of the time, human interpreters are concentrated on extracting features from local regions, while the global properties of the surveyed area could be missed. For this reason, a fast complementary tool, which allows both local and global analysis is needed. The final goal of our work is the creation of an interactive environment for AMD, which includes previously described image analysis methods. This user-interface could help in image interpretation, making it easier, more reliable and faster.

Acknowledgements. The overview of results, described in this paper, could be made in the context of the funded project: Airborne minefield detection in Mozambique (Pilot project DGVIII, coordinated by ITC).

References

[1] J. Cornelis, H. Sahli, M. Acheroy, and Y. Baudoin, "Anti personal mines, a world-wide problem: From political conscience towards humanitarian, research and industrial action," *Proceedings Sixth International Symposium on Measurement and Control in Robotics, IMEKO, BSMEE, BIRA*, pp. 1–5, May 1996.

[2] M. Acheroy, "Belgian project on humanitarian demining (HUDEM)," *Proceedings SUSDEM'97, International workshop on Sustainable Humanitarian Demining, Zagreb, Croatia*, pp. S7.1–S7.5, Sept 29 - Oct 1 1997.

[3] M. Sachne, L. van Kempen, D. Milojevic, H. Sahli, P. V. Ham, M. Acheroy, and J. Cornelis, "Mine detection by means of dynamic thermography: simulation and experiments," *IEE Second International Conference on the Detection of Abandoned Landmines (MD'98), Edinburgh, UK*, pp. 124–128, October 12-14 1998.

[4] C. Bruschini and B. Gros, "A survey of current sensor technology research for the detection of landmines," *Proceedings SUSDEM'97, International workshop on Sustainable Humanitarian Demining, Zagreb, Croatia*, pp. S6.18–S6.27, Sept 29 - Oct 1 1997.

[5] "http://etro.vub.ac.be/minedet."

[6] F. Guerne, "Buildng a sandbox with a carthesian gantry for sensor testing," *Proceedings SUSDEM'97, International workshop on Sustainable Humanitarian Demining, Zagreb, Croatia*, pp. S5.27–S5.33, Sept 29 - Oct 1 1997.

[7] V. Pizurica, A. Katartzis, J. Cornelis, and H. Sahli, "What can be expected from computerized image analysis techniques for minefield detection," *Submitted to 2nd International Symposium 'Operationalization of Remote Sensing', Enschede, Nederland*, 16-20 August 1999.

[8] V. Pizurica, A. Katartzis, and H. Sahli, "Supervised methods for linear minefield detection," Tech. Rep. IRIS-TR-0054, VUB-ETRO department, 1999.

[9] B. Williams and B. Blume, "Physics based sensor effects prediction applied to a multispectral mine detection algorithm," *SPIE, Orlando, Florida*, vol. 2496, pp. 798–809, 1995.

[10] J. K. Hackett, E. Gold, D. T. Long, E. Cloud, and H. Duvoisin, "Model-based approach to real-time target detection," *SPIE, Orlando, Florida*, vol. 1700, pp. 269–276, 1992.

[11] A. Banerji and J. Goutsias, "Detection of minelike targets using grayscale morphological image reconstruction," *SPIE, Orlando, Florida*, vol. 2496, pp. 836–849, 1995.

[12] S. Crocker, S. Ayasli, and T. Grosch, "Multistage processing for automatic minefield detection using low-frequency SAR," *SPIE, Orlando, Florida*, vol. 2496, pp. 823–833, 1995.

[13] T. O. Grosh, C. F. Lee, and E. M. Adams, "Detection of surface and buried mines with a UHF airborne SAR," *SPIE, Orlando, Florida*, vol. 2496, pp. 110–120, 1995.

[14] S. L. Earp, T. J. Elkins, and B. C. Conrath, "Detection of random minefields in clutter," *SPIE, Orlando, Florida*, vol. 2496, pp. 543–555, 1995.

[15] R. R. Muise and C. M. Smith, "A linear density algorithm for patterned minefield detection," *SPIE, Orlando, Florida*, vol. 2496, pp. 586–593, 1995.

[16] G. Robinson and B. L. Robinson, "Pattern minefield detection from inexact data," *SPIE, Orlando, Florida*, vol. 2496, pp. 568–574, 1995.

[17] B. Bargel, K. Bers, G. Stein, and G. Traeger, "Model-based sensor fusion for minefield detection," *SPIE, Orlando, Florida*, vol. 2496, pp. 510–518, 1995.

[18] D. E. Lake and D. M, "Identifying minefields in clutter via collinearity and regularity detection," *SPIE, Orlando, Florida*, vol. 2496, pp. 519–530, 1995.

[19] R. R. Muise and C. K. Chui, "A wavelet approach to detect discontinuities of intensity functions for minefield classification," *SPIE, Orlando, Florida*, vol. 2496, pp. 531–542, 1995.

[20] I. Pratikakis, H. Sahli, and J. Cornelis, "Low level image partitioning guided by the gradient watershed hierarchy," *Signal Processing*, vol. 75, pp. 173–195, 1999.

[21] J. Chanussot and P. Lambert, "An application of mathematical morphology to road network extraction on SAR images," *Proc. International Symposium on Mathematical Morphology, Amsterdam*, pp. 399–406, 1998.

[22] F. Tupin, H. Maitre, J. F. Mangin, J. M. Nicolas, and E. Pechersky, "Detection of linear features in SAR images: Application to road network extraction," *IEEE, Trans. on Geoscience and Remote Sensing*, vol. 36, no.2, pp. 434–453, March 1998.

[23] P. Boekaerts, E. Nyssen, and J. Cornelis, "Autoadaptive scene identification in multi-spectral satellite data," *AGARD Symposium on remote sensing, Tolouse, France*, pp. 21–1 21–8, April 1996.

Digital Signal/Image Processing For Mine Detection. Part 2 : Ground based Approach

L. van Kempen, A. Katartzis, V. Pizurica, J. Cornelis and H. Sahli
Department of Electronics - ETRO-IRIS
Vrije Universiteit Brussel
Pleinlaan 2, 1050 Brussel - Belgium

tel. +32/629 28 58 fax. +32/629 28 83
email : {lmkempen,akatarzi,vpizuric,jpcornel,hsahli}@etro.vub.ac.be

Keywords. Mine detection, image processing, GPR, IR camera, US reflectometry.

Abstract. Experiments on mine detection with short range ground-based sensors (GPR, dynamic and static IR imaging, US reflectometry) are reviewed. The emphasis is on the processing and pattern recognition algorithms, although these cannot be discussed without taking into account some of the physical principles of the sensors and data acquisition circumstances. The paper proposes some original approaches, which have primarily been evaluated in controlled test conditions. Further refinement and redesign are needed before going to real life situations.

1 Introduction.

Part 1 of the paper, in these same proceedings, describes how the ETRO group entered the field of "mine detection"; and it is dedicated to "Airborne Minefield Detection". Part 2 reviews the ground based approaches.

2 Theoretical Background and Materials.

2.1 The Ground Penetrating Radar.

2.1.1 Introduction. The Ground Penetrating Radar (GPR) is an active device that, in many cases, performs better than the classic metal detector for low metal AP mines. For this reason an important part of our work focuses on the processing of data produced by this particular sensor. We will start with an overview of the existing GPR technology. Next we will explain two approaches in processing the GPR data, the first is based on a pattern classification scheme, and the second aims at a better visualization of the data.

2.1.2 GPR Technology. Figure 1 provides an overview of the existing types of GPR's.

The first type is a *time domain* GPR with an *impulse system*, where the emitted pulse has a carrier frequency, modulated by a square envelope. This type of device operates in a limited frequency range, and has

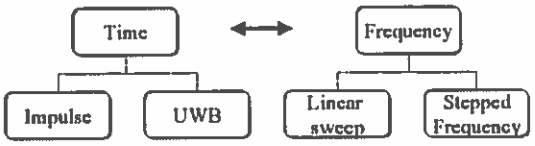

Figure 1: *An overview of the existing Ground Penetrating Radar types.*

in most cases a mono-cycle pulse. The second type of *time domain* GPR is the so called *Ultra Wide Band (UWB)* GPR, which emits a pulse without a carrier frequency. This way the spectral band of the emitted energy is very large.

The *frequency domain* GPR's transmit a signal with a changing carrier frequency over a chosen frequency range. This carrier frequency can be changed, either continuously (linear sweep), or with a fixed step.

Within our department, we have experience with both the *impulse time domain* and the *stepped frequency* GPR.

2.1.3 Processing towards pattern classification. The expected result of the processing of GPR data, is the final decision whether or not a mine is present. We tackle this problem, by a supervised classification algorithm that allows to distinguish between a number of classes, based on features, extracted from the data ([1],[2]).

A general classification problem can be solved in six stages, each of which will be explained in more detail.

i In the *pre-processing* stage the input data is passed through a number of filtering steps with the intent to reduce the noise as well as the background clutter, without deforming the information. It is important to remove as much non essential information (information that does not contribute to the distinction between objects) as possible. An example of such a non essential information is the distance between the antenna and the soil. The elimination of this problem is not simple in the case of rough terrains. Therefore a shifting mechanism has been designed so that the

resulting reflection from the air-ground interface can be eliminated from all A-scans in one single processing step.

ii The *detection* stage consists of a binary hypothesis testing (signal present versus signal absent), in order to eliminate beforehand the part of the data, that does not contain any object information.

iii The *feature estimation* stage reduces the data into a feature vector which represents the target. One way to estimate these features is on the basis of the one dimensional A-scans. This is done by transforming them into several domains (e.g. the *time* domain , the *Fourier* spectrum, the *auto-correlation*, the *Wigner-Ville* transform results, and the *Wavelet* transform results.) Another type of features can be estimated out of the two dimensional B-scan, based on the detection of the hyperbolas that are typically found in such images. The parameters of these structures give information about the object's position as well as its internal structure.

iv The *feature extraction* stage extracts out of the estimated feature vector only those features that are pertinent to the classification problem. This selection is done, based on a *learning set.*

v The *object model formulation* stage determines a set of parametric or non-parametric models for each object class considered. The models can be parametric multidimensional class conditional probability functions like the multivariate normal distribution.

vi The final *classification* step then compares the feature vector extracted out of an unknown data sample, with the different class models to determine the likelihood of being part of a mine object. The underlying decision function is the Bayesian one. Also a multiple classifier approach is used, where the classification is done based on the features given by the different domains separately, after which the classification results are combined in a second step. This combination uses the a posteriori probabilities given by each of the classifiers. The same type of combination can later be used in merging features given by different sensors.

2.1.4 Processing towards visualization This type of processing uses the three dimensional C-scan data, in order to get an idea about the shape of the object or its interaction with the radar beam.

We considered two types of such algorithms, the first being a three dimensional segmentation method based on the well known watershed technique ([3]). The second method is based on a technique called *Array Beam Imaging*. This method attempts to estimate the amount of energy that was reflected in each voxel of the subsurface, by shifting the A-scan signals, measured at the different positions on the surface, so that the signal parts, coming from that particular voxel will be added constructively.

2.2 Ultra Sound ([4], [5])

The idea of testing ultra sonic equipment for mine detection originated from two facts, the first being the presence of US test equipment for non-destructive material testing at our facility, and the second being the applicability of this type of equipment in wet or flooded circumstances. After some study, the similarity in general principle, as well as in the shape of the data, between US and impulse GPR, prompted the idea to develop processing tools, which are independent of the sensor. The tests showed also that the available equipment was not well-adapted to the mine-detection application (too high frequency probes, ...), so the tests were momentarily stopped.

2.3 Infra Red

2.3.1 Introduction The processing of images, given by thermal scanners can be envisioned in two ways. The first is the *dynamic* approach where an image sequence is processed in one batch, the second is the static approach where the processing is performed on one individual image.

2.3.2 Dynamic thermography ([6]) consists of processing a sequence of images of the same scene, submitted to a heating or a cooling (be it artificial or natural), so that the scene parts will follow different temperature curves in time, due to the variety in their specific nature (material, volume, shape ...).

The purpose of the processing is to produce an image with enhanced contrast between the objects due to *dynamic behavior difference*, and a number of scattergrams, on the basis of which a segmentation of the original image is derived.

The two methods, used to perform this processing are called the Karhunen-Loève Transformation and the Kittler and Young Transformation.

2.3.3 Static IR processing ([7]) The proposed type of processing, applied to IR images is based on Mathematical Morphology. Here the emphasis is laid on the enhancement, denoising and finally segmentation of individual images, using mathematical morphology tools.

2.4 Test Setup

The test setup that is available at the VUB campus consists of a sandbox (3x3x1.5m deep) filled with two soil types (sand and local soil) (see figure 2). Above it, an XY translation table is placed on which a number of sensors can be mounted. This table can scan the whole area of the sandbox with a step of 1mm. An impulse GPR and a metal detector are presently available, but new sensors can also be added without too much problems. Recently a second setup has been added for IR measurements. This includes an IR camera in the spectral region of 8-12 μm, a solar panel

to simulate the natural sunlight on the scene, and a translation support for this. Also an IR polarizer is available to perform some polarization experiments. This same setup is recently also used for millimeter wave measurements.

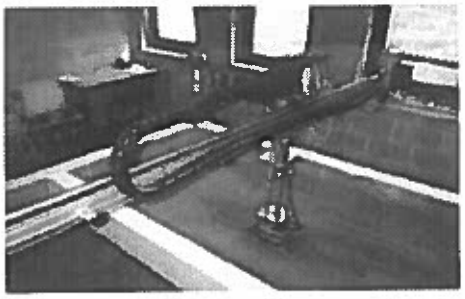

Figure 2: An overview of the available test setup.

2.5 Metal Detector

Modern metal detectors have become more and more refined and sensitive over the years, and it has often been said that they have reached their limits. However, recently metal detectors are used which are able to deliver additional information on the object under study, such as for example its depth, size and identity, or a rough bidimensional image.

A more detailed presentation of the electromagnetic detection of metallic objects using metal detectors, and their application to Humanitarian Demining can be found in "Metal Detectors for Humanitarian Demining: from Basic Principles to Modern Tools and Advanced Developments" by C. Bruschini in these same proceedings.

3 Experimental Results

3.1 Ground Penetrating Radar

An overview of the results for the pattern recognition approach applied on A-scans, can be found in [1]. In this paper we will put the emphasis on the results obtained for the B- and C-scan processing.

For the B-scan processing the aim was to detect the hyperbolas in the image. Figure 3 shows the detection results in a typical pre-processed B-scan image. This image contains four objects, two mines, a metal sphere and a rock. All objects are detected, by hyperbolas with the apexes at the correct horizontal position.

The comparison between the results for the *raw data* and those for the *pre-processed data* can be found in Table 1.

It can be seen that, for the pre-processed data, the estimated depth for all objects is approximately 5cm, which is the correct value, and the estimates for the velocity of propagation in the soil are approximately identical for the objects. Finally, the eccentricity of the hyperbolas is almost identical for all the objects.

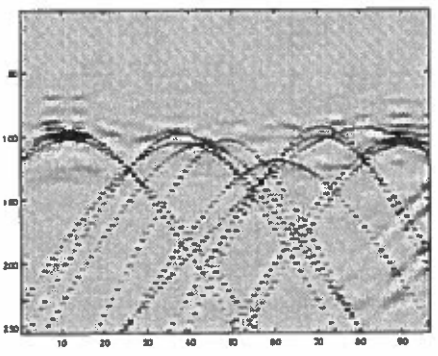

Figure 3: The detected hyperbolas in a pre-processed B-scan image.

Table 1: Feature Comparison between Raw and Pre-Processed Data

	Raw Data		
	Depth	Velocity	Eccentricity
PMA-3	4.7 cm	5.7e+7 m/s	20.5
Sphere	6.5 cm	6.4e+7 m/s	21.0
Rock	4.9 cm	6.7e+7 m/s	20.8
PMA-1	8.1 cm	7.0e+7 m/s	23.1
	Pre-processed Data		
	Depth	Velocity	Eccentricity
PMA-3	5.6 cm	6.9e+7 m/s	19.8
Sphere	6.1 cm	7.1e+7 m/s	19.9
Rock	6.4 cm	6.5e+7 m/s	19.1
PMA-1	5.6 cm	7.2e+7 m/s	19.8

For the C-scan processing two types of visualization were mentioned in the theoretical part: *three dimensional segmentation*, and *array beam imaging*.

An example of a result for the first method, using the watershed approach, can be found in figure 4.

In figure 4, subplots (a) and (b) show two horizontal slices of the original data. The final segmentation of subplot (c), clearly shows the result of the interaction between an object and a GPR waveform. Due to the fact that the GPR beam is not focused, the reflected energy has a hyperbolic distribution. This was already visible in the B-scan images, and the 3D segmentation shows the 3D hyperbolic shape very clearly.

An example of the results for the *array beam imaging* can be found in figure 5, which represents a mine, a metal sphere and a rock. Figures 5a-c show some representative slices of the original data. In none of these slices the objects are visible in a way they can be extracted. Figure 5d, shows the visualization after processing. One can see that at the positions of the objects there is a build-up in reflected energy which gives a good idea of the presence of said objects. Only a very small amount of clutter remains in the processed image.

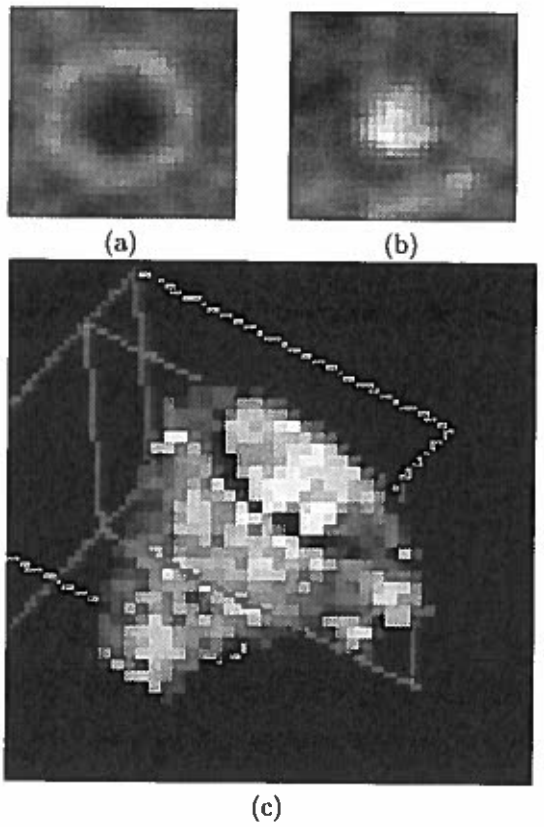

Figure 4: A result of the three dimensional segmentation on GPR data. (a) and (b) slices of the original data, (c) the 3D segmentation results.

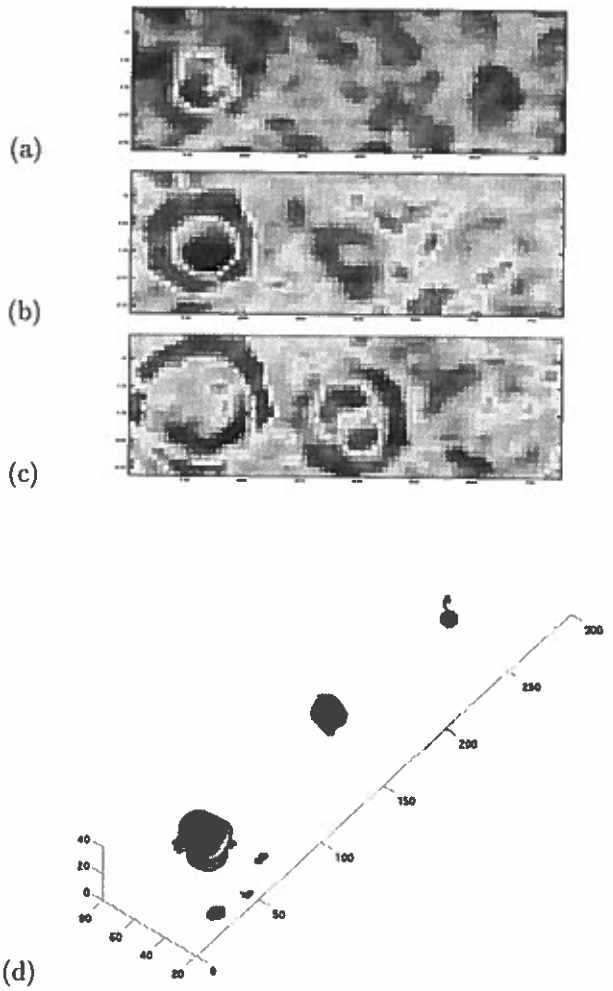

Figure 5: A result of the array beam imaging on GPR data. (a)-(c) are representative slices for the original data, (d) is the resulting visualization.

3.2 Ultra Sound

One of the main advantages of ultra sonic equipment is the confinement of the ultra sonic beam. Therefore in these kind of images there will be no blurring of the objects, and they can be visualized in great detail. Figure 6 shows the result of such a visualization: the three dimensional reconstruction of a scanned mine (the mine was placed under a layer of water).

The shape and structure of the mine can be clearly recognized in this kind of images.

3.3 Infra Red

The results of the application of the dynamic processing approach to a sequence of images that was acquired during 24 hours is demonstrated in figures 7 and 8.

The original image sequence (48 images) is represented by three sample images in figure 7.

In these images a change in contrast between the buried mine (in the lower left corner), and the gravel background, in function of time is visible. However, in none of the images, the contrast is such that the mine can be easily extracted.

Figure 8.a shows a scattergram, a plot of the distribution of pixel grey values in the two first transformed images. In the case of figure 8, the Kittler and Young transform is used. This scattergram shows a clear separation between the mine (small cluster) and the background. Figure 8.b shows the first transformed image, where the contrast enhancement due to the dynamic information in the sequence is quite clear. Figure 8.c finally represents the segmentation of the resulting image, based on the scattergram.

The results for the processing of the static IR images, based on mathematical morphology are summarized in figure 9. Figure 9.a shows one of the original images in the sequence (the object in the lower left corner is hardly visible). Figure 9.b shows the results after enhancement. The object is now visible, however, the signal to noise ratio in this image is bad, so a direct segmentation on this image will not prove to give good results. Figure 9.c shows the results after a smoothing and noise reduction algorithm was applied [7]. Here the regions belonging to the same part in the scene have received a more homogeneous grey value. Finally figure 9.d shows the segmentation results based on the watershed algorithm. One can see that not only the mine in the lower left corner was isolated, but also a mine in the center of the image, which was buried deeper.

Figure 6: A three dimensional reconstruction of a mine using ultra sonic data .

Figure 7: A number of sample images from the original sequence.

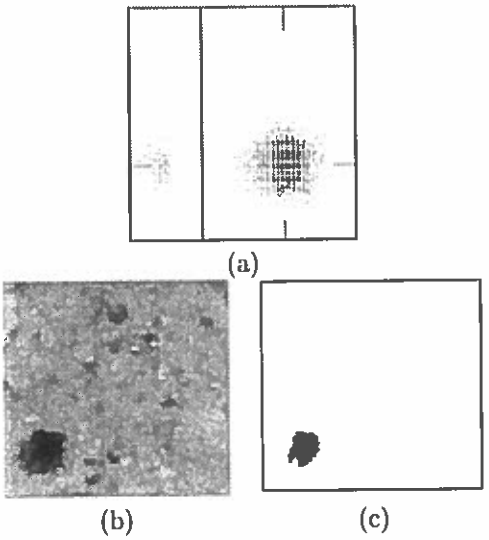

Figure 8: Histogram, first of the transformed images and segmentation results, based on dynamic processing.

4 Conclusions and Discussion

4.1 Ground Penetrating Radar

For this sensor, the research showed that since the GPR's and application circumstances are extremely diverse, the processing chain will never be completely independent of the GPR type. The same reasoning leads to the conclusion that a universal database of mine signatures, although useful for experiments, will not directly lead to generic solution methods. Instead, the suggestion of an open classifier which can be trained in the field is made. The training can then be done on a number of mines, which one expects to find locally and in the same time be adapted to the local soil properties.

Finally one can conclude that if the factor of shape has to be introduced in the recognition scheme, the necessity for acquiring regular C-scans will become imminent.

4.2 Ultra Sound

Since the experiments we performed with this sensor were limited, the conclusions we draw are globally the same as for GPR. However, although the setup that was used for our experiments was not ideal, the visual results are quite good. Due to the confinement of the ultra sonic beams the precision of scanning can be very high, leading to detailed data. However, both to reduce the acquisition time and to enhance the detection capabilities, it is suggested to use an array of probes in eventual future experiments. This, combined with an adapted processing (cfr. the phased array theory) can lead to good results, in those circumstances where other sensor types will perform less than optimal.

4.3 Infra Red

The results with the infra red data show that the presence of an anomaly in a scene can be detected and isolated. However in order to go a step further and have a recognition of these objects, a physical reasoning will always be necessary. This physical model will have to include a large number of variables such as environmental variables (air temperature, humidity, rain, time of day,...), local variables such as the characteristics of the ground, etc. Since such a model will be prone to errors, the use of IR equipment will probably stay in detecting objects, as a support of other sensor types. However an infrared feature that shows some promise is the use of polarization, which could at least result in a supplementary set of features for the distinction between natural and man made objects.

Acknowledgements. The overview of results, described in this paper, could be made in the context of the following funded projects: HUDEM (Mod Belgium, coordinated by RMA), VUB (research council), DEMINE (EU: HPCN 29902, coordinated by TUI).

The authors would like to thank the DeTeC (EPFL) group for the very constructive collaboration and the help for implementing the sensor test site at VUB.

References

[1] L. van Kempen, H. Sahli, E. Nyssen, and J. Cornelis, "Signal processing and pattern recognition methods for radar AP mine detection and identification," *IEE Second International Conference on the Detection of Abandoned Landmines (MD'98), Edinburgh, UK*, pp. 81–85, October 12-14 1998.

[2] H. Sahli, E. Nyssen, L. van Kempen, and

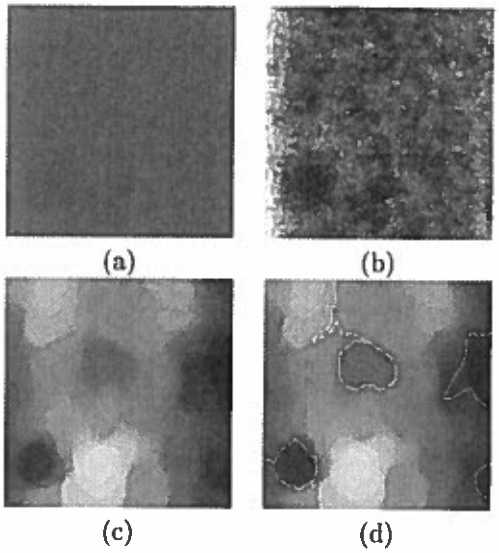

Figure 9: Static processing results: (a) original image, (b)enhanced image, (c) image after noise reduction and (d) segmented image.

J. Cornelis, "Feature extraction and classification methods for ultra-sonic and radar mine detection," *IEEE CESA'98 conference, Tunis, Tunesia*, pp. 82–87, April 1-4 1998.

[3] I. Pratikakis, H. Sahli, and J. Cornelis, "Low level image partitioning guided by the gradient watershed hierarchy," *Signal Processing*, vol. 75, pp. 173–195, 1999.

[4] L. van Kempen, E. Nyssen, H. Sahli, and J. Cornelis, "Pattern recognition experiments for ultra-sonic and radar AP-mine detection," *Proceedings SUSDEM'97, International workshop on Sustainable Humanitarian Demining, Zagreb, Croatia*, pp. S5.48–S5.54, Sept 29 - Oct 1 1997. Also Published in *Sustainable Humanitarian Demining: Trends, Techniques & Technologies* by the Humanitarean Demining Information Center at James Madison University, 1999, pp 297-304.

[5] R. Ekstein, "Anti-personal mine detection - signal processing and detection principles," Master's thesis, Vrije Universiteit Brussel, Pleinlaan 2, 1050 Brussels, Belgium, 1996-1997.

[6] L. van Kempen, M. Kaczmarec, H. Sahli, and J. Cornelis, "Dynamic infrared image sequence analysis for anti-personnel mine detection," *IEEE Benelux signal processing chapter, Signal processing symposium, Leuven, Belgium*, pp. 215–218, March 26-27 1998.

[7] G. Basterra, "Mathematical morphology techniques applied to anti-personnel mine detection," Master's thesis, Vrije Universiteit Brussel, Pleinlaan 2, 1050 Brussels, Belgium, 1998-1999.

Turning surface radar scans into three-dimensional buried mine positions

Colin Windsor, Lorenzo Capineri and Leonardo Masotti*
Department of Electronic Engineering, University of Florence,
Via S. Marta 3, 50139 Florence, Italy;
**and 21, Blackwater Way, Didcot, OX11 7RL, UK*

ABSTRACT
A method is presented for the rapid evaluation of buried object positions in three dimensions from sets of ground penetrating radar (GPR) range measurements. The "ringing" signal from the reflected object in any one scan is correlated with that of its neighbours to produce a set of range values. Randomly chosen sets of three range values are then used to solve analytically for the three co-ordinates of the mine position. A three-dimensional plot of the results is developed to give an intuitive image of the estimated buried object position and the relative uncertainty. The method is demonstrated using measurements recorded and made available by the DeTeC group at EPFL, Lausanne, Switzerland. The depth of a typical anti-personnel land mine buried at 100 mm nominal depth in sand is evaluated to around 25 mm accuracy and it position to around 30 mm.

Keywords: mine detection; radar; GPR; signal processing

1. INTRODUCTION

There is a clear need for rapid evaluation of the complex data patterns produced by ground penetrating radar (GPR) when used for the detection of buried anti-personnel mines. A review of the GPR method has been given by Daniels [1]. The problems of using GPR for the exacting task of detecting anti-personnel mines in the field have been reviewed in the Proceedings of the SusDem'97 Conference held in Zagreb in 1997 [2].

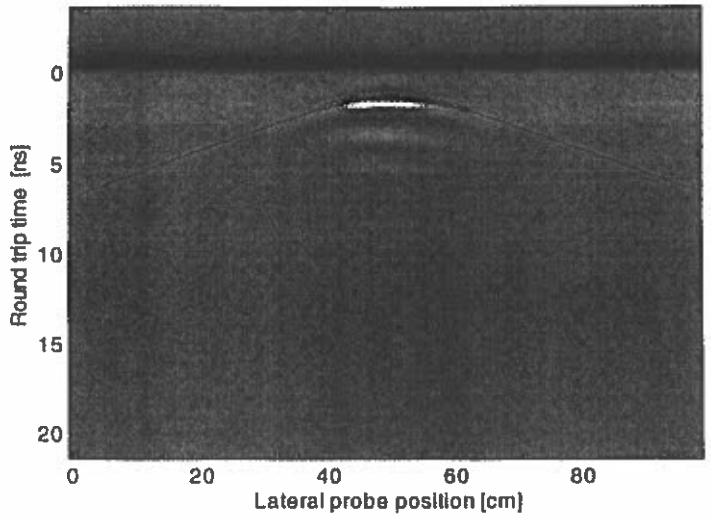

Fig. 1. The Ground Penetrating Radar (GPR) signal reflected from an anti-personnel mine buried in sand, recorded as a function of probe position, and elapsed time from the initial radar pulse. The grey scale image is fitted to the dynamic range of the reflected radar signal to form the B-scan of ultrasonic studies. The strong signal at nearly constant time is from the sand surface, the arc-like signal shows the changing range of the mine across the scan. The black circles show the results of the "correlation following" method described later, and the black curved line shows the calculated signal deduced from the three-dimensional position of the mine as found by the method.

The signal reflected from the mine at any given sensor position generally has several superposed "ringing" waveforms reflected from the ground surface, from the mine, and from other scattering centres such as rocks, tree roots, bottle tops, or shrapnel. A scan recorded as a function of sensor position, as in the "B-scan" of Figure 1, shows a nearly constant range for the ground surface, and a characteristic hyperbolic arc from the scattering centre indicating the changing range to the object as the sensor is moved.

Such patterns can be analysed to show the position along the scan of nearest approach to the object, but many such B-scans, taken along different sensor paths, must be analysed to determine the defect position in three-dimensions. The evaluation of such complex sets of scans requires great skill, since the patterns from several displays need to be assimilated. The problem is even more difficult in practice since the scans are frequently performed not as a simple raster along two orthogonal directions, as shown for example in Figure 2, but as a polar scan as a function of radius and angle from a given point, as a continuous scan produced for example by an oscillating arm travelling at a constant speed. To analyse such generalised scans requires the correlation of the signals between a given point (x_i,y_i) with a series of points (x_j,y_j) over the raster satisfying the condition that $|(x_i,y_i) - (x_j,y_j)|$ lies within the range of the signal from the object to be found.

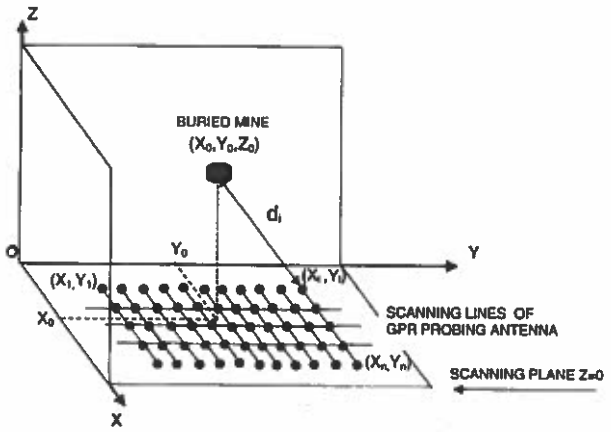

Fig. 2. A possible raster scan for a Ground Penetrating Radar source over a buried object at position (x_o,y_o,z_o). The scan may be analysed into a series of range measurements giving the distance d_i as a function of a series of n positions (x_i,y_i) $(i=1,n)$ of the sensor within the plane. In this figure the Z axis represents the depth coordinate.

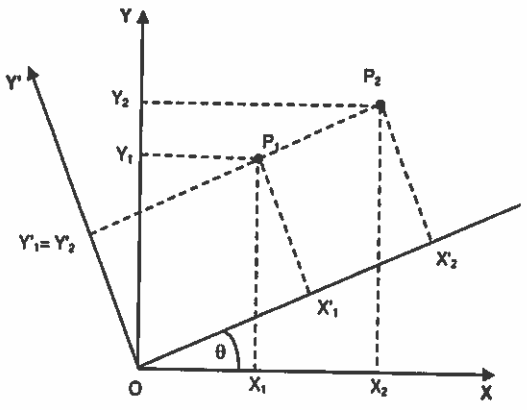

Fig. 3. The rotation of axes in the xy plane which enables two of the three selected positions (x_i,y_i) with i=1 and i=2 to become points (x_i',y_i') such that $y_1' = y_2'$, and so enable the equation for x_o' to be solved from a linear equation.

2. THEORY

Suppose the transmitted GPR pulse may be assumed to be a sharp delta-function at a time t=0. The reflected pulse, recorded as a function of the time of flight t_{tof} is then measured to form the "A-scan" of ultrasonics notation $A(t_{tof})$. For a point-like object at a position (x_o,y_o,z_o) the reflected signal will be centred on a time

$$t_{tof}(x_i,y_i) = t_o + 2\sqrt{[\,(x_i - x_o)^2 + (y_i - y_o)^2 + z_o^2\,]}/v \qquad (1)$$

depending on the velocity v of the radar pulse in the medium and the constant known time t_o of the signal reflected from the front surface of the medium. If these two constants are known, the time-of-flight signal may be immediately transformed into a range distance signal $d_i(x_i,y_i)$ such that

$$d_i(x_i,y_i) = v(\,t_{tof}(x_i,y_i) - t_o)/2 = \sqrt{[\,(x_i - x_o)^2 + (y_i - y_o)^2 + z_o^2\,]} \qquad (2)$$

In principle any three range signals with indices i_1, i_2 and i_3 can be used to solve for the three unknowns xo, yo and zo. For this three-dimensional case, the three quadratic equations can be reduced to linear equations by a rotation of axes in the xy plane. The first step is to subtract the expressions for d_1^2 from that of d_2^2 for giving

$$d_2^2 - d_1^2 = x_2^2 - x_1^2 - 2(x_2 - x_1)x_o + y_2^2 - y_1^2 - 2(y_2 - y_1)y_o \quad (3)$$

The terms involving y vanish in the special case when the points i_2 and i_1 lie parallel to the x axis so that $y_2 = y_1$. However even for

$$\tan\theta = (y_2 - y_1)/(x_2 - x_1) \quad (4)$$

the general case, the axes x and y may be rotated by an angle θ as shown in Figure 3, so that with respect to the transformed axes x', y' we have $y_2' = y_1'$. This occurs when
The equations for the transformed variables are then

$$x_i' = x_i \cos\theta + y_i \sin\theta ;$$
$$y_i' = - x_i \sin\theta + y_i \cos\theta . \quad (5)$$

Equation 3 then becomes in the transformed co-ordinates system

$$d_2^2 - d_1^2 = x_2'^2 - x_1'^2 - 2(x_2' - x_1')x_o', \quad (6)$$

from which x_o' is given by

$$x_o' = 0.5(d_2^2 - d_1^2 - x_2'^2 + x_1'^2)/(x_1' - x_2'). \quad (7)$$

It is now possible to use the analogue of equation 3 with points i_3 and i_1 to give the following expression for y_o'

$$y_o' = 0.5(d_3^2 - d_1^2 + (x_1' - x_o')^2 - (x_3' - x_o')^2 + y_1'^2 - y_3'^2)/(y_1' - y_3') \quad (8)$$

Having found x_o' and y_o' it is a simple matter to substitute in equation 2 with point i_1 to give the following value for z_o

$$z_o = \sqrt{[\, d_1^2 - (x_1' - x_o')^2 - (y_1' - y_o')^2 \,]}. \quad (9)$$

In practice many choices of the three $d_i(x_i,y_i)$ with $i=i_1$, i_2 and i_3, may not correspond to any real object position (x_o,y_o,z_o), give a negative square root argument and should be abandoned.
The true object position in the original co-ordinate system may now be evaluated from the inverse equations 5

$$x_o = x_o'\cos\theta - y_o'\sin\theta ;$$
$$y_o = x_o'\sin\theta + y_o'\cos\theta . \quad (10)$$

3. THE "CORRELATION FOLLOW" METHOD APPLIED TO A LAND MINE BURIED IN SAND

GPR scans from commonly found land mines buried in sand or soil have been collected by the DeTeC team at EPFL Lausanne Switzerland and have been made freely available [3]. Here we consider just one set of scans from a mine (type PFM) buried in sand at a nominal depth of 100mm.

The data acquisition used was a SPRscan from ERA Ltd., equipped with one 1 GHz antenna.
The scans take the form of two sets of raster scans along the X and Y axes over the mine as illustrated in Figure 2. Figure 1 gave an example scan showing a clear reflection from the mine without complications from other significant reflectors. The series consists of 21 B-scans along both the X and Y directions with at least some indication from the mine. The reflections from the mine in many of the scans can be correlated together so that the set of scans is particularly suited to demonstrate the present method. Later papers will describe more complex GPR scans including several overlapping arcs which could also be analysed, in principle, using the present method.

The "correlation follow" method has been recently described by Windsor and Capineri [4], and is used unchanged for the first stage of the analysis of each B-scan. The process of arc extraction can commence on any B-scan with a strong signal, by performing a search over the whole recorded scan below the strong surface reflection, for the position of maximum signal change. This position, defines a particular phase position within the ringing signal which will be maintained throughout the arc-extraction process.
The method searches the hyperbolic arc points following the maximum correlation between consecutive signals (A-scans) over a defined correlation window. When two arcs intersect or when the signal to noise ratio is low, the correlation becomes poor and the method attempts to recover this situation searching forward for a good correlation with signals relative to further lateral probe positions. During this search the correlation window is always placed on the direction calculated with an average local gradient. An average gradient can be calculated at each step with the last m points of the arc. This momentum term in the gradient, resulted effective to solve critical situations for arc extraction that otherwise could have led to premature end of the search or wrong search directions. The search methods ends when the signal to noise ratio is below a defined threshold or when all the allowed attempts failed to find a good correlation [5].

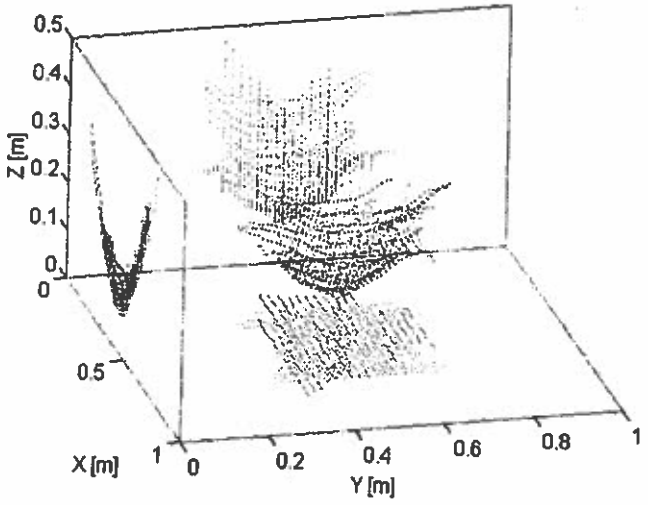

Fig. 4. (Left) Three-dimensional plot of extracted arcs from the data set of B-scan images for the buried mine in sand (type PFM). The projection on the cardinal planes are displayed together with the extracted arcs. Arcs points in black; projected points in grey.

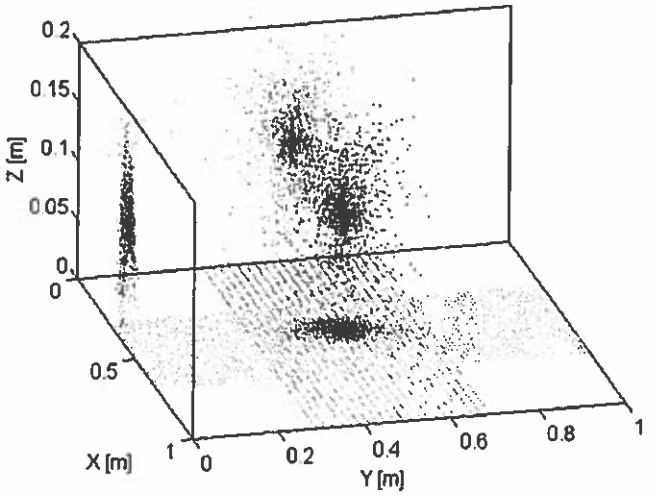

Fig. 5. (Right) Estimates of the position of the buried mine, at the final stage of the inversion process. The points within the accumulator space are displayed in black in real coordinates x,y,z. The z axis corresponds to depth, the x and y axes correspond to the GPR probe position within the plane of the scan. The centre of gravity of the spatial position is displayed as a three-dimensional (3D) cross. The projections of the distribution on the cardinal planes are displayed with grey points together with the centre of gravity position. The points have different weight but here are all displayed in black colour. The 3D cross position corresponds to the estimated buried object position and the spread of the distribution provides a qualitative information of the estimate uncertainty. In this case depth of the mine was estimated at the position (x,y,z)=(430,490,105)mm with standard deviations (29,25,23)mm.

4. THREE-DIMENSIONAL VISUALISATION OF RESULTS.

A test set of images was obtained by the DeTeC project [3]: the mine type PFM series of images was downloaded and processed from that database. The mine, a small air-delivered plastic anti-personnel mine with low metallic signature, was buried in a tank box filled with sand (estimated phase velocity $1.5*10^8$ m/s) at four different depths: 10mm, 30mm, 50mm and 100mm. Each set of measures consists of 21 B-scans on the X-direction and 21 B-scans on the Y-direction. The scan length of the radar probe is 1 meter, the distance between two parallel scans is 20mm. The collection of hyperbolic arcs extracted from images corresponding to a nominal mine depth of 100mm, can be displayed with a three-dimensional plot, as shown in Figure 4.
In the following three-dimensional plots, the reference system of Figure 1 was rotated to provide a more clear view of results. It can be observed that the ensemble of arcs is enveloped by an hyperbolic surface as predicted by the equation (1) of time of flight. The minimum of this surface corresponds to the lowest depth detected for the buried object. The regularity of the extracted arcs according to equation (1) can be easily checked in a quantitative and rapid way by the arcs' projections on Y-Z, X-Y and X-Z planes
The estimation of the buried object position is performed using this data set of points according to the inversion process described in section 2. For each triplet of points selected at random a possible object position is found. These positions are accumulated in a course of 3-dimensional accumulator space matrix and the process terminates when a maximum value is reached in any one cell of the accumulator. The centre of gravity of the points distribution in the accumulator is estimated and assumed to be the most likely object position. At the same time an associative accumulator is incremented detailing the coordinates of the possible object position. The accumulator contains floating points values in order to avoid the problem of X,Y and Z coordinates quantization. The points in the associative store can be displayed in real coordinates as shown with black points in Figure 5. The position of centre of gravity corresponding to the mine position is outlined by a 3D cross in Figure 5. In order to evaluate the accuracy of the positional estimates by eye, the variances of this distribution are presented as the projections of the points in gray color over the three cardinal planes.

	Nominal depth z=10mm		
	X	Y	Z
Centre of gravity [mm]	451	451	23
Standard deviation [mm]	29	32	12
	Nominal depth z=30mm		
	X	Y	Z
Centre of gravity [mm]	430	460	36
Standard deviation [mm]	23	28	18
	Nominal depth z=50mm		
	X	Y	z
Centre of gravity [mm]	414	479	42
Standard deviation [mm]	23	29	18
	Nominal depth z=100mm		
	X	Y	Z
Centre of gravity [mm]	430	499	105
Standard deviation [mm]	29	25	23

Table 1. The estimated position of a mine buried at different nominal depths in a sand box, from the original GPR images using the new method.

Moreover the length of the segments forming the 3D cross are equal to twice the standard deviation of the distributions. The set of 21 orthogonal lines on the scanning plane Z=0 in Figure 5 is a useful spatial reference for the determination of the X-Y coordinates of the buried object with respect to the raster scan with the GPR probe. The method was also tested with images from the same mine at smaller nominal depths. The results obtained by the automatic processing algorithm for each nominal depth (10mm, 30mm, 50mm and 100mm) are summarised in Table 1. For each image the buried mine centre of gravity is reported together with the relative standard deviations. The images were all similar to the example shown in Figure 1 in terms of signal to noise ratio, size and resolution. Two observations can be made on these preliminary results.

Firstly, the standard deviation of the depth (z-coordinate) in generally better than that of the x or y coordinates. This can be explained by the improved depth resolution given by our retention of the phase information in the back-scattered signal. It is easy to achieve values that are a small fraction of the wavelength calculated at the central frequency of 1GHz ($\lambda = v/f = 1.5\ 10^8\ /\ 1\ 10^9 = 150$ mm). Secondly the standard deviation of the depth estimate appears to worsen with deeper objects. This is probably due to the increased attenuation by the medium. The depth estimate at very short nominal depths, such as 10mm, appears to suffer from large systematic errors. This is probably caused by the strong interference between the reflected signals from the different surfaces of the mine, and from the air-sand interface.

CONCLUSIONS.

An algorithm has been developed to estimate the position of buried objects by processing three-dimensional data sets formed with GPR images. The main characteristics of the algorithm are:
1) independence from any particular GPR probe scanning method: suitability for test data taken at arbitrary probe positions
2) ability to correlate data from many scans, and so produce
a three-dimensional object position estimate
3) ability to estimate the probable error in the object position
4) ability to work with little operator intervention
5) fast processing speed
The algorithm has been tested on three-dimensional raster data collected using laboratory GPR by the DeTeC project for humanitarian demining [3]. The results show that a single buried landmine in a sandbox can be accurately detected within the depth range from 20 to 100 mm with an uncertainty better that 30mm. The present promising results obtained using this method will be extended by analysing further GPR images acquired in more realistic conditions. These need to include the use of real soil containing rocks, and the detection of the mine in the presence of other small metallic objects likely to be present in a minefield.

ACKNOWLEDGEMENTS.

This work was supported with the scientist mobility program of the University of Florence, Italy. We wish also to thank Prof. J.D. Nicoud at LAMI DeTec at Ecole' Polytechnique Lausanne, Switzerland.

REFERENCES

[1] Daniels D J, Surface penetrating radar for industrial and security applications, Microwave Journal, December 1994, pp 68-82

[2] SusDem'97 *International Workshop on Sustainable Humanitarian Demining Zagreb, Croatia, Sept 29 - Oct 1, 1997 , http://diwww.epfl.ch/w3lami/detec/susdem.html*

[3] Contact Prof. J-D Nicoud at LAMI-DeTeC , Swiss Federal Institute of Technology, IN-F Ecublens, CH-1015, Lausanne, Switzerland, Internet address
http://diwww.epfl.ch/w3lami/detec/gprsoft.html.

[4] C.G. Windsor, L. Capineri, *Automated object Positioning from Ground Penetrating Radar Images,* INSIGHT, J. of the British Institute of Non Destructive Testing, Vol. 40, N.7, July 1998, pp.482-488

[5] L. Capineri, C.G. Windsor and F di Zinno *Three Dimensional buried mine positions from arbitary radar surface scans* INSIGHT, Journal of the British Institute of Non Destructive Testing, Vol. 41, N.6, June 1999, pp.372-375

Mine Detection Using Infrared Imaging Technique

Mikael Georgson, Lars Pettersson, Stefan Sjökvist and Magnus Uppsäll

FOA Defence Research Establishment, P.O. Box 1165, SE- 581 11 Linköping , Sweden.

Keywords: Infrared Mine Detection, Thermal Modelling, Moisture.

ABSTRACT

The paper touches briefly on the theory of infrared radiation and the origin of thermal contrast in infrared imaging. Calculated temperature differences between the background and the surface above the buried object are compared to measured data from indoor experiments. Results from outdoor measurements are presented and show how the temperature difference can vary over a 24-hour period. The variation depends on the weather at the time as well as the weather before the measurement started. During periods of no precipitation there is a temperature difference of more than one degree Celsius for about 20 hours during a 24-hour period.

Introduction

The world wide problem of mine detection and clearance engage research groups on all continents. The techniques include metal detectors, ground penetrating radar, electronic noses and infrared, IR, imaging. Most of these techniques are solely used in hand held or vehicle mounted systems. However, an infrared system offers the possibility to scan a large area from an airborne platform. In such an application, the system can be used to point out contaminated areas instead of focusing on single mines.

To obtain a description of the behaviour of buried objects in soil, regardless of method, it is important to compare measurements with numerical simulations. A physical description of the interaction between the object and the surrounding allows an independent variation of parameters in order to study their influence separately.

This paper will discuss the possibilities and restrictions of using IR imaging technique in mine reconnaissance. Results of outdoor measurements on sand, gravel road and grass will be discussed as well as a comparison between measurements and calculations. The calculations were done using a thermodynamic description of the interaction between the sand and the object.

Theory

All bodies emit infrared radiation. For bodies at room temperature the maximum radiation is located at about 10 μm on the wavelength scale and at about 8 μm for a body at 373 K. In order to resolve objects using a thermal imaging system a difference in the emitted infrared radiation is required. This can be caused by either a temperature difference between the object and the background or an emittance difference of bodies at the same temperature. The thermal properties of mines are

different from the surrounding medium. This means that a contrast can be expected for surface laid mines when the environment and weather conditions are favourable. For buried mines the contrast occurs due to disturbances in the ground conditions. An object buried in soil change the conditions in the ground. The presence of an object alters the migration of water, which introduces a change in thermal conductivity and heat capacity, as these properties are dependent on the moisture content.

Model

A physical understanding of the origin of the thermal contrast is important to be able to predict the best possible conditions for mine detection. For that purpose numerical modelling[1] can be used to predict the thermal contrast. The model should include parameters such as air temperature, wind speed, solar irradiation, heat exchange with the atmosphere and soil moisture. The latter parameter plays an important role for the presence of thermal contrast. The model used for the calculations presented, in the following paragraphs, is based on the Finite Element Method. The conditions used in the calculations are the same as for the measurements and the model has been used to calculate the thermal behaviour for indoor as well as outdoor measurements. The calculations from the model have been compared to temperature measurements and readings from the thermal images from indoor registrations in dry sand. Figure 1 shows the temperature of the surface on top of a plastic AP mine, covered with about 5 mm of sand, and the background. The sand surface is irradiated with a solar panel, which intensity is varied for 8 hours to resemble the variation of the sun. The first pair of curves is the calculated values, the second pair shows values measured by temperature probes and the third is obtained from infrared images in the 8-12 μm region.

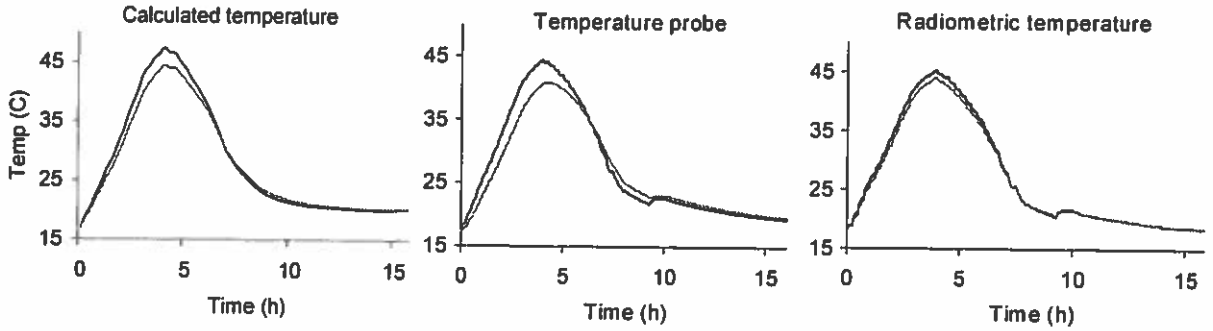

Figure 1. The graphs show temperature estimations for three different methods. The black curves show the surface temperature above the object and the grey curve the surface temperature for the background.

Figure 1 shows that the temperature is lower for the background than the area above the buried object, which is at a depth of about half a centimetre. The AP mine has a plastic shell, which is a poor heat conductor. For an aluminium-cased object the contrast is the reverse, due to a higher thermal conductivity than the surrounding. However, outdoor observations of measurements on aluminium cased wax have show the opposite contrast to the indoor measurement on metallic objects, which can be explained by inhomogeneous moisture content in the sand volume.
The results from the calculations can also be presented two dimensionally, showing how the isotherms penetrate the sand volume. Figure 2 show the isotherms at four different times during simulated solar irradiation for 16 hours for a volume containing aluminium cased wax with thermal properties similar to those of an AT mine.

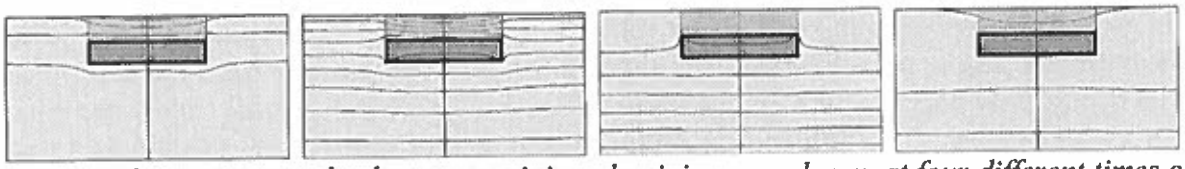

Figure 2. Isotherms in a sand volume, containing aluminium cased wax, at four different times of the day, from left to right, 8 am, 1 pm, 7 pm and midnight. At 8 am and 1 pm, the surface is absorbing energy, whereas it emits energy at 7 pm and midnight.

The first illustration of the temperature changes in the modulated volume show three isotherms and four different regions, the volume is beginning to warm up. The temperature difference between the regions is 1 degree Celsius. The second illustration shows the isotherms in the volume at 1 pm, which is close to maximum radiation. In the volume, there are several isotherms and it is clear from the shape of the isotherms that the aluminium shell conducts heat better than the surrounding. Furthermore, the isotherms are closer than in the first illustration, which is a result of an increased temperature.

At 7 pm, the surface starts to cool down. The isotherms near the aluminium surface have a different shape compared to the previous illustrations. This means that the heat is going in the opposite direction. This is even more clear in the last illustration. In this case the temperature is increasing with depth, in the first illustrations the highest temperature was on the surface. This means that from having a warmer area above the object as in the first illustration, it has now become cooler.

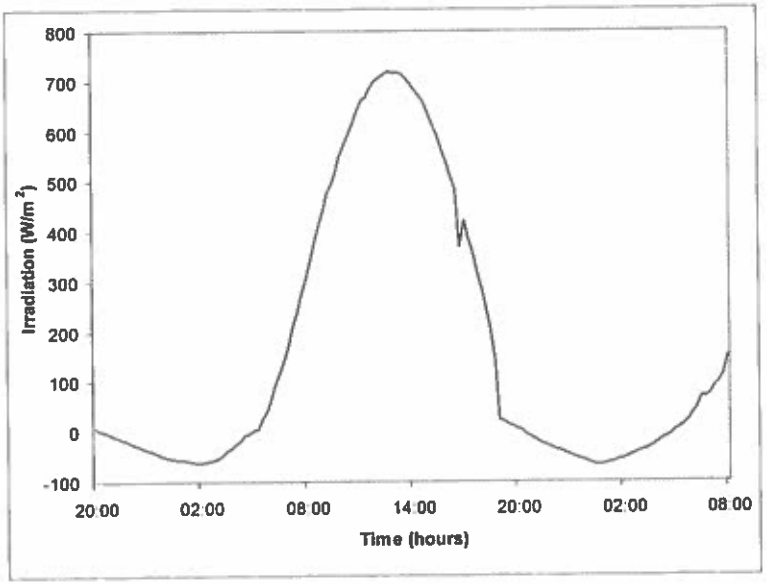

Figure 3. Time dependent irradiation used for calculating surface temperatures. Positive values are solar irradiation and negative are long wave emittance from the surface to the atmosphere.

The size of the object used in the calculations is 25 cm in diameter and 9 cm thick and buried at a depth of 5 cm. The sand volume above the object was assumed to be dryer than the rest of the volume. There was no moisture penetrating the sand volume from the sand surface. Instead, the moisture had to migrate from the sand volume towards the sand surface, as illustrated in figure 4, and the volume above the object will be dryer than the background. Consequently, the thermal capacity and heat conduction had lower values in this volume compared to the rest of the volume as the thermal properties are depending on the moisture[2].

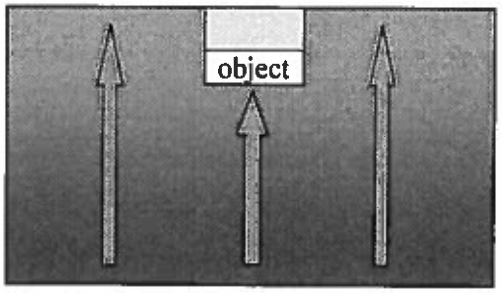

Figure 4. Mass transfer of water during periods of no rain.

The parameters, i. e. boundary conditions, used in the simulations for the heat exchange between the sand surface and the atmosphere are measured data from the weather station. The irradiation of the surface is according to the curve in figure 3. The curve has no wavelength dependence, i. e. it includes both the visible and the IR radiation. During daytime, the curve describes the solar irradiation in the visible and near infrared regions of the spectrum and the negative values during the night correspond to long wave emittance from the surface.
Figure 5 shows two infrared images of the same objects, appearing as bright spots in the upper right hand side corner of the left image. The image to the left shows the contrast at noon for two aluminium-cased objects, the same as discussed in connection with figure 7. The next image shows the contrast at midnight. What appeared as bright spots in the left image is dark in the right.

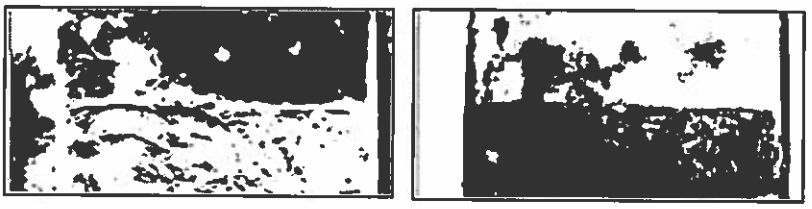

Figure 5. Two metallic objects in the upper right cornet of the two IR images registered at noon, left, and midnight, right.

Equipment and experiment

For the registration of the infrared images, an AGEMA Thermovision 900 system was used. Two cameras were used and images in the 2-5 μm and the 8-12 μm regions were recorded. The temperature resolution is 0.08 degree Celsius for the long wave camera and 0.1 degree for the short wave. Most of the analysis has been focused on the long wave band and the results presented in this paper are all from the long wave band. During the registration of the IR images the cameras were mounted about ten meters above the ground. The objects were buried in a box filled with sand. The size of the box is 5 by 3 m^2 and 0.7 m deep.
Weather data was collected using a system[3] that registered a number of parameters e. g. solar irradiation, air temperature and wind speed.

Results

Outdoor measurements done during a long period of dry weather show a contrast where the surface above the mine is warmer than the background. Using a lower value of thermal conductivity and heat capacity for the sand volume above the object compared to the background, the same values as for the calculations presented in figure 2, the calculation show the same contrast as the registration from the infrared camera. The calculated temperature variation is shown in figure 6. The grey curve is calculated for homogenous sand moisture using constant values for thermal conduction and heat capacity all around the object. The black curve shows the result from calculations using different values for thermal conductivity and heat capacity for the volume above the object and the rest of the volume.

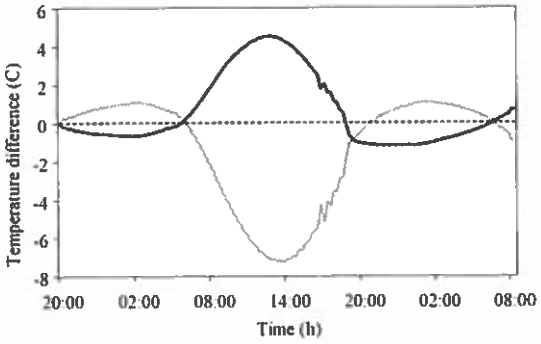

Figure 6. The grey curve is calculated for homogenous moisture and the black curve for different moisture contents in the volume.

Examples of measurement show that it is possible to find buried mines using the infrared technique. However, each situation is unique and success is dependent on both the environment and the weather influence on the soil surface.

The variation in thermal contrast is demonstrated in figure 7. The curves represent the temperature difference between the background near the object and the surface on top of the buried object as a function of time. The object is aluminium cased wax 25 cm in diameter and 9 cm thick. For the black curve the object is buried at a depth of 5 cm and for the grey curve the object is 15 cm deep. The shape of the temperature difference curves resembles the intensity curve of solar irradiation and indicates that the best time to look for buried objects is during the hours of high solar irradiation. Furthermore, the contrast is reversed during night. Consequently, there are two time intervals where there is no contrast between the object site and the background. These periods of low contrast can occur more frequently at unstable weather conditions.

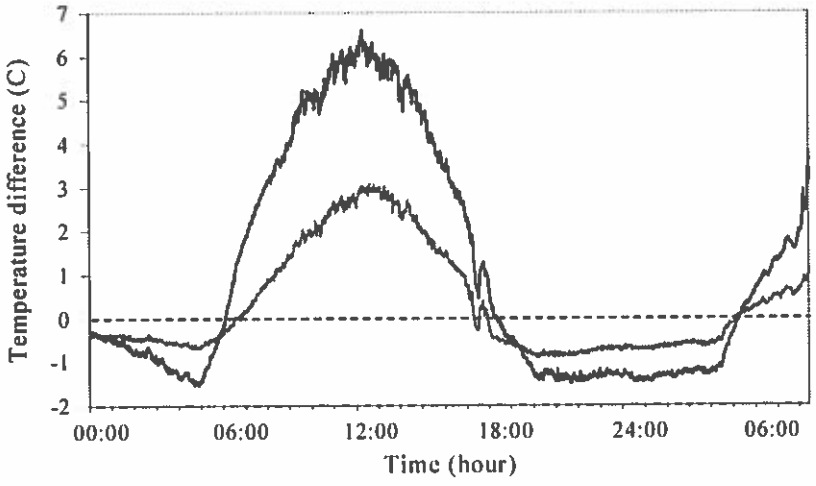

Figure 7. Temperature curves relative the background for buried objects at two different depths. The black curve represents an object 5 cm deep and the grey an object that is at a depth of 15 cm.

Immediately after burial of an object, a registration with infrared cameras will show effects of the digging rather than showing the presence of an object. With time this effect will fade away and the effect of the object will become clearer. An example of that is the temperature difference curves shown in figure 8. Registrations of two objects of the same kind as discussed in the previous paragraph were made. One had been buried for two weeks, black curve, and one for eight weeks, grey curve. After eight weeks the temperature difference curve is reversed to those of the indoor measurements on metallic objects. One explanation of the result from the registration of the more recent buried object is that two weeks was not enough for the dig marks to disappear and the sand is more homogenous with respect to moisture content.

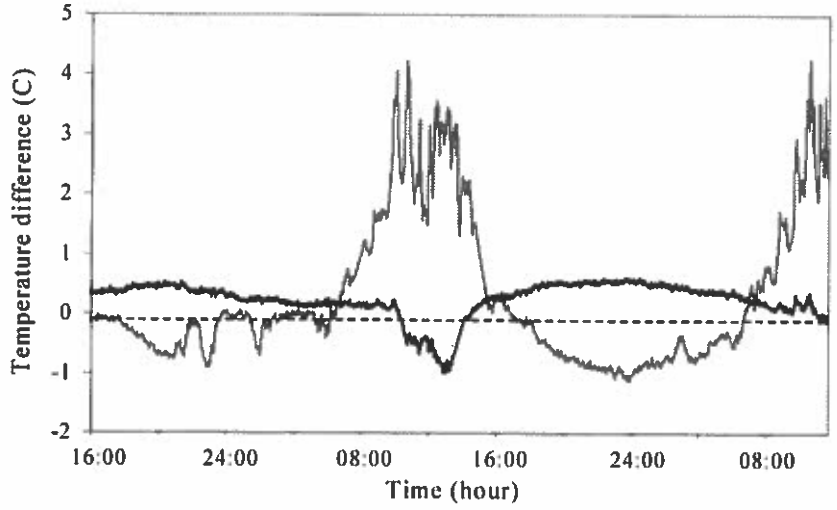

Figure 8. Registrations of objects at two separate occasions. The curves show the temperature difference as a function of time. The black curve represents the data recorded two weeks after burial and the grey curve the data recorded after eight weeks.

This discussion has focused on objects in sand. It is also possible to use infrared imaging for object detection in grass. However, this is an even more difficult situation with further restrictions when it comes to the possibility of detection. The soil properties become different and the background can vary in a short time giving rise clutter. Mine detection using infrared imaging systems will probably require an effective imaging processing[4].

References

1. S. Sjökvist, M. Georgson, S. Ringberg, D. Loyd, "Simulation of Thermal Contrast on Solar Radiated Sand Surfaces Containing Buried Minelike Objects." *2:nd Intern. Conf. on The Detection of Abandoned Land Mines*, pp 115-119, Edinburgh, U K, 12-14 October, 1998.
2. P. A. Jacobs, "Thermal Infrared Characterisation of Ground Targets and Backgrounds," *SPIE Optical Engineering Press*, ISBN 0-8194-2180-4, 1996
3. C. Nelsson and P. Nilsson, Ed. "Measurement Equipment at the Department of IR Systems," FOA-R--99-01111-615--SE, April, 1999.
4. M. Georgson, S. Ringberg, S. Sjökvist, M. Uppsäll, A. L. Christiansen. "Detection of Buried Objects with Infrared Imaging Technique, -Analysis of Outdoor Measurements."
2:nd Intern. Conf. on The Detection of Abandoned Land Mines, pp 120-123 Edinburgh, U K, 12-14 October, 1999

Searching dangerous terrain

Havlík, Š. and P. Scepko
Institute of Control Theory and Robotics, Slovak Academy of Sciences
Severná 5, 974 00 Banská Bystrica, Slovakia
Tel.: +421 -88-4152366, Fax.: +421-88-4152364,
E-mail: havlik@bb.sanet.sk

ABSTRACT.
Actual task of detection and neutralization of land mines abandoned on post battlefields is a big challenge for R&D in field of robotics. This paper briefly surveys problems and state of the art in development of robotic systems for this highly desirable humanitarian application. A concept of searching minefields is outlined. The development of a cable suspended platform with infrared camera and remotely controlled flail system with post cleaning verification are presented.

KEYWORDS: Demining, Sensing, Thermal imaging, Mobile Robot, Remote Control

1. INTRODUCTION

Much work has been done in the domain of detection and localization of mines. Beside known methods new sophisticated sensing principles able to detect and recognize mines as hidden objects are under development. As well as several vehicles equipped by demining technology are produced. [1].
Classic methods for detection and removing mines, used at present, are dangerous, too costly and considering the number of abandoned mines, are very slow. Within technologies for demining large mine polluted areas most frequently used are mechanical systems. Main drawback of this purely mechanical demining is that no system can satisfy the desired 100% reliability given for humanitarian mine cleaning. For this reason manual verification of cleaned area is required. For these reasons there is an urgent need to develop safe and efficient mine detection and demining methods. This is a big challenge for robotic research.

2. CONCEPT OF ROBOTIC DEMINING TECHNOLOGY

In general, the mine cleaning procedure consists of two tasks:
- *Detection and localization of land mines.*
- Neutralization i.e. removing or destruction of mines on place

Considering a robotic mine clearance technology an advanced system consists of following parts shown on Fig.1.

- ***Mobility system.*** Remotely controlled / autonomous / semiautonomous mobile (robotic) vehicle as the unified porter of other systems for detection and neutralization of mines is supposed. Solutions of such mobile robots are briefly discussed and two examples are given below.

- ***Multi-sensorial system for detection / recognition of mines.*** In principle, the sensory system can be situated on a special platform for scanning dangerous terrain, in front of the mobile vehicle, or, behind the vehicle (verification the demining procedure). A design example of the cable suspended robotic platform for scanning large operation space is given. Performing the scanning motions it is possible to create the map of all objects detected and recognized as mines. It is clear that no single sensor can detect all kinds of mines but fusion of information from several sensory systems is required.
- ***The system for destruction / neutralization of mines.*** Beside mechanical systems as for instance: rollers, ploughs, flails, rakes, ...etc, other principles that activate explosion of mines can be used. There are: explosive hoses, fuel air mixture, directed energy systems, laser, microwave or sniper rifle. Input data for these systems are positions / coordinates of objects recognized as mines.
- ***Control and communication systems.*** Principal requirement is that such a demining vehicle should operate in remote control mode, or, semi-autonomously. Concerning control a general system includes: mobility navigation / control, positioning the sensing or marking apparatus and the target positioning for destruction system. The communication system transfers large amount of control and sensory data to the operator's cabin.

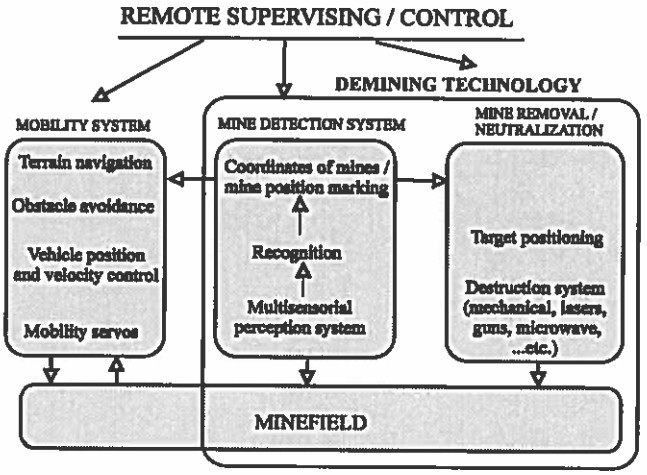

Fig.1. Global scheme of the semiautonomous robotic demining system

3. SEARCHING DANGEROUS TERRAIN

A robotic platform

Considering crucial working terrain condition and relatively large operation space the concept of the cable suspended robotic platform was designed [6,7].

The whole system, on Fig.2, consists of three columns with winch mechanisms, i.e. cable drivers and measuring systems built on remotely controlled vehicles. The ends of cables are fixed on the moving platform. This parallel kinematic structure exhibits 3 d.o.f. positional capability for the platform moving above the dangerous terrain. Controlling lengths of cables between the platform and end pulleys of winch mechanisms it is possible to move the platform to any position. The

central control system performs transformations and coordinated motion / position control of the platform with respect to a world reference frame. As obvious the geometry and actual operation space gives ground projection of the triangle created by fixation positions of three end pulleys A, B, C.
Regarding to this intended application this configuration exhibits some advantageous features as follows:

- Large workspace of operation, reconfigurable according to actual terrain conditions.
- Low weight and simple transport.
- Fast and simple installation on place.
- Operation / control in Cartesian coordinates defined directly on place.

The platform for this purpose is equipped by several ultrasound sensors what enables to control its height within a given distance over the dangerous terrain as well as to avoid any obstacles when perform searching motions.

Fixation of a sensing system (we intend to use the IR camera with two additional rotations) allows mapping the subspace in a given position of the platform. (Fig. 2)
Performing scanning motions it is possible to create the map of all objects detected and recognized as mines. (See Fig.3)

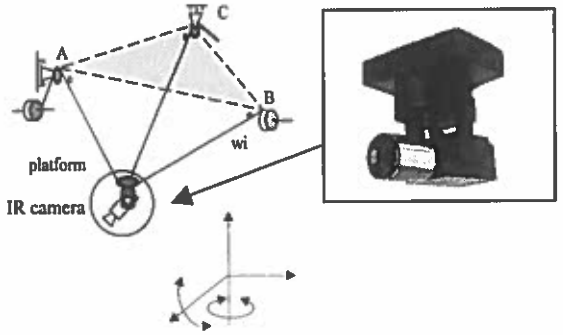

Fig.2. Searching system with IR camera

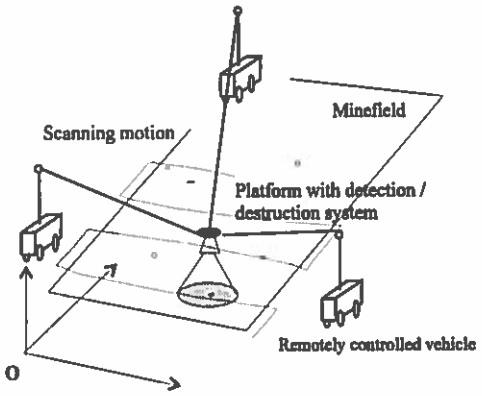

Fig.3. Concept of the searching operation

Four main problems have been solved for this system. There are:

- *Kinematic and force analysis* (motion and force transformation i.e. functions that relate actual motion and load values expressed in world reference coordinates and internal representation of control parameters i.e. cable length and internal forces).
- *Coordinated motion control* in world coordinates.
- *Dynamic analysis and control.*
- *Calibration,* i.e. to actualization of parameters in relations for motion and force transformations for a real arrangement of the whole system and its spatial geometry.

Sensing and thermal imaging

Infrared sensing and imaging is one of sensing technologies can be used for mine detection under some specific thermal conditions. The development of the IR camera which could be used for this purpose is briefly described below.

As follows from working conditions the sensing system should satisfy some principal requirements. There are:

- Robustness and long term operation
- Direct digital images and adequate sensitivity
- Ability to work in fusion with other detection systems

Based on theoretical analysis and design specifications [4,5] the first version of the system was built and some experimental measurements have been made.

Main functional parts of the thermal imaging system are shown on Fig.4. The system consists of four basic modules.

There are:

- optoelectronic module
- modules for analog and digital signal processing
- communication module

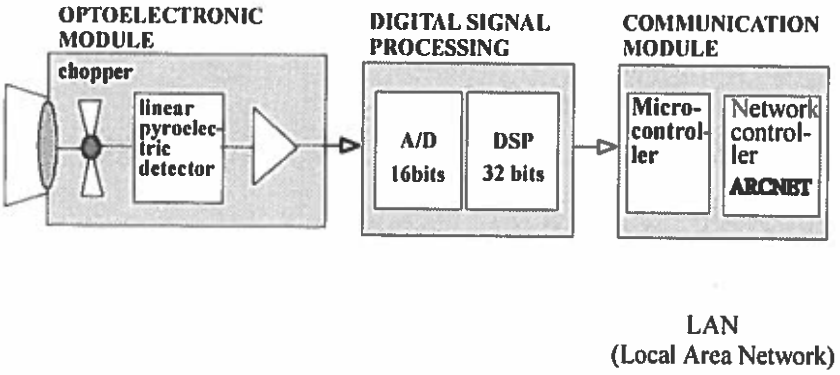

Fig.4. Main functional parts of the thermal imaging system

The uncooled detector consists of 128 pyroelectric elements arranged into a horizontal line. The desired 2D image is reached by scanning techniques. Two scanning modes are available:

- Moving by the detector inside the camera in vertical direction. The range of scanning zone is programmable. within 1 to 128 raws.
- Moving by the whole camera using external drives. This mode enables to scan the whole round scene, if desired.

What concerns to the performance specification the camera satisfies following parameters:

- spectral range of sensing	$\lambda = 8 - 12$ μm
- image dimensions	128 x 128
- number of temperature levels	16 bit (16389)
- adjustable measuring range of temperatures	0 -80 (or 50 – 1200) °C
- image frequency	2 Hz
- sensitivity (NEDT 20 °C with averaging 32x)	0,04 °C
- range of working temperature	-10 - +50 °C
- embedded signal processing (peak)	120 Mflops
- LAN interface (ARCNET)	5 Mb/s

Thermal signal / image processing

The thermal imaging system produces a temperature map. Each point represents a number that corresponds to a local temperature of objects transmitted by optics.

Remote sensing in case of mine detection / recognition require large amount of data processing and transfer. A useful tool seems to be a "Smart Thermal Camera" with embedded powerful signal processing module. In this case it is possible to process a great amount of image data directly in camera. Then processed /recognized objects / images are transmitted to operators console only. Processing thermal images includes SW general package which includes some basic image processing routines (camera calibration, filtering, temperature visualization, statistics, etc.) as well as some task related procedures that correspond to given processes / sensing areas, adjustable sensing sensitivity, etc.

Obviously, the SW recognition represents the main and dedicated part of the detection system. Learning algorithms including neural network approach are under study.

4. TELEOPERATED FLAILING SYSTEM

The demining system on Fig. 5, consists of following functional parts:

- The maneuvering vehicle.
- Two flailing mechanisms with rotating chains and hammers on ends. This mechanism can be manipulated in 2 d.o.f. according to working conditions.
- The radio communication system for teleoperation and remote mobility control as well as for manipulation with active flailing mechanisms.
- Television sensory system fixed on the platform with 2 d.o.f. positional capability.
- The operator's cabin with monitoring system.

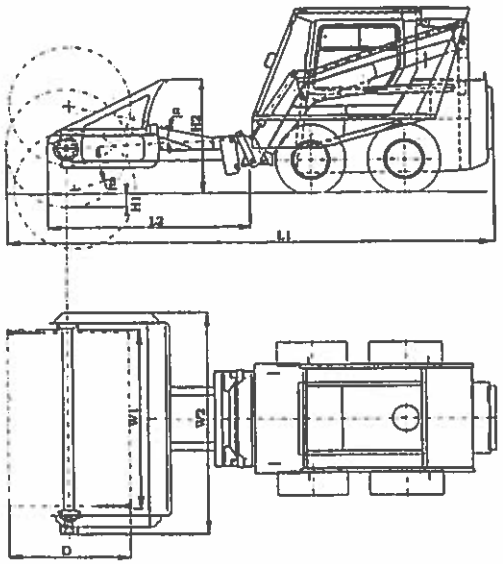

Fig.5. Side and top view on the demining vehicle
L1= 5282, L2 = 2180, W1 = 1985, W2 = 2457, D = 1300, H1 = 150 mm.

In order to satisfy maximal reliability (desired 100%) of the cleaned field crucial importance for this mechanical system play the mine detection systems.
What concerns to its placement, there are two possibilities:

a) The detection system is placed in front of the rotating flails. This brings several problems when consider vegetation as well as explosions of mines.
b) Detection system fixed behind the vehicle. From functional reason is is possible to verify yet cleaned area when terrain is practically without vegetation. By such an automatic way the need of human searching verification will be replaced. This concept was adopted in next.

5. CONCLUSION

Main attention in this research has been devoted to the development of the camera as well as terrain scanning system that exhibit specific features as mentioned above. According our preliminary experiments in order to detect hidden objects several improvements have to be made. There are:

- Thermal sensitivity / resolution of the camera should be about 0,05 °C , or less.
- Better results can be reached if the terrain to be searched is artificially radiated by a short thermal energy impulse from an additional source.
- A useful tool seems to be the equipment for precise camera positioning which allows sensing exactly the same thermal images in time sequence and compare thermal contrast considering different thermal conductivity.
- One of the limiting factor for using the IR detection technology is the homogenity of the searched terrain (vegetation, mud, stones, etc.). Considering cooperation with the demining flail system we consider to use this infrared camera together with other detection system for additional post searching the cleared field at first.

REFERENCES

[1] Proc. Int. Workshop on Sustainable Humanitarian Demining, Sept. 29 – Oct. 1, 1997, Zagreb, Croatia dtto in Sustainable humanitarian demining. Trends, Techniques and Technologies, Humanitarian demining Information Center, Madison University, 1998

[2] Holst, G.C. and Mc.Hugh, S.W.: Review of thermal imaging system performance. SPIE, Vol.1689 "Infrared Imaging Systems" (1992), pp.78-84

[3] Kawata, T. et al.: An inspection system for unmanned sewage disposal plants. 27 th ISIR Oct. 6-8, 1996, Milan, Italy, pp. 213-218.

[4] Kaplan H.: Machine vision: Photonic advances drive na exploding application market. Photonics Spectra, December 1996, pp. 72-79.

[5] Havlík, Š. Paník, J. and Ščepko, P.: Development of a thermal imaging system for robotics and automation. Proc. 5 th Int . Symp. on Measuerement and Control in Robotics (ISMCR'96), May, 9-11, 1996, Brussels, Belgium. pp. 140 -145

[6] Havlík Š: Concept, kinematic and control study of a 3 d.o.f. cable robot. Proc. IFAC Symp. on Robot Control, SYROCO 94, Sept. 19-21, Capri, ITALY, pp. 749-754

[7] Havlík, Š. and Kaek J.: A cable suspended robotic manipulator. Concept, kinematic and control study. Proc. Fourth Int. Symp. on Measurement and Control in Robotics. (ISMCR'95), June, 12 - 16. 1995, Smolenice Castle. Slovakia, pp. 237-242

EXPLODET : advanced nuclear techniques for humanitarian demining.

G. Nebbia, D. Fabris, M. Lunardon, G. Viesti
INFN Sezione di Padova and Dipartimento di Fisica dell'Universita' di Padova

M. Cinausero, E. Fioretto, S. Pesente, G. Prete
INFN Laboratori Nazionali di Legnaro

I.Lazzizzera, A. Sartori, G. Tecchiolli
INFN Sezione di Padova and Dipartimento di Fisica dell'Universita' di Trento

N. Cufaro-Petroni, G. D'Erasmo, G. Nardulli, M. Palomba, A. Pantaleo
INFN Sezione di Bari and Dipartimento di Fisica dell'Universita' di Bari

P. Prati, S. Zavatarelli
INFN Sezione di Genova and Dipartimento di Fisica dell'Universita' di Genova

V. Filippini
INFN Sezione di Pavia

R. Fonte, L. Pappalardo, S. Reito
INFN Sezione di Catania and Dipartimento di Fisica dell'Universita' di Catania

ABSTRACT :
The global problem of many countries infested with landmines demands new technical solutions in the localization and identification of hidden explosives, in particular anti-personnel landmines.
It is believed that only a combination of different sensors can fulfil the requirements of humanitarian demining activities.
In this respect, nuclear techniques employing neutrons have proven to be a viable tool in the identification of commonly used explosive at high nitrogen concentration.
Characteristic gamma rays emitted both in thermal neutron capture and in fast neutron inelastic scattering have been proposed as a signature of hidden explosives, in this sense a nuclear sensor is the only device capable of discriminating explosives from other hidden underground objects.
The present challenge is to conceive a cost-effective, mobile detection system based on nuclear techniques that can be operated in connection with other sensors in field conditions by a non specifically trained operator.

Key words : Thermal neutron analysis, detectors , landmine identification.

Introduction :

In the last few years the so-called "Landmine Crisis" has been brought to the attention of the general public because of the large impact played by abandoned landmines in the restoration of pre-war conditions of several countries after military operations were stopped. This crisis is due not only to the large amount of landmines spread over a number of countries around the world, but also by the low efficiency, intrinsic danger and high costs of the present humanitarian demining operations [1].

There is general political consensus , after the Ottawa treaty, to spur a technological development aimed at providing new tools for humanitarian demining operations, with the goal of decreasing at least by one order of magnitude the actual cost due for the neutralisation of a single explosive device. In this respect two different tools are needed : an "anomaly" detector and a bulk explosive detector. The first device should be able to perform a fast scan of the suspect area marking all places exhibiting a discontinuity in their thermal, electric or magnetic properties compared to the surrounding soil. In principle such detector does not identify that the discontinuity is caused by hidden explosive, unless a specific signature will become available in the future.
Therefore, in order to lower the false alarm rate presently characteristic of any "anomaly" detector, a bulk explosive device is also needed. Such device, only used to confirm the presence of explosive material in the previously marked target places , is foreseen to be based on one of the techniques presently under development such as the "artificial noses" the magnetic quadrupole resonance or nuclear reactions.

Theoretical background :

The italian Istituto Nazionale di Fisica Nucleare has started an R&D program called EXPLODET (EXPLOsive DETection), aimed at pushing the use of nuclear techniques in sensors designed for humanitarian demining once the state-of-the-art technical developments have been taken into account. An important part of such project is dedicated to the use of thermal neutron analysis , such technique , already tested in the past [2], is based on the neutron capture reaction on 14N contained in essentially all explosives in a much larger amount (about 20% by weight) than in most common materials and in soil (less than 1%).
The excited 15N nucleus thus formed de-excites with a probability of 18% by emitting a 10.8 MeV characteristic gamma ray , such radiation is higher in energy than all gamma radiation produced by neutron absorption in common materials, providing a rather unique signature for the presence of high concentrations of nitrogen.

Materials and methods :

In the foreseen optimisation of a nuclear sensor an important role is played by the neutron source. One has the possibility of using both radioactive sources such as Cf and AmBe or electronic sources generally based on the acceleration of a deuteron beam on a deuterium or tritium target.
The former have the advantage of the low price , small size and low weight, the latter , in particular the deuterium target ones have no radiation hazard once they are switched off.
The average energy of the neutrons emitted by fission sources as Cf is lower compared to sources based on (alpha-n) reactions such as AmBe, moreover the direct gamma radiation emitted by Cf sources presents a much softer spectrum than AmBe ones . As a cosequence Cf sources seem better suited for the present application, nevertheless the average energy of neutrons

produced by such radioactive sources is still very high compared to thermal energy needed to make the capture cross section in nitrogen useful for this application.
One then needs to design an optimum moderator to degrade the initial neutron energy into a range that allows the application of this technique. In the case of landmine detection the soil itself will act partially as a moderator producing a field of thermal neutrons in the vicinity of the target, MonteCarlo simulations show that the moderation capability of the soil strongly depends on the hydrogen content of the terrain (soil humidity), they also show that an increase of capture rate in nitrogen buried at typical landmine depth (about 20 cm.) should be obtained with the addition of an external moderator .
Moreover the neutron source should be embedded in some shielding material in order to reduce the external dose to a level not dangerous for the operator.
We have attacked this problem by experimentally measuring the flux of thermal and near-thermal neutrons produced by a Cf source inserted in a composite moderator made by a lead inner shell surrounded by a structure of high density poliethylene (HDPe) both in laboratory and field tests.
The detection of the 10.8 MeV gamma radiation emitted by the excited nitrogen nuclei has been the object of another part of the project in which different types of inorganic scintillators of different sizes have been tested.
For a field equipment one has considered design parameters such as dimensions and power requirements in the definition of the best detection apparatus, with this in mind we have proceeded to make experimental tests using standard NaI crystals 4"x 4" read out by photomultiplier tubes. Such detectors are traditionally used in high energy gamma detection for spectroscopy purposes, they have nevertheless a few drawbacks for the present application : the crystal itself is highly hygroscopic and thus needs to be sealed in an air tight container, the photomultiplier tubes are rather delicate , their gain response is affected by rate and temperature variations and they need a high voltage, high current power supply.
In this perspective he have performed a series of tests on CsI crystals of different sizes read out by a variety of silicon photodyodes (PD).
These solutions offer the following features : CsI is slightly denser than NaI and then the volume efficiency is somewhat better, light output is comparable, it is only slightly hygroscopic and needs no air tight sealing, it can be read out by silicon PD's biased at 40-50 Volts with virtually no current draining, moreover a typical PD is a very sturdy device with a size of 2x2 square centimetres and only a few millimetres thick. The important part of calibration of the apparatus and decision making is being implemented with the use of algorithms based on Artificial Neural Network (ANN) logic in order to render the sensor system completely automatic and its use viable to non specifically trained personnel.

Experimental results :

The study of the moderator composition and geometry has been performed using as an indicator for the flux of thermal neutrons a special detector made of a thin sheet of Cd mounted on a CsI crystal coupled with a PD and enclosed in a sealed container in such a way that the whole apparatus could be buried in the soil to test the neutron field in depth.
Cd has a large cross section for thermal and near thermal neutron capture (about 20 Kbarns) and de-excites with high probability via a 559 KeV gamma ray, so it is rather easy to use this signal to measure the relative thermalisation efficiency of the moderator.
Tests made in the laboratory showed that the optimum thickness of the HDPe moderator is about 5 cm. in the front direction, i.e. in between the source and the target, the side and back

parts also contribute (through multiple scattering) to the efficiency of the moderation process, their effectiveness saturates for a thickness of about 10 cm.
The same tests were done with the detecting device buried in the ground and an effect of the soil was evidenced since the overall moderation efficiency is increased when the target is positioned inside an open hole (4-8 cm. deep) in the ground, due to re-scattering effects by the terrain, while moderation and absorption by the terrain essentially cancel out when the sample is covered with soil.
Some effort was devoted to the optimisation of the detectors for the 10.8 MeV gamma radiation emitted by nitrogen.
For this purpose a sample of 800 g. of Melamine (a compound with a chemical structure similar to common explosives) has been used in the laboratory and irradiated with a flux of neutron moderated by a structure of HDPe with the optimum dimensions as described above.
Different sizes of CsI crystals (3"x 3" , 4"x 4") and NaI crystals (4"x 4") were used both with photomultiplier and PD red out.
The overall resolution and efficiency show best results for a combination of a 3"x 3" CsI crystal coupled to a PD of 28x28 square mm. , using a short (4 cm long) lucite light guide similar results are obtained using a 18x18 square mm. PD which is a factor 3 lower in price.
Resolution was tested on the 2.2 and 7.6 MeV gamma lines resulting from de-excitation of nuclei produced by thermal neutron capture in hydrogen and iron respectively, and resulted to be 6.1% and 2.1% to be compared with resolutions of 4.4% and 2.3% obtained for the same lines with a standard NaI crystal with photomultiplier read out.
The spectra obtained during these tests were then analysed using a self calibrating algorithm and a background subtraction based on a dynamical definition of a virtual background spectrum that make use of a single measurement instead of requiring two separate runs, one for the measurement and one for the background.
Study of the definition of the confidence level in detecting the nitrogen signal are still in progress and will be available within the end of this year.

Conclusions :

We are in the process of defining a prototype of a nuclear sensor for detecting landmines via the analysis of nitrogen content in a defined area in the ground.
The definition of the source-moderator assembly has been completed , also the detectors to be used in the apparatus have been defined and the construction of compact dedicated front-end electronics is under development, the decision making software is in progress and will be ready to be tested in field conditions within the year.

References :

[1] International Workshop on Localisation and Identification of APM, Report EUR 16329EN , 1995

[2] T.Gozani , Nucl. Instr. and Meth. B79, 601, 1993

Towards an Electronic Nose for Demining Based on Semiconductor Thin Films

M. Pardo[1], G. Niederjaufner, G. Benussi, E. Comini, G. Faglia and G. Sberveglieri

INFM and Gas Sensor Lab,
Dept. of Chemistry and Physics for Materials
University of Brescia, Via Valotti 9 - 25133 Brescia –Italy

ABSTRACT
The problem of sensing military grade TNT in air, sand and soil substrates is addressed by using tin dioxide thin film sensors. All measurements were carried out against their respective substrates with a static headspace sampling. It was found out that the detection can be performed in two steps. First an ANN, using as inputs features extracted from three SnO_2 catalyzed sensors (Pt and Au), distinguishes between the different substrate types, with or without TNT. Having determined the substrate, two bare sensors suffice to check if TNT is present. PCA plots show that the measurements quite clearly form two clusters.

Keywords: Electronic Nose, SnO_2 thin film sensors, static headspace sampling, neural networks

1) Introduction

The detection of unexploded ordnance such as antipersonnel mines is presently a lengthy and dangerous procedure. This task is carried out with the help of metal detectors or trained dogs. To render the detection more efficient various techniques are being proposed such as infrared spectrometry, radar and multispectral imagery analysis [1]. Recently the proposal of using sensors which try to detect an olfactory fingerprint of some constituents of the ordnance (electronic noses) has been put forward. In [2], for example, very low values (ppb) of DNT (2,4 dinitrotoluene) were sensed by SAW devices coated with polymers. In the preliminary study presented in this paper we attack the problem of recognizing TNT, even if in greater concentrations. At the present level of technology no single detection method can alone serve the purpose; data fusion seems to be mandatory for real applications.

The explosive charge of grenades, bombs and mines is made up of a primary or initiating and a secondary or high explosive charge. The primary explosive is easily triggered and immediately detonates. It is generally used to trigger the nearby secondary charge which forms almost the totality of the explosive. The secondary charge, having a high detonation speed (of the order of Km/s), produces a shock wave which is responsible for the destroying power of the weapon. It has to be stable in time and, on the contrary of the primary explosive, insensitive in order to be stocked and transported [3]. For military purposes, where high reliability is required, the mostly utilized secondary charge is TNT (2,4,6 trinitrotoluene) alone or in mixtures with components like RDX (cyclotrimethylenetrinitramine), HMX (cyclotetramethylenetetranitramine), PETN (pentaerythritol tetranitrate) and ammonium

[1] pardo@tflab.ing.unibs.it

picrate. The so called Composition B (40% TNT, 60% RDX, 1-4% wax) is used, by itself, for the production of projectiles, warheads and antipersonnel mines and as a starting material for the manufacturing of aluminized explosives. Others explosives such as nitrocellulose and nitroglycerin are largely used for civilian purposes but normally only for producing propellants by the army.
Since the vapour tension of RDX is negligible, we addressed the problem of sensing military grade TNT which has a vapour tension of 6 Pa at 80 ^{0}C [4]. The measurements were performed on TNT samples which also served to train dogs.

2) Experimental

Sensors

Five SnO_2-based sensors were deposited in a DC magnetron sputtering system from a pure Sn target according to the RGTO technique [5]. The RGTO (Rheotaxial Growth and Thermal Oxidation) technique consists of two steps: first the deposition a metallic film with DC magnetron sputtering from a tin target on a substrate, kept at a temperature higher than the melting point of the material, then the thermal oxidation in humid air in order to get a stoichiometric composition for the metal. The deposition of the metal on a substrate kept at temperature higher than the melting point of the metal (350°C) makes the film to grow with a high surface area. The thickness of the metallic film deposited is circa 300 nm for our samples. SEM micrograph of the surface the deposition show that there are spheres with dimensions ranging from 1 μm to 3 μm that aren't interconnected, hence there is no current flow between the contacts.
The metal-semiconductor phase transformation (Thermal Oxidation) is achieved by keeping the thin film in a furnace with a humid synthetic air flow (200 l/min) and making a thermal cycle of four hours at 250°C and thirty hours at 600°C. During these hours a little layer of oxide grow on the surfaces of the spheres and the second step at 600°C complete the oxidation. The oxygen incorporation in the lattice increases the volume of about the thirty percent, causing interconnection of the agglomerates and creating percolating paths for the current flow. A SEM image of the surface of the semiconductor film after thermal oxidation was taken; the agglomerates are porous and the porous surface is well suited for gas absorption [6].
To improve the sensitivity and the selectivity of the sensors we deposited a thin layer of noble metals as catalyst. For this special application we used two kinds of catalyst: Platinum and Gold. The thickness of these layers, deposited by sputtering onto the tin oxide surface at 300 for Platinum and 200°C for the others, was 4 and 5 nm respectively. TEM analysis shows that catalyzers form nanometric clusters.

1	2	3	4	5	6	7	8	9	10
0.3g TNT	Air	0.5g TNT + 2.5g soil	2.5g soil	0.6g TNT + 6g soil	6g soil	0.5g TNT + 2.5g sand	2.5g sand	0.45g TNT	Air

Table 1. The sample sequence

Sampling

Each sample shown in table 1 is introduced into a vial with a volume of 20cm^3 which is crimped with seal and septa. The vial is left in an incubation oven at 40°C for 30 minutes in order to reach gas-solid equilibrium. Part of the headspace is then extracted with a syringe and

injected, at strictly constant velocity, in the air flow which is used as carrier (static headspace scheme) [7].
Six successive extractions of the sequence shown in table 1 were performed separated by a time interval sufficient to reach equilibrium. As described in table 1 all measurements were carried out against their respective substrates. Sand for the manufacturing of concrete obtained by grinding pebbles was utilized. Since solid TNT in equilibrium is always present, all measurements refer to a saturation condition of the gas phase. This equilibrium is influenced by the substrate. In particular we expected the same results for the measurements with sand as for those with air and a smaller response for measurements with soil.

3) Data Analysis

For each response curve we preliminarily extracted one point of the baseline to see the drift and three tentative features, $R-R_0$, R/R_0 and R_0/R. The time evolution (60 points) of these features were then plotted for each sensor. This exploratory analysis permitted to make the following considerations:

1. Although a drift of the baseline is present the feature R/R_0 doesn't drift.
2. The catalyzed sensors do not distinguish between TNT + substrate and substrate alone (with the exception of the sand samples).
3. The bare sensors do distinguish between TNT + substrate and substrate alone but this difference is less than the difference between the various substrates.

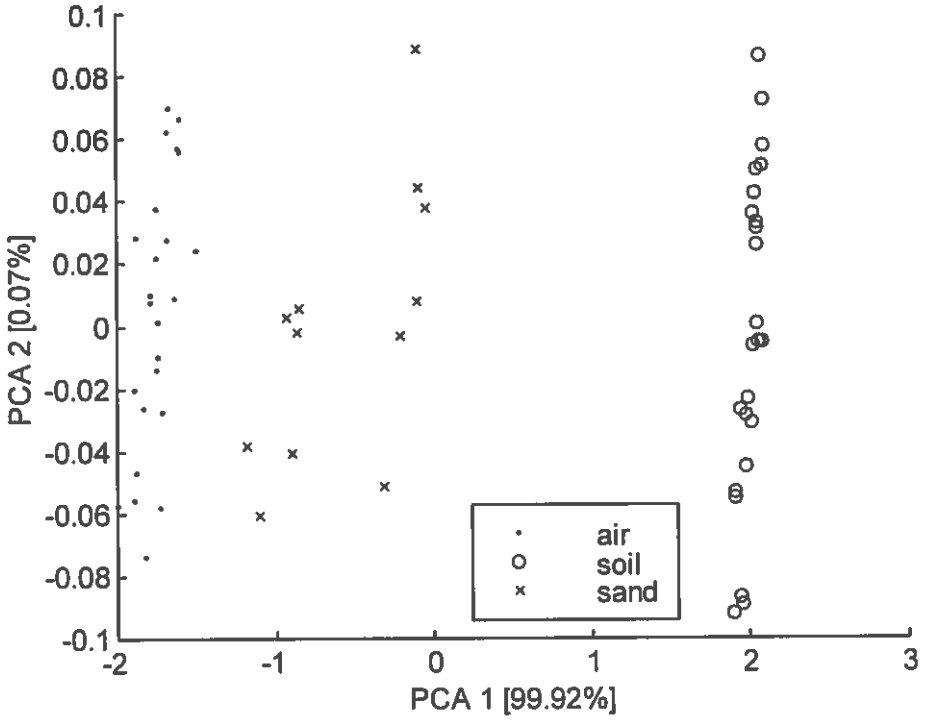

Fig. 1 PCA plot to distinguish between substrates.

These considerations lead us to split the data analysis in two steps:

1. Use the three catalyzed sensors to distinguish between the different substrate types, independently of the presence of TNT. The PCA plot for this separation task is shown in fig. 1. Three clusters can be recognized even if, as expected, there isn't much distance between sand and air.

The clusters are linearly separable. A 2-3-3 feedforward neural net was used to classify the data considering the scores of the two first PCs as inputs. The 16 test set patterns were correctly classified.

2. Check with the two bare sensors if TNT is present. A distinction in two clusters, i.e. TNT + substrate and substrate alone, for every fixed substrate type is evident from the PCA plots. See fig. 2 for the case of air. Being in a saturation condition at equilibrium there is no distinction between the two quantities of TNT (samples 1 and 9). In the case of the soil substrate a further distinction between the two different quantities of TNT is possible (samples 3 and 5).

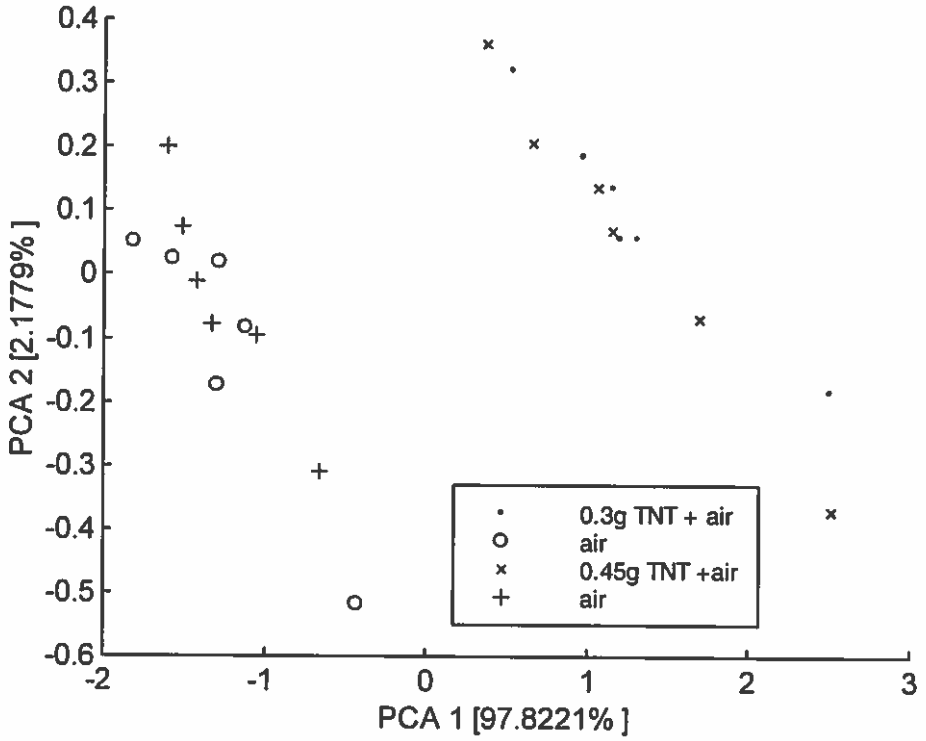

Fig. 2 Separation between air + TNT and air

4) Conclusions

We showed that the problem of sensing military grade TNT in air, sand and soil substrates can be addressed by using tin dioxide thin film sensors and pattern recognition techniques. Further work remains to be done regarding e.g. the reproducibility of the results between nominally equally prepared samples. Even the sensing property of the electronic nose when exposed to lower, more realistic concentrations of TNT vapor remains to be tested.

Acknowledgements

We thank Sorlini srl (Calvagese della Riviera, Italy) for hospitality and Dr. L. Regali for supervision during the measurements.

References

[1] X. Miao, M. Azimi-Sadjadi, B. Tian, A. Dubey, N. Witherspoon, Detection of Mines and Minelike Targets Using Principal Component and neural-Network Methods. IEEE Trans. Neur. Net. Vol 9 No 3, May 1998

[2] T. Mslna, R. Mowery, R. McGill, The Design of Silicone Polymers for Chemical Sensor Detection of Nitroaromatic Explosives. Proceedings of the International Meeting on Chemical Sensors, Bejing, 1998.

[3] S. Fordham, High Explosives and Propellants. Pergamon Press, 1980

[4] J. Boileau, C. Fauquignon, C. Napoly, Explosives. In Ulmann, 5th ed., Vol A10, 143-172, 1996

[5] G. Sberveglieri, G. Faglia, S. Groppelli, P. Nelli, A. Camanzi, A new technique for growing large surface area SnO_2 thin films (RGTO technique). Semicond. Sci. Technol., vol. 5, No 41 pp1231-1233, 1990

[6] W. Hellmich, Ch. Bosch-v. Braunmuehl, G. Mueller, G. Sberveglieri, M. Berti, and C. Perego, The kinetics of formation of gas-sensitive RGTO-SnO_2. Thin Solid Films, 263:231-237, 1995.

[7] M. Pardo, G. Niederjaufner, E. Comini, G. Faglia and G. Sberveglieri, Use of an electronic nose to classify different types of Italian cheeses. Proceedings of the 5th International Symposium on Olfaction & Electronic Nose, Baltimora, 1998, Technomic Publishers

How far can we push the chemical resolution of solid state gas sensors ?

Arnaldo D'Amico, Corrado Di Natale, Alessandro Mantini, Antonella Macagnano, Roberto Paolesse, Davide D'Amico*

*Dept. of Electronic Engineering and *Dept. of Chemical Science and Technologies, University of Rome "Tor Vergata"*
Via di Tor Vergata, 00133 Roma; Italy
email: damico@eln.uniroma2.it
PSM – CNR, Area della Ricerca di Roma "Tor Vergata"

ABSTRACT
Humanitarian demining is creating a broad interest on behalf of academic institutions, public research institutes, and industries as well.
This paper comments on some of the available mine detection techniques, such as nuclear quadrupole resonance and that based on the utilisation of neutrons for instance, and considers the possibility offered by solid state gas sensors. In particular, those based on resonators quartzes and SAW microbalances coated by biomaterials for the TNT detection will be illustrated. A perspective on the chemical resolution improvement, whose basic idea is taken from the working mechanism of living beings olfactory system, is illustrated as an alternative and promising research path.

Keywords: Chemical sensors, Nuclear quadrupole resonance, Microbalance Biosensor, Neural Networks

Introduction

Humanitarian demining is gradually creating a diffuse social consent and a growing interest on behalf of researchers belonging to different scientific areas who foresee, through a interdisciplinary and co-ordinated action possibilities giving prositive contributions to the detection of explosive with adequate resolution levels.
The many countries that have buried mines and threatened the life of people are calling for new more efficient and effective technical solutions able to localise and identify explosives especially those of anti-personnel mines. A new scientific approach to this important problem and a more pronounced effort in terms of number of researchers and founds, is mandatory in order to find the more appropriate solution in a time as short as possible.
A challenge may be represented by multisensors systems, which should combine different detecting techniques based on different chemical-physical principles. So far, a variety of approaches have been considered: radar technologies, optical and infrared systems, metal detection, direct mechanical scraping and, recently, other proposed solutions consider possibility of using artificial olfactory systems, nuclear instrumentation, x-rays, nuclear quadrupole resonance. This last also includes pattern recognition techniques, new biomaterials as chemically interactive materials for sensing molecules belonging to the class of explosives such as TNT. Among the many obstacles to mine clearance it is worth mentioning the high soil conductivity and metal contamination (different pieces of metals, etc.) which represent a serious problem for the metal detection techniques. Also the

vegetation represents a serious obstacle because it infers a slow down in the demining work. Infact, in some cases trees can seriously prevent demining machines for being used. Trained dogs may represent an interesting help for demining. Anyway, it suffers of many drawbacks such as the long training time, the fatigue showed on behalf of even suitable dogs, the tendency of dogs to pay little attention on the job, and the lack of communication means between dogs and trainers.
The best and fully satisfactory solution for demining as not yet found; if resolution could be improved solid-state gas sensors could represent a positive turn, while we have to think that new systems characterized by high-amplification, could play a substantial role.

Detection techniques.
Nuclear quadrupole resonance (NQR) is a mean of mine localisation based on the detection, by portable systems, of radio frequency signals coming from ^{14}N nuclei which are normally present into explosives; so it can be considered an r.f. Spectroscopy. In this context transitions of atomic nuclei, which have the form of electric quadrupole, are promoted by a suitable radiation externally induced. The frequency of the output signal depends on the quadrupole characteristic constants (coupling coefficient), asymmetry parameters, and surrounding conditions. The main drawback here is the fact that NQR depends on the chemical structure of the particular nitrogenous molecules under detection and discrimination cannot be so easy.
In practice r.f. bursts with a frequency close to the NQR frequency, and with a given duty cycle, are sent to the ^{14}N nuclei, and echoes showing the presence of ^{14}N, can be detected among bursts by detectors operating at about 1 MHz.
In the case of the Neutrons Technique, neutrons are sent toward ^{14}N nuclei and the detection of gamma rays emitted during the thermal neutron capture reaction from ^{14}N can be considered a sign of the presence of explosive containing nitrogen atoms. The main concern in this technique is the construction of a suitable mobile and low cost system eventually to be utilised in combination with other complementary techniques. One of the main problem here seems to be the background noise coming from competing reactions due to other materials present into the soil, such as silicon for instance.
Another technique called Ground Penetrating Radar (GPR) is based on the electromagnetic reflections. The penetration depth depends on the absorption function of the ground type and on the frequency of the antenna. In this technique a reflected signal is received and correlated to the depth of the reflecting source. Images can be taken and studied for the best interpretation that requires knowledge of geological and geomorphologic characteristics of the ground tectonic.
Finally images of land mines can also be produced by the use of positron-electron pair production induced by photons of energies of the order of MeV. In practical cases we can imagine to have TNT bombarded by neutrons. The ^{14}N will become a source of γ-rays of a sufficient energy to generate e^+-e^- pairs in a lead based detector. Identification of the TNT position is possible, once the background noise is, via software, substantially reduced.

Quartz Microbalance Biosensor

Quartz Microbalance Biosensors represent an important step ahead among the many attempts oriented to the mine detection problem. The principle utilised in this context is well known in its simplified version. A slice of quartz is used to control with a high stability (10^{-6} at least) an electronic oscillator. A changeable mass applied as a load to the quartz, induce a frequency change (Δf), given in a first approximation by the Sauerbray relationship:

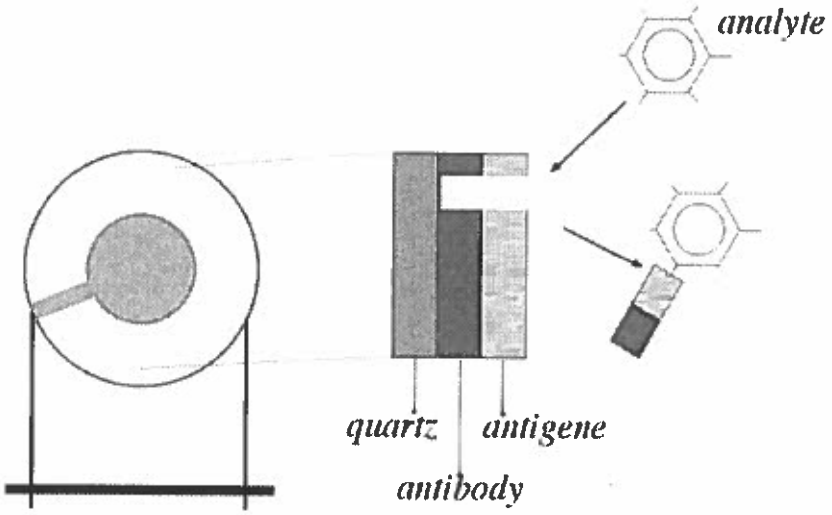

Figure 1: the principle of the high-resolution QMB biosensor.

$$\Delta f = -2.3 \cdot 10^{-6} f_0^2 \frac{\Delta m}{A}$$

Where f_0 is the unperturbed frequency, A is the quartz area, Δm is the mass change of the coating. This last is, in the case of QMB biosensor, a biomaterial such as an antibody sensitive to TNT. In demining applications, the QMB biosensor has already been tested in a two step approach. The first deals with the collection and compression of the vapour atmosphere, the second concerns its analysis. In the first step, an amount of air above a given field is drawn through a filter, able to absorb TNT molecules and then concentrated by a factor as large as 10^6, in a liquid medium. The quartz coated by an antibody is used to detect the TNT molecules. As a result of this process part of the antibody, captured by the TNT, dissolves into the liquid, leaving the overall weight of the quartz slightly reduced, and this generate an increase of the oscillator frequency. The reason of the frequency change can be related to the TNT concentration into the liquid (about 10^{-12}).
In virtue of the compression process, the total system can detect 10^{-12} ppm in about 3-5 minutes. Weak points of this system are the non-constant overall reproducibility and the non-uniform consumption of the chemically interactive material such as the specific antibody for the TNT.
Figure 1 shows the QMB biosensor principle.
Surface acoustic wave (SAW) devices also represent a promising mass transducer to be utilised for in liquid operation. In these devices the sensing action is given by surface acoustic waves acting as a probe of the mechanical and electrical properties of the surface coated by the antibody. The release of the antibody, induced by the TNT molecules, is detected as a change of the surface wave velocity, which produces a frequency change oscillator of which the SAW represent a delay line element. By this device, due to the intrinsic sensitivity with respect to the QMB, it is possible, in principle, to gain an order of magnitude of the ultimate resolution so to reach 10^{-7} ppm, in optimised noise conditions.

New directions and Conclusions

Olfactory systems of living beings suggest a way that may be followed, as another potential possibility, when we look forward very high-resolution sensors.

The nature has developed a biostructure very close to the concept of chemical amplification by which, for any activated receptor, a flow of a high number of ions across the cilia wall through channels opened by chemical actuators stimulated by exited receptors driven proteins. It would be extremely important to conceive, design and fabricate prototypes of solid state chemical amplifiers, where a useful signal suitable for pre-processing actions in conventional electronic devices, is triggered by a single molecule of TNT type for instance. In order to follow this idea, a substantial effort may be necessary at interdisciplinary level where combined competence's in the field of chemistry, interfaces, solid-state electronic devices and modeling represent the cultural ingredients to approach the fabrication of new generation sensors for the solution of the mines problems. Candidates for this new type of device are the electron multipliers and photoelectron multipliers, but also ionisation chambers can have a potential value.
In the meantime the use of combined systems seems to represent a possible way which can overcome the numerous drawbacks: nucelar systels and solid state biosensors. The only certain thing is that we must move faster to solve this problem is we want to have the number of victims substantially reduced.

Acknowledgement:
We acknowledge the support of the CNR - Finalised Project MADESS II, subproject Sensors.

References:
Proceedings of the Demining Technologies – International Exhibitions, Workshops and Training Courses, 29 Sept. 1 Oct. 1998, Joint Research Center, Ispra (Va); Italy

Combining results from different mine detection techniques

Colin Windsor and Lorenzo Capineri*

Department of Electronic Engineering, University of Florence,
Via S. Marta 3, 50139 Florence, Italy;
**and 21, Blackwater Way, Didcot, OX11 7RL, UK*

ABSTRACT

The life-threatening nature of mine detection means that operators instinctively see that combinations of detection techniques give greater certainty than any one alone. For example, they will not trust ground penetrating radar, until they have confirmed the indication with a metal detector and sealed its presence by prodding. These and the further methods of infra-red thermography, ultrasonics, thermal neutron capture, the artificial nose and visual detection can all be used in mine detection. This review sketches each technique and the diverse properties of the mine which they each measure. It then describes the principal methods available for combining the results from different techniques, in particular the Bayes method of partial probabilities, and the method of neural networks. Some examples are given from the literature.

Keywords: mine detection; data fusion; neural networks

1. INTRODUCTION

The human interface with the world includes the senses of sight, touch, hearing, smell and taste. Each one gives a quite different view of the world by measuring different properties of objects it may contain. Sight gives a three-dimensional image of its light reflectivity, shape and position. Touch measures its three-dimensional position with some additional texture and hardness information. Hearing records the sounds emitted by the object. Smell and taste record the chemicals it emits. The human brain is able to combine the information from all these senses, in order to make the best possible classification of the object. This is the process of data fusion - the combination of different types of measurement from a given object in order to make a classification.

Data fusion is sometime applied to the combination of different measurements of the same kind. For example our eyes take two two-dimensional images and fuse them to produce a three-dimensional picture of the field of view. Similarly a raster of radar scans can be analysed to construct a three-dimensional image of an object. We shall not include this aspect of data fusion in this review.

Figure 1 illustrates data fusion in mine detection. The field of view contains a mine, a lump of rock, a piece of plastic, a bottle top and a tin can. The metal detector shows up the tin can strongly, the bottle top less strongly and the mine only through a weak signal. The radar shows up all the objects, with a varying intensity roughly in proportion to their volume. The chemical nitrogen detector shows up just the plastic and the mine. No one technique discriminates the mine from the other objects. However the combination of all the three sensors shows up the mine uniquely.

2. THE TECHNIQUES OF MINE DETECTION

The main techniques used for anti-personal mine detection are given in Table 1, and will be described in turn.

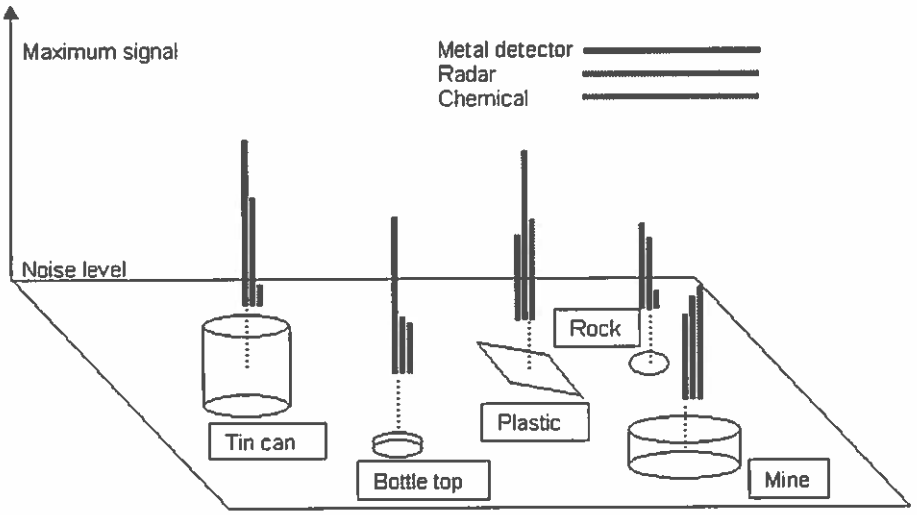

Fig. 1. A piece of ground containing a buried mine, together with a tin can, and bottle top, a rock and a piece of plastic. The three histograms show the metal detector, radar and chemical signals from each object. Only the mine returns a significant combination of positive signals from all three techniques.

Table 1

	Technique	Material property
MD	Metal detector	Conductivity
GPR	Radar	Dielectric
NC	Neutron capture	^{14}N concentration
	Thermography	Heat capacity Pemissivity
US	Ultrasonics	Elastic modulus/ Acoustic impedance
V	Visual	Surface appearance
P	Prodding	Hardness

Table 2

Classes		"mine" ,j=1	"no mine" j=2
i	Technique		
1	Metal Detector	$P(X_1 \mid C_1)$	$P(X_1 \mid C_2)$
2	G P R	$P(X_2 \mid C_1)$	$P(X_2 \mid C_2)$
3	Neutron Capture	$P(X_3 \mid C_1)$	$P(X_3 \mid C_2)$

Metal Detection

The traditional tool of the operator remains the electromagnetic metal detector. A pulse of current in windings in the detector induces eddy currents in any metal object. The eddy currents in turn produce a magnetic field which can be detected by electromagnetic induction in sensitive coils within the metal detector. The measured signal is dependent on the distance between the detector and the metal object, the amount of metal in the object and the conductivity of the metal object. Metal detectors are very sensitive, and can be built into arrays. They are cheap, reliable and easily tested and calibrated [1].

Ground Penetrating Radar

The electromagnetic spectrum is readily absorbed at most wavelengths by soil and sand. However at Ultra High Frequencies of say 500 MHz the radiation can penetrate the required 100's of millimetres necessary for buried mine detection. At this frequency the wavelength an average soil is around 200 mm, so that detection of mines becomes possible [2]. Generally an Ultra Wide Band ground Radar delivers a short pulse of radiation which is reflected from any object whose dielectric constant is different from the surrounding medium. In practice there is a reasonable contrast between soil or sand and the plastic and air of mines. However there is also good contrast with a solid piece of rock or metal. The time-of-flight between the initial pulse and the reflected signal can be used to determine the object range provided that the velocity of the radiation in the medium is known. For a point-like object, whose size is small compared with the wavelength, the reflected signal as a function of time-of-flight takes a "ringing" form with several ripples around a principle peak. The detailed shape of the reflection is determined by the form of the original pulse, the shape of the object, and whether the reflection comes from the top or the bottom surface of the object. Stepped or multifrequency

Radar can also be used to measure the variation of soil electrical impedance that can contains indications of the presence of a mine.

Neutron Capture
Explosives generally contain around 20% of atomic nitrogen, much in excess of the 1% level in most soils. This can be detected to good sensitivity from the gamma ray of characteristic 10.8 MeV energy emitted when a thermal neutron is captured. Both thermal neutrons and high energy gamma rays penetrate well through several centimetres of soil. The thermal neutrons are typically generated using a californium isotope source surrounded by a hydrogenous moderator which slows the neutrons down. The emitted gamma rays can be detected by a sodium iodide scintillator surrounded by photomultiplier tubes [3]. The method is not particularly sensitive but is strongly specific to the nitrogen target element.

Thermography or emissivity
A pulse of heat incident on the ground diffuses down into the soil and differentially heats up any buried object according to its heat capacity. An infra-red camera looking at the soil some milli-seconds later will see the heat flowing back to the surface and show any object of either higher or lower heat capacity as a dark or light shadow respectively [4]. The method is quick and can cover a wide area at a time. It is sensitive for objects just below the surface, but is sensitivity decays rapidly as the distance of the object from the surface increases. It is not essential to provide a pulse of heat since there will always be natural thermal gradients in the soil caused by the daily changes in temperature as the sun rises and falls. The water content of the sand or soil is an important factor in the actual difference observed.

Ultrasonics
Sound waves readily penetrate soil but their wavelength is too long to give any definition to a buried mine. The familiar medical high-definition ultrasonic scans are performed at millimetre wavelengths where scattering from sand or soil is rather high. However at the 100 mm wavelengths of 100kHz-frequencies a reasonable penetration through soil is possible with a specific design of highly efficient ultrasonic transducers. The problem remains that scattering can take place from any interface where the elastic modulus or the acoustic impedance of the material changes. Stones and cracks in the soil remain strong scatterers of ultrasonic radiation, so that any signal is superposed on a background of scattering from the medium.
Besides their low efficiency, air coupled transducer or laser induced acoustic pulses must be employed to avoid dangerous pressure on the ground that can trigger a buried mine.

Visual
All demining operators would begin by examining the surface of the ground beneath them. They would assimilate the type of ground, sand, soil or clay. They would search for signs of disturbed earth. Any metal or litter showing at the surface would be used to gauge the probability that more might be lying beneath the surface. They would note the position of any feature, such as a tree or bush, that defines the area and may restrict the use of other techniques.

Prodding
The other traditional tool of the operator is the simple stick which is gently prodded into the earth around the mine. The soft earth or sand gives way to the stick, while the relatively hard mine resists it. With skill the exact position of the mine is readily determined. The human skills of data fusion are well demonstrated in this progress, where the position to insert the stick is subjectively evaluated from the view of the ground and the measurements previously made with a metal detector. It is not too difficult to imagine some of these skills being applied by a robotic prodder in the future.

3. Theory of Data Fusion

Suppose we are using a series of N_T techniques T_i, where i=1, N_T to provide information on the presence or otherwise of a mine. For example for the first three techniques in Table 1, N_T =3 where T_1 = MD (metal detection), T_2 = GPR (radar) and T_3 = NC (neutron capture). We may think of this as a classification problem between N_C classes C_j, where j=1, N_C. Since we have just two classes representing the presence or absence of a mine, N_C =2 and C_1 = "mine" and C_2 = "no mine".

The most straightforward use of data fusion is when one or more variables measured by each technique T_i, have been processed to give a single variable X_i, representing the probability that a significant signal above the noise has been detected. For example a metal detector in typical terrain may have some background level B, with standard deviation σ, and a significant signal may be taken to be one with a magnitude greater than three standard deviations above the background. That is $X_1 > B+3\sigma$. We might then use historical experimental data to deduce the probability P_1 that the class C_1 = "mine" results from the experimental measurement X_1. Such probabilities are generally written in the form $P(X_i|C_j)$ representing the probability that measurement X_i will result in the classification C_j.
Now suppose that measurements have been made with N_T =3 techniques, MD, GPR and NC respectively, giving three probabilities $P(X_i \mid C_j)$ with i=1,3. An important result is that if the techniques are effectively independent, then a joint probability may be defined which is the product of the three individual probabilities

$$P(X \mid C_j) = \Pi_{i=1,3}\ P(X_i \mid C_j).$$

The example we have chosen is a good one in that the metal detector, radar and neutron capture techniques are independent in that they measure mutually exclusive features of the mine. The metal detector measures metal content, the radar dielectric contrast and the neutron capture nitrogen content. We may therefore use the probability product with confidence, and multiply the mine probability maps we have measured with each technique together to evaluate an overall probability. Figure 2 shows an example from the literature of a two technique probability distribution.
In general a matrix of probabilities may be defined with probabilities for each technique and for each class. In the present case we have the matrix shown in Table 2.
The story is more complicated than this in that we may be omitting a most important factor. This is the *a-priori* probability that a certain type of object may be present. For example in a given minefield there may be a mine only every 100 square metres, so that the *a-priori* "mine" probability $P(C_1)=0.01 m^{-2}$. However there may a much greater number of detectable objects that are not mines. Perhaps the pieces of metal, cans, bottle tops and the like occur every square metre so that the "no mine" *a-priori* probability is $P(C_2)=1.0\ m^{-2}$. If we neglect this factor we shall record too many false alarm "mine" classifications and the overall probability of successful classification will not be optimal. The factor may be allowed for using Bayes theorem, which states that

$$P(C_j \mid X) = P(X \mid C_j).\ P(C_j)/\ P(X)$$

The Bayesian probability $P(C_j \mid X)$ represents the conditional probability of obtaining the class C_j given the vector of inputs X. The denominator P(X) is essentially a normalising parameter reflecting the probability of recording the input value X . Since this is independent of class is does not alter the overall classification probability. In the case of mine detection there is another factor to be taken into consideration. That is the consequential penalty from a miss-classification. For example if a bottle-top is miss-classified as a mine, we have the false alarm situation and the result is some slight inconvenience. However if a mine is misclassified as a bottle-top we have a potentially life-threatening situation. We may therefore define a class weight $W(C_j)$, depending on the class C_j, representing the factor by which we wish to increase the probability of each classification class to make due allowance for the consequences of any miss-classification. Our modified Bayes' theorem might then become

$$P(C_j \mid X_i) = P(X_i \mid C_j).\ W(C_j)\ .\ P(C_j)/\ P(X_i).$$

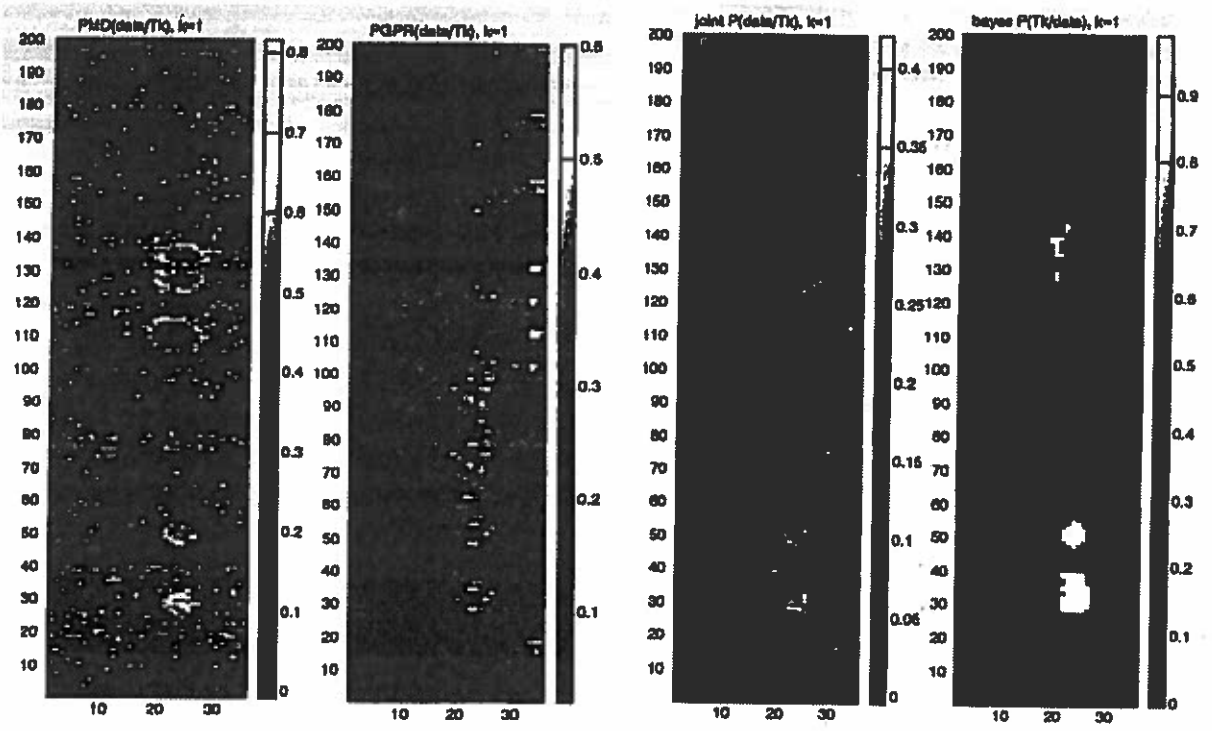

Fig. 2. From left to right, an area of ground containing several mines examined by (i) a metal detector, (ii) ground penetrating radar, (iii) the joint product probability, and (iv) the Bayes probability. In all cases the grey scale level indicates the probability with dark corresponding to low, white to high

In de-mining we might put for the "mine" class W (C_1)=1000 and for the "no mine"class W(C_2) =1, thus more than cancelling the *a-priori* probability factor and ensuring that any mines are given a high weighted conditional probability.

4. Neural Network Data Fusion.

In the above approach we have treated the mine probability factors $P(C_j \mid X_i)$ for each class C_j and technique X_i as evaluated independently, and then multiplied these probabilities together to give the overall probability. This has to be done because the signals from the individual techniques, say the metal detector signal and the radar signal, are assumed to be independent. Adding the respective signals together in any linear combination will not arrive at a any true basis for estimating the probability of a mine. Neural networks provide a non-linear discriminator which can combine inputs from two or more techniques in a way which will result in a valid probability of estimating the likelihood of a class, for example the probability of a mine being present [5].

The essence of the neural network method is training by examples. In the mine detection application, one might consider the objects in Figure 1 as individual training examples, which would be supplemented by "noise" examples where no identified object was present but the individual techniques naturally record the signal present from the soil, or sand. The signals from each techniques may here be represented by the intensities of the bar histograms shown in Figure 1(again we assume that there is only one input per technique, but that need not be the case in general). These signals become the input signals of the neural net as illustrated in Figure 3.

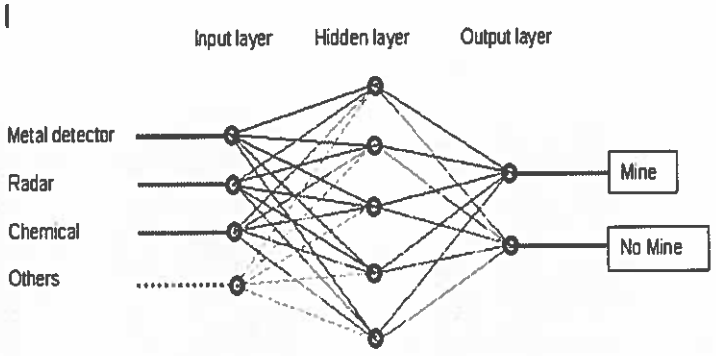

Fig. 3. A multi-layer perceptron neural network. Inputs from each mine-detection technique are fanned out to the hidden layer of "neurons" which perform a weighted sum of the input signals which undergoes a non-linear transformation to form the hidden layer signal. These signals are similarly summed in the output layer neurons to form output signals representing the "mine" and "no mine" probabilities.

Figure 3 shows an illustration of the multi-layer perceptron network which is widely used in classification problems [6]. The connections are thought to mimic the layered form of our visual cortex. One or more input signals from each detection technique used are fanned out to a "hidden" layer. Each unit in this layer represents a biological neuron and can act in parallel in performing a computation involving summing the input signals weighted by a variable amount w representing the biological synapse strength. The neuron performs a non-linear computation, usually through a sigmoidal function to give an output which is sent to the next layer. In a training process, sets of inputs from each object in the training data set are presented to the network sequentially. The class of the training object is known and may be used to define target outputs say 1,0 for the mine and 0,1 for all the other objects, including the noise examples. The weights w are then adjusted until the network outputs match their targets as nearly as possible. The training proceeds iteratively by presenting each example many times until the agreement, as represented by the squared difference between the target and the network output, is minimised.

CONCLUSIONS

The paper reviewed the main concepts of data fusion that is important for automatic target recognition based on data acquired with different techniques. The basic theory of data fusion is revised considering the application of mine detection which cannot accept misclassifications of mines. Finally the paper includes the basic concepts of data fusion with neural networks because this method can generalise the classification process when carefully trained, similarly to the deminers that they use their experience and senses.

REFERENCES

[1] C Bruschini, "Evaluation of a Commercial Visualising Metal Detector", Sustainable Humanitarian Demining. Mid Valley Press, Verona, VA, USA 314 325, 1998.

[2] D J Daniels, Surface penetrating radar for industrial and security applications, Microwave Journal, December 1994, pp 68-82

[3] T Gozoni, Nucl. Inst. Meth., B79, 601, 1993.

[4] G C Holst and S W McHugh, "Review of Thermal Imaging System Performance", SPIE, Vol 1689, "Infrared Imaging Systems", 78-84, 1992.

[5] M D Richard and R P Lippmann, "Neural Network Classifiers Estimate Bayesian *a posteriori* Probabilities", Neural Computation, 3, 461-493 (1991)

[6] C Bishop, "Neural Networks for Pattern Recognition", Oxford University Press 1995.

Multi Sensor Mine Signature Measurements at the JRC

J. Dean[i], A. Franchois[ii], J. Fortuny[i], D. Tarchi[i], G. Nesti[i], B. Hosgood[i], G. Andreoli[i] and A. Sieber[i].

[i] Technologies for Detection and Positioning; Anti-Personnel Mines, Space Applications Institute, EC Joint Research centre, Ispra (VA) Italy,
[ii] TTE Division, Section EM Faculty of Electrical Engineering Eindhoven University of Technology P.O. Box 513, 5600 MB Eindhoven The Netherlands

Keywords: mine signature, data fusion

Mine signature measurements have been performed at the experimental facilities of the Joint Research Centre of the European Commission, including far-field radar measurements at the European Microwave Signature Laboratory (EMSL), near-field GPR measurements with the Linear SAR facility (LISA), and thermal infrared measurements at European Goniometric Facility (EGO). The targets were reference objects, army training surrogate APL mines, simulant APL mines and mine-like objects. The environments were sand and soil at various humidities, gravel, mixtures of gravel and soil with and without vegetation cover.

In EMSL, full-polarimetric ultra-wideband backscatter measurements used a stepped-frequency radar in the range 0.3 - 9.5 GHz on targets in free space and buried. These data can be processed to extract typical target features. Near-field cross-polarisation measurements were done with LISA for targets buried in dry sand. FDTD simulations, which compared well to some measurements, indicated that the early time response may contain useful feature information. The response depends on the characteristics of the surrounding medium but not so much on the target depth. Environments also have been characterised. Using plane layers of material effective complex permittivity was derived from the measured the backscatter coefficient at perpendicular incidence. Checks with an open-ended probe and a ring resonator were also done.

In the European Goniometric Facility (EGO), a series of test measurements of the Bi-directional Reflection Distribution Function (BRDF) has been made. The spectra of a selection of mines were measured in the 400-2500 nm range. For partially or totally exposed targets, plastics and rubber presented clear spectral characteristics. A further step for future work is to determine the minimum exposed portion of a mine, which is necessary to give a significant signature.

A high-resolution CCD camera working in the near infrared range (NIR) was also employed in the goniometer to characterise the response of these mines at different angles of observation and illumination. BRDF measurements in VIS/NIR and thermal infrared (TIR) ranges of selected soil types were also made, including flat and Gaussian rough surfaces of those materials, in order to characterise the environmental conditions. In the TIR range using the 6-20 micro-metres band, a significant change in BRDF, due to specular reflection, was observed for some materials of the limited samples of APLs available, when the target was partially or totally exposed. While for plastics and rubber the signatures were not meaningful, metals, e.g. copper and steel tripwires, yielded a significant specular component. In addition, in the outdoor test area, under ideal conditions with the mine a few centimetres below the surface of dry sand, the presence of a foreign object could be recognised by scanning with a TIR radiometer. With vegetation cover however, recognition was practically impossible according to test results. Some measurements have also been made to study the long term variations in the temperatures of buried objects using a TIR radiometer.

Results of these measurements are being made available together with sensor evaluation results, for the use of researchers and data fusion algorithm developers, in a database

Sensor systems and near-field inversion algorithms for microwave imaging of buried objects

Ch. Pichot[1], C. Dourthe[2], E. Guillanton[1], J.Y. Dauvignac[1], I. Aliferis[1,3], P. Millot[4]

[1]Laboratoire d'Electronique, Antennes et Télécommunications
Université de Nice-Sophia-Antipolis/CNRS
250 Rue A. Einstein, Bât. 4, 06560 Valbonne, France

[2]Centre d'Enseignement et de Recherche en Modélisation,
Informatique et Calcul Scientifique/INRIA,
2004 route des Lucioles, BP 93, 06902 Sophia Antipolis, France.

[3]Department of Electrical and Computer Engineering
National Technical University of Athens
Iroon Polytechniou 9, 157 73 Zografou, Athens, Greece

[4] Département ElectroMagnétisme et Radar
ONERA/CERT
2 avenue E. Belin, BP 4025, 31055 Toulouse Cedex 4, France

ABSTRACT

The detection and identification of buried inhomogeneities using electromagnetic waves are of crucial importance for nondestructive testing in military or humanitarian applications. The paper deals with investigations on different signal processing methods, ultra wide-band transmitting and receiving antennas for a multifrequency-multistatic system. Two classes of algorithms are considered here. For the first class, a global qualitative reconstruction based either on Diffraction Tomography or a SAR-like algorithm is presented, delivering tomographic images for detecting the objects and obtaining an idea of the shapes. In the second class, a quantitative algorithm has been developed for reconstructing the complex permittivity profile of the buried objects.

Keywords: microwave imaging, tomography, Ultra Wide Band antennas, SAR

1. Introduction

The detection and identification of buried inhomogeneities using electromagnetic waves are of crucial importance for nondestructive testing in military or humanitarian applications. Step frequency ground penetrating radar (GPR) can be an attractive option for such applications. Sensors that are used in radar systems e.g. resistively loaded dipoles, biconical antennas and bow-tie antennas are required to transmit at least octave or ideally decade signals. The paper deals with investigations on different signal processing methods, ultra wide-band transmitting and receiving antennas and sensor arrangement systems.
Two classes of algorithms are considered here. For the first class, a global qualitative reconstruction based either on Diffraction Tomography or a SAR-like algorithm is presented, delivering tomographic images for detecting the objects and obtaining an idea of the shapes. In the second class, a quantitative algorithm has been developed for reconstructing the complex permittivity profile of the buried objects. The nature of such an inverse scattering problem being strongly nonlinear and ill-posed, the study has concerned a spatial iterative reconstruction algorithm based on a numerical method and able to give an efficient solution. This algorithm is therefore computationally more intense and cannot be used, at the moment, for real or quasi-real

time tomographic reconstructions but for post-processing of the measured data. Using multifrequency operation, the different algorithms process the backscattered field signal generated by the buried inhomogeneities and measured by a synthetic probing line. Concerning the approach based on diffraction tomography (DT), the method originally developed for multifrequency and plane wave illumination has been extended recently in order to take into account the near-field pattern of the broadband antenna illuminating the buried object. The SAR-like algorithm called compensated near-field SAR takes into account the presence of soil with a given permittivity. The third algorithm is based on an integral representation of the EM field and the moment method to generate matrix relations. A biconjugate gradient (BiCG) method is used is used to minimize a cost functional in order to retrieve the contrast permittivity and conductivity profiles of buried inhomogeneities. A regularization procedure has been derived recently using Edge-Preserving (EP) potential functions. This regularization scheme has been implemented in the BiCG method and the enhancement is significant. The near-field pattern of the transmitting antenna is also taking into account and incorporated in the reconstruction algorithm.
Investigations have been made on the design and performance (return loss, radiation pattern, antenna gain) of a new ultra-wide band antenna (bandwidth of more than one decade) offering new capabilities as sensor in connection with the inversion algorithms.
Tomographic reconstructions of buried objects with the different algorithms are considered for situations of practical interest using bow-tie antennas, conventional medium gain antennas and new ultra-wide band antennas as transmitter and sensor.

2. Imaging algorithms

2.1 Qualitative diffraction tomography

The geometry (Fig. 1) is two-dimensional and we consider two different media $\{D_i\}_{i=1,2}$. The presence of two media is not restrictive and the theory can be easily generalized to M different stratifications. The object region D_d is in general inhomogeneous and embedded in a lossy medium D_2 (soil). Each domain $\{D_i\}_{i=1,2,d}$ is characterized by dielectric permittivity ε_{ri} and conductivity σ_i, respectively we assume to be frequency independent in the considered bandwidth. The buried object is illuminated by means of a transmitting antenna, located in the air (domain D_1) or in contact with the soil at different step frequencies and for different positions x_s of the transmitting antenna.

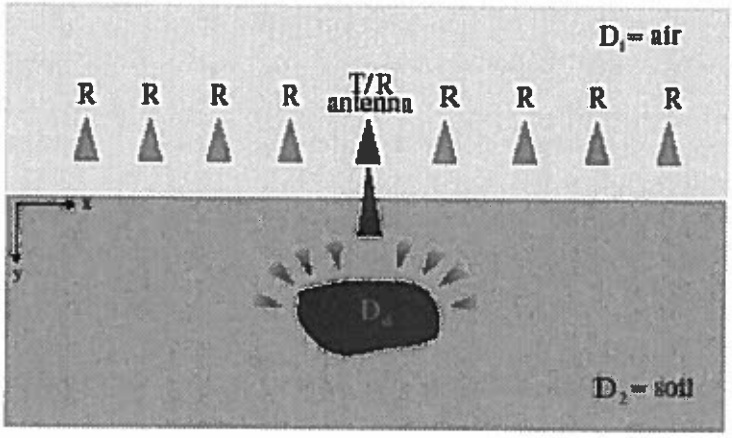

Fig. 1. Geometry of the problem.

At each position of the transmitting antenna, the scattered E^D field is measured on a synthetic probing line situated in the domain D_1 or at the interface air-soil D_1/D_2. The z-component of the scattered field in the electromagnetic 2D-TM case may be formulated as an integral representation for every angular frequency ω

$$E_z^D(x,y,x_S) = \int_{D_d} \left[k_i^2(x',y') - k_2^2\right] E_z^D(x',y',x_S) G(x,y,x',y')\,dx'\,dy' \qquad (1)$$

where $k_i^2(x,y) = \omega^2\mu_0(\varepsilon_0\varepsilon_n(x,y) + j\frac{\sigma_i(x,y)}{\omega})$, x_S is the location of the transmitting antenna along the x axis and where G(x,y,x'y') is the Green's function of the stratified media configuration.
We consider the spatial distribution of normalized induced current density

$$K(x,y,x_S) = \left\{\frac{k_D^2(x,y)}{k_3^2} - 1\right\}\left\{1 + \frac{E_z^D(x,y,x_S)}{E_z^I(x-x_S,y)}\right\} \tag{2}$$

where E^I $(x-x_S,y)$ is the incident field. The spectral decomposition $A_1(\eta)$ or plane-wave decomposition of the near-field pattern of the transmitting antenna in free-space is defined for each angular frequency by

$$A_1(\eta') = \int_{-\infty}^{+\infty} E_z^I(x'-x_S,0)e^{-2\pi j\eta'(x'-x_S)}dx' \tag{3}$$

By using the Green's function of the stratified media defined with a Fourier transform as

$$G(x,y_1,x',y') = \int_{-\infty}^{+\infty}\Theta(\nu')e^{-j[\gamma_1(\nu')y_1 - \gamma_2(\nu')y']}e^{2\pi j\nu'(x-x')}d\nu' \tag{4}$$

with $\gamma_i(\nu') = \sqrt{k_i^2 - 4\pi^2\nu'^2}$ i = 1,2 and where $\Theta(\nu')$ is a function of $\gamma_i(\nu')$.
The 2D spatial Fourier transform of the currents is defined by

$$\hat{K}(\alpha,\beta,x_S) = \int_{\Re^2} K(x,y,x_S)e^{-2\pi j(\alpha x+\beta y)}dxdy \tag{5}$$

Assuming that the induced currents are independent of the position x_S of the source, one obtains for every angular frequency ω the spectral relation

$$\hat{K}(\alpha,\beta) = \frac{e^{j\gamma_1(\nu)y_1}}{k_3^2 A_1(\eta)T_\perp(\eta)\Theta(\nu)}\hat{E}_z^D(\nu,\eta,y_1) \tag{6}$$

where $E_z^D(\nu,\eta,y_1)$ is the 2D spatial Fourier transform of the scattered field measured along the probing line L_1 situated at a height y_1 (in our case $y_1 = 0$) and $T_\perp(\eta')$ is the reflection coefficient of each component of the plane-wave expansion at the interface air-ground D_1/D_2.
In order to take advantage of conventional Fourier transforms, we must consider real dual variables such as $\nu \in \Re$, $\eta \in \Re$, $\alpha = \nu - \eta \in \Re$ and $\beta = \frac{-1}{2\pi}[\gamma_2(\nu) + \gamma_2(\eta)] \in \Re$.
The one-to-one relationship (6) via Fourier transforms relates for each angular frequency ω the 2D Fourier transform of the scattered field $E_z^D(\nu,\eta,y_1)$ at various source location x_S to the 2D Fourier transform $\hat{K}$ on a specific arc in the Fourier domain. From data on arcs in the Fourier space for different angular frequencies and source locations, an approximate image of the object by means of the induced currents can be obtained [1].
In many imaging methods, the incident field is assumed to be a plane wave. This is not realistic in the present context for two reasons. First, the near-field pattern of a real transmitting antenna cannot be assumed to be a plane wave. Second, with the multifrequency technique the near-field pattern changes considerably across the broad frequency band of the transmitting antenna. For numerical simulations and experiments we use a bow-tie transmitting antenna and the near-field pattern has been computed with a surface finite element (SFEM) method [2].
In order to show the performance of the reconstruction algorithm, reconstructions from synthetic and experimental data are compared using a bow-tie transmitting in the frequency range [0.8, 1.3] GHz with 50 MHz frequency steps and 37 transmitting and receiving locations. The test case is a plastic tube (rectangular cross-section 30 × 18 cm^2) buried at a depth of 30 cm with $\varepsilon_{r1} = 3$ and $\sigma_1 = 0$ S/m. The background medium D_2 is a sandy soil ($\varepsilon_{r2} = 2.55$ and $\sigma_2 = 2.21\ 10^{-3}$ S/m).

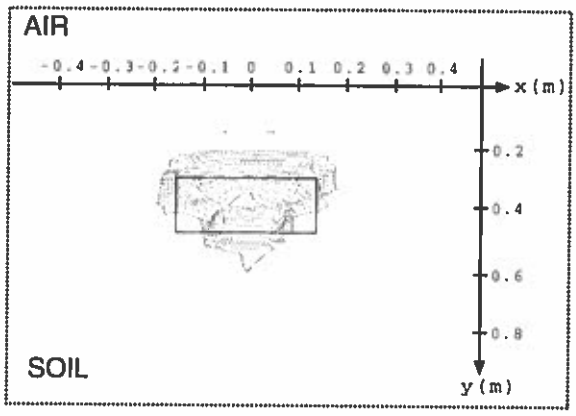

Fig. 2. Image from synthetic data.

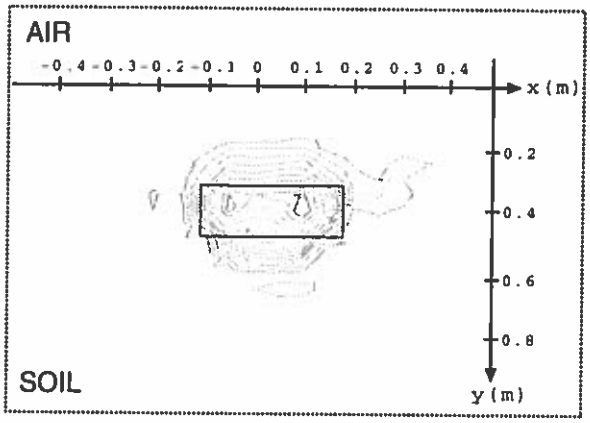

Fig. 3. Image from experimental data.

2.2 Quantitative reconstruction tomography

The forward problem can be solved using the moment method (MoM) with pulse basis functions and point-matching, which transforms integral equations into matrix equations as

$$\begin{cases} E^I = (I - G^O C(\varepsilon_r, \sigma))E \\ E^D = G^R C(\varepsilon_r, \sigma) \end{cases} \tag{7}$$

with complex contrast function $C(x,y) = \left[\varepsilon_m(x,y) - \varepsilon_{r_2}\right] + j\dfrac{\sigma_D(x,y) - \sigma_2}{\omega\varepsilon_0}$

The rectangular image (or test domain) containing the region D_d is divided into $N = N_x \times N_y$ elementary square cells. For highly contrasted objects and/or face with strongly noisy data, the inverse scattering problem becomes more ill-posed. The introduction of some a priori information is needed in order to reconstruct a regular solution. The solution is modeled as a piecewise constant profile, and we minimize the nonlinear cost functional

$$J_{EP}(\varepsilon_r, \sigma) = \sum_{f=1}^{NF}\sum_{s=1}^{NS}\left\|\rho_{s,f}(\varepsilon_r, \sigma)\right\|_{L_1}^2 + \sum_{p=1}^{NX}\sum_{q=1}^{NY}\varsigma_{\varepsilon_r}^2\varphi\left(\frac{\left\|(\nabla\varepsilon_r)_{p,q}\right\|}{\delta_{\varepsilon_r}}\right) + \sum_{p=1}^{NX}\sum_{q=1}^{NY}\varsigma_\sigma^2\varphi\left(\frac{\left\|(\nabla\sigma)_{p,q}\right\|}{\delta_\sigma}\right) \tag{8}$$

where $\rho_{s,f} = E^D - G^R C(\varepsilon_r, \sigma)(I - G^O C(\varepsilon_r, \sigma))^{-1} E^I$

The weighting parameters $\varsigma_{\varepsilon_r}$ and ς_σ fix the influence of the regularization. The parameters δ_{ε_r} and δ_σ fix the level on the gradient norm above a discontinuity is preserved, and under which is smoothed. The regularizing function φ is real and defined to perform an isotropic smoothing in the homogeneous areas of the image, while preserving edges [3]. The minimization of J is performed using a Biconjugate Gradient (BiCG) scheme applied to ε_r and σ

$$\varepsilon_r^{k+1} = \varepsilon_r^k + \alpha_{\varepsilon_r}^k \eta_{\varepsilon_r}^k \qquad\qquad \sigma^{k+1} = \sigma^k + \alpha_\sigma^k \eta_\sigma^k \tag{9}$$

where $\eta_{\varepsilon_r}^k$ and η_σ^k are the Polak-Ribière update directions and $\alpha_{\varepsilon_r}^k$ and α_σ^k are the complex parameters (weight factors). Reconstructions from simulated data using the near-field pattern of the bow-tie transmitting antenna are presented in the case of a square test domain of side 13.5 cm embedded in a sandy soil ($\varepsilon_{r_2} = 2.55$ and $\sigma_2 = 4.\ 10^{-3}$ S/m) at a depth of about 24 cm. The test domain is discretized into 9 × 9 subsquares of 1.5 × 1.5 cm^2 and contains a lossless object ($\varepsilon_{r_D} =$ 3) with 5 × 5 subsquares. The scattered field data are collected with 11 receiver stations equally sampled along a probing line of about 1 m length utilizing 3 frequencies (0.8 GHz, 1.05 GHz, 1.3 GHz). No initial guess is used in the iterative procedure. The reconstructed permittivity profile is shown in Fig. 4. After 500 iteration steps, the relative mean square error on ε_r is $\mathrm{Err}(\varepsilon_r) = 9.3\ 10^{-4}$.

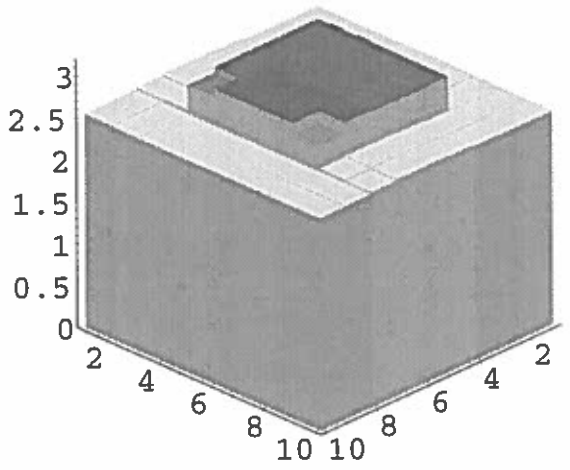

Fig. 4. Image from synthetic data with edge-preserving regularization.

2.3 SAR-like algorithm

For this case, the system uses a quasi-monostatic configuration where two close antennas are viewing towards the ground at 0.5 m to 1.5 m high and move step by step along a 3 m long rail (Fig. 5).

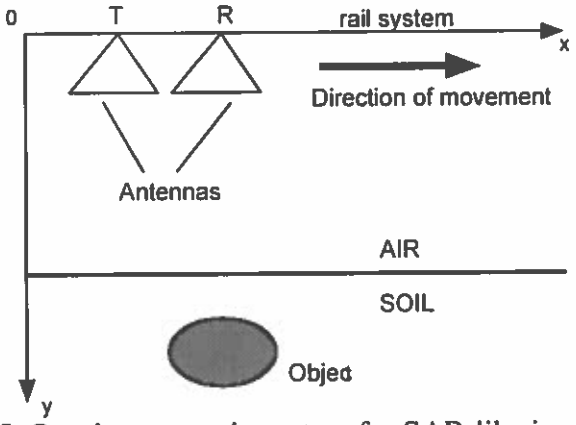

Fig.5. Quasi-monostatic system for SAR-like imaging

At each step (every $\lambda/4$ = 2.5 cm), a stepped-frequency "chirp" (UWB waveform) from 500 MHz to 5 GHz is transmitted. The processing algorithm starts from the complex matrix $N_f \times N_a$ of the received signals for a given set of discrete frequencies N_f and antenna positions N_a. One can show that the distribution of the object reflectivity $\eta(x,y)$ is given by the following expression [4] for a frequency f_i and a given position on the rail x_j :

$$\eta(x,y) = \sum_{f_i} \sum_{x_j} S_r(f_i, x_j) e^{j\frac{4\pi}{c} f_i \left[\sqrt{(x_i - x_j)^2 + h^2} + \sqrt{\varepsilon_r}\left(\sqrt{(x - x_i)^2 + (y - h)^2}\right)\right]} \qquad (11)$$

where h is the rail height and x_I is the abscissa of the impact (or inflection) point I of a ray on the soil [4]. In the soil, $\varepsilon_r = \varepsilon'_r - j\varepsilon''_r$ and generally both ε'_r and ε''_r depend on the frequency (dispersion). Doing this, the phase becomes complex and this means that we introduce the compensation of attenuation versus frequency by an exponential term. The unkown x_i can be computed using the Snell's law. In practice, to avoid ambiguities in distance, more than 500 frequencies are used. For computing the reconstructed image from (11), we take profit of Fast Fourier transform. In Fig. 6 is shown a reconstructed image from experimental data for a surrogate plastic (with minimum metal content) AP mine (10 cm diameter) buried at 5 cm in sandy soil with 3% water content utilizing the frequency band [1, 5] GHz.

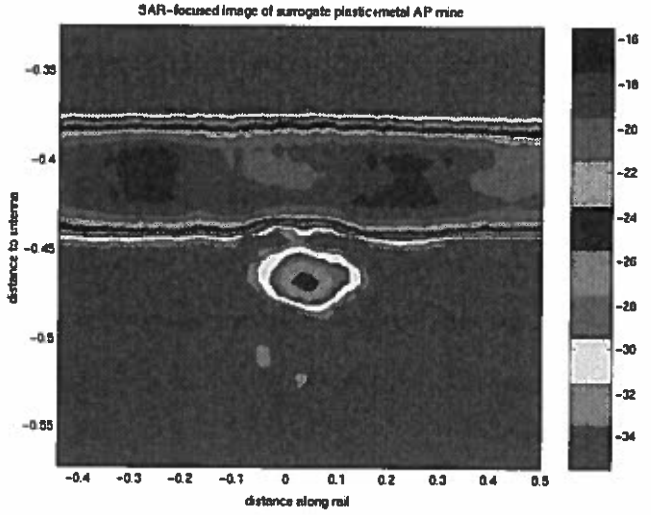

Fig.6. SAR image of a surrogate AP mine

3. Ultra-wide band antennas

Tapered slot antennas offering ultra wide bandwidth of more than one decade [500 MHz, 11 GHz] have been designed and realized as transmitter and sensor. These antennas present interesting characteristics in terms of near-field patterns and gain. The level of cross-polarization is less than -24 dB over the frequency range [1, 6] GHz. Another advantage of these antennas concerns their integration in an array without requiring significant space.
Experimental reconstructions using SAR-like algorithm have been obtained with these antennas and compared to those obtained with conventional gain horn antennas on different buried objects of practical interest and mine-like objects. An experimental study has been carried out in order to develop a new microwave imaging system.

Acknowledgments

The authors wish to thank France Télécom/CNET La Turbie for providing the computer resources in the numerical simulation of bow-tie antenna. The authors also thanks the LCPC in Nantes and the LRPC in Rouen (French Publics Works Laboratories) for their support in this study.

References

[1] C. Dourthe, Ch. Pichot, "Microwave imaging algorithms for arbitrary space and time incident waveforms using ultrawide bandwidth GPR Technique", *EUREL Conf. Publication on the detection of abandoned land mines*, pp. 124-127, 1996.

[2] P. Ratajczak, P. Brachat, J.L. Guiraud, "Rigorous analysis of three-dimensional structures incorporating dielectrics", *IEEE Trans. Antennas Propagat.*, vol. 42, No. 8, pp. 1077-1088, 1994.

[3] P. Lobel, L. Blanc-Féraud, Ch. Pichot, M. Barlaud, "A new regularization scheme for inverse scattering", *Inverse Problems*, vol. 13, pp. 403-410, 1997.

[4] P. Millot, Ch. Pichot, "Introduction of the electromagnetic properties of soils in near-field SAR processing for subsurface imaging of buried objects", *Proceed. Physics in Signal and Image Processing* (PSIP'99) (17-21 January 1999, Versailles, France), p. 210-214.

[5] E. Guillanton, J.Y. Dauvignac, Ch. Pichot, J. Cashman, "A new design tapered slot antenna for ultra-wideband applications", *Microwave Opt. Technol. Lett.*, vol. 19, No. 4, pp. 286-289, 1998.

3D Polarimetric Diffraction Tomographic Imaging of Buried Objects

K.J. Langenberg K. Mayer
Dept. Electrical EngineeringUniversity of Kassel
D-34109 Kassel, Germany

ABSTRACT
Diffraction tomographic imaging is based upon twodimensional measurements of scattered wavefields --- in one scalar component --- either in a frequency or in an angular diversity mode resulting in a threedimensional data field. With the help of the Fourier Diffraction Slice Theorem, which is a solution to the inverse scattering problem within the linearizing approximations associated either with the name of Born or Kirchhoff, this 3D data field can be mapped into the image space via the Fourier space of the object; this provides a fast and effective scheme which additionally allows for the starightforward implementation of various standard signal processing techniques. Recently, we have been able to extend this algorithm to vector wave fields --- like electromagnetic waves --- thus accounting for polarization diversity explicitly. Various checks of this polarimetric diffraction tomographic imaging scheme against synthetic data could prove its superiority over scalar imaging. In particular, we have produced synthetic 3D time domain data and pertinent images for tendon ducts buried in concrete below steel reinforcement, and several mine models buried in dry sand for varying parameters.

Keywords: Tomography, Inversion Methods, 3D visualization

Fully Polarised 3D-SAR GPR for the Recognition of Hidden Mines

G. Alli, A. Bicci, G. De Pasquale, G. Manacorda, G. Pinelli, S. Sensani
Ingegneria dei Sistemi (IDS) S. p.A.
Via Livornese 1019 - 56010 Pisa (Italy)
Tel.+39 50 312411 - Fax. +39 50 3124201 - E-mail: g.pinelli@ids-spa.it

ABSTRACT

This paper reports on the feasibility study for a large, fully polarised, 3D-SAR Ground Penetrating Radar (GPR) array for the identification of landmines (ATM, APL) and unexploded ordnance (UXO). It also reports on some of the numerical techniques developed for the automatic detection and identification of mines and UXO in real time while the array is scanning the subsoil. Examples of the application of such techniques to GPR measurements of APM buried in real ground are also presented.
Such a GPR array and associated signal processing represents IDS contribution to the ANGEL Project (EUREKA! framework) for a multi-sensor system for the elimination of landmines.

Keywords: Mine, GPR, Array, 3D-SAR

1. Introduction

Every day, we know of damages to people due to mines. Official estimates talk of about 100 million Anti Personnel Mines (APM) hidden in the ground [1]. Presently the scientific community is busy in research to design a system which will be able to locate ATM (Anti-Tank Mines), APM and UXO buried in the subsoil. Unfortunately, finding and removing them is a difficult problem. This is particularly true for the APMs which are often small (diameter of 5-6cm) and with very low metallic content. Hence, to individuate APMs, there is a need for sensors which are both more sensitive than the ones currently available and capable of extracting enough physical information useful for the discrimination of buried objects. In other words, the problem of finding mines can be divided in two stages: the *detection stage* where all the buried objects should be revealed and the *classification stage* where mines should be discriminated from unwanted objects such as stones and tree roots.
In the past 10-15 years many techniques have been applied to the detection of mines, including Metal Detectors (MD), Biological Detectors (BD), Infra Red (IR) sensors and GPR. Each of these have proven some capability of performing the job but none is singularly able to do it with the reliability required by humanitarian demining standards. For this reason many humanitarian demining systems currently under development relay on the joint use of more than one of these sensors. The ANGEL project for which IDS has began the development of the GPR sensor also follows this principle integrating, on top of the GPR, IR, BD and MD sensors on an unmanned vehicle [1].Furthermore, given that the vehicle should move at about 5 Km/h and break before stepping on a mine, it was required that the sensors data processing should be done in real time so that vectorised data can be transmitted to the control unit where data fusion from the various sensors gives the final decision on the presence of a dangerous object.

[1] ANGEL system is composed not only by the land vehicle, but also by other platforms. For more details about the ANGEL project visit www.gtd.es/angel_1.asp.

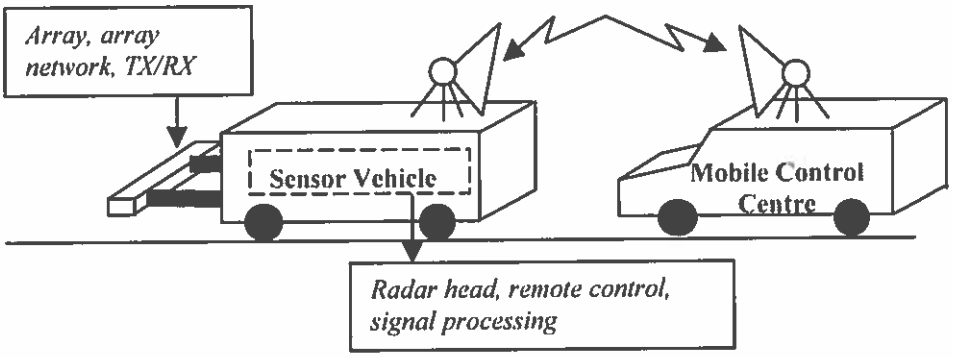

Fig. 1 – Architecture of ANGEL's Multi-Sensor and Control Vehicles. The Multi Sensor Vehicle carries the GPR *array subsistem* in front of the vehicle and the *on-board subsystem* including the GPR signal processing unit

2. Theoretical Background

The main characteristics (i.e. frequency, bandwidth, etc.) of the GPR array are determined by its suitability in the detection of small, low metal content, shallow buried APM in the presence of a lossy, possibly inhomogeneous medium (soil). Propagation losses, antenna size and size of the target to be detected dictate the frequency band of propagation [2] imposing severe constraints to the radar design and making the task of designing such a radar far from trivial.

The GPR feasibility study has moved along an accurate system analysis which has investigated the parameters affecting the radar performance. Intense simulation has been performed, concentrating on an array configuration capable of guaranteeing the signal-to-noise ratio (SNR) and the signal-to-clutter ratio (SCR) needed to obtain the detection and discrimination of the hidden mines. Experimental activities have verified the results of such simulations.

For effective detection and discrimination of the most difficult targets (i.e. non-metal APM as small as 5-6 cm in diameter) there is a need for:

- SNR and SCR sufficient to detect APM. In particular, the GPR system has to guarantee a signal to clutter plus thermal noise ratio higher than *0db*;
- Resolutions with respect to the three main directions (x = array alignment direction, y = array (vehicle) movement direction, z = depth direction) finer than the APM size;

SNR and resolution are two conflicting requirements: the SNR requirement limits the maximum frequency to be irradiated in the terrain and hence the resolution. The analysis performed has identified the 2 GHz central frequency with a 100% relative bandwidth as a viable and effective solution.

With such a choice (taking as a reference for the soil a dielectric constant equal to 9), the expected range (depth) resolution is about 2.5 cm. [3]. The resolution along the others directions (x and y directions) can be increased through focusing techniques. In order to reduce system complexity, a linear 2D array to focus along the array direction is used, while the array movement is exploited to focus, by following SAR principles, along the array movement. The maximum attainable cross-range resolution is expected to be 4 cm. [2]

Detection and classification must be performed with the lowest computational load (lower than 1 Gflops/s). Taking into account that the communication link is shared with other sensors, we have established that the final data throughput required by the GPR must be lower than 10Mbit/s.

3. System Description

Taking into account the aforementioned stringent requirements, the proposed GPR architecture (see Fig. 2) is constituted by a radar ("*radar head*") which pilots a fully polarimetric linear 2D array.

[2] For antenna beam width of 120° and maximum antenna footprint at the target depth

This architecture permits us to apply *3D-SAR* techniques, to increase SCR and SNR through a reduction of the volumetric resolution cell (*"detection processor"*, in which all the objects are revealed).

Once the buried objects are revealed, they have to be classified, i.e. we must discriminate between mines and unwanted targets such as stones or tree-roots (*classification stage*). To this end, *features* must be extracted from the detected objects. These features can be derived in the time-frequency domain (STFT, Wavelet Transform, Wigner-Ville distribution, etc.) by exploiting the same co-polarised radar channels used in the detection stage. However, polarimetric information (such as polarimetric invariants) derived from cross-polarised radar channels are also believed to be useful in discriminating mines by unwanted targets. Hence the array architecture includes several *feature extractor blocks* (see *"classification processor"* in Fig. 2) composed of both co-polar (HH,VV) and cross-polar (HV) radar channels.

The radar channels acquired by the array subsystem, after A/D conversion, are pre-processed by single DSP's which act on the acquired A-scan (range/time filtering and gain).

Then, the pre-processed data are sent to the *data manager block*, having the following functions:

- For each possible target position, the HH radar channels involved in the *detection stage* are located in a squared area of *0.8x0.8m* centred on the target. Hence, the data manager has to control the radar channels involved in each detection block.
- When a target has been detected, an *alarm zone* around the effective target position is identified. In this case, the classification stage should be applied for each volumetric element (voxel) of a cubic volume centred around the alarm zone. So, for each voxel, the HH-VV-HV radar channels involved in the *classification stage* are selected and, for each channel, the feature extraction procedure is applied. The extracted features are then correlated to produce the final recognition result.

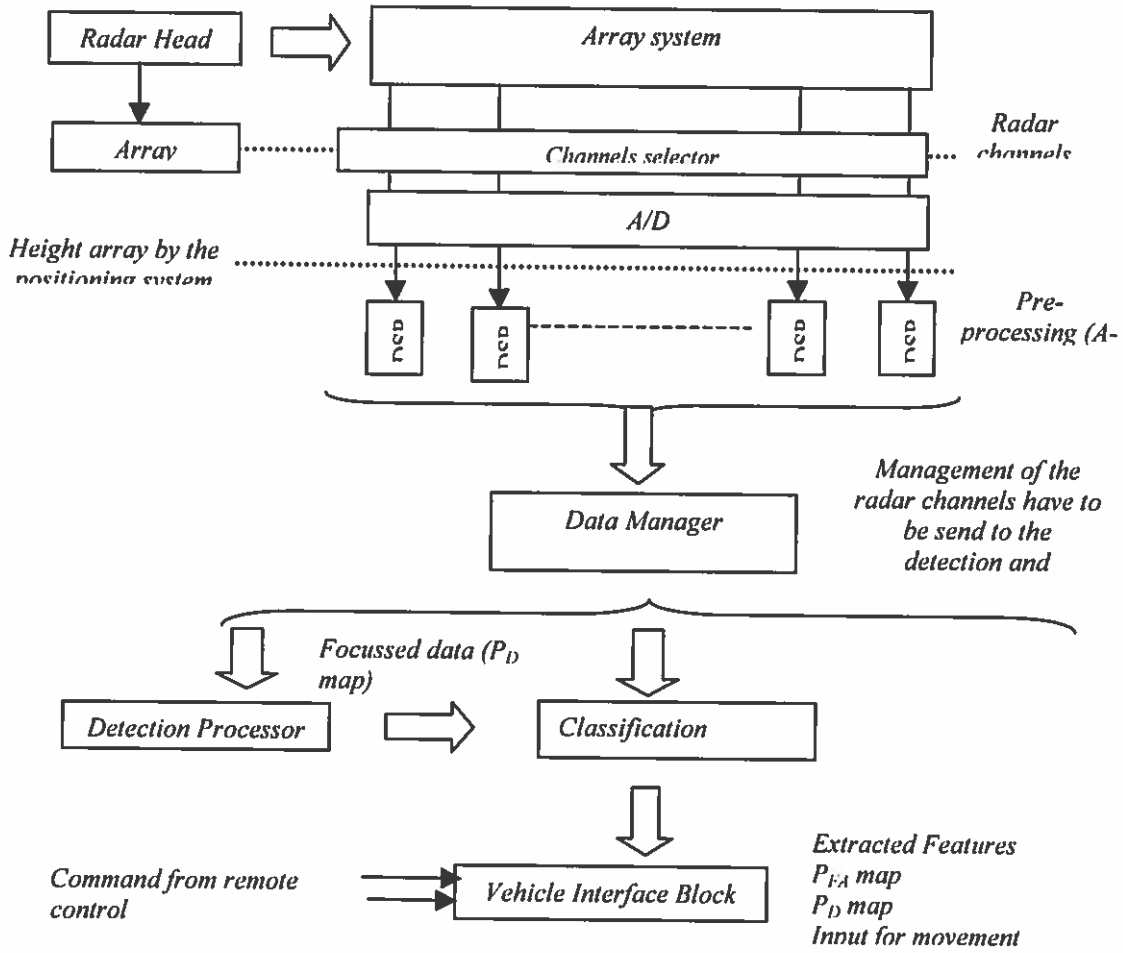

Fig. 2 - General Architecture of the ANGEL GPR Design

In such a way, for each voxel belonging to the cubic data volume surrounding the alarm zone, the classification stage is carried out in two steps: first, data from each of the three radar channels (HH,VV,VH) are sent to a feature extractor block that derives the features along A-scan and second, the extracted features, are sent to another block which correlates all the features. In the end, the classification results are sent to the *vehicle interface block* (extracted features, correct detection probability map, false alarm probability map) to be displayed.

4. Simulation Results

In this section, some simulation results relevant to the array architecture design are presented. Performance have been evaluated in terms of cross-range resolution and main/side lobe ratio as a function of number of elements (TX/RX), number and type of radar channels. Considering, for the sake of simplicity, a non-polarimetric array with $n_{rx} = n$ receivers and $n_{tx} = n\text{-}1$ transmitters, the number of channels exploited is $n*n\text{-}1$. The set of resulting radar channels is reported in the matrix of Fig. 3.
Fig. 3 also shows five different channel configurations, considered in the simulation example reported in the following.

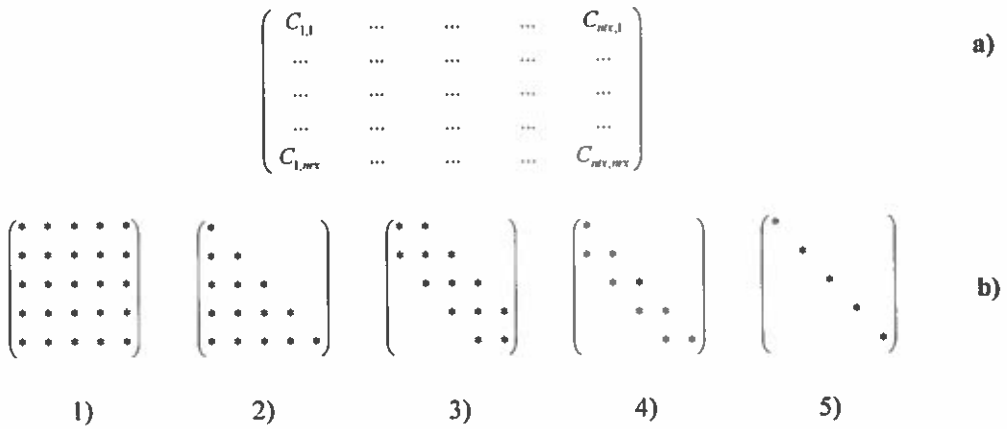

Fig. 3 – Matrix of the available radar channels (a) and different array configurations (b), 1) *all channels* 2) *Monostatic plus bistatic* 3) *Monostatic plus near bistatic* 4) *Monostatic plus near homologous bistatic* 5) *Only Monostatic*

The performance obtained in terms of –3dB cross-range resolution and main/side lobe ratio (dB) is reported in Fig. 4.

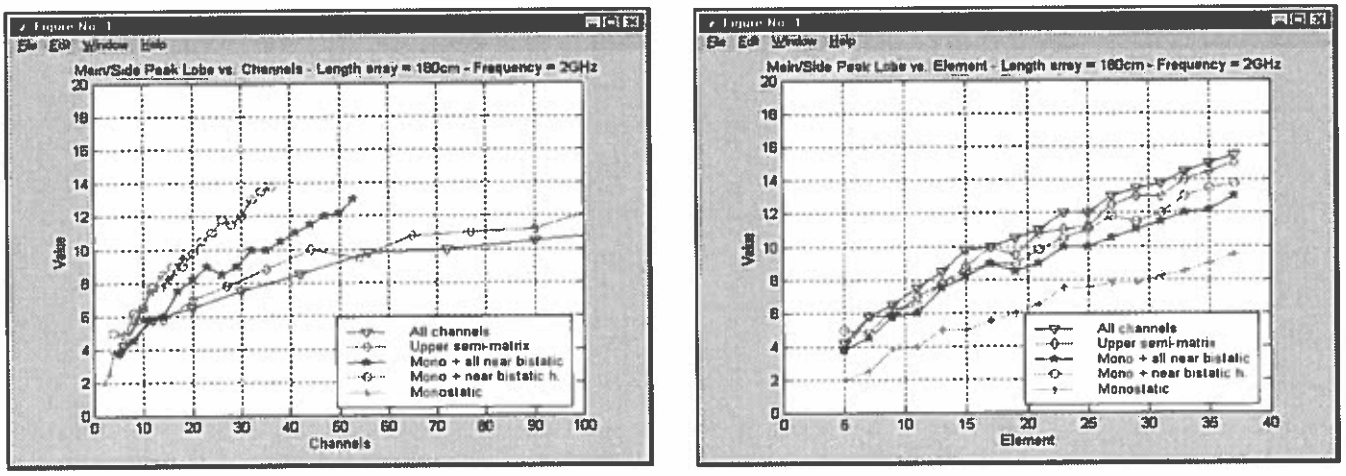

Fig. 4 –Performance for different array sampling, array length=2m, bandwidth=2GHz

The main results are:

- Resolution does not change with the array sampling (about *3.5-4cm* for the configurations (3)-(4)-(5) and about *5cm* for the configurations (1)-(2))
- Side lobes degrade with the decreasing of the number of radar elements (TX/RX) and channels.
- Monostatic and pseudo-monostatic configurations provide the best lobe performance for the same number of channels.
- Intensive use of bistatic channels provides better lobe performance for the same number of elements.

Therefore, the problem of determining the optimum configuration is not easy. In particular, the choice depends on the weight assigned to the performance indexes (resolution, side lobes) and cost indexes (number of elements and number of radar channels). A possible criterion could be to choose the array configuration that minimises the costs (=number of elements and radar channels) and provides acceptable performance in terms of resolution and side lobes. For example, by imposing the following requirements: 1) Minimum Cross Range Resolution = *4cm* 2)minimum Main/Side Lobe Ratio of *10dB*, we conclude that the configuration (4) with array sampling of *8.2cm* allows the optimisation of the number of radar channels (*22*) and elements (*23*).
Based on this kind of analysis the following polarimetric array architecture has been defined:

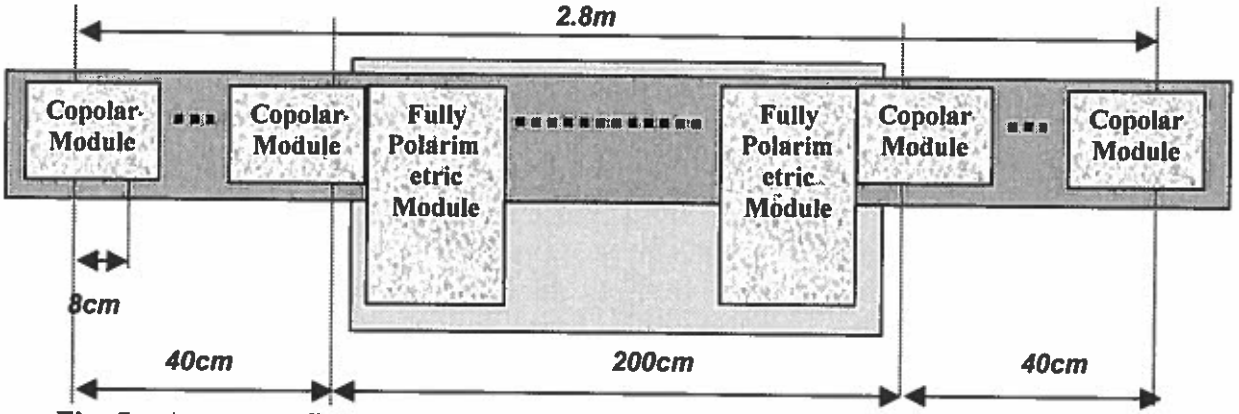

Fig. 5 – Array configuration (85 radiating elements; 115 channels). Length: 280 cm.

The proposed architecture can be easily scaled if we accept to relax the initial requirements. A simpler configuration, scaled to a length of 140 cm, needs 49 radiating elements, with 37 used channels. This configuration requires a *data rate* of 77 Ksample/s, a *computational load* of about 128 Mflop/s and a *data throughput* (data flow to the ANGEL central unit) of 2.1 Mbit/s.

6. Automatic Target Identification

As reported in the previous sections, the target identification is carried out through two sequential steps: the detection stage and the classification stage. The latter extracts features from the detected target and submits them to a classifier for discrimination purposes.
Many feature extraction algorithms (Short Time Fourier Transform (STFT), Wavelet Transform, Singularity Expansion Method (SEM), Polarimetric Invariant Method, etc.) and classification techniques (Neural Network) have been studied with the objective of defining the proper identification scheme.
Fig. 6 shows an example of a processing technique based on local spectrum analysis both for enhancing the target signal level and for distinguishing interesting targets (mines) from clutter.

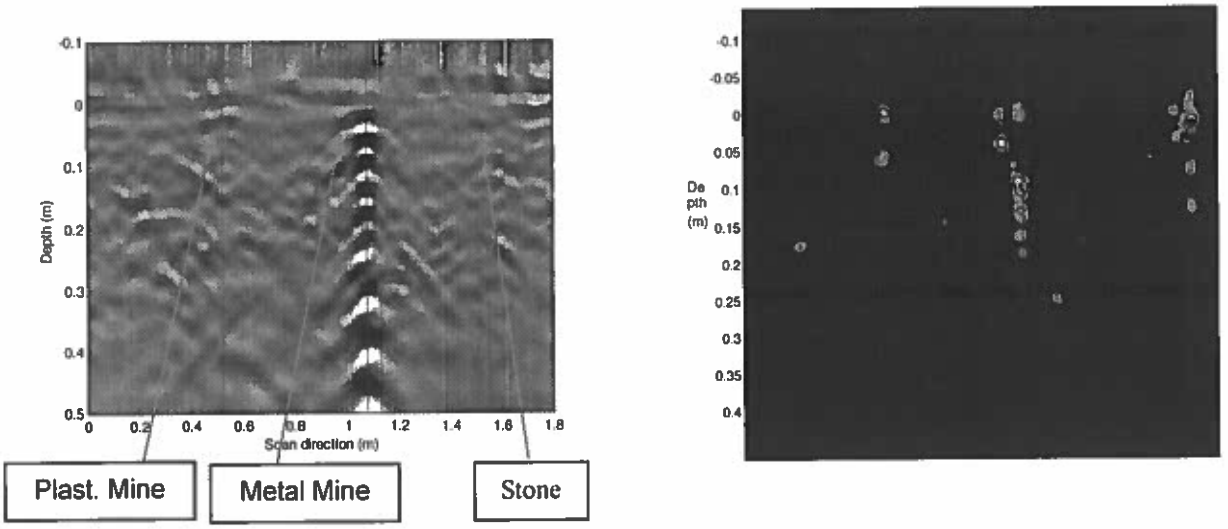

Fig. 6 – Example of the application of an STFT based algorithm to a (pre-processed) GPR map. Left: pre-processed map (both plastic and metal mines are APM with a diameter of about 6 cm.). Right: processed map.

7. Conclusions

In this paper, it has been presented the contribute of IDS to the ANGEL project in the definition of an UWB, 3D-SAR, full polarised radar system specifically tailored to the identification (detection and recognition) of the hidden mines and UXO. Through this system, the demining operation can be conducted by means of a single pass on the investigated strip terrain. The radar system pilots an array of antennas conceived as scalable. For a swath 1m wide, the array has 49 radar elements (both Tx and Rx) and exploits 37 (monostatic plus near bistatic full polarised) radar channels. For such a configuration, the system guarantees a resolution along the three dimensions equal or finer than 4cm with a main-to-side lobe ratio of at least 10dB.

7. References

[1] J.Walker, "Moore's law in the minefield", Proceeding of WAPM, 1995.
[2] D.J.Daniels, "Surface Penetrating Radar", The Institute of Electrical Engineers, London (UK), 1996
[3] H.Brunzell, "Detection and Classification of buried objects using impulse radar measurements", Technical Report of the Department of Applied Electronics, Chalmers University, 1996.

Ultra-Wide Band Impulse Radar for Stand-off and Stand-over Searching of Land Mines and UXO in Subsurface Region and Vegetation

A. Boryssenko
Scientific Research Company "Diascarb"
P.O. Box 370 Kyiv 253222 UKRAINE
E-mail: aab@public.ua.net

ABSTRACT
Subsurface or ground-penetrating radar is used namely for land mine detection in the "stand-over" mode when radar's antennas are spaced directly over searching area with continues or step-by-step scanning motion to implement the synthetic-aperture technique. There is also other, less applicable now, version of radar demining operation, i.e. a "stand-off" mode when searching object hidden in vegetation and beneath ground surface are located ahead moving platform with radar mounted on it. In the process of platform motion a synthetic-aperture technique is implemented offering into single framework solution for mine detection and discrimination problems in stand-off and stand-over modes.

Keywords: Ground Penetrating Radar, Ultra-Wide Band Radar, Stand-off Radar Mode, Stand-over Radar Mode

PROBLEM BACKGROUND

Subsurface-penetrating or ground-penetrating radars (GPR) are widely used all around the world to solve variety problems of science, engineering etc [1]. Due to ultra-wide band (UWB) performances implemented by impulse or step-frequency technique resulted in high spatial resolution achieved those radars are applied for demining also [2, 4-6]. The author shares the division of possible GPR applications for land mine problems into two main groups [2].

The first, so-called "stand-over" operation is based on using radar as common GPR system when radar antennas must be deployed directly over/on surface under investigation. Inherently low directivity of UWB antennas or their large diameter of footprint makes worse radar spatial resolution in plane. In order to face this obstacle the synthetic-aperture technique by continues or step-by-step antenna scanning is used. The stand-over radar demining applications are dominant and vegetation is serious obstacle for normal operation in such mode.

The second method of radar application for land mine detection is characterized by the "stand-off" radar position in respect to searching minefield and less employed than the stand-over mode. Two realizations of the stand-off method are known the author. The Jacor radar experimental system [3] is able to detect and identify buried mines in subsurface and vegetation at safe distance before moving vehicle where radar is boarded. Continues wave stepped-frequency radar was being used in the Jacor project with target discrimination technique based on analysis of resonance's responses of hidden objects. Other implementation of the stand-off operation for demining is a UWB synthetic-aperture polarimetric radar system mounted to the basket of a telescoping boom lift, which has been developed for minefield detection namely but not separated mines [4].

The novel concept of the stand-off radar operation for land mine detection problems is under theoretical and experimental investigations in this paper. It demands taking into consideration some principal problem's aspects like optimization of radar electronics and functioning/processing algorithms with chosen detection strategy, estimation of probabilistic terrain and vegetation features and so on.

STAND-OFF RADAR CONCEPT

The author has conducted before theoretical and experimental studies to apply UWB impulse radar by some adaptation of common GPR system to microwave imaging of hidden objects in opaque media. The primary goal was to develop UWB radar-based system to find automatically in real-time invisible hidden objects in dense grass or vegetation at the safe distance before the moving platform with radar housed on it [7]. In this case only stand-off mode of radar operation is applicable and author adopts in this paper the concept of radar microwave imaging to the demining problems by introduction of special kind of the stand-off radar technique, both the equipment and the signal processing.

Operations in the stand-over and stand-off modes are presented in Fig. 1 a,b where electromagnetic illumination of surface is shown schematically by rays. Note that segments of equivalent double-traveling time, which are printed by radar beam over surface under limits of conical antenna pattern, have sufficiently different geometrical shapes for both modes. This offers some opportunities in the case of the stand-off mode due to better distribution in time echo signals scattered by various parts of surface background illuminated by radar. Noticed that intensity of background scattering is lower for the stand-off mode than for the stand-over one as seen clearly in Fig. 1 a,b.

At the same time, target echo is shifting consequently in time due to stand-off radar motion through scene of interest (Fig. 1 c,d) that implements the effective synthetic-aperture technique to obtain acceptable target discrimination in plane. For comparison, due to a round shape of equivalent double traveling-time curves in the stand-over mode some uncertainty of target spatial position is evident in Fig. 1a in contrast to Fig. 1b-d where there is only a uncertainty about target position in respect to the axis along which radar moves through scene of interest (Fig. 2c,d). The last uncertainty is removed easy by application of receiving antenna array.

Low directivity features of the UWB antennas mentioned above cause also strong background scattering that mask useful target echo signals. These unfavorable events can be overcome by employment special signal processing technique that based on deriving of statistical differences between target echo and background discussed in the next section.

The stand-off mode is attractive also due to the fact that radar antenna operates in stable air-field media in contrast to the stand-over mode when antenna is disturbed by terrain with probabilistic electrical features and its rough surface, as well as due to vegetation cover with evident stochastic properties. The last factor, i.e. vegetation, is serious obstacle for normal operation in the stand-over mode while both subsurface and hidden in vegetation mines should be detected by radar operating in the stand-off mode. Beyond doubt a more safety factor of the stand-off mode operation in minefield in contrast to the stand-over one is important too.

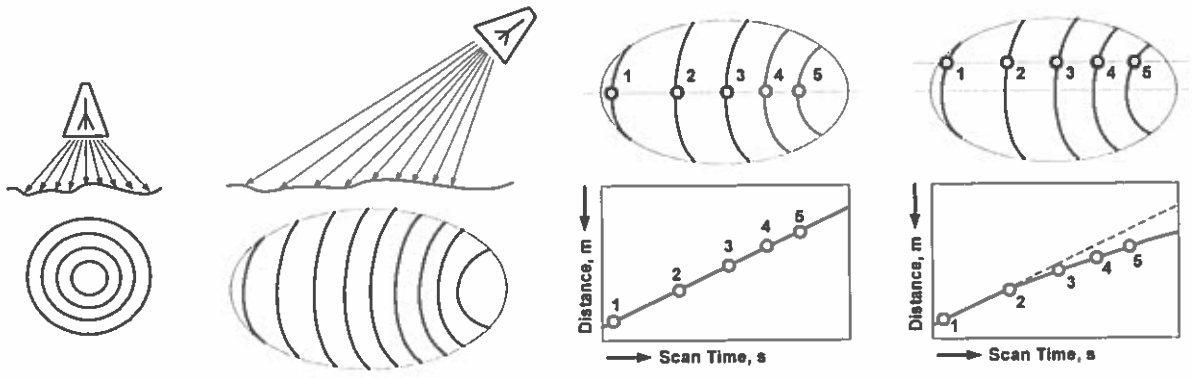

Fig. 1 Schematic presentation of operation radar in stand-over mode (a) and stand-off one (b). Trajectory of mutual convergence of radar and target in the act of radar stand-off survey: (c) target is laid on the axis of radar motion, (d) target is shifted from the axis of radar motion.

EXPERIMENTAL AND SIGNAL PROCESSING TECHNIQUES

Basically, the proposed radar demining system on moving platform (Fig. 2) with radar mounted on it can operate sequentially in two operation stages: 1) at far distance in the stand-off mode to detect harmful objects located beneath ground surface and covered by vegetation; 2) at short distance resulted from radar-target approach in the stand-over mode used mostly for radar demining at present. In order to examine this radar concept, laboratory and field tests have been conducted. The developed experimental set-up that consists of modified impulse radar (Fig. 3a) of the 1GHz middle frequency band, monostatic Tx-Rx antennas arrangement, control and processing electronics, computer with control/processing real-time software. The total 500 MHz – 1.5 GHz frequency band used is optimal and compromises to achieve maximum spatial resolution and minimum signal attenuation under real operation conditions in vegetation and subsurface soil regions.

Transmitting Tx antenna is driving by pulse with front duration ≤ 0.2 nanoseconds, amplitude of about 35 V, pulse repetition rate of 10 microseconds. Stroboscopic receiver unit is employed in radar with 0.0125 nanoseconds time resolution. The bow-tie antennas with backed reflector and the TEM horn antennas have been used. The 12 bit 500 kHz sampling frequency ADC and Analog Device ADSP-2105 digital signal processor (DSP) have been employed that installed both on computer card boarded in computer via the standard PCI bus. Radar returns data stored by computer has 512 samples per each radar's sounding period, i.e. trace. Radar is able to give out 20-50 traces per second that is preferable value for movable radar carrier. Total performance factor of radar is 140 dB and its total dynamic range is 120 dB including internal analog summation implemented in the receiver unit.

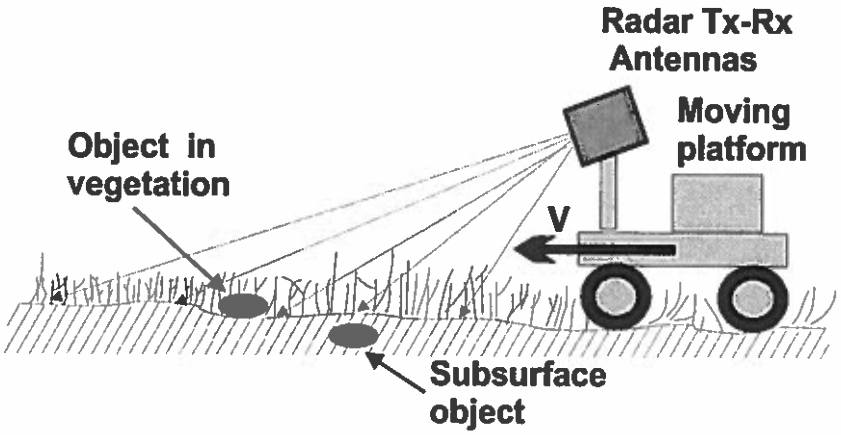

Fig. 2. Schematic presentation of the stand-off radar operation for detection objects hidden under ground surface and in vegetation cover before moving platform with radar boarded.

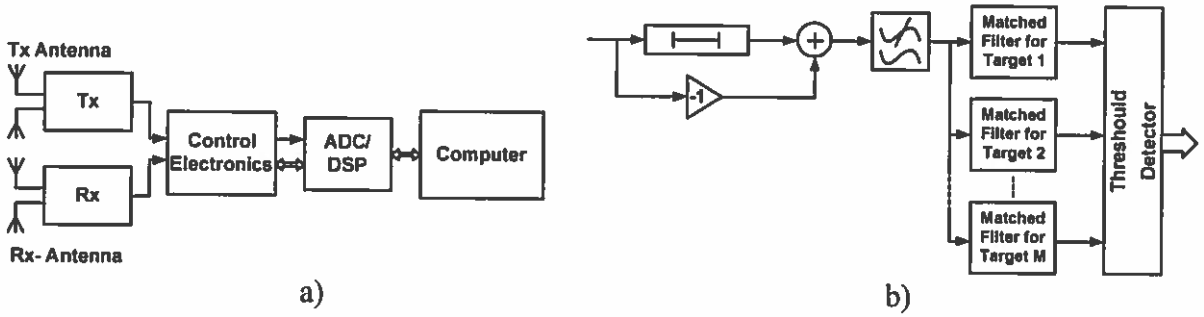

Fig. 3. (a) Principal components of UWB impulse radar used in experimental set-up where Tx is transmitter, Rx is receiver, ADC/DSP is analog-to-digital converter and digital signal

processing computer card. (b) Signal processing block diagram with principal algorithms implemented numerically by DSP capabilities.

Along with discussed above radar equipment, the key factor is necessary signal processing to ensure required functioning of radar system in large degree. The primary goal of radar data processing is compensation of background masking effects. In order to discriminate a target under powerful background masking, a difference between target echo and background scattering must exist. These distinctive properties are forced by relative statistical uniformity of background scattering in contrast to target echo signals that can be described by signal-to-background ratio (SBR). Typical value of SBR is no more than -10db and less for unprocessed radar return and should be improved during the data processing procedure. To do this, a Doppler processing is implemented by computing a difference between radar returns obtained for two neighbor successive radar traces like it is diagrammed in Fig. 3b. This Doppler processing fulfilled is similar to common moving target indication for suppression of passive interference signals. Such filtering has been implemented in real-time mode by the DSP.

The next task to be solved is improving SBR and signal-to-clutter ratio (SCR) to ensure required radar performances that can be summarized in receiver operation characteristic (ROC) [5]. Let note that in contrast to classical theory of optimal detector [4,5] where detection rate and false alarm rate are determined by signal-to-noise ratio (SNR) in the presented stand-off system both SBR and SCR are determining factor mostly. Next operating block in Fig. 3b after subtraction shows a linear filtration to minimize non-compensate residual interface signals to improve finally SBR. Also in Fig. 3b linear matched filter for some set of target's signatures and the threshold detector are employed. Algorithms to perform matched filtering or some kind of the E-pulse technique [6] is able to improve SCR as well as other kinds of signal processing methods (joint time-frequency analysis, wavelet analysis etc.). Note that among possible signal processing approaches those are preferable here, which offer their DSP implementation for real-time operation. This problem demands special considerations to optimize detection strategy in radar and this work is in progress now.

The 2-D presentation of radar operation scene like one in Fig. 1c-d is also important aspect of data processing and its visualization in the process of experimental studies allows implementing 2-D signal and image processing techniques. Those questions being complex require special consideration too and they are illustrated in some degree in the next section where experimental results are shown and discussed.

EXPERIMENTAL RESULTS AND DISCUSSIONS

Typical results of experimental studies to locate target buried in vegetation is presented in Fig. 4 that corresponds to antenna height 1.5 m over surface. The searching area extends ahead from radar up to the distance 5 m and is covered by radar line of sight (angle of sight is 60^0). The object detected in Fig. 4 was a stone of about square shape with about 8-cm side hidden in the 10-15 cm grass. Others kind of mine-like objects, including ones located under the Earth surface at the depth of 3-5 cm were under testing also. Radar data have been recorded and presented in distance-time format where vertical axis is distance from object to radar and horizontal one is current time coordinate that is similar to the B-scan of GPR radargrams. The key operational phases of radar return processing to discriminate target echo produced by single appointed scaterer in vegetation before moving vehicle with radar is depicted in Fig. 4.

As seen in Fig. 4, a original data (the upper image) is under powerful masking interference's signals due to background scattering and the following images phases show data after its processing to eliminate interference and extract signal scattered by detecting target. A trajectory of mutual approach of target and radar is visible in Fig. 2 as fuzzy line drawn from the below-left corner to the upper-right one. This line is observable very difficulty for original data and clearly visible after processing. Inclination of trajectory line is determined by velocity V of mutual approach of target and radar that was about 1.5 m/s for considered case to detect

harmful objects before moving vehicle. This magnitude of velocity is very high, of course, for demining and its decreasing improves substantially the system total performances like ROC.

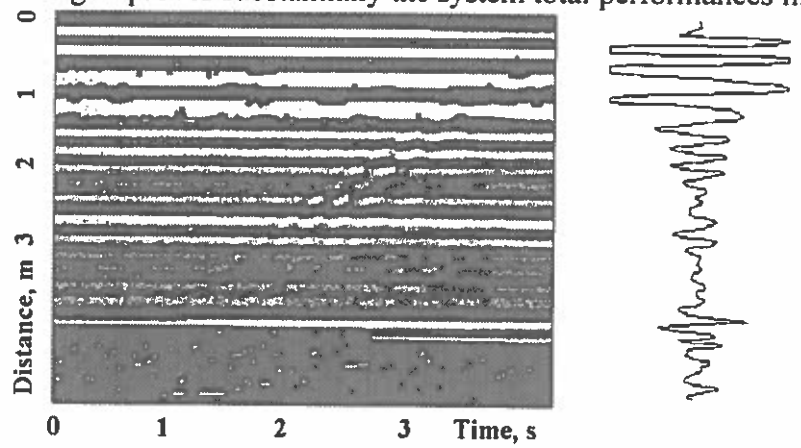

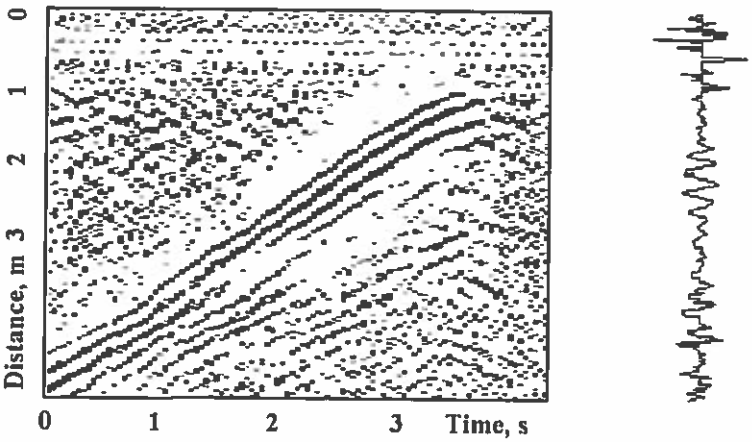

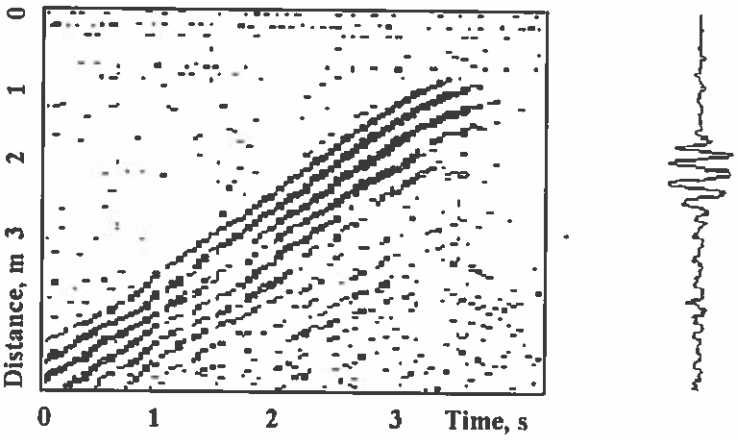

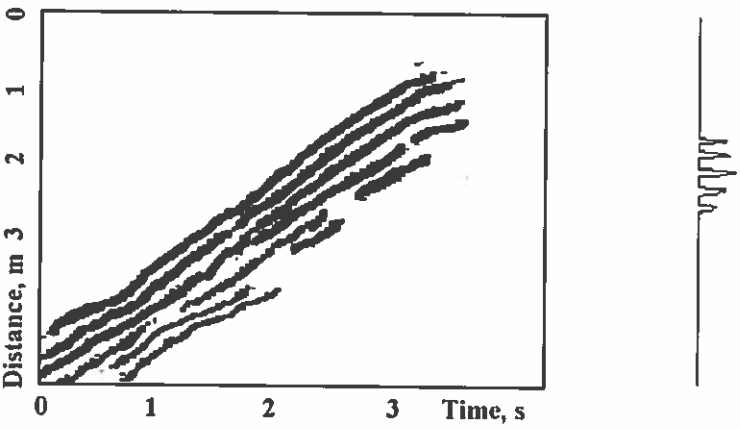

Fig. 4. Experimental data processing to discriminate the target echo masked initially by strong background scattering and picked out later as result of signal processing applied.

Residual uncompensated noise after the Doppler filtration that forced due to unavoidable fluctuations of background scattering resulted from radar movement and background heterogeneity is presented firstly in the upper image in Fig. 4 and eliminating entirely later. The right part of Fig. 4 includes a signal waveform for various processing stages that demonstrates waveform transformation and discriminations of useful signal components masked initially by a background scattering. Note that definite targets have specific waveforms can be applied for target discriminations. The upper waveform in Fig. 4a, presents initial waveform of echo signal with low SBR (about -10 dB) while the two lower waveforms have SBR>20 dB.

CONCLUSSIONS

As seen clearly in Fig. 4, the signal processing employed in accordance with Fig. 3b demonstrates effective discrimination of target echo under background masking. Detailed studying of signal-clutter discrimination technique based on recognition of target echo signatures and influence of SCR achieved on the total radar performances like ROC is subject of the current author research efforts.

Other important aspects of problem must be considered and studied theoretically, numerically and experimentally. This includes optimization of system total performances and effectiveness of implementation of real-time DSP processing, application of novel methods of pattern recognition, formation of electronic maps and libraries with their maintenance to store target signatures, improving target detectability due to high detection rate while minimizing the number of false alarm, application a receiving array and full-polarimetric concept etc. The final goal is to build advanced radar for both stand-off and stand-over demining operations.

There are no principal physical and technical limitations to create such radar system for demining problems that based on modern microwave, analogous and digit electronics as well as hardware and software signal processing techniques. It is also valuable to employ a data fusion approaches, i.e. combination of radar data and other remote sensing data given by various sensors, which may be installed on same robotics-like platform including metal detector, infrared, NQR and others sensors etc.

ACKNOWLEDGEMENTS

The author wishes to thank to Mr. and Mrs. Schakirovs for their generous support of the presented studies.

REFERENCES

[1] "Proceedings of the international conference on ground-penetrating radar", Lawrence, USA, May 1998.
[2] D. Daniels, "Ground probing radar techniques for mine detection", In [1].
[3] "Stand-off mine detection radar system", http://www.jacor.com/eme/smdr.html
[4] L. Carin, N. Geng, M. McClure, J. Sicina, L. Nguyen, "Ultra-wide-band synthetic aperture radar for mine-field detection", *IEEE AP magazine*, Vol. 41, No. 1, 1999, pp. 18-33.
[5] T. Dogaru, L. Carin, "Time-domain sensing of target buried under a rough air-ground interface", *IEEE Transactions on AP*, Vol. 46, No. 3, 1998,pp. 360-372.
[6] P. Ilavarasan, J. Ross, E. Rothwell, K. Chen, D. Nyquist, "Performance of an automated radar target discrimination scheme using E pulses and S pulses", *IEEE Transaction on AP*, Vol., 41, No. 5, 1993, pp. 582-588.
[7] A. Boryssenko, "Active microwave imaging in opaque media", *Accepted to the XXVIth URSI General Assembly*, Toronto, Canada, August 13-21, 1999.

Passive Mine Detection by Estimation of Statistical Properties of the Natural Electromagnetic Background Radiation

A. Boryssenko, V. Polishchuk
Scientific Research Company Diascarb
P.O. Box 370, 253222, Kyiv, Ukraine
E-mail: diascarb@public.ua.net

ABSTRACT

A presented method of mine detection hidden beneath terrain surface is geophysical method based on the following natural phenomenon. In general, when a land mine is buried beneath the Earth's surface, as well as any other foreign matter inside it, the media features are disturbed including natural electromagnetic background radiation (NEMBR). We can measure these disturbances by estimation of statistical variance of the local low-frequency pulsed NEMBR in surrounding space over searching territory. It was found empirically that strong statistical correlation exist between buried underground objects and variations of the Earth's NEMBR fields measured above searching area.

Keywords: Natural Electromagnetic Background Radiation, Correlation Coefficient, Magnetic Inductor Device

INTRODUCTION

It is well known terrifying figures about presence over 100,000,000 landmines in the different parts of the world and necessity to develop novel effective demining techniques due to limited capabilities of existing ones. Most of such methods and tools are based on advanced geophysical remote sensing like one implemented here that based on estimation of the statistical variations of the pulsed Earth's NEMBR fields.

Let consider firstly what is an electromagnetic background that can be proposed to apply for a mine detection. It was found experimentally that numerous geophysical processes in the Earth interior cause electromagnetic radiation in the low frequency band (0.1-100 kHz). This natural electromagnetic emission can be registered near the Earth's surface by an inductor devices as pulse stochastic electromagnetic radiation.

There are two reasons to study this phenomenon, i.e., firstly, in practical geology to forecast large-scale catastrophic events like earthquake or mudslide and, secondly, to detect buried underground objects by their passive remote sensing. This sensing is implemented by measurement and estimation of statistical variations of the pulsed Earth's NEMBR. A strong statistical correlation exists between location of underground object and extreme statistical behavior of the NEMBR registered over territory with buried object because subsurface objects vary the performances electromagnetic background as foreign matter [1].

This paper provides basic information concerning application of such passive remote sensing technique for land mine detection problems. To demonstrate these opportunities, results of some experimental examinations carried out by authors to detect mine-like target hidden beneath terrain surface are shown and discussed below.

RESEARCH METHODOLOGY

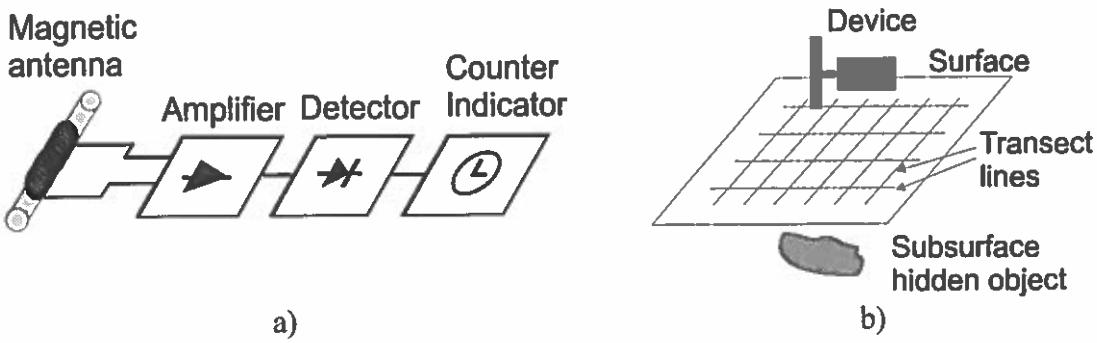

Fig. 1. (a) Schematic presentation of used device to register electromagnetic background radiation. (b) Measurement set-up with device moving (scanning) over searching territory along transect lines that formed, as a rule, orthogonal grid over searching area.

To measure pulsed NEMBR disturbed due to presence of foreign matter in subsurface media a magnetic inductor device with electronic registration of the flux density speed or pulse repetition rate can be employed. The simplified schematic structure of this electronic device is presented in Fig. 1a. The device includes a magnetic loop antenna with ferrite corner and electrostatic shielding, amplifier with 60-90 dB gain factor, amplitude pick detector, digital counter with indicator to display current pulse repetition in the arrangement without computer. In real a computer with ADC/DSP card has been used for storage of measured data and its real-time processing. Note that special preventive measures to minimize influence of computer wide spectrum electromagentic emission on measured NEMBR should be employed.

Application of device in the act of field survey is depicted by convection in Fig. 1b where vertical and horizontal orientations (polarizations) of a receiving ferrite antenna, which is located during measurement at the height of about 10-25 cm meter over the surface, can be used. Fixed over the Earth surface an electromagnetic pulsed radiation as pulse repetition frequency in each survey point is a mixture with industrial, atmospheric and computer interference signals. But those components have different statistical features and can be separated by corresponding statistical signal processing technique like one considered later.

In the connection of physical nature of the natural electromagnetic pulsed emission it is expedient to apply probabilistic mathematical methods, in particular correlation analysis to estimate statistical features of the NEMBR. Let consider the measured values of pulse repetition rate in two neighbor descrete readout points, i.e. x_i and y_i along same transect line where $i=1...n$ and n is total number of measurements in each readout points. Now, a theoretical correlation coefficient T as measure of statistical dependence between x_i series and y_i series is expressed like below:

$$T = \frac{\sum_{i=1}^{n}(x_i \cdot y_i)}{\sqrt{\sum_{i=1}^{n} x_i^2} \cdot \sqrt{\sum_{i=1}^{n} y_i^2}} \qquad (1)$$

And the empirical correlation coefficient E is determined by expression:

$$E = \frac{\sum_{i=1}^{n}(x_i \cdot y_i) - \frac{1}{n} \cdot \sum_{i=1}^{n} x_i \cdot \sum_{i=1}^{n} y_i}{\sqrt{\sum_{i=1}^{n} x_i^2 - \frac{1}{n} \cdot \left(\sum_{i=1}^{n} x_i\right)^2} \cdot \sqrt{\sum_{i=1}^{n} y_i^2 - \frac{1}{n} \cdot \left(\sum_{i=1}^{n} y_i\right)^2}} \quad (2)$$

The theoretical correlation coefficient T accepts values rather close to unit, therefore it is convenient to use instead it other magnitude like modified theoretical correlation coefficients R:

$$R = 1/(1-T) \quad (3)$$

EXPERIMENTAL RESULTS AND DISCUSSIONS

Mine simulators with ferro and non-ferro content like fluorocarbon polymer one have been used during field examination under realistic condition in loamy/sandy soils with/without vegetation cover. Mine-like object was being buried beneath the ground surface at the depth of about 5-15 cm as shown schematically in Fig.2a. The following optimal strategy of data gathering has been found effective. The area of survey site has been covered by grid of transect lines with the step of about 5 cm between nodes of grid. The total length of each transect line was 1m. A magnetic inductor device with antenna gear and computer interface via ADC/DSP card and corresponding processing software developed has been used to estimate the NEMBR statistical features measured along each transect line.

The typical results of such explorations for the fluorocarbon polymer disk-shaped mine simulator of 10 cm diameter and 2.5 cm height is shown in Fig. 2b,c where the two principal statistic performances, i.e. theoretical R (1) and empirical E (3) statistical correlation factors are represented. The data in Fig. 2b,c have been registered along transect line laid directly over buried target and demonstrates clearly strong correlation between spatial position of mine simulator beneath surface and pick of the correlation factors obtained when device is spaced directly over the mine simulator.

CONCLUSIONS

It seems reasonable utilization of NEMBR sensor technique as part of multi-sensor demining system with data fusion strategy employed. There is also positive authors' experience to apply a NEMBR sensor array to improve spatial resolution with simultaneous decreasing number of scan motions necessary to cover same searching area. To perfect target-clutter discrimination, i.e. to improve target detectability due to high detection rate while minimazing the number of false alarm operation with controlled stabilized false alarm rate, it will be useful creation of the database of target signature containing a set of statistical features like considered above, as well as high-order statistic (spectra) performances.

REFERENCES

V. Polishchuk, A. Boryssenko, I. Nefedova, "Passive detection of subsurface objects by using of the Earth natural pulsed electromagnetic field", *Proc. of Conference on Physical Methods and Means to Monitor Environment, Materials and Products LEOTEST'99*, Lviv, 1999, pp.89-90. (In Russian).

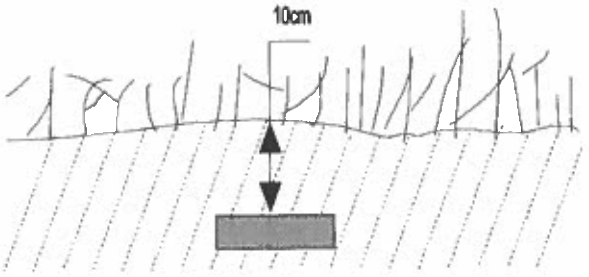

a)

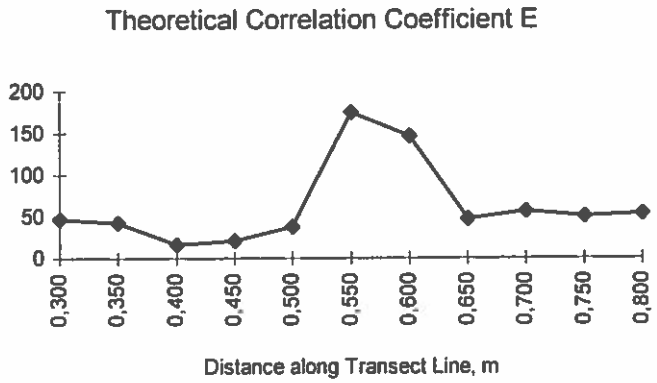

b)

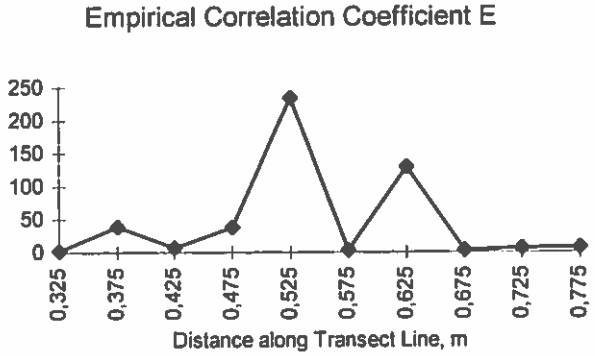

c)

Fig. 2. Experiment to detect hidden mine-like target by estimation of statistical variation of the pulsed Earth's NEMBR: (a) schematic presentation of problem's transect with hidden mine-like subsurface target; (b)-(c) experimental value of theoretical R (3) and empirical E (2) correlation coefficients correspondingly with evident pick anomaly over place where target is located really.

Handheld Magnetic System for Standoff Real Time Mine and UXO Detection

Yuri Bregman, Hovav Zafrir and Zeev Zalevsky
SOREQ Nuclear Research Center, Yavne 81800, Israel
Tel-Aviv University, Faculty of Engineering, Department of Physical Electronics, Tel-Aviv 69978, Israel

ABSTRACT
This paper introduces an advanced handheld system which combines both a sophisticated super resolving detection algorithm and state of the art magnetic sensors used for real time landmine and unexploded ordinance (UXO) detection. The algorithm is based upon the Pseudo-Wavelet transform, which is able to deal with signals embedded in strong noises, and features high spatial resolution capability and low computation complexity.

Key words: Magnetic detection, Landmines, UXO, Wavelet transform

1. Introduction

The main demand in humanitarian demining is the removal of at least 99.6 per cent of mines or munitions over large areas utilizing efficient and cost effective equipment. The existing portable metal detection equipment is the most reliable current method of finding mines, yet it is obviously very slow and extremely dangerous. However, most commercial metal detectors are not able to detect minimum-metal plastic mines from the distance of more than 5-10 cm. There is a demand for sensitive standoff detectors in order to make those mines fully reachable from the distance of at least several tens of cm. On the other hand the majority of suspected areas have no mines at all and the most cost-effective tool for demining would be a standoff "survey sensor" for marking actual minefields.

SOREQ NRC is implementing the final integration stage of a handheld magnetic system for standoff real time mine and UXO detection. The system is a combination of a sophisticated super resolving detection algorithm and state of the art magnetic sensors. The system is equipped with two potassium vapor magnetometers. The magnetic sensors are installed in a transverse horizontal gradiometric configuration and the input to the detection algorithm is the difference between the readout of the sensors. This array diminishes most of the geological background, magnetic noise caused by operator movement as well as diurnal variations of the Earth's magnetic field. Despite the gradiometric configuration, the influence of those factors is not fully diminished and a residual noise remains. The above mentioned effects are treated as noise by the super resolving detection algorithm.

The handheld system is the advanced derivative of the ground robotic system that was introduced in Refs. [1-3] where its real time, wide coverage and standoff detection capabilities were tested with real targets ranging from low metal plastic AP mines to air bombs.

In this paper we introduce a super resolving automatic detection algorithm for the magnetic handheld system based upon a Wavelet transform. The proposed approach allows an operator to obtain automatic detection with very low signal to noise ratios and better detection resolution.

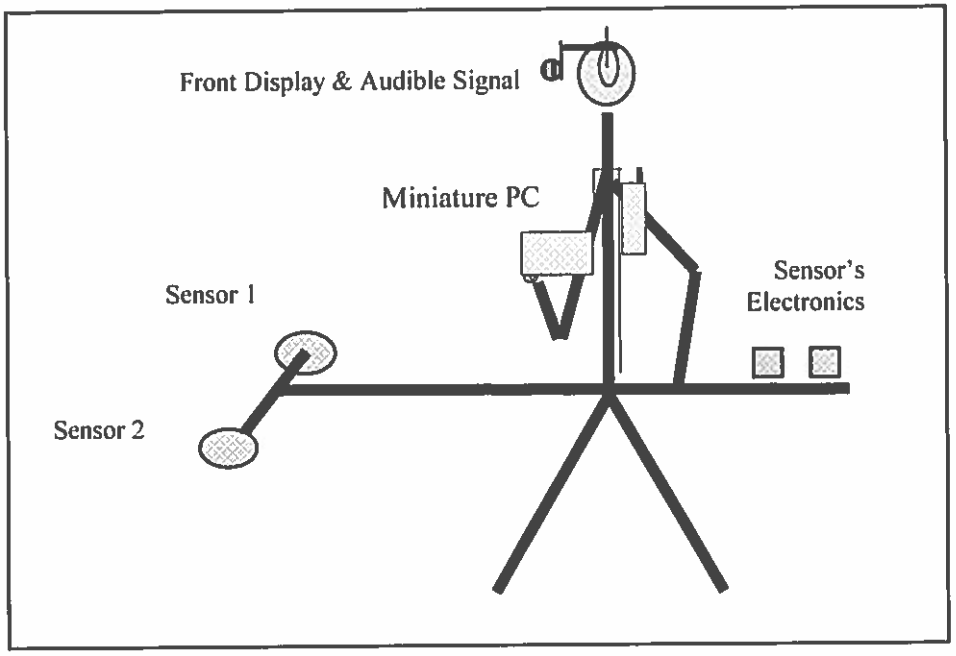

Figure 1. Handheld magnetic detection system

2. Theoretical background

Magnetic targets may be regarded as point dipoles. The magnetic anomaly caused due to those objects is considered by the Wavelet-based algorithm as a target signal, which is to be detected within the embedding noises. The magnitude of the field of a magnetic dipole can be expressed as [4, p.110]:

$$F = \frac{M\sqrt{4\cos^2\theta + sin^2\theta}}{r^3} \tag{1}$$

where M is the magnitude of the magnetic moment, r is the distance between the detector and the target and θ is the angle created between the vector connecting the target with the detector and the direction of the Earth's magnetic field.
The magnetic anomaly of a point dipole which is measured with the total field magnetometer is the component of **F** in the direction of **M** and may be approximated as:

$$H = \frac{M(3\cos^2\theta - 1)}{r^3} \tag{2}$$

We assume here that the Earth's magnetic field has the inclination 45° and declination 0° (that is about the real direction of the Earth's magnetic field in Israel). We assume that the direction of **M** coincides with the direction of Earth's magnetic field as well.

3. The Pseudo-Wavelet-based Algorithm

The Wavelet transform is a useful transformation for analyzing transient and seismic signals [5-7]. It may be expressed as a correlation operation between an input signal and a scaled base function called the mother Wavelet. Assuming that the background noise is a white noise it is well known that the matched filtering is the optimal operation regarding the signal to noise (SNR) criteria [8]. According to this theorem if an object f is to be detected within the signal g, a correlation operation is to be performed:

$$C_{fg}(b) = \int g(x')f(b-x')dx' \tag{3}$$

If g is identical to f a sharp correlation peak will appear. Its maximum indicates the relative position of f within g. If g includes f embedded with white noise, this operation will obtain the optimal detection in the sense of SNR and the optimal position estimation of f within g.

Observing again Eq. 2 reveals that, approximately, the variation of the distance of the magnetic dipole r is a scale operation of the original function. Thus, we aim to apply the matched filtering theorem for different factors of the filter, which means to create a matched Wavelet filter for obtaining the optimal automatic detection. Mathematically, the desired operation should be:

$$C_{fg}(b,a) = \int g(x)f\left(\frac{x-b}{a}\right)dx \tag{4}$$

where g is the input data and f is the pattern we wish to identify within the input. f is the dipole pattern obtained from Eq. 2. One may notice that Eq. 4 is identical to the Wavelet transform if f is the mother Wavelet function [5]. The admissible condition must fulfill $\int f(x)dx = 0$ in order to be able to perform the inverse Wavelet transform. Since the magnetic dipole is not obligate to this condition, we will call the algorithm the pseudo-Wavelet transform.

The mother Wavelet function f is determined according to Eq. 2. Obviously it highly depends upon the scanning direction. The performance of the algorithm will be much better for the South-North scanning line direction.

Since the shift parameter b is continuous and the scale parameter a is discrete, we may define the analog of the hybrid Wavelet transform. From Eq. 2 it may be seen that the distance variations influence the scale according to a^3. Since in the hybrid Wavelet the scale factors are powers of 2 (2^n where n=0,1,2...) we obtain:

$$a^3 = 2^n \rightarrow a = \exp\left(\frac{\ln 2}{3} \times n\right) n = 0,1,2... \tag{5}$$

4. Algorithmic Analysis

The following simulations examined different performance aspects of the pseudo-Wavelet matched algorithm, its ability to deal with signals embedded in strong noises, spatial resolution capability and low computation complexity. Fig. 2 demonstrates the ability of the algorithm to deal with detection of signals in low SNR. In Fig. 2a the magnetic dipole is embedded in a noise so strong that it is difficult to recognize the signal within it. For this simulation the detectors were located 1.5 m apart and 0.5 above the ground. The dipole with magnetic moment of 0.012 A-m² was 0.1 m below the South-North scanning line, and 2.3 m aside and 10 m along it. A white Gaussian noise and a linear trend modeled the background. Fig. 2b is the output obtained. Indeed a sharp correlation peak points out the existence of the dipole within the input data.

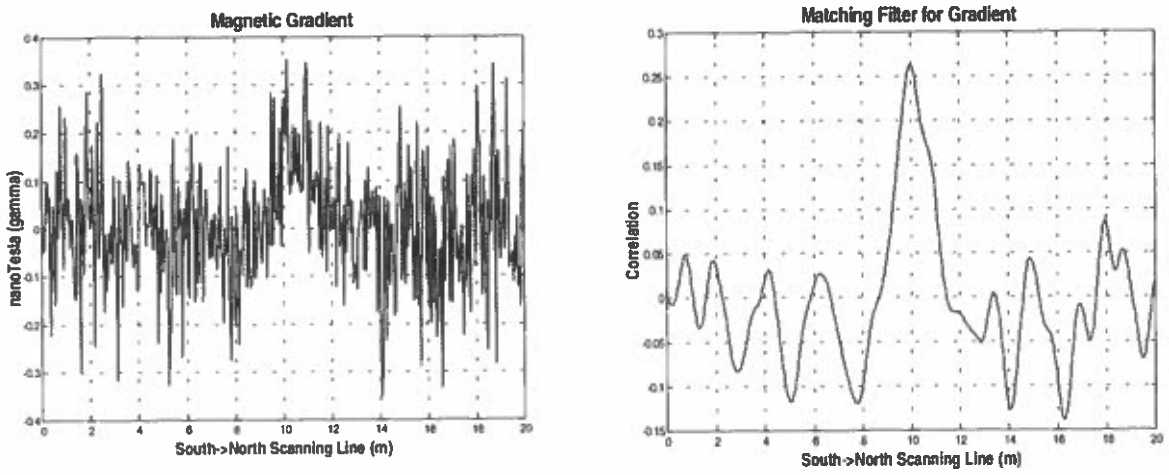

a). b).

Fig. 2: The ability of the algorithm to deal with a detection of signals in low SNR. a). The input data. b). The obtained correlation peak.

Fig. 3 examines the spatial resolution (target separation capability) in the presence of noise. The handheld detection system has the same configuration as in the previous simulation. The input signal included two dipoles with magnetic moments of 0.012 A-m², one at a depth of 0.1 m and 1.4 m aside and the other at 0.2 m and 1.5 m, respectively. The separation distance in the South-North scanning direction was a parameter. Fig. 3a suits a separation distance of 1.1 m between the two dipoles. Fig. 3b presents a cross section (for specific scale) of the pseudo-Wavelet plane obtained for this case, which yields the correlation peak picture.

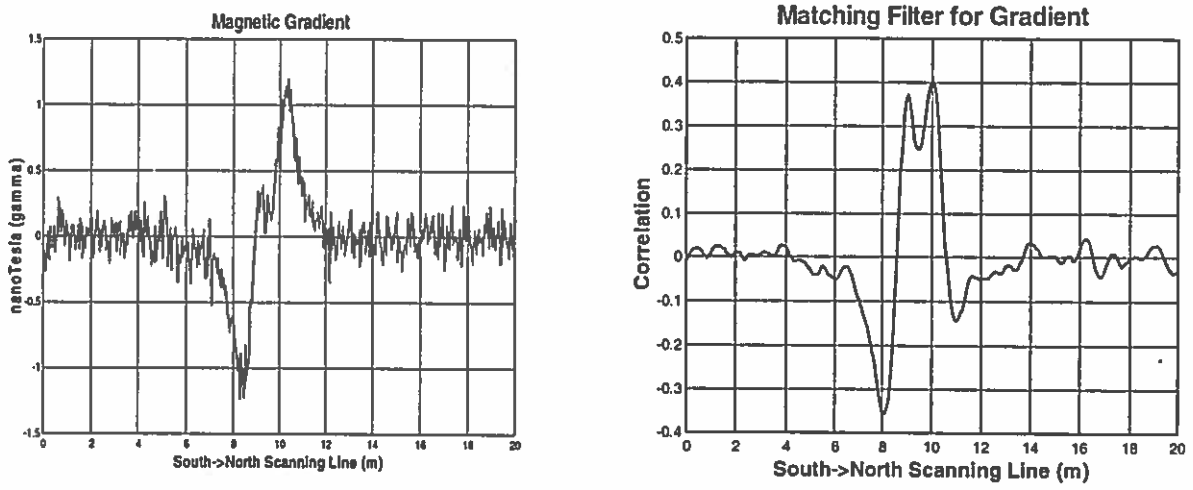

a). b).

Fig. 3: The separation ability of the algorithm.
a). The input data containing two dipoles. b). The obtained correlation peaks.

5. Experimental results

The capabilities of potassium vapor magnetometers to detect low-metal antipersonnel mines, specified by their metallic strikers, were demonstrated during a survey near Eilat, the southern Israeli city on the Gulf of Aqaba. The soil was unconsolidated gravel composed of metamorphic, magmatic and sedimentary pebbles. Fig.4 exhibits the magnetic response of the horizontal gradient, measured along a test line with and without two Israel No.10 AP plastic mines buried to a depth of 50 cm [9, p. 364]).

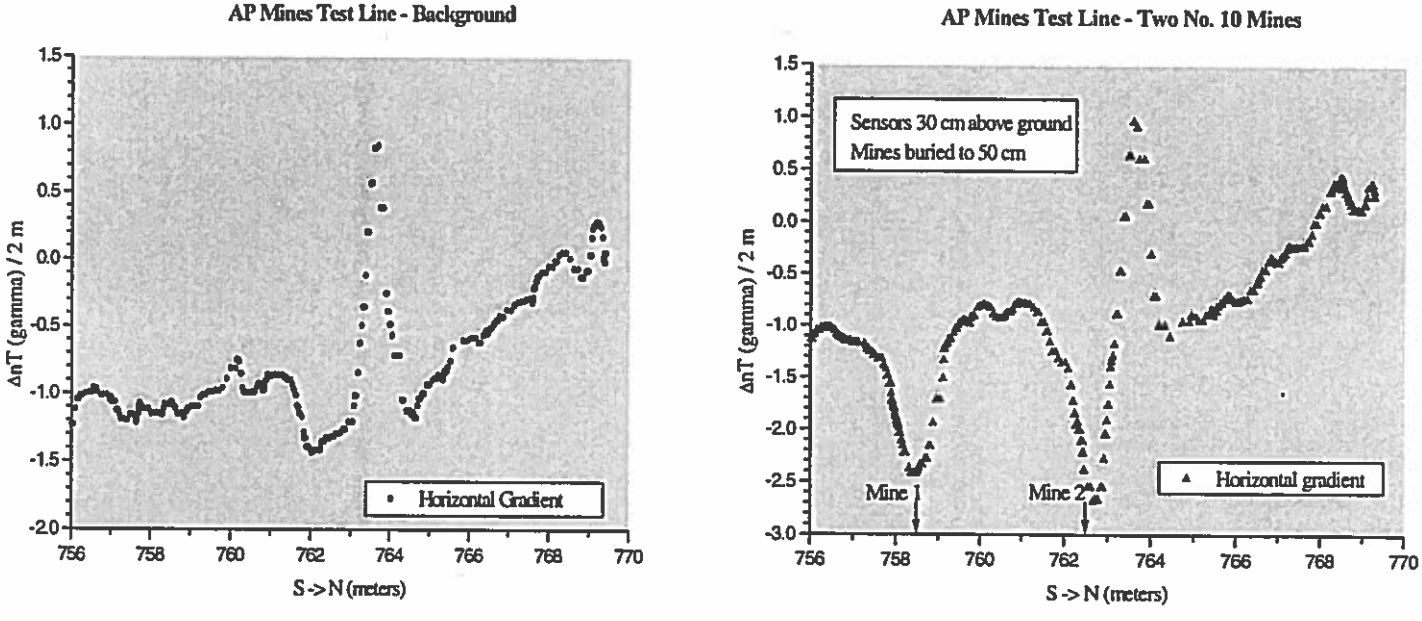

Fig. 4: Magnetic response of plastic mines

6. Final discussion

This paper has introduced a handheld magnetic system for standoff real time mine and unexploded ordinance (UXO) detection that includes Wavelet based algorithm. Theoretical analysis, computer simulation and partial experimental results have demonstrated system's capabilities. SOREQ is planning to introduce a demonstration handheld system prototype, by the end of 1999.

References:

1. H.Zafrir, Y.Bregman, D.Wolf and S.Hershler, "Super-sensitive magnetic and GPR ground robotic system for real time and wide coverage, UXO detection and mapping", The Fourth Unexploded Ordinance Detection and Range-Remediation Conference, p. 387-393 (1997).
2. H.Zafrir, Y.Bregman, D.Wolf and S.Hershler, "Super-sensitive, real time and wide coverage, all terrain ground robotic & hand held systems for mine and UXO detection and mapping", "Detection of abandoned land mines", Conference Publication No 458, IEE, p. 208-212 (1998).
3. Z.Zalevsky, Y.Bregman, H.Zafrir, "Super Resolving Magnetic Robotic System for Wide Coverage Real Time UXO Detection", Detection and Remediation Technologies for Mines and Minelike Targets IV, Proc. of SPIE **3710**, 1999 (to appear).
4. W.M.Telford, L.P.Geldart, R.E.Sheriff, D.A.Keys, "Applied Geophysics", Cambridge University Press, 1986.
5. H.Szu, Y.Sheng and J.Chen, "Wavelet transform as a bank of matched filters," Appl. Opt. **31**, p.3267-3277 (1992).
6. J.Caulfield and H.Szu, "Parallel discrete and continuous Wavelet transforms," Opt. Eng. **31**, 1835-1839 (1992).
7. R. K.Martinet, J.Morlet, and A. Grossmann, " Analysis of sound patterns through Wavelet transforms," Int. J. Patt. Rec., Artificial Intell. **1** (2), 273-302 (1987).
8. Y.Bitran, Z.Zalevsky, D.Mendlovic and R.Dorsch, "Performance analysis of the fractional correlation operation," Appl. Opt. **35**, 297-303 (1996).
9. Jane's Mines and Mine Clearance, edited by C.King, First Edition, 1996-97.

Detecting of anti-tank mines having dielectric sheath under curved rough surface by ground penetrating radar with long pulse duration

Chernokalov A.G.
Korolev Rocket and Space Corporation "Energia"

Druchinin S.V.
Moscow Institute of Physics and Technology (MIPT)

Izyumov S.V.
Joint stock company "Geological Prospecting" Rus. Ltd.

ABSTRACT

A problem of detecting of mines having dielectric sheath by ground penetrating radar is considered. Dimension of antennas was greater than the size of mines. Large roughness of the surface leads to a clutter and false objects after processing of signals. It is shown, that in this case a correlation processing and the focusing with a procedure of selecting and testing of objects can give images of mines, placed at small depths, but some false objects remain in the images. To check suspicious objects and obtain detailed images of mines one should use an another high frequency radar.

Keywords: ground penetrating radar, anti-tank mines, correlation processing, focusing

Introduction

A problem of detecting of anti-tank mines having dielectric sheath by ground penetrating radar (GPR) when roughness of the surface is large enough is considered. Development of systems for detecting of mines in such conditions is urgent because acts of diversions remain frequent. Detecting of mines under railroads is also considered. This work has been carried out to order of and jointly with Ministry of the Russian Federation for Civil Defense, Emergencies and Elimination of Consequences of Natural Disasters.

Theoretical background

Usually, in such systems radars use sufficiently short pulses to obtain detailed images of mines. We try to use antennas with greater dimensions and to measure signals with greater step between neighboring antennas positions. The using of wider pulses and large antennas sometimes enables to diminish influence of roughness of the ground surface, and may give better results for moist clayey soils, where losses are very large. Moreover, greater step in measurements is useful for rapid survey. Optimal design of mine detector may combine low and high frequency GPR systems, the first for rapid survey and detecting, the second for additional testing of sites and detailed imaging of mines.

The antennas, which are used in the GPR, are of the slot type. To enlarge a signal, passed to the ground, one should place the antennas closely to the ground surface. An influence of the spacing between the antenna and the ground surface to antenna's characteristics was considered in [1]. Variations of this spacing or roughness of the surface cause inconstancy of the signal of the radar, passed directly between transmitting and receiving antennas. This inconstancy is an obstacle in a problem of detecting of mines. Because the mines are usually buried at small depths, size of

antennas and wavelengths of the GPR are comparable with the depths, the signals, reflected from the mines, are not separated in time from the signal, passed directly between antennas. When the distance between antennas is large comparable with the depths, the presence of mines cause variations of the signal, passed directly between antennas. The inconstancy of this signal due to roughness of the surface leads to a clutter and "false" objects.

Materials and methods

A brief description of the GPR

The radar has been developed in MIPT and joint stock company "Geological Prospecting" Rus. Ltd. The radar uses separate transmitting and receiving antennas. Antenna have size 40×40×10 cm, distance between centers of antennas is 0.65 m. Fig.1 shows a signal, measured above a metallic sheet 0.4×1 m buried at a depth 1 m in sandy soil with moderate moisture. A signal 1 is a signal, passed directly between antennas, 2- the reflected signal.

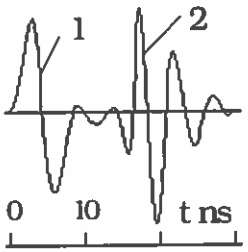

Fig.1

Methods of processing of signals

The software of the GPR includes several methods of processing of signals: inverse filtration, correlation and wavelet- correlation methods, least mean square method with regularization and auto- correlation processing. Three- dimension image of objects is obtained by focusing (migration).

Signal, passed directly between the antennas, is subtracted from measured signals before the processing. To find this signal the following methods are used.

a) This signal is found by averaging of signals along the ground surface. The inconstancy of a spacing between the antennas and the ground leads to variations of radar's frequency range. In GPR system described above that may be approximately taken into account by compression or strain in time scale of the first two oscillations of this averaged signal. By this way the averaged signal is fitted to each signal before the subtraction.

b) More accurate method consists in the following. Because the shape of the GPR signal, passed directly between the antennas, varies due to roughness of the surface, we measure in advance many waveforms on a rough surface, corresponding to all possible spacings between the antennas and ground surface. These measurements are performed on a site, where no objects were buried. Then when we subtract the signal passed directly between antennas, we choice the best suited waveform among previously written sample waveforms.

Due to inconstancy of the GPR signal (an influence of irregularity of the surface) and errors in determining of a signal, passed directly between antennas, a clutter appears after this subtraction near the ground surface. Focusing can somewhat filtrate this clutter.

Methods of processing of signals (except the auto- correlation method) require calibrating signals, measured in advance. Correlation and auto- correlation processing enable to compare measured reflected signals and calibrating signals, reflected from various mines, and choose the best suited waveform. Such processing in high frequency GPR may be used to identify a sort of mines. Auto- correlation processing is most effective when the shape of the reflected signal differs greatly from the calibrating signals. This processing finds correlation between reflected signals, measured in closely spaced positions of antennas.

Focusing is performed after the processing of signals. After the focusing a procedure of selecting and testing of objects is performed. This procedure consists in the following. In the image, obtained by focusing, we find local maxima and select points, in which the amplitude is greater, then a certain level, around each maximum. Then we search a signal, reflected from such "object", in the measured signals. If this reflected signal is found in a certain number of antennas positions, in which this reflection may be found, this "object" remains in the image, and the signal, reflected

from it, is subtracted from the measured signals. Otherwise, it is removed from the image. This procedure enables to find separately local and extended objects and to filtrate "false" objects and clutter.

Experimental results

Results of testing the GPR on site with curved ground surface

The GPR was tested on site with moist sandy-clayey soil and curved, irregular surface. The anti- tank mine in dielectric sheath with diameter about 23 cm and thickness 10-12 cm was buried at a depth 20 cm of its top side. An anti- infantry mine having dielectric sheath, diameter about 10 cm and thickness 5,3 cm was buried at a depth 17 cm of its top side. The irregularities of the surface were of the order of 10 cm in height and 0.5-1 m in length. Antennas were placed on the surface, but most part of apertures of antennas was not in close contact with the soil. The spacing between the antenna and the surface has an influence on antenna characteristics and on GPR signal. Antenna system was moved along parallel lines, and the signals were measured in points of grid with a step 0.2 m along both directions. A line of motion was parallel to direction between the antennas.

The anti-tank mine has been detected only after the processing of signals, focusing and procedure of selecting and testing of objects. The anti- infantry mine has not been detected because its size is very small. Antennas were moved along three parallel lines. Results of measurements and processing of signals for the central line are shown on Fig.2. Fig.2a) shows the signals after subtraction of the averaged signal, passed directly between the antennas. These signals include a clutter, which is due to irregularity of the surface. Fig.3,4 show results of 2-dimensional focusing (vertical sections) without a) and with b) the procedure of selecting and testing of objects for the central and neighboring line of motion of antennas. Fig.5 shows a result of 3-dimensional focusing with the selecting and testing procedure.

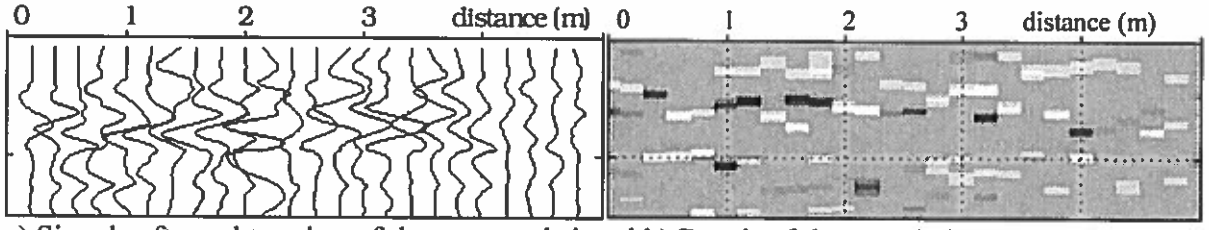

a) Signals after subtraction of the averaged signal b) Result of the correlation processing

Fig.2 Results of measurements and processing

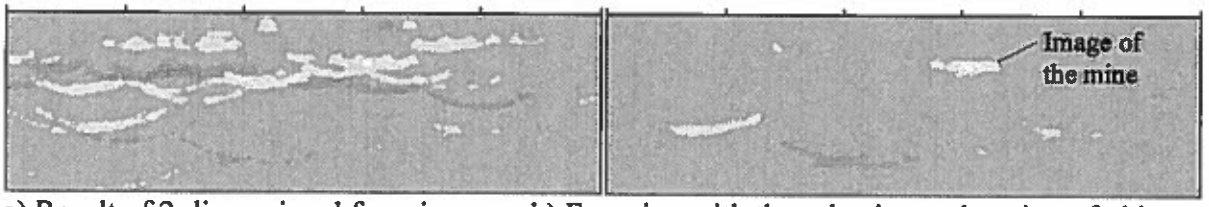

a) Result of 2-dimensional focusing b) Focusing with the selecting and testing of objects

Fig.3 Results of focusing without and with the selecting and testing procedure.

a) Result of 2-dimensional focusing b) Focusing with the selecting and testing of objects

Fig.4 Results of focusing for neighboring line of motion of antennas.

The anti-tank mine is not seen on Fig.2. On Fig.3b),4b) it is clearly distinguished. On Fig.3a),4a) it is also seen but a number of "false" objects is large enough and it is difficult to distinct the image of the mine. The image of the mine is greater than its actual size and slightly irregular. This is because large wavelengths, used in the GPR, large distance between antennas and large step between positions of antenna system. For the last two reasons the depth of the image is somewhat greater, that actual depth of the mine. Polarity of reflected signals is shown by colors. A sign of the reflected signal is positive, that corresponds to the ratio of dielectric constants of the mine and the moist soil.

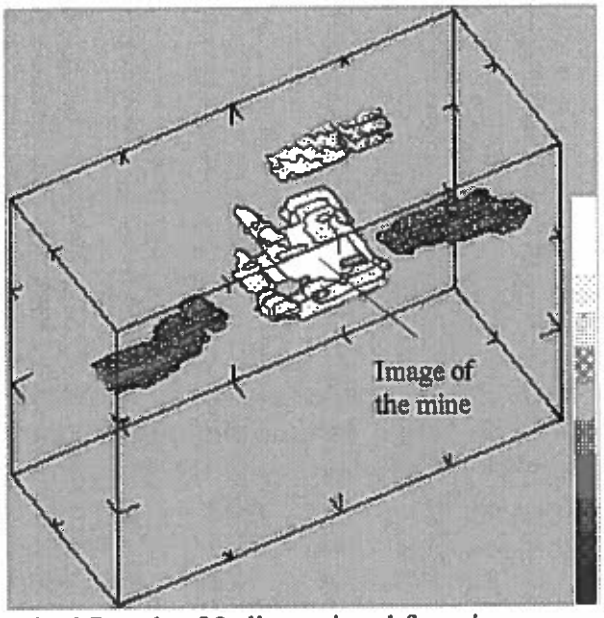

Fig.5 Result of 3-dimensional focusing

Apart from the image of the mine some false "objects" appear in the images. To check suspicious images and select actual mines one should use the another high frequency GPR.

For more rapid survey the antennas should move at a height about 10-20 cm along the ground surface. Now we develop such GPR.

A testing the GPR on railroads

The GPR was tested on sections of railroad with reinforced concrete and wooden sleepers. The antennas were covered by resistive material on sides and below the antenna to diminish parasitic reflections from rails. A layer of easily deformable resistive material between the antenna and the ground surface diminishes influence of roughness of the surface and diminishes a number of oscillations in the signal. Polarization was perpendicular to sleepers, made of reinforced concrete. Variations of GPR signals were very large due to sleepers. Mines, even having metallic sheath, placed below sleepers, have not been detected. Now we work on this problem.

Final discussion

Testing of the GPR shows, that the using of the GPR may have good prospects for detection of anti-tank mines on rough curved surface together with high frequency GPR for detailed imaging. Processing of signals and focusing with the procedure of selecting and testing of objects enable to find anti-tank mines, having dielectric sheath, by this low frequency GPR.

References

1. S.V. Druchinin, "Analysis of Characteristics of a Slot Antenna Used in Georadar", in *Proc. 7th International Conference on Ground Penetrating Radar*, Lawrence, Kansas, USA, May 27-30, vol.2, pp.643-648, 1998.

Target identification in Humanitarian demining using weak activation IR methods

Constantin Th. Coutsomitros[1], Athina Kokonozi[2]
Fivos Andritsos[3] , Ioannis Vakalis[4],
Lorenzo van Wijk[5] .
European Commission - Joint Research Centre - Ispra
Institute for Systems Informatics and Safety TP: 680
21026 Ispra (VA), Italy
[1]constantin.coutsomitros@jrc.it *tel: (+39) 0332 785171, Fax: (+39) 0332 786053,* [2]athina.kokonozi@jrc.it *tel: (+39) 0332 785172,* [3]fivos.andritsos@jrc.it *tel: (+39) 0332 789599, Fax: (+39) 0332 789392,* [4]ioannis.vakalis@jrc.it *tel: (+39) 0332 789117,* [5] lorenzo.van-wijk@jrc.it *tel: (+39) 0332 786224.*

ABSTRACT

Infrared spectral measurements have been shown, under different laboratory conditions, to detect buried plastic anti-personal mines (APM). Small temperature differences were applied between the landmine and its surrounding by heating and cooling. Different static test were performed with the mine partially or totally covered by sand and/or vegetation. The maximum depth of the buried mines was about 1 cm, which is a typical depth for an APM. In addition the use of the IR camera images fused with other sensorial information and expert knowledge to enhance the identification process of the suspect object is described.

Keywords: IR imaging, demining, data fusion, weak activation.

INTRODUCTION

Effective and efficient demining tools and methods are required to eliminate the threat of million buried mines. The main goal is to reduce false alarms, as deminers experience a ratio of 100-1000 false alarms for each effective mine detected.

Different demining technologies have been developed relying on sensors able to detect a particular feature of the mine, like its electrical, magnetic or thermal properties or trace elements of its explosive. The changing conditions and the varying features makes the usage of a single sensor inadequate. Moreover, the detection (localisation of a potentially dangerous object) and the identification of a given suspect object must be treated separately, since in actual de-mining as well as in future scenarios they are the object of different techniques [1].

Forward Looking Infra Red (FLIR) is a technique that yielded interesting results in the detection of anti-personal mines. Coupled with image treatment procedures FLIR allows the visualisation of the localised object in order to check whether it is a mine or a false alarm.

The working principle of this sensor is based on the measurement of temperature contrast, due to the different emissivity between the areas where the mine is localised and its surrounding. The thermal characteristics of the mine, the soil and the air determine the dynamic properties of the heat transfer phenomena. But the environment conditions and the burying operations can affect the measurements.

Several studies [2] have shown the in-ground vertical temperature gradient to be a good indicator for the thermal contrast between the mine and the surroundings. A different approach is followed in [3] where a linear coefficient links the temperature contrast and the temperature gradient with the type of the road and the position where the temperature was measured. It was also observed that this correlation could be affected by the environment conditions. Promising results were obtained using the Automatic Target Recognition (ATR) method for detection and landmine extraction from IR scenes [4]. Two other methods for extracting the difference in dynamic temperature response between objects were proposed by using the Karhuen-Loeve Transformation (KLT) and the Kitter-Young Transformation (KYT) [5]. In order to use the dynamic information that IR images contain, a theoretical model, and the numerical simulator based on that model is described [6].

In this study the experimental results on landmine identification using IR imager technique are presented. The measurements were performed in the laboratory under controlled conditions. The experimental set-up used is described in the next section. Weak activation was caused by cooling and heating respectively the observed area, in order to designate the factors affecting the demining operation with an IR imager. Some of the images in this work were obtained under extreme conditions not corresponding to real situations, in order to calibrate the method (see images A to D).

Im(A): the operator's hand is close to the buried mine, which is totally covered by sand. Obviously very weak streams of heat, emitted by the hand, are enough to create a temperature contrast.
Im(B): the mine was heated and placed on the sand and under leaves. Then the system was cooled before the acquisition.
Im(C): the mine was heated and then placed under the sand, totally covered. Before the acquisition the system was cooled.
Im(D): the small mine was heated and placed under leaves and under sand, totally covered. Before the acquisition the system was cooled.

Im (A) **Im (B)** **Im (C)**

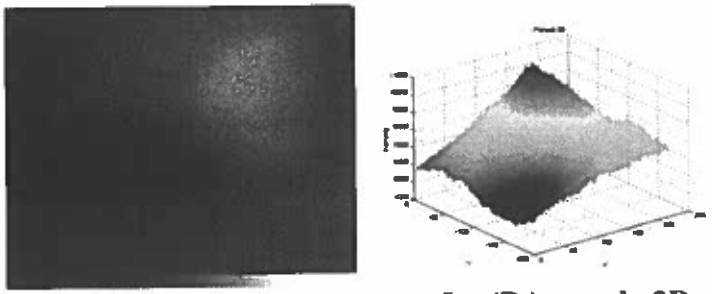

Im (D) **Im (D) pseudo 3D**

EXPERIMENTAL SETUP

IR camera

An Inframetric 760 model equipped either with an 8–12 μm and 3–12 μm spectral range sensor was used to evaluate temperature spectra. The detector is made off mercury, cadmium and tellurium and is able to detect temperature differences about 0.1. A thermomechanical cooling system improves the sensor's heat sensitivity by keeping its temperature at 77°K. The IR video camera has a 20–50 mm lens and is interfaced with a video and a small computer in order to save the collected images in digitised form. The light intensity is converted into 8 bits of gray level information ranging from 0 to 255 for each pixel and the sensor output image is saved in a 207 x 256 pixel array. The system is able to save up to 20 images. . The camera is inclined downward by 30 degrees. An IR 100 W was used for warming up the landmine or the sand.

Image pre-processing

Clearly, a poor contrast is expected between target and surrounding, as the temperature differences are very low. Thereby after the image acquisition some pre-processing is required to enhance specific image features. Image enhancement is performed to improve the raw image by suppressing noise and to emphasise structures. This will make segmentation easier.

The pre-processing steps include gaussian filtering, Sobel edge detecting and histogram stretching. The pixel values are replaced with their corresponding colour value by performing a lookup table transformation using the 'jet' colormap of Matlab. Then the detail and noise in the original image are removed performing a gaussian filter convolution. After 3x3 Sobel convolution kernels were applied to the smoothed image to emphasise the regions between the low and high spatial frequencies. Finally a minimum and maximum threshold are set in order to separate out areas with pixels having a high absolute magnitude value of the gradient. The pixels having intensity within the range of these two values are stretched proportional to their intensity. All the pixels with intensity less than the minimum are replaced to zero and those with intensity greater than the maximum to 255.

See images: Im (D) pseudo 3D, Im(2) sobel, Im(3) sobeltresh.

USE OF IR CAMERA INFORMATION WITH OTHER SENSOR DATA.

We described the weak activation technique as an identification method for buried suspect objects. This means that this method is more likely to be used after we received an alarm signal from the same or another sensor.

It is widely accepted that the use of one method - one sensor techniques are error prone because of the variety of the conditions and the types of the buried objects. We have thus designed a scheme to fuse the IR images with information from other sensor in an attempt to enhance the identification method [7]. This scheme (Fig.1) involves feature recognition algorithms and the use of CAD mine database where the appropriate combination of extracted features could lead to identifying one or more mine types with probability attached.

IR Image

Metal Detector

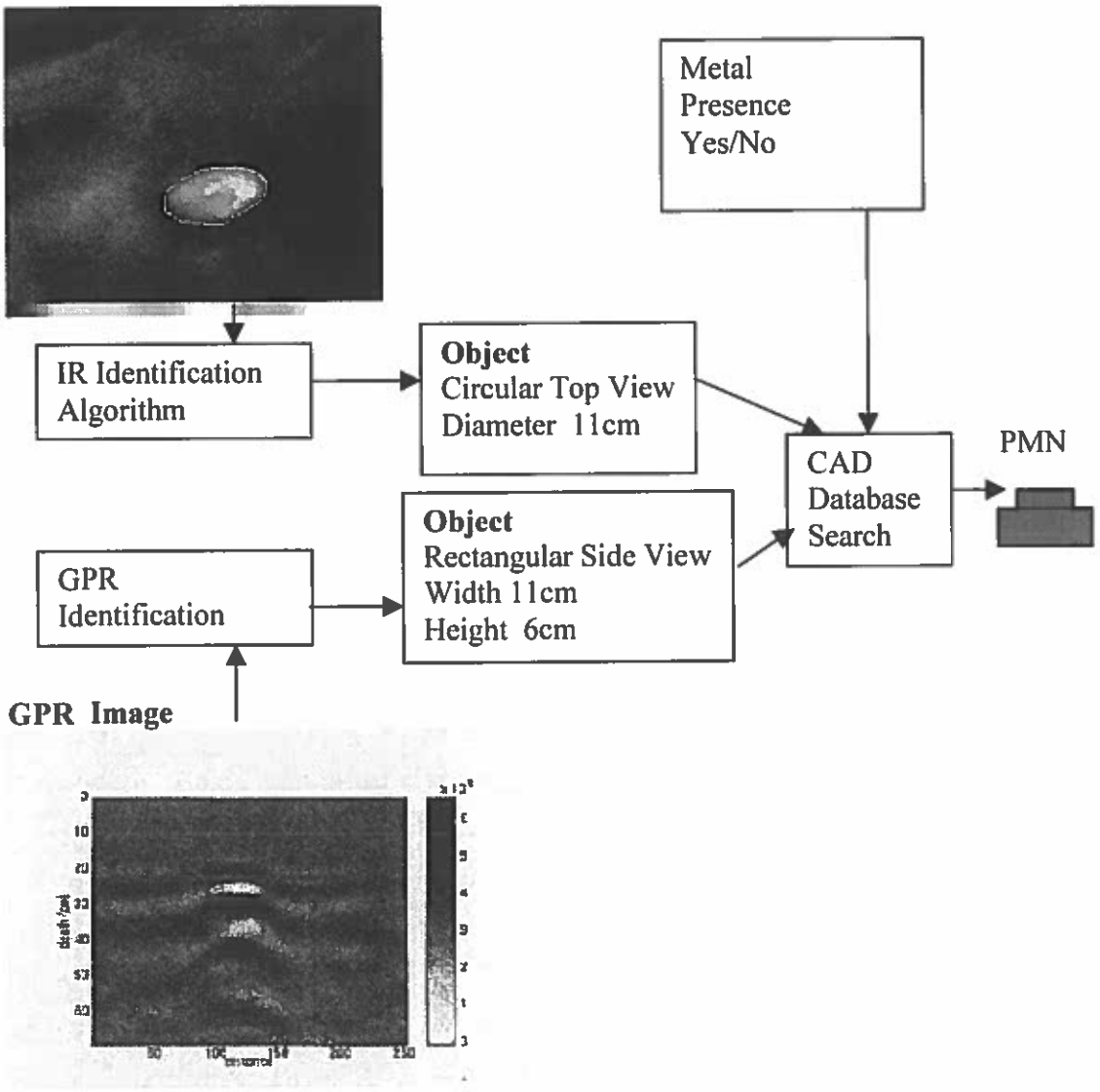

Fig. 1 A Sensor Fusion scheme using a CAD mine database

RESULTS AND DISCUSSION

There are two methods to obtain image acquisition using Infrared camera:

• ***Passive methods.*** The results are determined by the weather conditions and by the day-period of the acquisition. It has been observed that the acquired images are more distinct, if the acquisition is on midday [6]. No artificial changes of the temperature are caused, the acquisition takes place under the existing environment conditions.

• ***Active methods.*** In this case we alter the environmental conditions of the experimental set-up. Streams of heated/cooled air are directed towards the area focused by the IR imager. Ripples on the soil surface over the mine during the mine burying operations, can effect the temperature difference between the perturbed soil surface and its immediate surroundings. These types of phenomena are detectable with the IR imager, and cause false or distorted observations. In order to avoid them, we eliminate the tracks of the perturbed soil, with a spatula. In real conditions the smoothing of the soil is caused by natural phenomena.

The acquired images are classified according to the different laboratory conditions. The background temperature was about 18°C. We caused temperature difference to the sand (heating and cooling) with a hairdryer just in order to show that small amounts of energy are needed to create the temperature gradient between the buried mine and the surrounding area.

(1). The mines are on the surface.

Im(1): two plastic mines of different shape are placed on the surface. No temperature difference was caused.

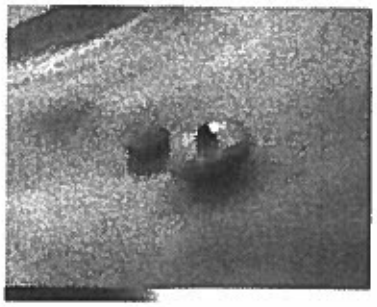

Im(1)

Im(2)

Im(3)

Im(2) sobel

Im (3) sobeltresh

(2). The sand was heated

Im(2): Both two mines are totally covered by sand. It can be observed that the top of the bigger mine as we can has different temperature compared to the rest part of the mine.
Im(3): The mine is totally covered by the sand.
The following images [Im(8), Im(9), Im(10)] acquired with a time delay of about 30".
Im(4): the mine is on the sand and partly covered by grass.
Im(5): the mine is on the sand and covered patially by more grass.
Im(6): the mine is on the sand and totally covered by grass.

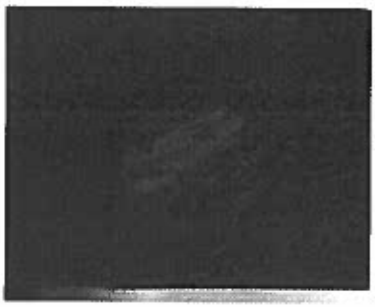

Im(4)

Im(5)

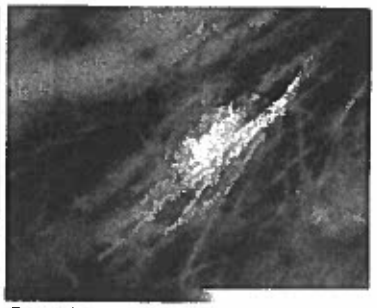

Im(6)

(3). The sand was cooled.
Im(7): both mines are totally covered only by sand.

Im(7) **Im(8)** **Im(9)**

(4). No temperature change was caused.
Im(8): the mine is partially covered by sand the top cover is visible.
Im(9): the mine is on the sand partly covered by grass.

Acknowledgments
We would like to thank Dr A.C.Lucia and Dr F.Sorel for their interest in this work, and for many fruitful discussions.

REFERENCES:

1) F. Andritsos, "*An information tool for humanitarian demining: Mine Identification Core Module*", Technical Note No I.98.232, JRC-ISIS, Nov. 1998.
2) Kevin Russell, John McFee and Wayne Sirovyak, "*Remote Performance Prediction for Infrared Imaging of Buried Mines* " (SPIE, Vol. 3079 pp. 762-769, 1997).
3) Jean-Robert Simard"*Improved Landmine Detection Capability (ILDC): Systematic approach to the detection of buried mines using passive IR imaging*". (SPIE Vol. 2765 pp. 489-499, 1996)
4) Peter Ngan, Sigberto A.Garcia, Eugene Cloud, Herbert Duvoisin, Dan Long and Jay Hackett, "*Developed of automatic target recognition for infrared sensor-based close range land mine detector*", (SPIE Vol. 2496,pp. 881-889, 1995).
5) Luc van Kempen, Mariusz Kaczmarec, Hichem Sahli, Jan Cornelis "*Dynamic infrared image sequence analysis for anti-personnel mine detection*". (IEEE Benelux Signal Processing Chapter, 1998, Leuven Belgium, pp. 215-218, March 26-27, 1998).
6) M. Schachne, L. van Kempen, D. Milojevic, H. Sahli, Ph. Van Ham, M. Acheroy, J. Cornelis "*Mine Detection by means of Dynamic Thermography: Simulation and Experiments*" [IEE Second International Conference on the Detection of Abandoned Landmines (MD'98), Edinburgh, UK, pp. 124-128, 12-14 October1998]
7) W. McMichael "*Data fusion for vehicle-borne mine detection*" (IEE "Detection of abandoned mines", Conference Publication No. 431, 7-9 October 1996)

WIDE-SPAN SYSTEMS OF MINE DETECTION

S.I. Ivashov, V.I. Makarenkov,
V.V. Razevig, V.N. Sablin,
A.P. Sheyko, I.A. Vasilyev

The Central Research Institute of Radio & Electronic Systems (TsNIIRES JSC)
69, Prospect Mira, Moscow, 129110, Russia
tel: +7 (095) 281 4797
Fax: +7 (095) 288 5880
E-mail: tsniires@tsniires.ru

KEYWORDS:

mine detection, wide-span system.

INTRODUCTION

The existing systems of detection of plastic-body mines planted in the soil use, as a rule, HF transducers. The detection principle of these systems is associated with measuring the variations in the dielectric properties of the soil in the place of minelaying. In view of the low contrast of a mine, the level of false alarms in a mine detector appears to be unacceptably high at a sufficient level of detection. This relates primarily to the reflections of HF signals from cultural and natural heterogeneities present in the soil and its surface.

One of the methods to overcome arising difficulties is the use of wide-span mine detection systems. The advantages of wide-span systems include their higher efficiency and the possibility of reducing the probability of false alarms in the course of mine clearance due to space selection.

Similar problems arise in the subsurface location when detecting lengthy objects in the soil, such as cables, pipes, fragments of old foundations, etc. In this case reflections from subsurface objects present correlated sequences which are well identifiable even at a high level of local reflections. And in the case of detection of subsurface mines, mines can be distinguished from the local heterogeneities of the soil by their shape and size because the characteristic size of an antitank mine is known. It is about 20...30 cm.

EXPERIMENTAL SYSTEM

To test these possibilities, a mock-up of a wide-span mine detector involving HF transducers was developed in the end of 80s. The mock-up is presenting a series of mine detectors arranged in a line, together with a mechanical gear providing for the movement of this mine detector above the ground. The mine detector mock-up is shown on Figure 1.

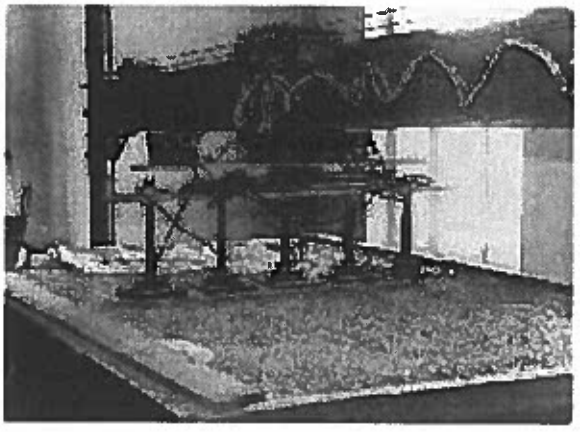

Figure 1: General view of the experimental installation. The working frequency of transducers is 600 MHz.

The working frequency of transducers is 600 MHz. The movement of the wide-span mine detector mock-up was performed above the surface of the proving ground. The dimension of the test sport is 2 m wide and 6 m long in its surveying plan and 1.5 m deep. The signals of the mine detector transducers were transmitted

through an interface for further processing to a computer. Each signal level from the receiver of the mine detector transducer corresponds to a certain level of the density of pixels on the picture.

The picture of the soil surface under investigation was formed as follows. Each transducer formed one picture line. By adding up picture lines, a two-dimensional picture was formed.

EXPERIMENTAL RESULTS

The Russian-made TM-62M type antitank mine was used as a metallic-body mine, and the Italian TC-6.1 type antitank mine was used to simulate plastic-body mines. The pictures of these mines are shown on Figures 2 and 3.

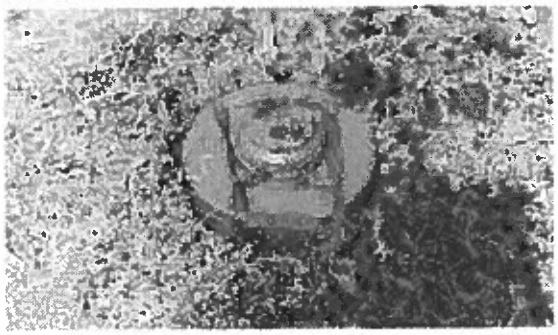

Figure 2: TM-62M type metallic-body antitank mine

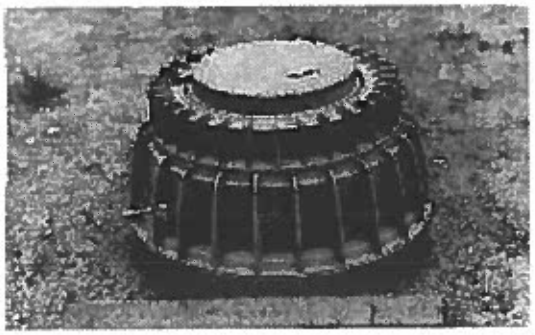

Figure 3: TC-6.1 type plastic-body antitank mine

We can present some experimental results. Figure 4 shows the HF image of a plastic-body antitank mine placed in the soil. The other picture on Figure 5 shows the image of two mines in its center, one of which is in a metallic body (left side) and the other one is in a plastic body. There are a metal pipe cut in the lower left corner of the picture, a 30 by 30 cm^2 metal plate in the lower right corner and a brick in the upper right corner. All these objects are buried in the soil at a depth from 5 to 10 cm.

The analysis of HF images on Figures 4 and 5 shows that the image of a mine presents two arcs perpendicular to the direction of the movement of transducers and a dark mark between them.

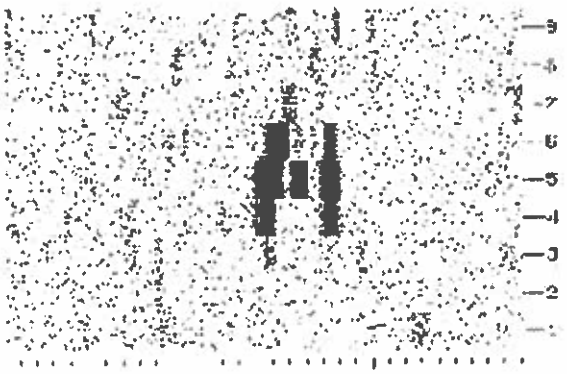

Figure 4: HF image of a plastic-body antitank mine in the soil

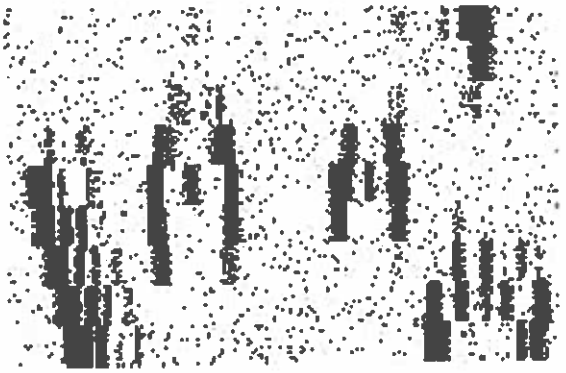

Figure 5: HF image of antitank mines and different objects in the soil.

The characteristic size of the obtained images of mines is close to the size of a mine in plan, about from 30 to 40 cm. Also, it should be noted that the shape, which is taken by a mine on the picture, is determined both by the size of a mine itself and the design of the transducers of a wide-span mine detector. The further experiments have shown that this image of a mine is sufficiently immune to the cultural and natural clutter of the soil.

In view of this circumstance, the space-filtering algorithm «identifying» mines in the soil by the characteristic shape of their images was proposed. In order to perform identification, let us use a correlation filter with a recognition matrix which depends on the shape and size of objects to be searched. You can see it on screen.

$$\mathbf{F}_{j,n} = \left\| f_{j,n} \right\| = \begin{vmatrix} 0 & 1 & 1 & 1 & 0 & 0 & 0 & 0 & 1 & 1 & 1 & 0 \\ 1 & 1 & 1 & 0 & 0 & 1 & 1 & 0 & 0 & 1 & 1 & 1 \\ 0 & 1 & 1 & 1 & 0 & 0 & 0 & 0 & 1 & 1 & 1 & 0 \end{vmatrix}; \quad \begin{matrix} j=1,2,3; \\ n=1,2,.. \end{matrix} \quad (1)$$

The following algorithm will be chosen as a procedure of recognition.

Let us establish a relation between each element of the HF image brightness matrix $\|m_{i,k}\|$ and the element of the matrix $\|l_{i,k}\|$, which is calculated as follows:

$$l_{i,k} = \Theta\left(\sum_{j=1}^{3} \sum_{n=1}^{12} f_{j,n} \cdot m_{i+j-2,k+n-5} - p \right), \quad (2)$$

where: p - the value of the detection threshold.

The function $\Theta(x)$ in the expression (2) is determined as follows:

$$\Theta(x) = \begin{cases} 1; & for\ x > 0. \\ 0; & for\ x \le 0. \end{cases}, \quad (3)$$

A target background environment meeting actual conditions was created to determine the efficiency of mine identification against the background of the soil clutter. For this purpose holes and mounds were made in the surface of the soil of the experimental spot, and a brick, a metal pipe cut and a metal plate were buried in the soil. Also, three antitank mines were buried in the soil, one of them being in a metal body and another two being in a plastic body. The surveying of the surface of the experimental spot resulted in an image shown on Figure 6.

The result of filtering the HF image shown on Figure 6 by using the above algorithm is given on Figure 7. This Figure shows that all three mines have been detected. At the same time linear-shaped objects and the occasional heterogeneities of the background are completely filtered and removed from the image.

The new device was making last year. You can see it on foreground of Figure 8. The main task of this device is to receive pictures of different antitank and antipersonnel mines in the ground at different depth

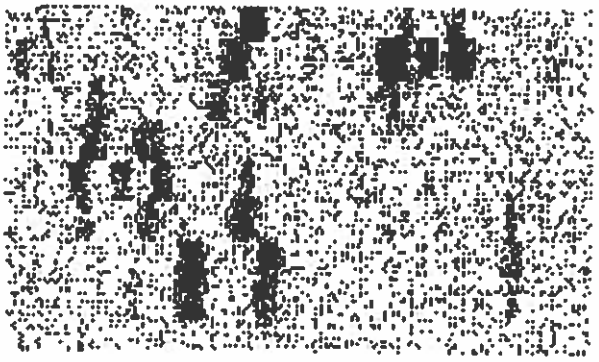

Figure 6: Initial HF image of the proving ground with mines and other things

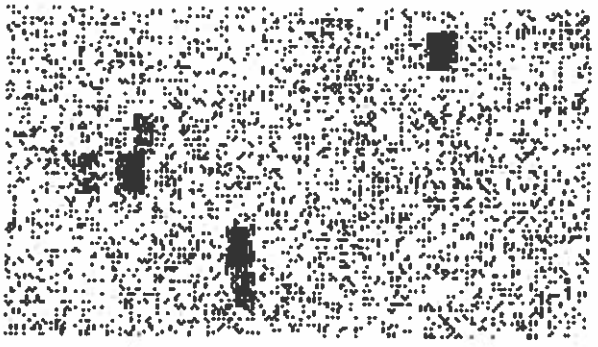

Figure 7: Result of filtering the HF image shown on Figure 6

Figure 8: General view of the modern experimental installation.
The working frequencies of transducer are from 1.5 to 2.0 GHz.

Test spots with different types of soil are on background of the Figure 8. We are using different types of soil in experiments: sand, black soil and loam.

On Figure 9 you can see different types of mines under investigation now.

Figure 9: General view of different mines under investigation

This work founds as subsequent development in the recently designed MiRascan ground-probing radar that makes it possible to detect and identify slightly deepened (up to 20 cm) objects by their shape. The principle of the multifrequency sounding of the condensed media (such as construction structures, soils, etc.) was assumed as a basis of the radar design.

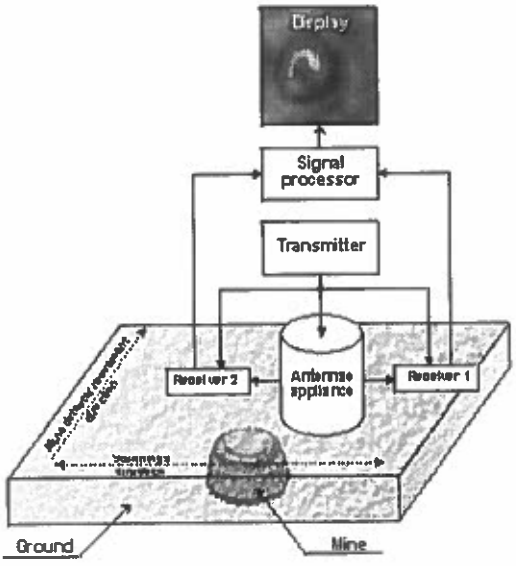

Figure 10. Block diagram of MiRascan radar

Figure 10 presents the block diagram of the MiRascan radar. The radar has five operational frequencies in the range from 1.5 to 2.0 GHz, and its signal is received in two polarizations. Power emitted by the generator on each frequency switched in sequence amounts to 10 mW, which provides for the complete safety of staff. The successive reception of signals on each frequency and in both polarizations is conducted in the process of scanning of the ground surface. Frequency switching rate is such that it provides for the spatial matching of the radio images on separate frequencies.

The scanning in the lateral direction is carried out at the expense of electromechanical movement of the SHF device of the radar, and in the longitudinal direction due to the movement of the entire radar. The scanning results are displayed in the form of gray scale images on the monitor screen. Since it is difficult for an operator to perform a simultaneous analysis of all images on different frequencies, one animated image is formed in which sequential frames correspond to different frequencies.

The mock-up of the mine detector makes it feasible to survey the lane of movement 112 cm wide and to display the scanning results on the screen of a personal portable computer in real time.

There is HF animation images of Russian antitank mines TM-62M and TM-62P3 with plastic and metallic bodies.

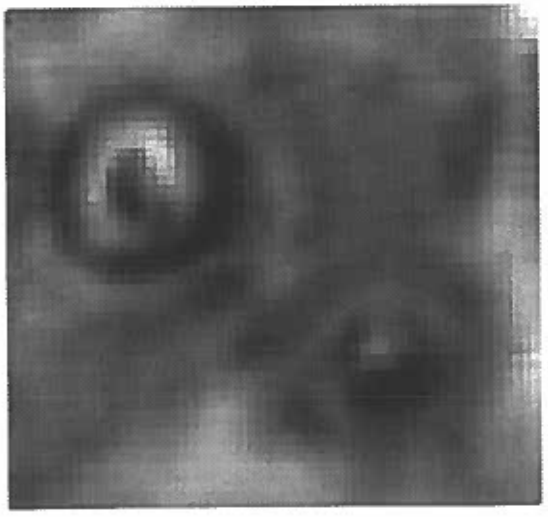

Figure 11: HF animation images of Russian antitank mines TM-62M and TM-62P3

The HF animation images of Italian TC-6.1 and TC-2.5 antitank mines are shown on Figure 12.

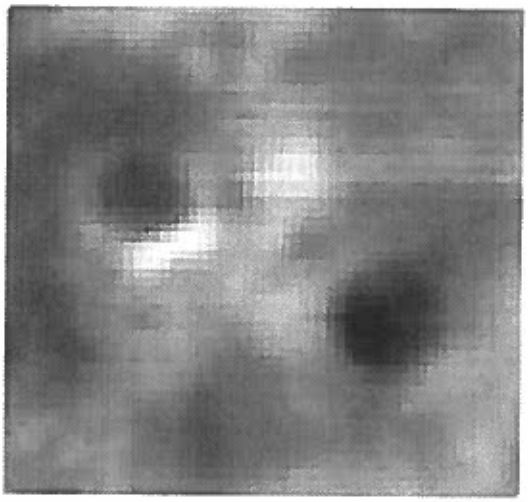

Figure 12: HF animation images of Italian antitank mines TC-6.1 and TC-2.5

Now you see a Russian antipersonnel PMN mine in sand on Figure 13.

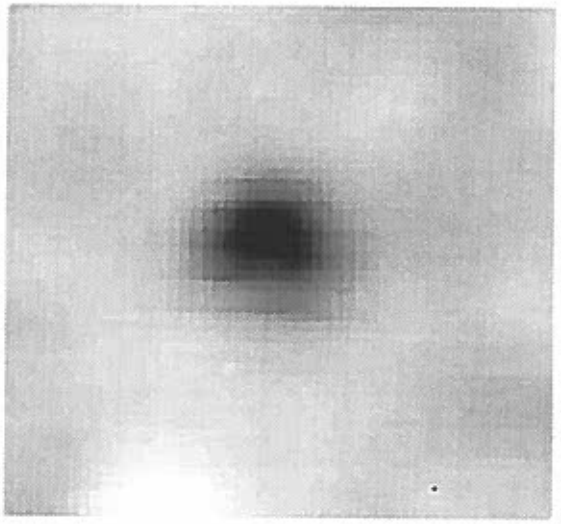

Figure 13: HF animation images of Russian antipersonnel PMN mine in sand

Russian antitank PTM-3 mine was dug in sand on depth 5 cm. This mine has form of a rectangular container with square cross. The container's sizes equal 84×84×330 mm. The HF animation image of antitank PTM-3 mine is given on Figure 14. It is visible that this image cardinally differs from all previous.

The arrangement of the mines on the site with the sandy soil is presented in this picture above. The results of the site surface scanning at constant frequency are given below it.

Figure 14: HF animation images of Russian antitank PTM-3 mine in sand

CONCLUSION

To improve detection characteristics, the above-discussed wide-span mine detector based on HF transducers are complemented by ferrosondes. In this case a coincidence circuit could be used in several channels of a mine detector to reduce false alarms.

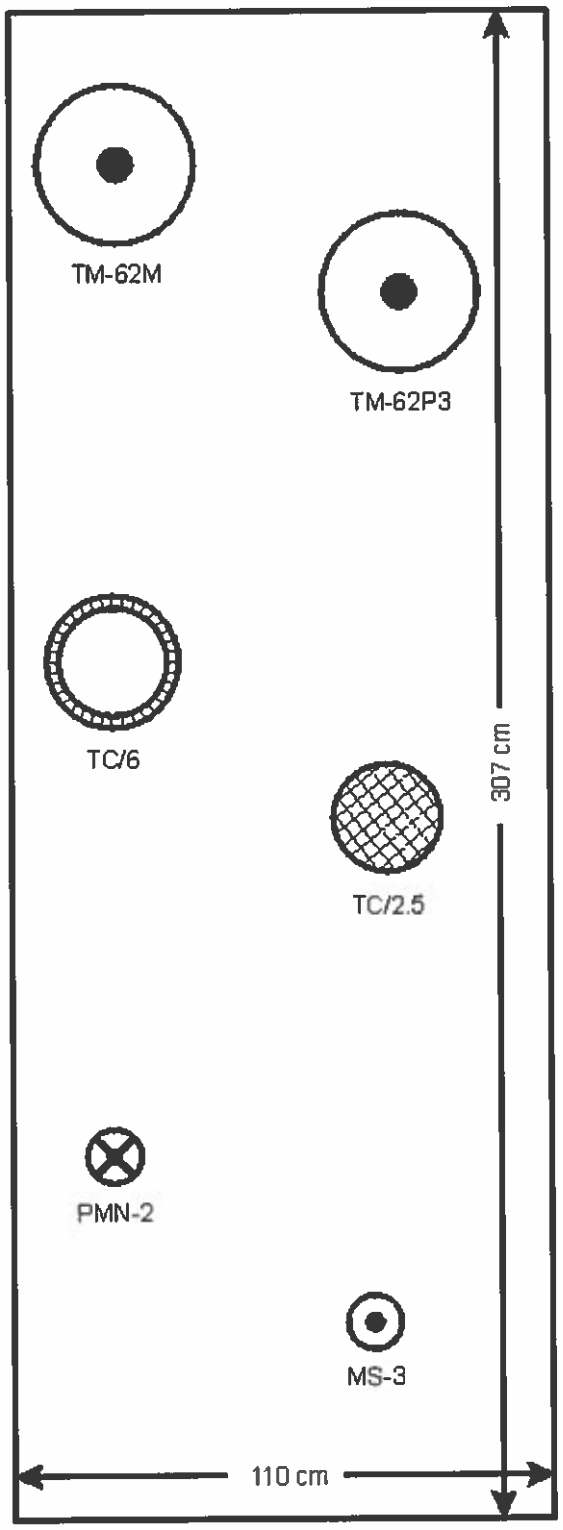

Figure 15: Diagram of mines arrangement in the proving ground

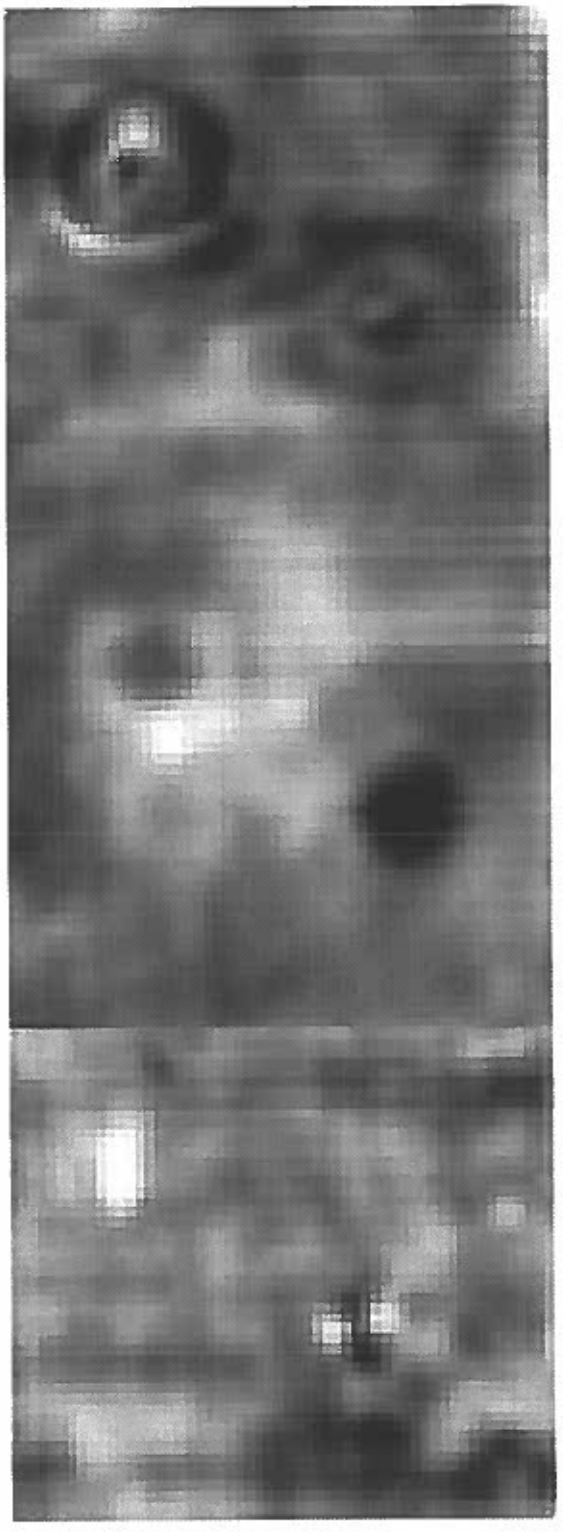

Figure 16: Radio images of mine mock-ups in the examined lane with sandy soil

Direct Imaging of Explosives

E.A. Knapp[1], *A.W. Saunders*[1], *and W.P. Trower*[1]

ABSTRACT

We describe here our Nitrogen Camera technique with which we have produced images of elemental nitrogen in concentrations and with surface densities typical of buried plastic anti-personnel mines[2]*. We show intensity images, obtained under laboratory conditions, of nitrogen in a plastic anti-personnel mine simulant and in SEMTEX. We summarize our progress in creating the technology to field our Nitrogen Camera, the most important of which is a mobile 70 MeV racetrack microtron.*

Keywords: land mine detection, Nitrogen Camera, gamma-ray imaging, race-track microtron

1. INTRODUCTION

Any technique that can detect nitrogen concentrations can be used to screen for concealed explosives. However, if images of nitrogen in concentrations typical of buried anti-personnel mines can be obtained, then a robust screening technology can be built. Although three-dimensional nitrogen images are desirable, more important are a collateral of carbon and oxygen images since with them the rejection of non-explosive nitrogenous material is almost assured.

Present mine clearing teams rely on hand-held magnetometers to register tiny metal detonating caps and wires in small plastic land mines with the result that the vast majority of their efforts are devoted to retrieving harmless metal fragments which liter combat areas. Mine clearing productivity would be greatly improved if the explosive material itself could be directly detected. Any such detector would need to be insensitive to metal, register all explosives, and produce images of the nitrogen, carbon, and oxygen in explosive objects. No such fieldable instrument, based on a nuclear or any other technique, now exists.

Our Nitrogen Camera, which we have demonstrated experimentally and are developing, meets all of these criteria[3]. The basis of our technique is an electron accelerator that produces photonuclear reactions whose decays are detected. A mobile vehicle mounted Nitrogen Camera could be effective in detecting buried mines, either in an active battlefield situation or in the clearing of abandoned military munitions. We describe here our Nitrogen Camera system as it moves from a laboratory proven technology that directly images explosives with high efficiency into the field.

2. PHYSICS

Our ability to image explosives results from an observation made over a decade ago by the late Luis Alvarez and one of the authors. They noted that high-energy photons interact with the chemical elements in explosives to generate a unique signature. This signature can identify unambiguously and to construct images of the explosives marker element - nitrogen, carbon, and oxygen.

When high-energy photons from an accelerator source are flashed onto an object in a high-intensity pulse, a variety of radioisotopes are produced, almost all of which decay with half-lives of seconds or longer, as seen in Fig. 1. However, if nitrogen, carbon, or oxygen are present, radioisotopes are

[1] World Physics Technologies, Inc., 1105 Highland Circle, Blacksburg VA 24060 USA.

produced that β decay with very short half-lives, ~10-20 ms, which hold two advantages for the detection of our marker elements, as seen in Fig. 2. First, almost all of the produced marker isotopes decay and can be observed in a brief time window after the flash. Second, and more important, the recorded time histories of these markers are significantly different from those of all other isotopic products thus automatically giving clear signals of the nitrogen, carbon, or oxygen present. To obtain separate images of our three markers, the energy of the electron beam that produces the photons flashed on the object is varied. No other photonuclear reactions produce such short half-life products so that mines and unexploded ordnance can be uniquely distinguished from the material that surrounds them. This invention realizes this fact.

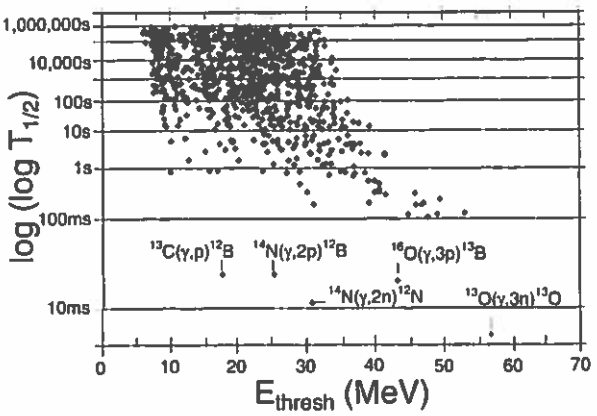

Fig. 1. β decaying radionuclei photoproduced on stable isotopes with abundance >1 % resulting in three or fewer nucleons.

To detect our five explosives marker reactions, we record all γ rays, whose energies exceed ~1 MeV, with time after they are created in the manner of Fig. 2. The vast majority of these γ rays come from bremsstrahlung of decay electrons and positrons, some result from the annihilation of positrons with environmental electrons, and a small number arise from the de-excitation of nuclei stranded in excited states after the parent nucleus β decays.

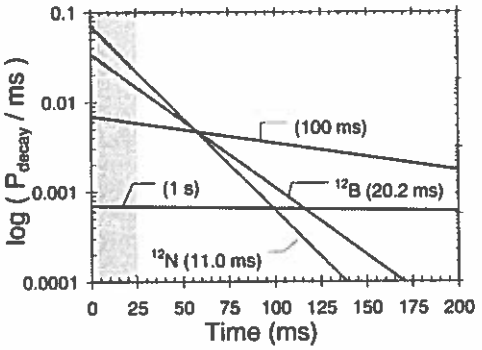

Fig. 2. β-decay probability with time.

Table I. Production of our explosives marker radionuclei.

Isotopic Fraction	Reaction	$E_\gamma^{threshold}$ (MeV)	Decay	$T_{1/2}$ (ms)	$Yield_{production}$ P_{prod}(25MeV)/e⁻	P_{prod}(50MeV)/e⁻	P_{prod}(70MeV)/e⁻
.011	^{13}C (γ,1n) ^{12}B	17.5	β^-	20.2	1.2×10^{-8}	5.4×10^{-8}	6.3×10^{-8}
.996	^{14}N (γ,2p) ^{12}B	25.1	β^-	20.2	-	9.2×10^{-10}	1.9×10^{-9}
.996	^{14}N (γ,2n) ^{12}N	30.6	β^+	11.0	-	8.4×10^{-7}	1.2×10^{-6}
.998	^{16}O (γ,3p) ^{13}B	43.2	β^-	17.4	-	1.4×10^{-13}	6.9×10^{-12}
.998	^{16}O (γ,3n) ^{13}O	52.1	β^+	8.6	-	-	7.1×10^{-9}

To create our marker reactions, we pass 25, 50, and 70 MeV electrons through a tantalum radiator to produce photons whose spectra are seen in Fig. 3(a). These photons interact with our marker nuclei according to the cross sections of Fig. 3(b). Note that 50 MeV electrons, for example, produce vanishingly few 50 MeV photons but many 17 MeV photons. So a 50 MeV electron beam will create nitrogen radionuclei but also many carbon radionuclei. We calculate the probability that a beam electron will produce a radioisotope from a mole of marker isotope, by multiplying the photon flux by the reaction cross section, energy bin by energy bin which we sum and present in Table I as production yields.

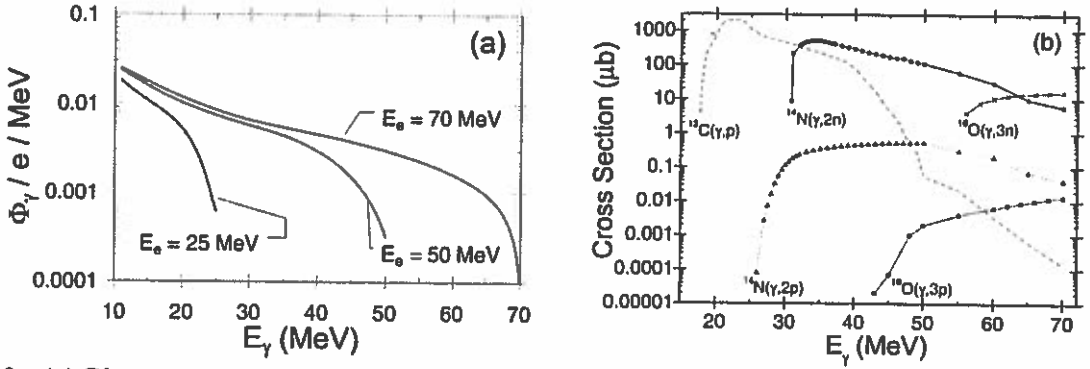

Fig. 3. (a) Photon spectra from electrons on a radiator and (b) marker reaction cross sections.

Our rapidly decaying marker radionuclei emit a positron or an electron whose energies are distributed as seen in Fig. 4(a). Each β ray collides with the atomic electrons of the object and radiates a succession of γ rays until it comes to rest. The γ-ray spectra from these β decays are shown in Fig. 4(b). It is the totality of these γ rays with energy greater than ~1 MeV recorded with time after the photon flash that reveals our explosives marker elements.

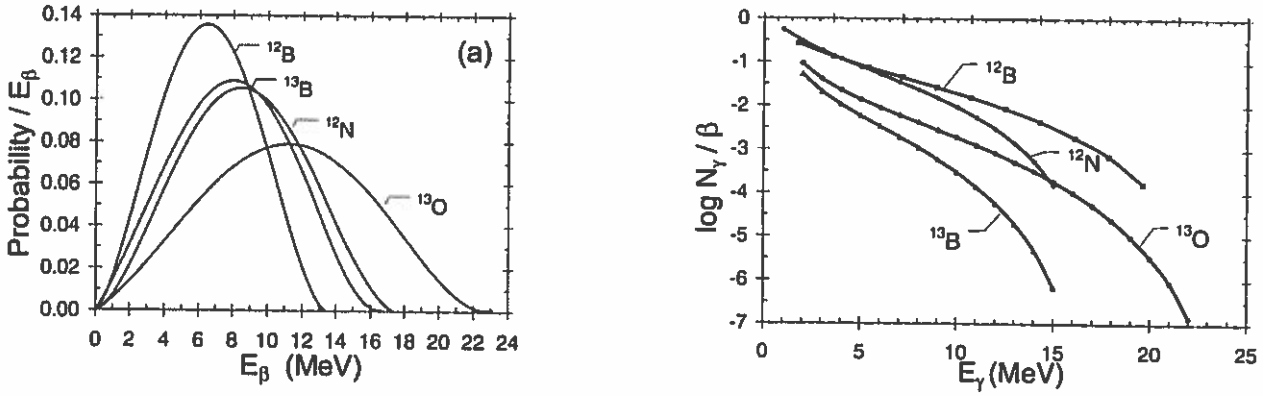

Fig. 4. Marker radioisotopes (a) β-decay and (b) resulting γ-ray bremsstrahlung spectra.

Operationally, after the probing photons are flashed on an object, we wait ~5-10 ms for the neutrons produced with the photons to be slowed and captured and the photomultiplier tubes to settle down before we begin recording γ rays in 1 ms time intervals. Marker elements produce count sequences that fall with the characteristic half-life of the particular radioisotope. In our 20 ms detection window of Fig. 2, ^{12}N (52%), ^{12}B (42%), 100 ms isotope (12%), and 1 s isotope (1%) will decay.

Table II. Decay of our explosives marker radionuclei.

Reaction	Decay	$E_\beta^{end\ point}$ (MeV)	Yield$_{decay}$ P_γ (25 MeV)/e$^-$	P_γ (50 MeV)/e$^-$	P_γ (70 MeV)/e$^-$
^{13}C (γ,1n) ^{12}B	β^-	13.3	1.5×10^{-8}	6.6×10^{-8}	7.7×10^{-8}
^{14}N (γ,2p) ^{12}B	β^-	13.3	-	1.1×10^{-9}	2.4×10^{-9}
^{14}N (γ,2n) ^{12}N	β^+	17.3	-	2.2×10^{-6}	3.3×10^{-6}
^{16}O (γ,3p) ^{13}B	β^-	16.6	-	1.3×10^{-14}	6.8×10^{-13}
^{16}O (γ,3n) ^{13}O	β^+	23.1	-	-	1.4×10^{-9}

By exposing an object to flashes of photons with three different energy distributions, we determine separately the relative abundance of our three explosives marker elements: 25 MeV electrons will

produce carbon, 50 MeV - both nitrogen and carbon, and 70 MeV - oxygen, nitrogen, and carbon. The decay yields, the probability of a beam electron producing bremsstrahlung γ rays with energy above 1 MeV, are listed in Table II. Actual detection yields can be calculated from these decay yields once the detector type (i.e., efficiency, pulse shape, and electronics chain characteristics) and geometry (i.e., size and stand-off distance) are specified.

3. EXPERIMENTS

We proved our Nitrogen Camera idea in experiments using the racetrack microtron at the Royal Institute of Technology (KTH) in Stockholm, Sweden[4]. Their accelerator produced electrons with energies from 5 to 50 MeV selectable in steps of 3.3 MeV with pulse currents on good days as large as ~18 mA delivered in 5 μs-long pulses at rates of 1 to 10 Hz. As the electron beam passed though a 1 mm tantalum radiator, it produced a flash of photons with energies distributed as seen in Fig. 3(a) where ~85% of these photons fell inside a 2 cm diameter spot on an object located ~1 m away. The photon flash from the electron beam produced a variety of radioisotopes in the volume below the spot including our explosives markers when electron energy exceeded their reaction threshold energy. These produced radionuclei immediately began to decay and, in the ensuing sea of γ rays, we sought our explosives markers.

All manner of γ rays fell on our crude detectors (four 5" fast photomultiplier tubes coupled to 5" plastic scintillator cylinders) located a half meter upstream from, and pointing at, the spot where the photons were flashed. The individual detector signals were fed into constant-fraction discriminators and aggregated in a linear fan-in before being sent to a multi-scalar data acquisition board resident in a computer backplane. Fig. 5 shows the γ ray time spectra resulting from single ~4 mA, 50 MeV electron pulses on a 1" thick aluminum plate and on the center of a 2" × 2" 300 g carbon block attached to the plate. Subtracting the raw counts from these two flashes, bin by bin, and fitting the residual spectrum to an exponential gives 22.3±1.5 ms in reasonable agreement with the ^{12}B half-life.

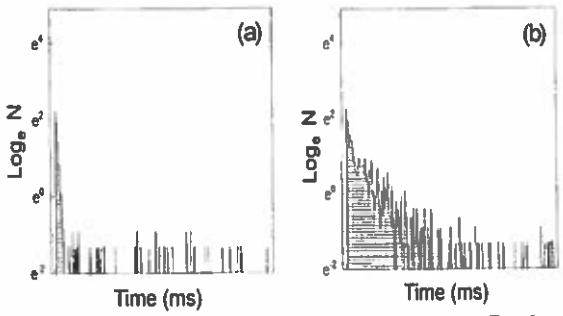

Fig. 5. Counts from single photon flash: (a) plate and (b) carbon block on that plate.

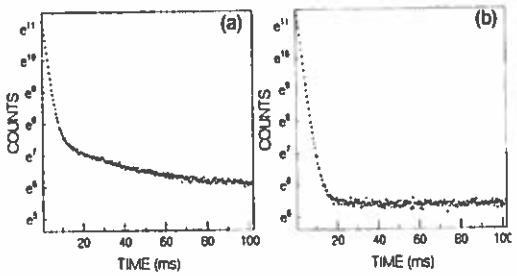

Fig. 6. Time spectra for 50 MeV electrons on (a) a melamine object and (b) room air.

Time spectra from 300 g of melamine ($C_3N_6H_3$) and from room air subjected to ~1,500 photon flashes produced by ~1 mA, 50 MeV, 10 Hz electrons are seen in Fig. 6. The first ~10 ms after the photon flash form a common small time-peak containing ~66% of the counts. Long-lived (>100 ms) radionuclei produced the common flat background that increased roughly with the number of photon flashes squared at our pulse repetition rate and increased linearly with the object matter density. Subtracting these two features leaves a melamine signal with ~17% of the counts and a half-life of ~18.6 ms, between that of ^{12}N and ^{12}B.

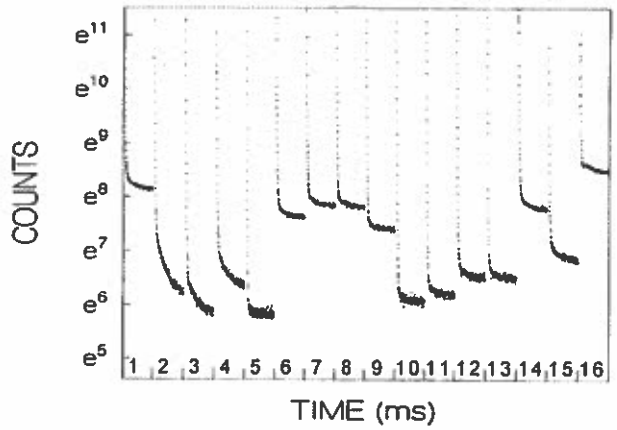

Fig. 7. γ-ray time spectra for 16 samples.

We obtained experimental time spectra for many materials and all but one (titanium) of the ten most abundant elements that comprise 99.48% of the earth's crust. We also irradiated 17 other elements and three explosives - SEMTEX, dynamite, and C3[5]. We saw no signals other than those from nitrogen or carbon. (Our accelerator energy and current were too low to produce the oxygen markers.) The 100 ms spectra, excited when multi-pulse 50 MeV electron beam photons were flashed on 16 samples, are shown in Fig. 7: (1) Al, (2) medium plastic mine, (3) small plastic mine, (4) small metal mine, (5) air, (6) granite paving brick, (7) soil, (8) sand, (9) KBr, (10) Mg, (11) $CaSO_4$, (12) $NaBiO_8$, (13) H_2O, (14) Fe, (15) Teflon, and (16) Pb. Samples 2-4 indicate the presence of nitrogen by the slope of their decay while samples 1, 7-9, 14, 16 have a large mass density as indicated by the their large long-time count rate. We conclude from these and other multi-flash data that: (1) Large-time noise is small and well behaved and so can be ignored, (2) Small-time noise is brief and so its time domain can be excluded, and (3) The Nitrogen Camera signal is robust - an object with ~125 g of nitrogen below a spot when flashed with photons resulting from a single 8 mA, 50 MeV electron pulse gave ~100 counts above a ~5 count background in detectors ~1 m away.

4. IMAGES

To obtain images of explosives marker element distributions in an object, we scanned our photon flash vertically by deflecting the electron beam pulse-by-pulse over the tantalum radiator in 15 steps with a bi-directional programmed magnet power supply. The photons produced a 30 cm strip of 15 evenly spaced 2 cm diameter spots at the rate of 1 Hz/flash. The object was attached in a double blind procedure at random locations and in various orientations to the downstream face of a large 1" thick aluminum plate. This plate provided support for the objects being interrogated and also background counts typical of a ~2" overburden of loose soil in which anti-personnel mines are commonly buried. The plate was moved horizontally, transverse, and at a right angle to the photons at 6 cm/s as the beam was stepped vertically. The resulting saw tooth pattern produced images of 180 pixels in ~2.5 min.

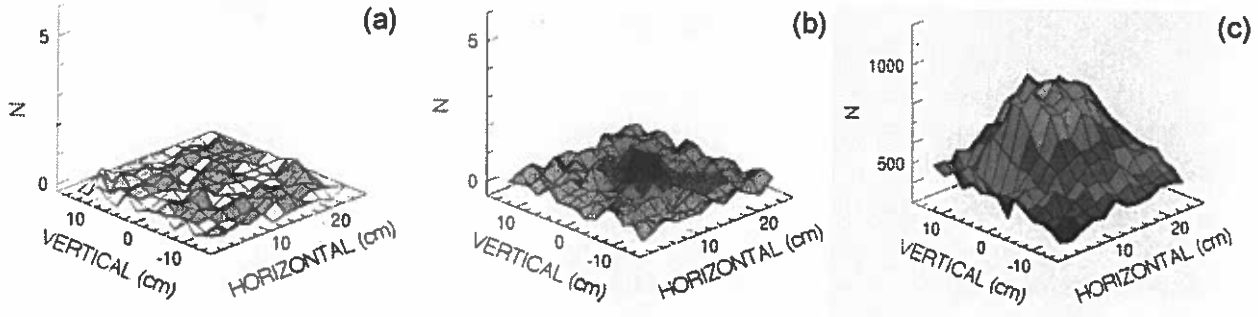

Fig. 8. Plastic "land mine" response to photons from (a) 30, (b) 40, and 50 MeV electrons.

Images of a medium size plastic melamine-filled land mine is shown in Fig. 8. The mine is evident only at the highest energy and there is no hint of a carbon signal despite melamine being ~1/3 carbon by weight, because only one out of a hundred carbon atoms is ^{13}C. Thus we will use 50 MeV

electrons for our initial explosives scans since even a substantial carbon content is unlikely to make an image relative to a comparable amount of nitrogen. ~125 g of the SEMTEX in a 2" diameter cylinder scanned with photons from a 50 MeV electron beam is imaged in Fig. 9. Twice this amount of SEMTEX brought down Pan Am 103[6] in 1988.

We made all our images by simply aggregating the raw pixel counts in each 1 ms time bin during the interval between 10 and 60 ms after the photon flash. These data were not corrected, normalized, or adjusted. Because we obtained these images under ideal laboratory conditions and despite the fact that we have not been able to anticipate any substantial problems, field conditions will surely degrade our signal in unanticipatable ways.

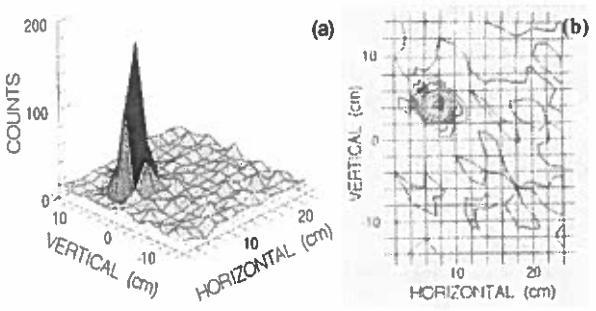

Fig. 9. 50 MeV electrons in SEMTEX: Intensity (a) image and (b) contour map.

5. THE ENABLING HARDWARE

To field the Nitrogen Camera, we have had to develop several technologies, the most challenging of which was the photon source, a mobile, rugged, reliable 70 MeV electron accelerator to provide ~50 mA beam pulses at ~20 Hz with energy changeable pulse to pulse. Further, since the source is to be vehicle mounted, it had to be small, be lightweight, and use power efficiently. Finally, because its operators would have modest technical skills, its start up, operation, and diagnostics has to be highly automated. We began designing our racetrack microtron in 1992 with Russian colleagues[7]. We have been forced to develop new approaches so as to realize our 0.6 x 0.5 x 1.3 m^3 accelerator that weighs ~3,000 kg, and only requires ~25 kW of operating power. The three most significant innovations are: (1) A narrow rectangular cavity biperiodic accelerating-focusing structure to reduce the size and allow the 1st orbit beam to clear the structure; (2) Large rare earth permanent magnet dipoles which halve the overall microtron power consumption, reduce its size and weight, and simplify its construction and operation; and (3) a 40-beam 6.6 MW/6kW klystron that now provides 300 nC beam pulses at 70 MeV, soon to be 750 nC.

REFERENCES and FOOTNOTES

2. W.P. Trower, A.W. Saunders, and V.I. Shvedunov, **Nitrogen Camera: Detection of Anti-Personnel Mines**, in **Terrorism and Counterterrorism Methods and Technologies**, W. Ishimoto, ed. (SPIE, Bellingham, 1997) v. 2933, p. 58.
3. We have not investigated the oxygen reactions because we lacked an electron beam with sufficient energy and intensity. We will attempt to detect oxygen reactions in experiments we will conduct before this conference.
4. H. Babic and M. Sedlacek, **A Method for Stabilizing Particle Orbits in the Race-Track Microtron**, Nucl. Instrum. Meth. **56** (1967) 170.
5. Explosives loaned to us by Nobel Chemicals, Ltd., Stockholm, Sweden.
6. **Report of the President's Commission on Aviation Security and Terrorism** (U.S. GPO, Washington, 1990).
7. E.A. Knapp, A.W. Saunders, V.I. Shvedunov, and W.P. Trower, **A Mobile Racetrack Microtron**, Nucl. Instrum. Meth. **B139** (1998) 517 and W.P. Trower, A.I. Karev, V.N. Melekhin, V.I. Shvedunov, and N.P. Sobenin, **Design of a Mobile 70 MeV Race-Track Microtron for the Carbon/Nitrogen Cameras**, Nucl. Instrum. Meth. **B99** (1995) 736.

3D visualization of data acquired by laboratory UWB GPR in the scope of mine detection

N. Milisavljevic, B. Scheers, Y.Yvinec, M. Acheroy,
Royal Military Academy, Brussels, Belgium

Abstract: *In this paper, we present a laboratory version of ultrawideband (UWB) ground penetrating radar (GPR) system that we developed, as well as data acquired by this system and our 3D visualization method performed on this data. This is a part of work done for the moment at the Royal Military Academy (RMA) in the scope of the Belgian HUDEM[1] project. The main purpose of this on-going work on UWB GPR is to analyze possibilities to detect and visualize buried landmines and other buried objects (false alarms) and therefore to test the ability to distinguish (identify) them.*

Keywords: mine detection, laboratory UWB GPR, TEM horn antennas, 3D visualization.

INTRODUCTION

One of the most promising technologies for detection and identification of buried landmines is the ground penetrating radar (GPR) [1]. Since antipersonnel (AP) mines are not buried at great depth and are very small objects, a conventional GPR is not very well suited to detect the mines without failure and to discriminate between a mine and a mine-like target. Because of that, in the frame of the HUDEM project, the RMA has started research on the detection of AP mines by means of UWB GPR [2], i.e. GPR using ultra-short electromagnetic pulses (shorter than 200ps). One of the main advantages of this type of GPR is a high depth resolution; our idea is to use this benefit for 3D visualization of the buried objects, and, by this, to "visually" detect landmines and distinguish them from other buried objects.

In the first part of the paper a laboratory version of the UWB GPR is presented, as well as reasons for its development. After that, the development of very small UWB directive TEM horn antennas is discussed. Finally, the ideas for 3D visualization of data acquired by such a system are described, and results of this method are given.

The work presented in this paper is still under progress and improvement.

LABORATORY UWB GPR SYSTEM

Classical GPRs are mostly designed for geophysical applications and use central frequencies below 1 GHz. As AP landmines are small objects, higher frequencies are needed for a better depth resolution and detailed echo. For example, in order to obtain a depth resolution of 3 cm, in the worst case (ε_r of the soil very small), frequencies up to 3GHz are needed. High frequencies can also be very useful to detect shallow buried landmines. Unfortunately, when mines are buried too deep and the frequency is too

[1] The HUDEM (HUmanitarian DEMining) project is the technology exploration project on humanitarian demining launched by the Belgian Minister of Defense with funding provided by his Department, the Ministry of Foreign Affairs and the State Secretariat for Development Aid. The Royal Military Academy (RMA) - Brussels is in charge of overall project management and coordination of an active collaboration between several Belgian universities.

high, it is possible that nothing would be detected because of the dramatically increased attenuation of the soil with frequency. So, to be sure to detect something, low frequencies are needed as well. A solution to this dilemma is the use of a large bandwidth in order to benefit from the advantage of both low and high frequencies. Such a large bandwidth can be obtained by a time-domain (carrier-free) UWB GPR or a SFCW (Stepped Frequency CW), and these two types of GPR are usually found in demining applications.

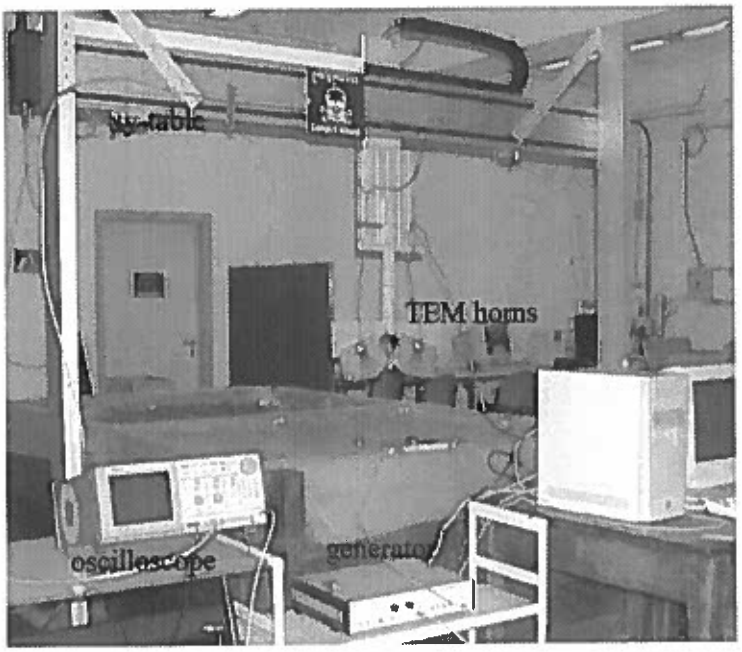

Figure 1: The UWB GPR system set-up

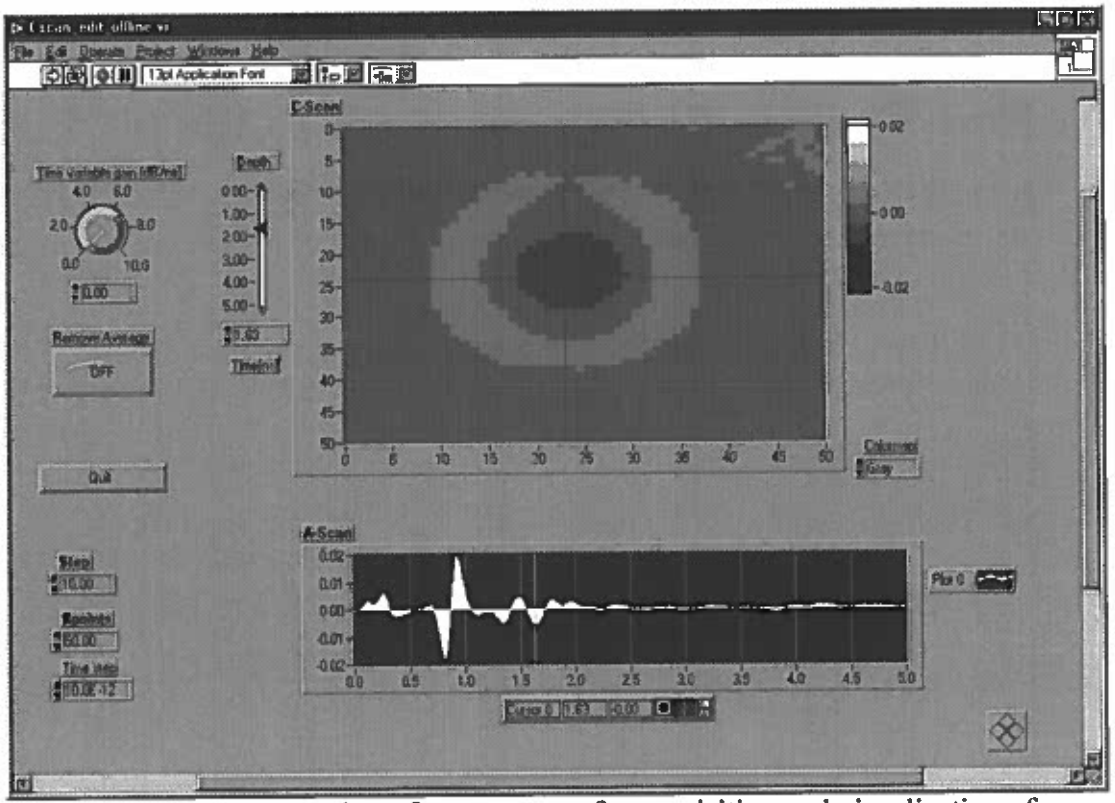

Figure 2: A screen-shot of our program for acquisition and visualization of raw A- and C-scans

In order to study its advantages and drawbacks, we made a laboratory version of a time-domain UWB GPR system. Its components are mainly off-the-shelf laboratory equipment, while the antennas are developed in the RMA. On the transmitting side of the system, a Picosecond Pulse Labs step-generator is used; the amplitude of the generated step is 10V, the rise-time is 45ps, and waveform purity is high. This step-signal is then transformed by an impulse-forming network to an impulse with maximum amplitude of 2.5V and a FWHM of less than 100ps. The impulse is fed to a Tx-Rx antenna pair, designed for this large bandwidth (more about antennas is given in the next section). On the receiver side, a 6GHz digitizing oscilloscope is used for measuring the backscattered signal. The oscilloscope has an internal delay line, a 14 bit resolution and can average up to 10,000 times, to obtain a higher dynamic range. The oscilloscope data is collected by a computer using a GPIB bus. The antenna pair is mounted on a xy-table of 2m by 2.5m and 2m high (see Fig. 1). This table is computer-controlled and has a precision of less than 0.1mm. In the scanning area of the table, two boxes are placed, 1.5m by 1.5m each and 0.8m deep; one of them is filled with sand, the other one with loam. The permittivity of both types of soil is fully characterized in function of frequency and moisture content. The whole setup is controlled by a computer, that commands, via a serial connection, the position of the xy-table scanning head and collects the data (A-scans) from the oscilloscope. The program that runs on the computer allows visualization of the A-, B- and C-scans (see Fig. 2), performing basic signal and image processing and saving the data.

DIELECTRIC-FILLED TEM HORN ANTENNAS DEVELOPMENT

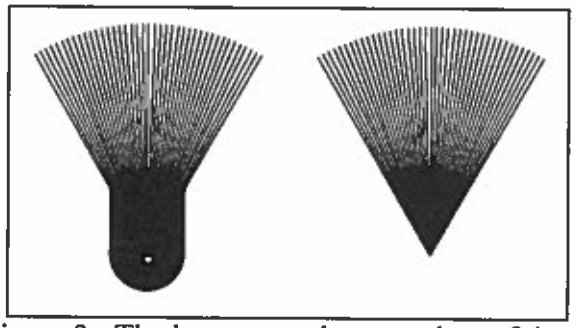

Figure 3 : The bottom- and upper-plate of the antenna etched on a PCB

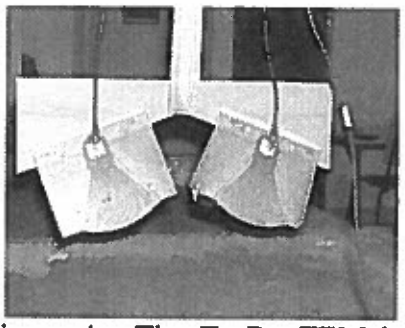

Figure 4 : The Tx-Rx TEM horn antenna pair

Taking into account the UWB approach, we decided to develop our own antennas. Since we wanted very small antennas which can be used-off ground and radiate over a large bandwidth (between 500MHz and 4GHz), we chose a travelling wave TEM horn [3] antenna[2], that consists of a pair of triangular conductors (antenna plates) forming a V structure. In order to reduce the physical size of the antenna, without changing the bandwidth and to improve the directivity, the antenna is filled with a dielectric ($\varepsilon_r \approx 3$). The antenna plates were etched[3] on a printed circuit board (PCB) and terminated by a 50Ω load, by putting two 100Ω SMD resistors in parallel between the antenna plate extremities. We also replaced the antenna plates by a set of 41 wires (see Fig. 3). The distance between the wires is too small to influence the antenna characteristics, but it forces the currents to be radial. Also, that limits the

[2] It is called a travelling wave TEM horn antenna because it guides mainly a spherical TEM-like mode between the two antenna plates.

[3] Etching the antenna plates also limits the weight of the plates and increases the precision in fabrication.

surface of conducting metal, which is very important when using the antennas in combination with a metal detector (due to the lamination of the antenna plates, the metal detector will be only weakly influenced by the presence of the antennas). The final realisation of the antennas is shown on Fig. 4. Their dimensions are small: a physical antenna aperture is 12cm by 6cm.

3D VISUALIZATION OF ACQUIRED DATA – DESCRIPTION OF METHOD

Data acquired by the described system proved to us that this type of GPR has a high depth resolution. Thanks to that, we came to the idea to perform 3D presentation of the data in order to visualize buried objects and hence detect landmines as well as distinguish them from other, non-dangerous buried objects (stones, cans etc).

Our method for 3D visualization proceeds as follows: After collecting A-scans, we perform envelope detection (by finding absolute values of the Hilbert transform, see Fig. 5) on each of the A-scans, and then we join them in adequate C-scans (see Fig. 6). That is the starting point for our further processing, in order to visualize objects that we measured. On each of the C-scans some image preprocessing tools are applied, including filtering, smoothing and thresholding; the same threshold-level is chosen for all C-scans, to preserve just higher signal amplitudes. After that, detection of edges on thresholded images is done. Finally, detected edges from each of the C-scans are joined, taking into account their physical meaning, i.e. the depth that they describe, the position in the measured volume etc., and, by that, a 3D visualization of the buried object is obtained. The program for visualization that we developed makes it possible to rotate (i.e. to see from different angles) this 3D image, to easily distinguish various depths by assigning colours to chains from specific C-scans (i.e. a colour of a chain describes its depth position). Also, it is possible to choose (change) the threshold-level and see its influence on the shape of chains and 3D objects.

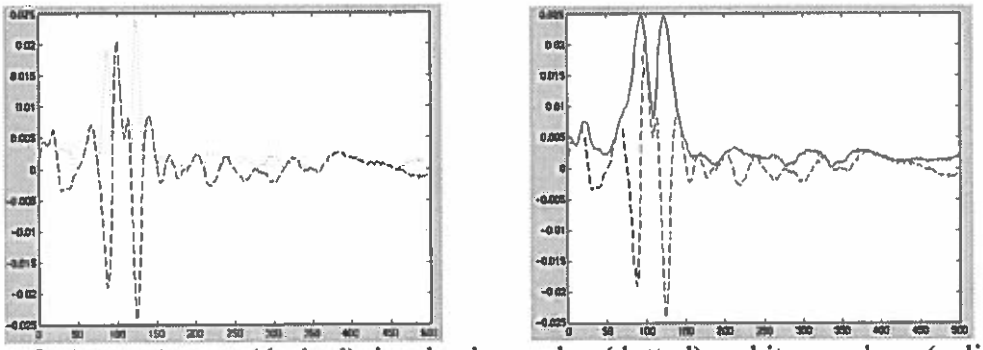

Fig. 5: A raw A-scan (dashed), its absolute value (dotted) and its envelope (solid)

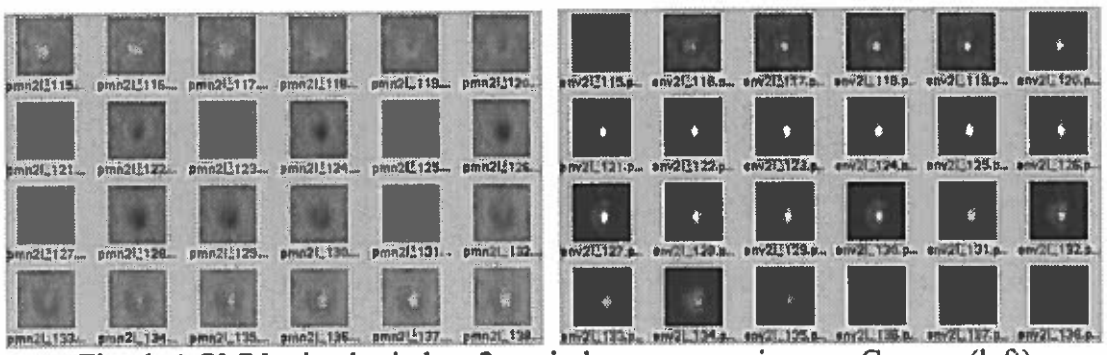

Fig. 6: A PMN mine buried on 2 cm in loam: successive raw C-scans (left) and after envelope detection (right)

3D VISUALIZATION OF ACQUIRED DATA – RESULTS

Results of this method, applied on the data acquired by our GPR system when a PMN mine was buried around 2cm below the soil surface in sand, are given on Fig. 7; the typical shape of one side of the PMN case can be easily noticed[4]. If a slightly higher threshold-level is chosen, the results are as on Fig. 8. It can be seen that the basic shape is preserved, i.e. that the influence of the threshold-level is not critical.

Some other results of this method are shown on Fig. 9.

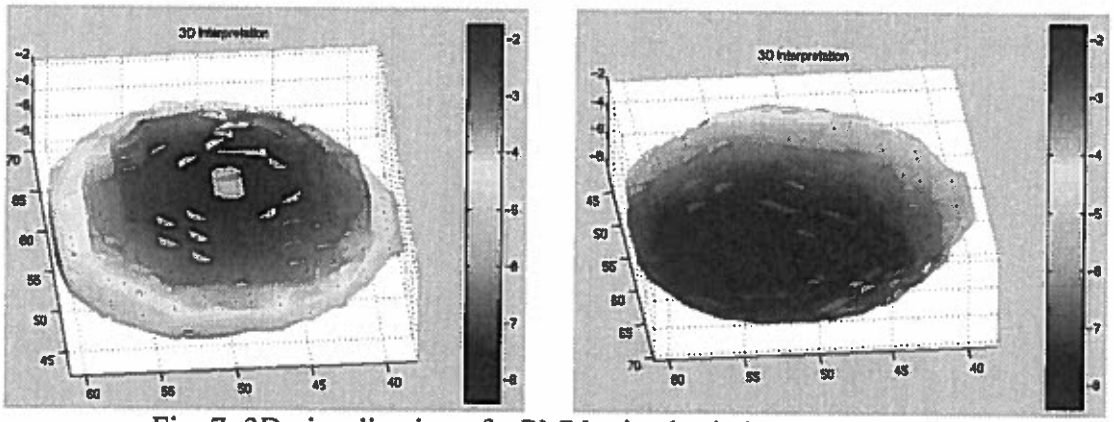

Fig. 7: 3D visualization of a PMN mine buried on 2cm in sand:
two views – up (left) and bottom (right); threshold-level is 145 (scale 0-255)

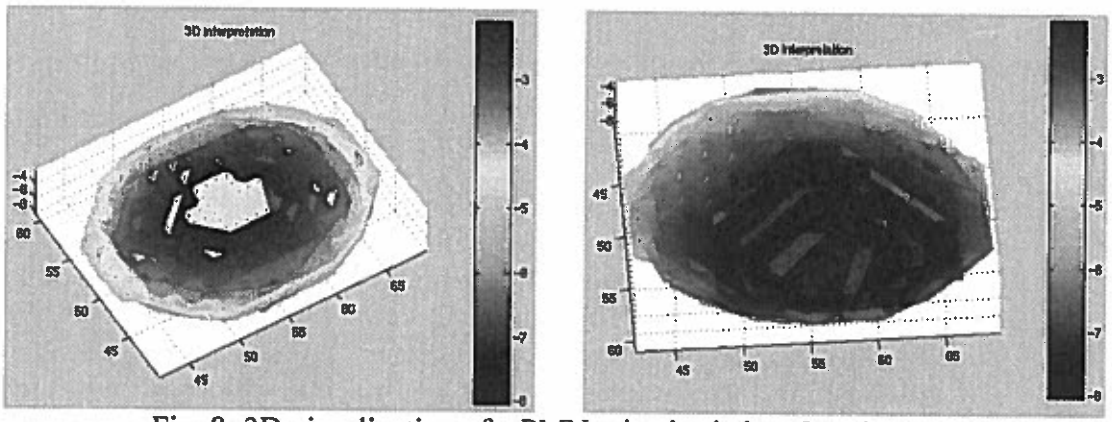

Fig. 8: 3D visualization of a PMN mine buried on 2cm in sand:
two views – up (left) and bottom (right); threshold-level is 155 (scale 0-255)

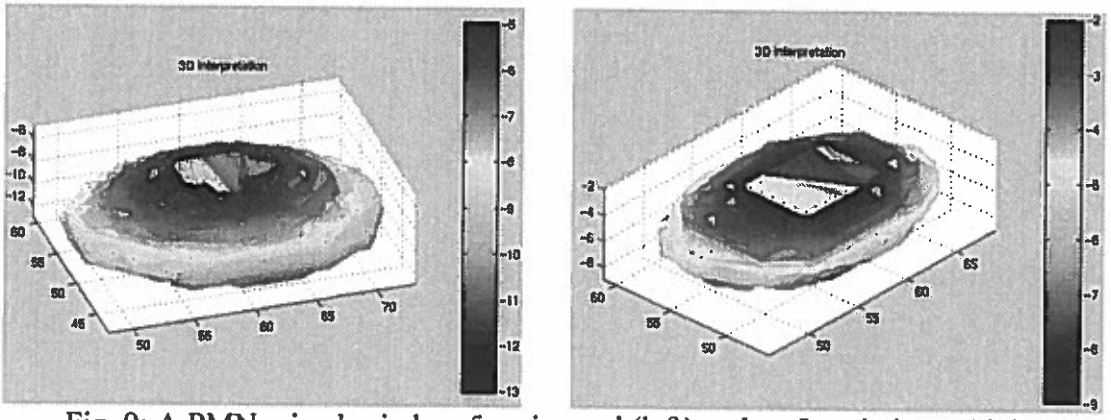

Fig. 9: A PMN mine buried on 5cm in sand (left) and on 2cm in loam (right)

[4] Remark for all figures in this chapter: the depth (z-axis) is given in [cm], while other two axes are in pixels, and size of one pixel is 1cmx1cm. Since the data is not focused, dimensions of mines are larger than in reality, i.e. mines are stretched (it will be solved in future work by migration).

On the left sides of Figures 10 and 11 photos of a VS-50 and a PMN mine are given, respectively, and on the right sides are results of 3D presentation of the measurements of these two mines. It can be concluded that shapes of mines are preserved.

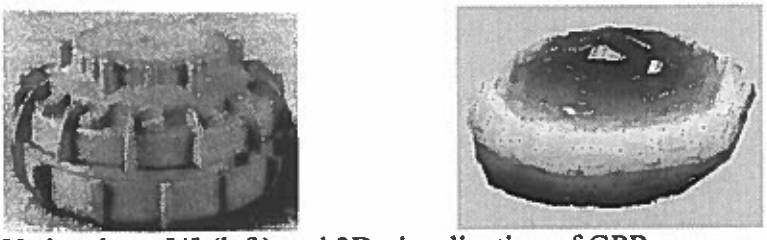

Fig. 10: VS-50: its photo [4] (left) and 3D visualization of GPR measurements (right)

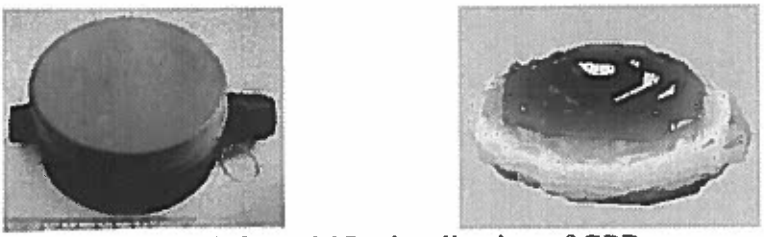

Fig. 11: PMN: its photo [4] (left) and 3D visualization of GPR measurements (right)

CONCLUSION AND FUTURE WORK

Results obtained by our laboratory version of UWB GPR system prove that this technology is promising for mine detection. Since the depth resolution of such a system is very good, we have been trying to take advantage of it and visualize acquired data in 3D. The first results of our 3D visualization method show that it is possible to extract the shape of a buried object, but further improvements are necessary, especially in the sense of the data focusing, so that dimensions of detected objects are proportional to the real dimensions. Therefore, our next step will be to find an efficient migration method. There is one more reason why our program for 3D visualization is still in progress and improvement. Namely, we are aware that we are dealing, by the current method, with a lot of data that has to be processed in order to visualize buried objects (but, speed of data processing is not low!). In future work, we will investigate possibilities to reduce the amount of data for processing.

Our hope and belief is that 3D visualization of UWB GPR images has a great potential for realistic mine detection situations, because it should help a deminer to simply "see" what is hidden below the ground surface in a simple, easily understandable way.

REFERENCES

1. Daniels D.J., 1996, *Surface-penetrating radar*, IEE, London, UK.
2. Scheers B., Piette M., Vander Vorst A., 1998, "The detection of AP mines using UWB GPR", IEE, Second International Conference, The Detection of Abandoned Land Mines, Edinburgh, UK
3. Baum C.E., 1995, "Low-Frequency-Compensated TEM Horn", Sensor and Simulation Notes Nr. 377, Phillips Laboratory.
4. "MineFacts" humanitarian demining database: http://www.demining.brtrc.com/cgi-win/runwin.exe?MINE:SearchDB

A Method of Metal Objects Identification by Electromagnetic Means

Piotr Szyngiera
Institute of Electronics, Silesian Technical University
Gliwice, Poland
email: szyna@boss.iele.polsl.gliwice.pl

ABSTRACT
The process of searching for land mines by means of a metal detector is always connected with motion of the sensor. In this paper, a simple method is given that utilises the sensor movement to produce graphical signature of an object. It is achieved by displaying in-phase and quadrature signals on an impedance plane where target characteristics are observed by an operator as well as can be further processed by digital signal processing means including for example digital filtering and neural networks analysis. The method can be inexpensive alternative for multifrequency detectors or can compliments these methods.

Key words: Metal detector, eddy current patterns, target recognition, electromagnetic methods

Introduction

Magnetic and electromagnetic metal detection as one of the methods of buried landmines and unexploded ordnance location has its golden years beyond. Introduction of non-metal land mines caused development necessity of other location methods yet did not eliminate metal detectors. Contrary, metal detectors are still widely used and proofed to be one of the most useful tools in the field. Their low cost, simple design and easy usage make them inevitable tool for every demining team. There is also a widely spread misconception that electromagnetic methods are not up-to-date and soon they will be totally substituted by other locating techniques. In practice, however, electromagnetic instruments are constantly being improved what still ranks them high at the list of the most widely used demining equipment. This short paper deals with another method of possible electromagnetic metal detector improvement.

To discriminate or not to discriminate?

There are two basic types of electromagnetic metal detectors: pulse induction (PI) and continuous wave (CW) detectors. PI detectors are very simple, deep seeking instruments capable of operating even in extreme background condition. On the other hand, however, the power drain is considerably high and the sensitivity to small low conductive metals is insufficient. Continuos wave detectors, operating at frequencies from 1 kHz to 50 kHz, are extremely sensitive even for tiniest metal objects but are more complicated, heavier and background noise susceptible. CW detectors are also known for its good discriminating capability.

Distinguishing different targets is desirable in many applications but this feature seemed to be irrelevant for demining purposes. However, recent tendencies show that metal target characterisation would be very helpful in process of buried UXO locating. The identification surely helps to distinguish buried ordnance from trash and thus minimises false alarm rates that cause drop of a deminer concentration and enlarges risk of injuries.

There are some methods of characterising buried ordnance by secondary field analysis either in time or frequency domain. Recent developments concentrate on multiperiod techniques for PI detectors and multifrequency methods [8,9] for CW metal detectors. Some of them have been successfully implemented, some are still developed with very promising results. However, none of the methods are sufficient for all searching conditions.

Below one of the frequency domain method is briefly discussed and a new approach to the eddy-current metal detector signals analysis is proposed. The method provides easy and inexpensive target recognition, especially those made of ferrous metals.

Electromagnetic induction sensor properties

The main part of every metal detector is its sensor, often called a search head. Such a sensor consist of at least one transmit coil that produces primary field and a receive coil (or coils) that sense the secondary field. The coils have to be situated in such a way so the receive signal is nulled. There are many possible arrangements of those transmit and receive coils that fulfil this demand (see fig. 1).

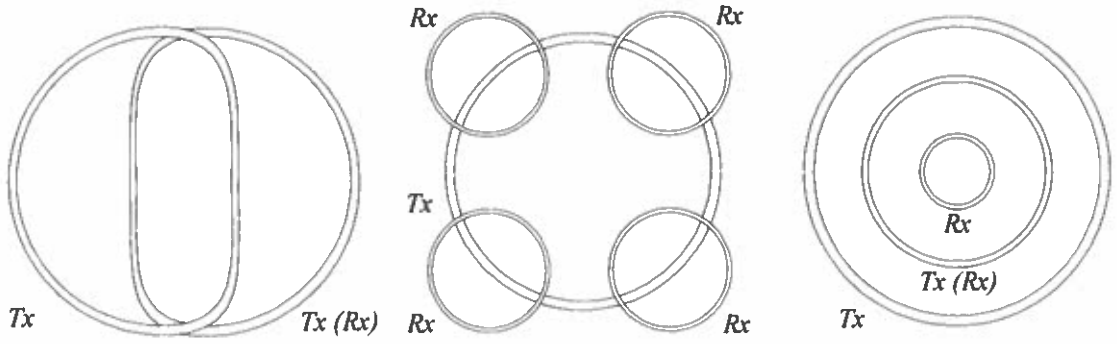

Fig. 1 Examples of balanced sensors. From left to right: Coincidental (double D) - e.g. Minelab F1A4, multicoil -e.g. Fourdee AN/PSS-11, Concentric -e.g. Geophex GEM3 [6] -note that the inner coil can be either receive or transmit (bucking).

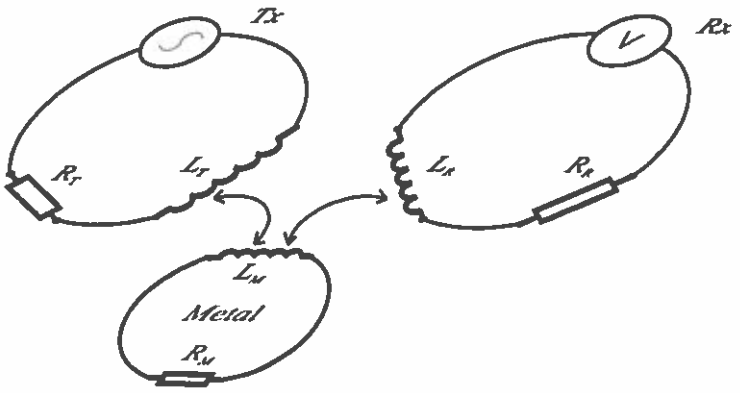

Fig. 2 Electrical model of a balanced search sensor.

Target characterisation capability can be easily evaluated by means of electrical methods (including SPICE modelling) if we assume that the sensor and the metal are represented by lossy inductors (see fig. 2) [2,4].

Since the transmit and receive coils are balanced, there is no mutual inductance. A metal object within the detection range of the sensor causes the coils to unbalance and as a consequence a receive signal is produced. The strength of the signal depends mainly on the distance to the sensor, provided the object is made of relatively well conducting material [2]. Information about the metal electrical properties lies in the phase angle of the receive signal (see fig. 3).

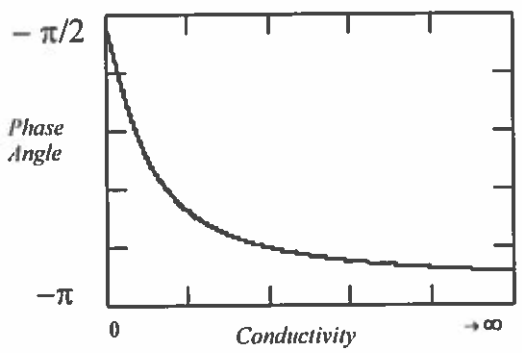

Fig. 3 Receive signal phase angle versus non-ferrous metal conductivity

This feature is widely used in discriminating and target identifying metal detectors. Multifrequency metal detectors also utilise this feature yet the phase measurement is done at several frequencies (at least two) to cancel out influence from permeable environment [7,9].

How to make use of the sensor motion

The process of searching for buried ordnance is always connected with the motion of the sensor over a suspected area. The sensor motion is often used in CW detectors for filtering out low frequency signals caused either by varying background conditions or sensor height. Fig. 4 shows how such a sensor reacts to buried objects when being swept. If we compare the two responses from purely conductive (non-ferrous metal) and purely permeable object (mineralised stone, for instance) the differences are clearly visible. However, signal components from conductive and permeable object (steel, for example) are very difficult to interpret without additional processing. One of the methods is maximum signal detection and

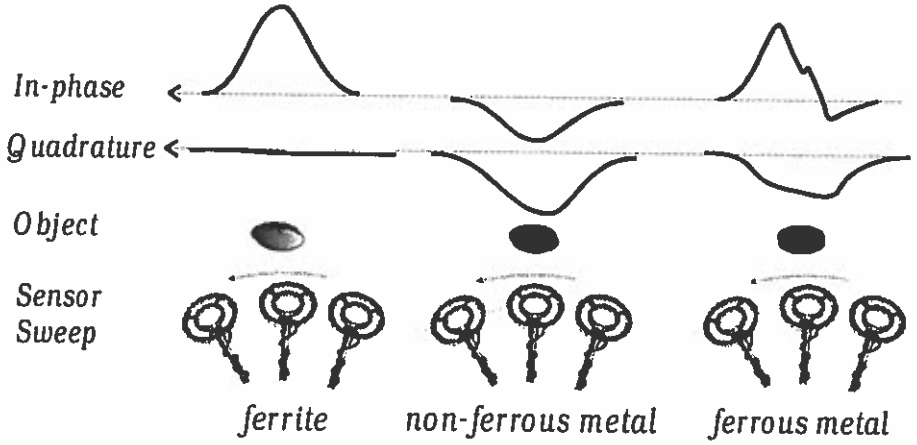

Fig. 4 Comparison of sample responses from various objects

then calculating phase shift for this particular value. This method however causes significant loss of information and produce very ambiguous results for ferrous metals.

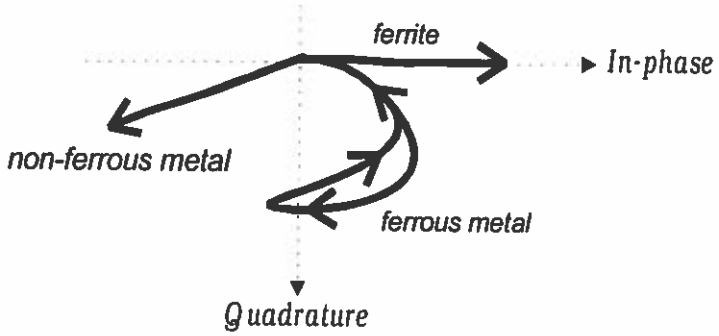

Fig. 5 Responses on the impedance plane

If the receive signal is presented on an impedance plane, during sweeping the sensor a graph is created (see fig. 5). This method is similar to eddy-current pattern method used for detection material flaws in non-destructive testing [5]. For non-ferrous metals such a trajectory is represented by a line, whose angle depends on electrical properties of the object. For ferrous metals the shape is more complicated but still there are some common features for certain types of objects that enables an operator to evaluate what is beneath the sensor.

Some practical results

Method of displaying metal detector signals on impedance plane was implemented in Institute of Electronics, Gliwice on a laboratory model and as an extension unit to commercially available metal detector (for reference only). A simplified block diagram of the laboratory model is shown on Fig 6.

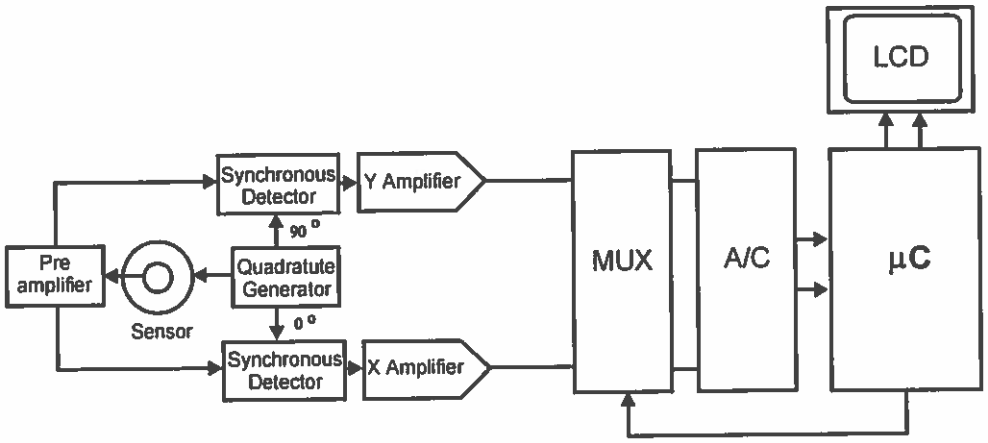

Fig. 6 Simplified block diagram of the target identifying metal detector

The sensor is of co-axial type operating at 5kHz. The trajectories together with calculated phase shift and signal strength are displayed on LCD module. Some trajectories captured by means of a DSO are shown on Figs. 7, 8 and 9. Purely conductive or permeable objects moving horizontally to the sensor are represented by straight line whereas steel plates (or other ferrous objects with flat surfaces) draw loop-like patterns. Curved lines are produced for elongated iron objects (not shown).

Since the laboratory model was based on 12-bit A/C converter, it works well for relatively big objects only. For coin size objects, effective target recognition was 10-15 cm. Modern digital metal detectors have 18 bits resolution, so smaller objects can certainly be represented more precisely. Some problems were encountered when multiply metal objects were in the range of the sensor (which was 40cm diameter). The resulting trajectories were mostly of circular shape, what made impossible to distinguish separate targets. Even though, it helps to note that more targets are present, and "target masking" effect is greatly reduced. Trajectories similar in shape (elipsoidal) were observed when a non-ferrous metal was situated within highly permeable patches (simulated by a ferrite powder).

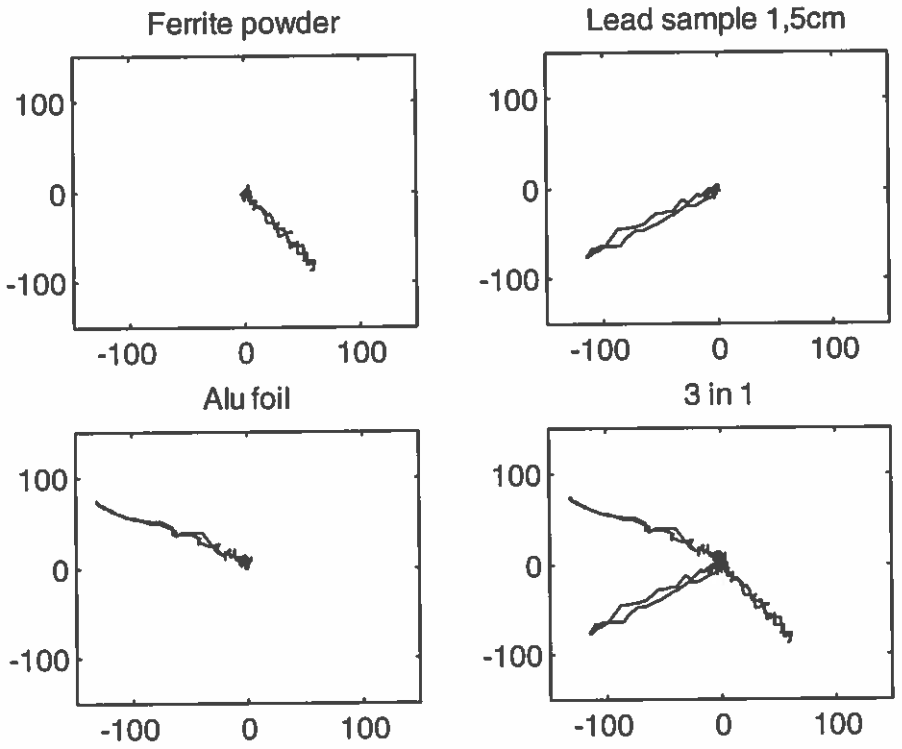

Fig. 7 Trajectories produced by objects having either purely conductive or permeable properties (note: patterns are tilted due to phase shift at bandpass preamplifier)

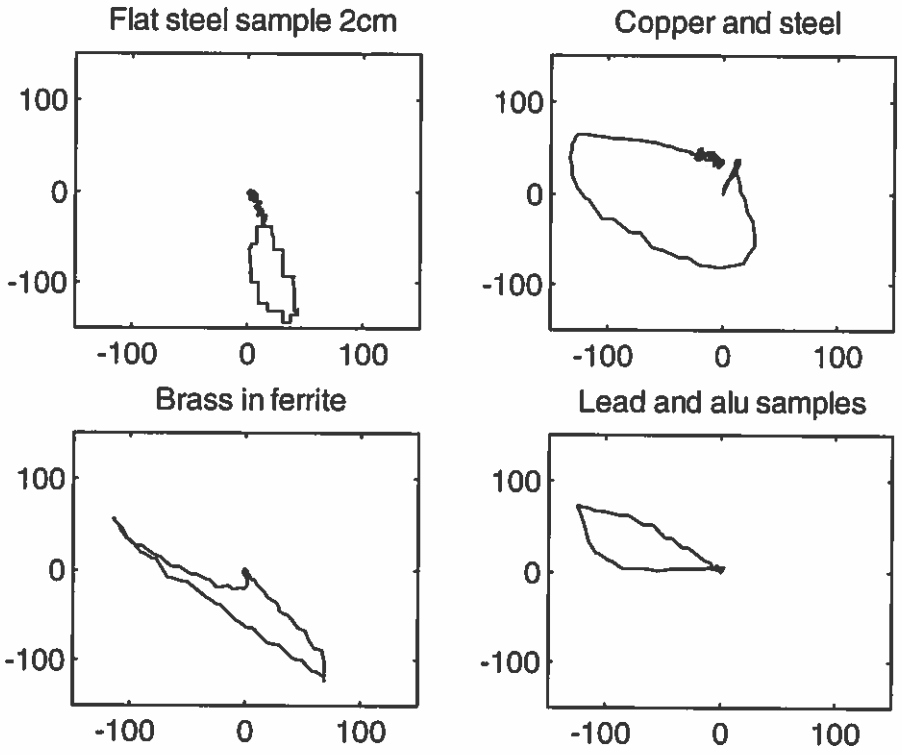

Fig. 8 Trajectories produced by objects having both purely conductive and permeable properties and multiply targets lying close to each other.

Conclusions

Target characterisation by means of displaying receive signals on an impedance plane is an inexpensive method of distinguishing sought object from metal debris often found on minefields. The method does not require special design of a sensor, as it would work virtually on any balanced coil configurations. These sensors are theoretically well defined and readily available. Further development is aimed at noise cancellation (well known digital methods can be applied [3,5]) and spatial resolution improvements. 3D imaging (where third dimension would be frequency or sensor placement - see fig. 7 for reference) is being investigated.

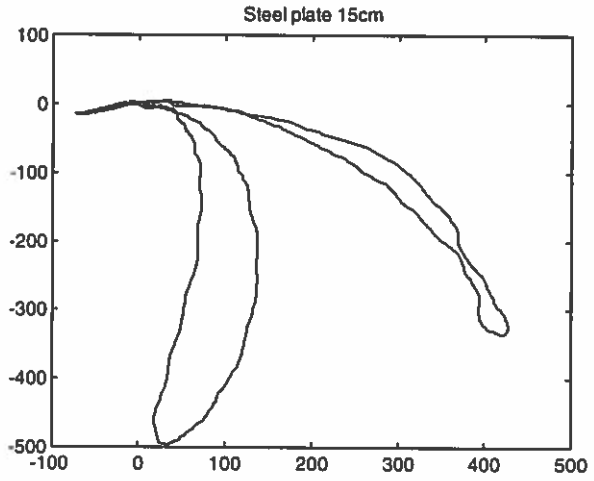

Fig. 9 Illustration of approaching a steel plate (10x10cm) by a concentric sensor. From right: pattern produced at the edge of the sensor and a pattern at the centre of the sensor.

Certainly this method alone would not provide 100% reliable metal detection and target recognition. It can be used as an aid in fields where many surface metal trashes are present and the mine types are well characterised in advance.

References

[1] Szyngiera P., "Eddy-Current Trajectory Pattern Method Applied for Metal Objects Recognition", Non-Destructive Testing Conference, Poznan, Poland 1995 (Proceedings in Polish),

[2] Szyngiera P., "Metal Detector Balanced Search Loop Properties Analysis", Optoelectronic and Electronic Sensor Conference, Szczyrk, Poland 1996 (Proceedings in Polish)

[3] Szyngiera P., Wojtasik A., "Wavelet Transformation Applied for Eddy-Current Metal Detector Signals Analysis" Conference of Telecommunication, Bydgoszcz, Poland 1998 (Proceedings in Polish).

[4] McNeil JD, "Electromagnetic Terrain Conductivity Measurement at Low Induction Numbers", Technical Note TN-6, Geonics Ltd, 1980

[5] Stepinski T., "Analysis of Eddy Current Patterns", The British Journal of NDT, vol. 32, no12, 1990

[6] Won I.J. et all, "GEM-3 Monostatic Broadband Electromagnetic Induction Sensor", JEEG, Vol. 2 Issue 1, March 1997

[7] Candy B., "A Method and Apparatus of Discrimination Detection Using Multiple Frequencies to Determine a Recognizable Profile of an Undesirable Substance", USA patent no 4942360, 1990

[8] Won I.J. et all, "Electromagnetic Induction Spectroscopy", JEEG Vol. 3 Issue 1, March 1998

[9] Shoemaker D., "Plural Frequency Method and System for Identifying Metal Object in a Background Environment Using a Target Model", USA patent no 5642050, 1997